Sustainable Process and Supply Chain Design with Consideration of Economic Constraints, Climate Change, and Food-Energy-Water Nexus

Dissertation

Presented in Partial Fulfillment of the Requirements for the Degree Doctor of Philosophy in the Graduate School of The Ohio State University

By

Kyuha Lee, B.E., M.E.

Graduate Program in Chemical Engineering

The Ohio State University

2020

Dissertation Committee:

Bhavik R. Bakshi, Advisor

Jeffrey M. Bielicki

Sami Khanal

James F. Rathman

Abstract

Sustainability assessment has become one of the essential tools for process and supply chain design problems to ensure the well-being of future generations. Sustainability assessment methods such as life cycle assessment have been used to identify opportunities for improvement of technologies and help the decision-making process. However, environmental impacts may result in ecological overshoot and shift across space, time, flows, and disciplines. To avoid unintended outcomes due to burden shifting, sustainability assessment methods need to account for ecosystem services, multiple spatial scales, temporal dynamics, multiple flows, and cross-disciplinary effects. This dissertation contributes to advance the methods for sustainability assessment, sustainable process design, and sustainable supply chain design by considering market constraints, climate change effects, and the nexus of multiple flows.

Decisions made by approaches that only consider the environmental domain could result in unexpected outcomes due to burden shifting to economic and social domains. For example, the conventional sustainability assessment approaches assume advanced technologies can be adopted by the market due to technological advances. However, the market does not always choose the "best" technology because of market effects, such as market demand and economic resource availability. These unintended consequences could occur through the entire supply chain at multiple spatial scales. In

this dissertation, a novel multiscale technology choice modeling framework is introduced to take account of market constraints as a consequential approach for designing engineering processes and supply chain networks. The case study focuses on the installation of new green urea production systems in a watershed where there are limited supplies of resources, such as water and land. This multiscale consequential framework is useful for modeling the substitution effects of emerging technologies while considering market constraints.

The consequences of climate change on industrial systems can be studied using the multiscale consequential framework as well since climate change affects future resource availability. The impacts of climate change on the urea manufacturing systems and potential adaptation strategies to maintain their productivity are discussed. To make the manufacturing systems robust to climate change, the systems need to be designed to be flexible to the increased risk of water scarcity and warmer temperatures. A climate-resilient process design approach is explored to ensure the operability of manufacturing processes by employing a flexibility analysis approach.

Addressing the challenge of climate change will also require the use of technologies that treat CO_2 as a valuable resource instead of a waste that is simply dumped into the atmosphere or underground. Novel insights into the food-energy-water-ecosystem nexus are discussed while examining the economic feasibility and environmental benefits of CO_2 conversion technologies. Various technological and agro-ecological alternatives are considered to improve the sustainability of food-energy-water (FEW) activities. Additionally, a modeling framework for spatially-explicit sustainability

assessment is developed. In this framework, the spatially-explicit sustainability of regional FEW systems can be examined while considering flows across multiple regions at multiple spatial scales.

Other contributions of this dissertation include a carbon footprint analysis of biomimetic carbon fixation technologies and understanding the effect of societal consumption on the FEW nexus.

Dedicated to my wife and parents.

Acknowledgments

I would like to express my deepest appreciation to my advisor, Dr. Bhavik Bakshi, for providing invaluable guidance and giving me many research opportunities throughout my Ph.D. years. I have always been motivated by his enthusiasm for sustainability research. I simply cannot thank enough for his constant encouragement and all the feedback.

I would like to extend my sincere thanks to Dr. Sami Khanal, who has been my collaborator for multiple projects, for her valuable advice about the watershed and climate modeling. Many of the research works would not have been possible without her help. I would also like to thank Dr. Jeff Bielicki, Dr. Jim Rathman, Dr. Liang-Shih Fan, and Dr. Nick Brunelli for serving as my committee members for my qualifying exam, candidacy exam, and Ph.D. defense. Their comments and feedback through the exams have helped me improve the quality of my research.

I am also very grateful to all of my collaborators. Dr. Sintov and Ian gave me an invaluable opportunity to work on the social aspects of sustainability. Dr. Parquette and CAPS project members (Dr. Tabita, Dr. Sundaresan, Dr. Satagopan, Dr. Sun, and Parker) have provided a great amount of assistance for a research project on carbon fixation technologies. Also, I would like to extend my gratitude to Dr. Irwin and DRFEWS project members for providing me with insightful comments on spatially-explicit sustainability assessment work. All these multidisciplinary research

projects have truly broadened my research perspective and interests. I would also like to acknowledge research funding sources: the OSU Sustainable and Resilient Economy (now the OSU Sustainability Institute) program, Battelle Memorial Institute, Ohio Water Resources Center, NSF Sustainability Research Networks grant CBET-1444745, NSF INFEWS grant SBE-1739909, and NSF grant CBET-1804943.

I must also thank my fellow group members in Sustainable Engineering Research Group, Varsha, Xinyu (Priscilla), Tapajyoti (TJ), Michael, Utkarsh, Vyom, Yaz, Ying, Soomin, Mu, Xiangming (Shaun), Ruonan, Jingying, Shubhankar, Amrita, Vivek, and Kevin. All the comments and feedback through our meetings have been extremely valuable.

Many thanks to the members of Young Timothy Christian Fellowship. They have helped me and my wife in various ways and have given support for my Ph.D. studies. Most importantly, I would like to thank my wife and all the family members for supporting me throughout the years.

Vita

December 2, 1985	Born - Seoul, Republic of Korea
2005–2009	B. E. Chemical Science and Engineering, Kobe University Kobe, Japan
2009–2011	M. E. Chemical System Engineering, The University of Tokyo Tokyo, Japan
2015–present	Graduate Research Associate, Lowrie Department of Chemical and Biomolecular Engineering, The Ohio State University Columbus, OH, USA

Publications

Research Publications

Lee, K. and Bakshi, B.R., "Energy-water-CO_2 nexus of fossil fuel based power generation." *Advances in Carbon Management Technologies: Carbon Removal, Renewable and Nuclear Energy, Volume 1*, Ed. by Subhas K. Sikdar and Frank Princiotta, CRC Press, 2020.

Bakshi, B.R., Ghosh, T., and Lee, K., "Engineering, Markets, and Human Behavior: An Essential Integration for Decisions toward Sustainability." *Current Opinion in Chemical Engineering* 26, 164–169, 2019.

Lee, K., Ghosh, T., and Bakshi, B.R., "Toward Multiscale Consequential Sustainable Process Design: Including the Effects of Economy and Resource Constraints with Application to Green Urea Production in a Watershed." *Chemical Engineering Science* 207, 725–743, 2019.

Ghosh, T., Lee, K., and Bakshi, B.R., "Integrating Market Models and Price Effects in a Multiscale Sustainable Process Design Framework." *Computer Aided Chemical Engineering* 47, 175–180, 2019.

Lee, K., Kim, A.Y., and Lee, J.K., "Fullerene Coated Indium Tin Oxide Counter Electrode of Prussian Blue Electrode for Enhanced Electrochromic Properties." *Solar Energy Materials & Solar Cells* 139, 44–50, 2015.

Lee, K., Kim, A.Y., Park, J.H., Jung, H.G., Choi, W., Lee, H.Y., and Lee, J.K., "Effect of Micro-Patterned Fluorine-Doped Tin Oxide Films on Electrochromic Properties of Prussian Blue Films." *Applied Surface Science* 313, 864–869, 2014.

Kim, A.Y., Lee, K., Park, J.H., Byun, D., and Lee, J.K., "Double-Layer Effect on Electrothermal Properties of Transparent Heaters." *Physica Status Solidi A* 211 (8), 1923–1927, 2014.

Choi, K.O., Yoon, S.H., Kim, W.S., Lee, K., Yang, C.M., Han, J.H., Kang, C.J., Choi, Y.J., and Yoon, T.S., "Morphological Dependence of Hydrothermally Synthesized ZnO Nanowires on Synthesis Temperature and Molar Concentration." *Physica Status Solidi A* 210 (7), 1448–1453, 2013.

Fields of Study

Major Field: Chemical Engineering

Studies in:

Sustainable Engineering
Process Systems Engineering
Environmental Impact Assessment
Food-Energy-Water Nexus

Table of Contents

Page

List of Tables

List of Figures

Chapter 1: Introduction

Sustainability assessment is a tool to guide decision-making for improving the sustainability of products, processes, and systems. Due to the multidisciplinary nature of this challenge, scholars from diverse disciplines have endeavored to advance sustainability assessment methods. Life cycle assessment (LCA) is one of the most well-known and well-established sustainability assessment methods. Based on LCA, numerous sustainability assessment modeling frameworks have been developed to avoid unintended harm from solutions. To claim sustainability, six necessary but not sufficient requirements for sustainability assessment methods have been proposed.[9] These requirements can be used to evaluate the performance of modeling frameworks.

1. Consider the demand for ecosystem services (e.g., CO_2 emissions). Requirement 1 is satisfied by most of the methods including conventional LCA.

2. Consider the supply of ecosystem services (e.g., carbon sequestration) to avoid ecological overshoot. Only a few methods such as techno-ecological synergy (TES)[10] and specific case studies that consider ecosystem services meet Requirement 2.

3. Consider temporal dynamics of activities. Requirement 3 involves dynamic modeling of processes and systems.[11]

4. Consider multiple spatial scales to avoid shifting of impacts across scales. Multiscale modeling methods such as hybrid LCA[12] and process-to-planet (P2P) frameworks[13] address Requirement 4.

5. Consider multiple environmental flows to capture their interactions. Requirement 5 accounts for the interactions between multiple flows such as food, energy, and water (FEW) nexus.[14,15]

6. Consider cross-disciplinary effects to avoid unexpected outcomes from other disciplinary domains. Requirement 6 considers the consequences of economic, social, and ecological domains on the environmental domain.[16,17]

In the area of chemical engineering, the sustainability of manufacturing and industrial processes also needs to be examined based on the sustainability assessment criteria above. In this dissertation, novel sustainable process and supply chain design approaches, whose main contributions are aimed to satisfy Requirement 6, and advanced sustainability assessment approaches that address Requirements 2, 4, and 5 are explored.

1.1 Motivation

1.1.1 Consequences of Economic Constraints on Technological Systems

Conventional sustainable engineering approaches, such as sustainable process design and sustainable supply chain design, aim to develop production systems and supply chain networks that have high efficiency, low cost, and low environmental impacts. These approaches implicitly assume that the optimal solution can be fully adopted by the market and society due to their environmental and economic benefits.

However, the market does not always choose the "best" solution because the extent to which technology is adopted depends on many non-technological factors such as its effect on market prices, constraints on the availability of raw materials and other resources, and human preferences. For instance, economic or ecological resources, such as labor, capital, minerals, water, and land area, may not be enough to meet the market demand for an advanced technology. Governmental regulations could hinder the adoption of a certain technology. Also, sub-optimal decisions could be made by economic agents due to subjective preferences.[18] In that case, the market selects among multiple technologies to satisfy the demand and to avoid violating regulations. Economic rebound may also occur if the more efficient new technology results in increased total resource use when adopted in society. In this sense, there are some gaps between engineering decisions based on technological advances and market decisions based on the economy and human preferences.

Consequential modeling approaches, such as consequential LCA (CLCA), try to capture the consequences of life cycle modeling decisions on the real-world economy to fill those gaps.[19,20] For example, many previous CLCA approaches investigate the change in environmental impacts by employing marginal data which are about temporal changes in most affected technologies.[21,22] However, the consequences of decisions that are attributed to the conventional (attributional) approach could be incurred across the entire economy.[23] More recent CLCA approaches utilize sophisticated economic models, such as general or partial equilibrium models, to account for consequences on broader economic systems.[24–26] The equilibrium-based approaches are useful for including market price changes as a consequence in the model, but not suitable to assess consequences at a smaller scale because the product resolution in

the equilibrium models is usually very low.[18] Also, they do not take account of the economic constraints addressed above and lack a multiscale framework.

The rectangular choice-of-technology (RCOT) model was developed to account for market constraints and multiple technology uses in analyzing economic systems.[27,28] In the RCOT model, when there are not enough market resources available to satisfy the commodity demand using the "best" technology, the market employs a different technology or multiple technologies simultaneously. In this sense, the RCOT approach can reflect market effects as a consequence in the model. However, none of the previous studies apply the RCOT framework to multiscale models and to solve engineering design problems.

1.1.2 Consequences of Climate Change on Technological Systems

Given the looming specter of climate change, it is essential that process systems are designed to be resilient to such a future. Manufacturing and industrial processes and their supply chains are major contributors to greenhouse gas (GHG) emissions, and thus to climate change. Many systems also rely heavily on water resources, both for generating steam and for cooling the process. However, water resources could be affected by drought under future climate change due to the projected increase in temperature and variability in precipitation. To combat climate change and its impacts, there is a need for the implementation of technologies and policy changes that reduce CO_2 emissions. Also, designs of industrial processes and supply networks need to be flexible in terms of projected climate change to maintain their productivity. The impacts of climate change have mainly been investigated on the operability of power plants[29,30] and agricultural systems.[31,32] However, studies on climate change impacts

on chemical and manufacturing processes are still lacking. To ensure the operability and productivity of chemical processes to changes in climate, the consequences of climate change on such processes and supply chain networks need to be investigated.

To examine climate change impacts on process design and supply chain design problems, various design constraints, such as projected water availability, water temperature, and target CO_2 mitigation level, can be considered. For example, if the water temperature gets warmer due to climate change, the systems that use water for cooling are likely to withdraw and consume more water to keep the same cooling performance. If this is the case, the increased risk of water scarcity may be a critical constraint for the design problems. Alternatively, equipment may need to be redesigned to increase the heat transfer area or coefficients. This could incur a financial cost. Also, future chemical processes may need to regulate their GHG emissions and adopt greener supply chains. In this context, the consequences of climate change on process and supply chain design need to be studied to ensure manufacturing systems to be resilient and robust to climate change.

1.1.3 Sustainable Food-Energy-Water-Ecosystem Nexus Modeling

In addressing the impacts of limited resources and climate change on technological systems, it is also crucial to understand the interactions between multiple environmental flows (Requirement 5). For instance, thermoelectric power plants generate electricity while withdrawing large quantities of water from a watershed. Therefore, increasing electricity generation could increase water stress and contribute to climate change. Also, farming practices that increase food production deteriorate water quality due to nutrient runoff. To prevent shifting of environmental impacts across

multiple flows, therefore, the FEW nexus needs to be understood in assessing the sustainability of technological systems.

Also, since the supply of natural resources is limited, it is important to consider the carrying capacity of ecosystems that support the activities of technological systems (Requirement 2). For example, in addressing the environmental sustainability of a power plant, the amount of water consumed by the power plant should be smaller than the amount of renewable water available to the plant. Otherwise, the power plant will likely fail at some point because water resources will become scarce. Similarly, farming produces food but releases significant amounts of nutrient emissions to the watershed where the supply of nutrient retention service is limited. To claim sustainability, therefore, the interactions between FEW flows and ecosystem flows need to be studied. Bakshi et al. developed the TES framework to account for the role of ecosystems in assessing the sustainability of technological systems.[10] In this framework, the demand for ecosystem services imposed by human activities, which correspond to the emissions and resource use, must not exceed the capacity of corresponding ecosystem services. This condition needs to be satisfied to claim the environmental sustainability of any activities.

From the life cycle perspective, the sustainability of FEW systems in a certain region needs to be assessed while accounting for inter-regional flows across the region to avoid shifting impacts outside the region. Also, technologies, economic activities, environmental interventions, and the supply of ecosystem services are varied with regions. Due to the regional heterogeneity, therefore, various multi-regional assessment approaches have been developed. Multi-regional input-output (MRIO)[33] and regionalized LCA[34] models evaluate regional sustainability by considering inter-regional

flows at the economy and value chain scales, respectively. Liu et al. developed a framework for regionalized techno-ecological synergies in LCA (TES-LCA) that accounts for regional ecosystem services at the value chain scale.[35] Such regionalized LCA-derived models need to account for multiple spatial scales using a hybrid modeling approach (Requirement 3). Therefore, there is a need for an integrated modeling framework of multiscale and multi-regional sustainability assessment that accounts for inter-regional flows and regional ecosystem services at multiple scales.

1.2 Objectives

Figure 1.1 represents the overview of the research topics in this dissertation. The main objective is to develop novel modeling frameworks that advance approaches for sustainability assessment and sustainable process and supply chain design. Along with the motivation stated in Section 1.1, objectives for the research topics can be classified into three sub-objectives. Each sub-objective focuses on Requirements for sustainability assessment as follows:

1. Develop a consequential multiscale modeling framework that accounts for economic constraints for sustainable process and supply chain design problems. The focus is to address Requirements 4 and 6.

2. Develop a climate-resilient process and supply chain design framework to investigate the consequences of climate change on manufacturing systems. Requirement 3 is partially addressed by modeling the impacts of future climate change on manufacturing systems.

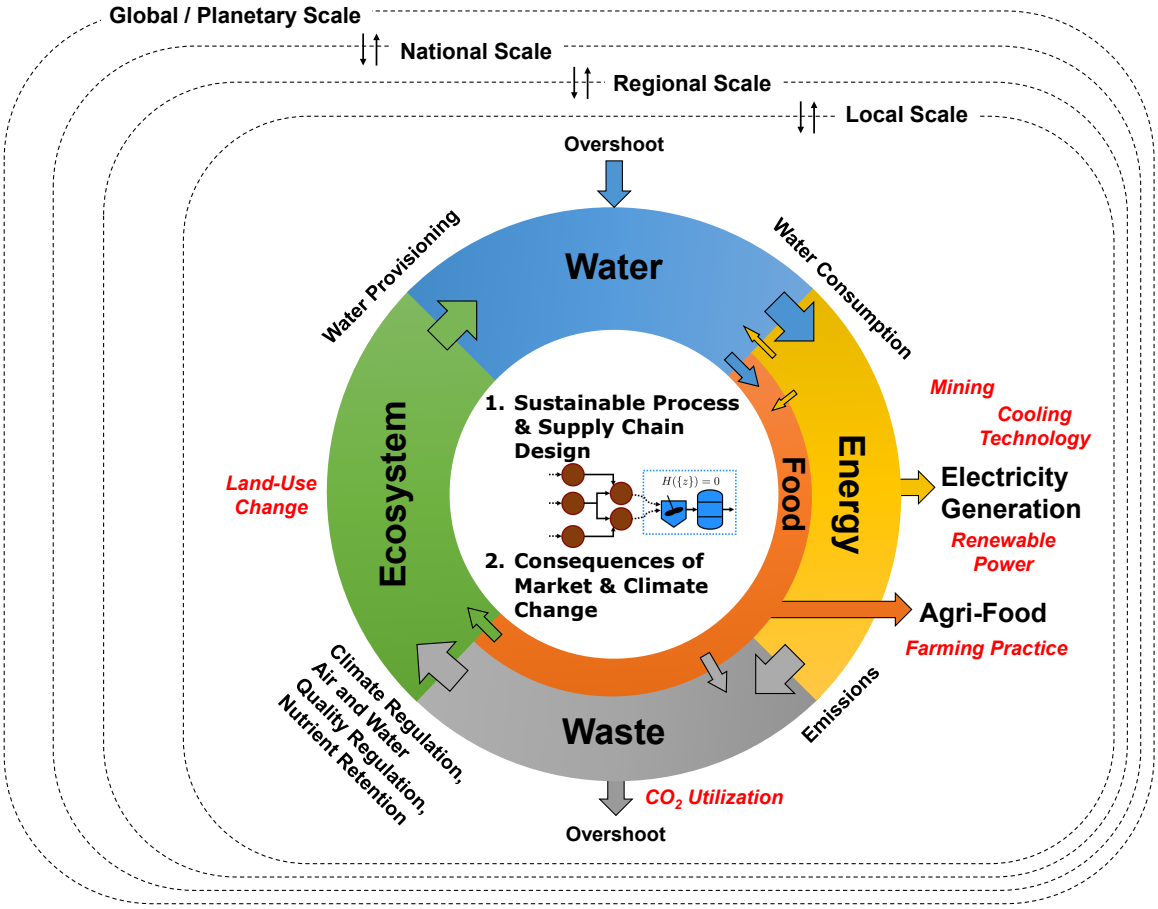

Figure 1.1: Overview of the research topics.

3. Develop a food-energy-water-ecosystem nexus modeling framework to assess the sustainability of regional FEW systems. The focus is to address Requirements 2, 4, and 5.

1.3 Contributions

Research work in this dissertation contributes to the field of sustainable engineering by developing advanced quantitative approaches for sustainability assessment, sustainable process design, and sustainable supply chain design problems. General

computational frameworks are proposed to address not only the consequences of market constraints and climate change on process and supply chain design but also the nexus of food-energy-water-ecosystem. The proposed frameworks can be employed for various applications. Specific contributions are as follows.

- A multiscale technology choice modeling framework is developed to perform a consequential study in solving process and supply chain design problems. The framework integrates process engineering, life cycle, and economy models. Also, market constraints are considered as a consequential approach to avoid unintended outcomes due to cross-disciplinary effects. Multiple technology options can be considered at each spatial scale in the developed framework. For instance, multiple process design models for competing technologies can be considered to optimize multiple production systems at the equipment scale. The framework is particularly useful to examine the adoption of emerging technologies in the constrained market.

- A climate-resilient process and supply chain design framework is developed to minimize the monetary loss due to climate disturbances and maintain the operability of manufacturing systems under climate change. The developed framework can account for the consequences of climate change on manufacturing systems design. Traditional process systems engineering methods that address uncertain parameters (e.g., flexibility analysis) can be employed to develop climate-resilient design solutions. Adaptation strategies for manufacturing systems to climate change can be addressed as well by including mitigation strategies as alternative options.

- A food-energy-water-ecosystem nexus framework is developed to investigate the absolute sustainability of regional FEW systems. The traditional FEW nexus framework is extended to include waste and ecosystem flows to identify the interactions between FEW systems and ecosystems. This allows us to explore the opportunities for improvement of FEW systems not only from technological aspects but also from agro-ecological aspects. Also, a general computational framework for spatially-explicit absolute LCA is developed. This is a multiscale and multi-regional FEW nexus modeling framework that integrates various existing LCA-derived models. The general framework can be employed for various spatially-explicit case studies.

- Other contributions of this dissertation include a carbon footprint analysis of biomimetic carbon fixation technologies and understanding the effect of societal consumption on the FEW nexus. Conventional sustainability assessment methods such as process LCA (PLCA) and environmentally-extended input-output (EEIO) analysis are employed to examine how the emerging carbon fixation technologies could be improved to reduce the footprint and investigate the correlation between household consumption behaviors and FEW impacts, respectively.

1.4 Organization

Figure 1.2 summarizes research topics in this dissertation and spatial scales that each topic addresses. The rest of the dissertation is organized as follows. Chapter 2 provides a brief background of existing sustainability assessment methods that the research projects in this dissertation are based on. The existing methods described

in Chapter 2 include PLCA, EEIO analysis, MRIO, and integrated hybrid LCA. In Chapters 3 and 4, EEIO and PLCA modeling approaches are applied to investigate FEW footprints of household consumption and a carbon footprint of biomimetic carbon fixation technologies with RubisCO immobilization, respectively. These two projects employ the conventional sustainability assessment methods, and therefore, they only satisfy Requirement 1. To address the research problems described in Section 1.1, novel modeling approaches need to be developed. Chapter 5 introduces a consequential multiscale modeling framework that considers the consequences of economic constraints on SPD and SSCD. A case study is conducted for green urea production systems in a watershed. In Chapter 6, the consequences of climate disturbances on manufacturing systems are investigated, and climate-resilient process design approaches are proposed. Chapter 7 explores sustainable watershed management strategies with technological and agro-ecological options by investigating the interactions between FEW systems and ecosystems. Chapter 8 describes a multiscale and multi-regional modeling framework for spatially-explicit absolute sustainability assessment to investigate the sustainability of regional FEW systems. Finally, Chapter 9 summarizes the conclusions of the dissertation and describes potential future work. In Appendices, two additional PLCA projects are described: life cycle CO_2 emissions of the coal-to-liquids process and a carbon footprint of the solar panel facility in the Columbus Zoo parking lot.

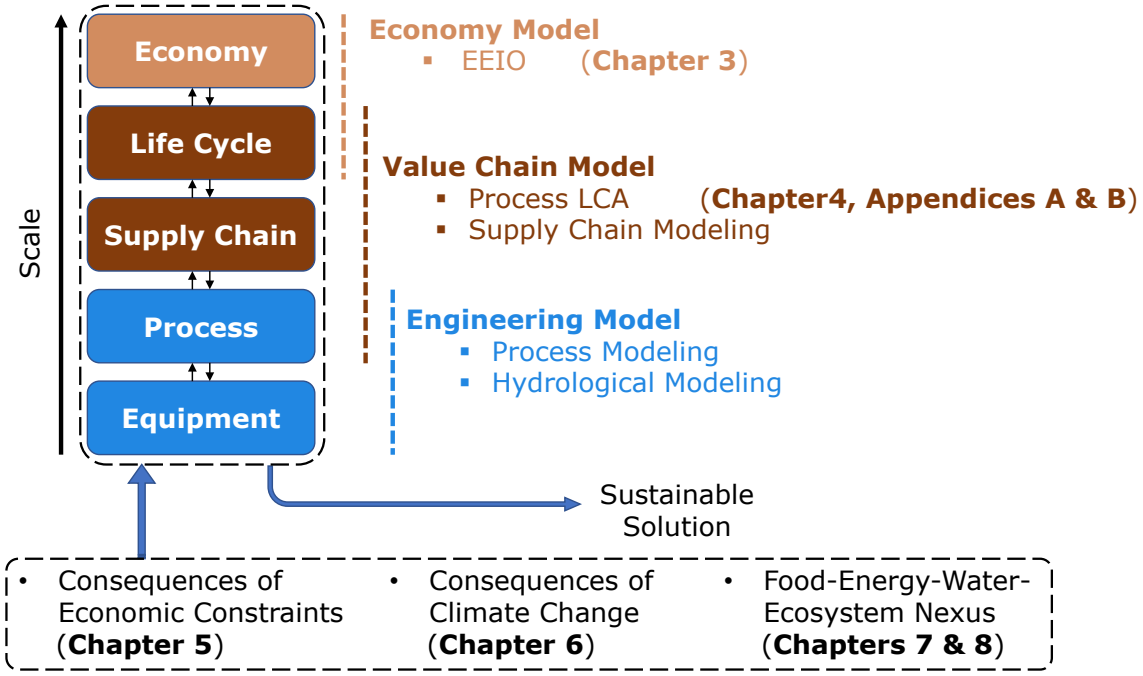

Figure 1.2: Research topics and spatial scales that each topic addresses.

Chapter 2: Background

This chapter describes various existing methods to account for the direct and indirect input from human activities into nature. These methods include life cycle assessment (LCA) and footprint analysis. The demand for ecosystem services can be defined as emissions and resource use from human activities. These environmental interventions can be quantified by various existing sustainability assessment methods. The mathematical formulation and characteristics of various LCA models are described. Also, data sources and software programs to conduct LCA studies are introduced.

2.1 Quantifying the Demand for Ecosystem Services

Sustainability assessment methods such as LCA and footprint analysis calculate environmental impacts (e.g., greenhouse gas emissions and water consumption, etc.) of products and processes. Those environmental impacts are referred to as the demand for ecosystem services (D_k). D_k represents the demand for an ecosystem service k. For instance, CO_2 emissions from an industrial facility (D_{CO_2}) are demanded by a forest ecosystem that provides a carbon sequestration service to the facility. Likewise, water consumption from the facility is defined as the demand for a water provisioning service (D_{water}) from a watershed ecosystem. In this sense, the demand for ecosystem

services means environmental impacts from processes and economic activities. Table 2.1 shows some examples of demands for ecosystem services and their corresponding supplies of ecosystem services.[10,36]

In the sustainability assessment methods, environmental impacts of processes and economic activities can be quantified by mathematical calculations that are addressed in Section 2.2. Quantifying the demand for ecosystem services relies on the existing methods of LCA and footprint analysis. The rest of this section describes approaches to quantify the demand for ecosystem services by using the LCA method with an example of electricity generation.

LCA has been developed for decades to quantify environmental impacts of products or processes throughout their life cycle that ranges from the extraction phase of upstream resources (e.g., fossil resources) to the end-of-life phase (e.g., waste disposal and recycling). Therefore, LCA is often called a cradle-to-grave analysis. Figure 2.1 shows the system boundary of an example LCA study: LCA of electricity generation. The left-hand side corresponds to the extraction of upstream resources for electricity generation, while the right-hand side corresponds to the downstream processes of electricity.

Table 2.1: Examples of the demand and supply of ecosystem services.

Ecosystem service (k)	**Demand for ecosystem service (D_k)**	**Supply of ecosystem service (S_k)**	**Key ecosystem contributor**
Climate change regulation	GHG emissions	Carbon sequestration	Forest, Grassland
Air quality regulation	Air pollutant emissions	Air pollutant removal	Forest, Grassland
Nutrient retention	Nutrient runoff	Nutrient removal	Wetland
Water quality regulation	Water pollutant emissions	Water pollutant removal	Wetland
Water provisioning	Freshwater consumption	Freshwater supply	Watershed
Fossil energy source provisioning	Fossil resource consumption	Fossil resource supply	Geosystem
Soil retention	Soil erosion	Soil formation	Soil
Pollination	Pollinators needed	Pollinators available	Plant

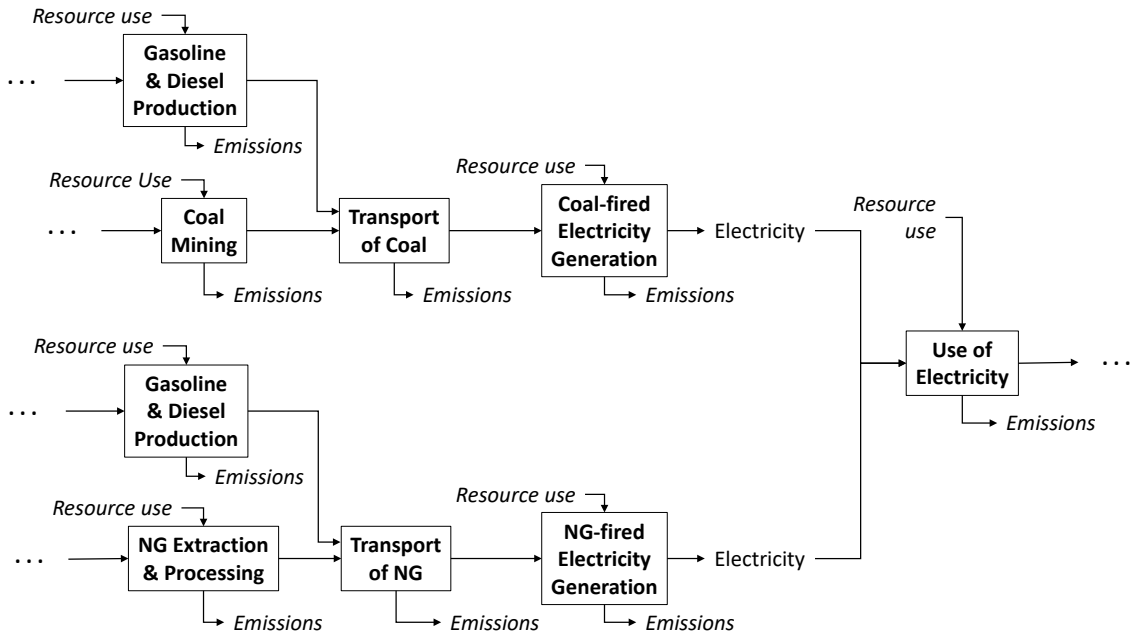

Figure 2.1: System boundary of an example LCA study on the comparison between coal-fired electricity and NG-fired electricity. Bold boxes represent processes and italics represent environmental intervention flows.

LCA has been standardized by ISO[37] and follows four steps as shown below.

1. **Goal and scope definition**: In conducting an LCA study, the goal of LCA study, a functional unit, and a system boundary need to be defined first. With respect to the electricity example shown in Fig. 2.1, the goal is to compare life cycle greenhouse gas emissions (i.e., global warming potential) of two product systems for electricity: coal-fired electricity and NG-fired electricity. Many LCA works are comparative studies between more than two product systems since the results obtained from LCA represent relative indicators, not the absolute ones. Therefore, one of the main purposes for conducting LCA studies is to recommend practices that are less bad between the options. A functional unit

needs to be defined properly to be common between the options for the goal. In this example, the functional unit can be kilowatt-hour (kWh) of electricity. Also, the system boundary is defined based on the goal of LCA study and data availability. The system boundary needs to include upstream and downstream processes of a product to avoid shifting of impacts across the life cycle because each process in the life cycle has its own environmental impacts. If all options in the study share the same downstream phases as shown in Fig. 2.1, the use and end-of-life phases can be excluded from the analysis. Such an LCA study is called a cradle-to-gate analysis.

2. **Life cycle inventory analysis**: In this step, every required life cycle inventory (LCI) data is collected from a variety of data sources. Some typical LCI data sources are introduced in Section 2.3. The type of data includes, but not limited to the amounts of product inputs, main product, by-products, co-products, resource use, and emissions.

3. **Life cycle impact assessment**: Life cycle resource use and emissions are calculated based on the LCI data collected in the previous step. Life cycle impact indicators, such as global warming and eutrophication potentials, are calculated using life cycle impact assessment (LCIA) characterization factors. The resulting life cycle impacts can be normalized and aggregated using normalization factors and weighting factors, respectively, depending on the goal that is defined in the first step. The details for mathematical calculations are addressed in Section 2.2.

4. **Interpretation of results**: In the last step, LCIA results are interpreted to make recommendations to reduce life cycle impacts. Hotspot inventories with respect to life cycle impact indicators can be identified as well. This step helps make decisions to change practices less bad to the environment.

2.2 Methods to Quantify the Direct and Indirect Demand

LCA can calculate direct and indirect environmental impacts (i.e., direct and indirect demands for ecosystem services) of products and processes. The direct demand means on-site resource consumption and emissions from an immediate process that produces the desired product. The indirect demand refers to the resource consumption and emissions from upstream and downstream processes. For example, the direct CO_2 emissions of coal-fired electricity is the on-site CO_2 emissions from the coal-fired electricity generation. On the other hand, the indirect CO_2 emissions for coal-fired electricity include CO_2 emissions from the upstream processes, such as coal mining and transportation of coal. The sum of direct and indirect emissions corresponds to the life cycle emission.

An LCA model consists of two equations: the product transaction equation and the environmental intervention equation. The product transaction equation contains data about the transaction of products between processes to produce the desired amount of a final product (i.e., final demand of a product). The environmental intervention equation calculates direct and indirect resource use and emissions for the final demand. In terms of the electricity example in Fig. 2.1, the transaction equation calculates how many coal and NG products are needed to produce 1 kWh of electricity, which is the final demand in this example. Also, the intervention equation

calculates the amounts of direct and indirect emissions and resource use to produce 1 kWh of electricity.

Depending on the goal and scope of LCA study, a different way of formulating LCA models are required. For example, if it is expected that detailed LCI data are easily available from LCI databases, process-based LCA model could be appropriate since the model contains a lot of process details. If it is too demanding to collect numerous LCI data along the life cycle, environmentally-extended input-output (EEIO) model could be suitable because the model accounts for the entire economy. The EEIO model covers the entire life cycle activities in return for the details of process data. Table 2.2 compares the pros and cons of various LCA models. In the following section, the mathematical formulation for those LCA models is introduced. Underbar (e.g., $\underline{A}$) and overbar (e.g., $\overline{A}$) notations in the mathematical formulation refer to value chain process scale for the process-based LCA model and economy scale for the EEIO model, respectively.

2.2.1 Process-based LCA

Process-based LCA model is based on process data in physical units (e.g., kg, m^3, and MJ). The product transaction equation of this model can be formulated using physical process data as follows.

$$\underline{A}\underline{s} = \underline{f},$$

$$\text{where } \underline{A} = \begin{bmatrix} \underline{a}_{11} & \underline{a}_{12} & \cdots & \underline{a}_{1n} \\ \underline{a}_{21} & \underline{a}_{22} & \cdots & \underline{a}_{2n} \\ \vdots & \vdots & \ddots & \vdots \\ \underline{a}_{m1} & \underline{a}_{m2} & \cdots & \underline{a}_{mn} \end{bmatrix} = \{\underline{a}_{ij}\} \in \mathbb{R}^{m \times n}, \ \underline{s} = \begin{bmatrix} \underline{s}_1 \\ \underline{s}_2 \\ \vdots \\ \underline{s}_n \end{bmatrix}, \text{ and } \underline{f} = \begin{bmatrix} \underline{f}_1 \\ \underline{f}_2 \\ \vdots \\ \underline{f}_m \end{bmatrix}.$$

$\underline{A}$ matrix is called a technology matrix that contains data about product input and output flows between processes. The rows ($i = 1, 2, \cdots, m$) and columns ($j = 1, 2, \cdots, n$) of $\underline{A}$ matrix correspond to products and processes, respectively. In most cases, the number of products is equal to the number of processes (i.e., $m = n$). $\underline{s}$ and $\underline{f}$ represent a scaling vector for each process (j) and a final demand vector for each product (i), respectively. $\underline{s}$ vector is determined by $\underline{s} = \underline{A}^{-1}\underline{f}$.

With respect to the electricity example, figure 2.2 shows partial LCI data that are collected for the process-based LCA model. $\underline{A}$ matrices for coal electricity (A^{coal})

Table 2.2: Pros and cons of various LCA models.

Pros	Cons
Process-based LCA model	
	− Collecting LCI data is time-consuming work.
+ The model has a lot of process details.	− Commercial LCI databases are expensive.
+ Free LCI databases are available.	− It is technically impossible to cover the entire life cycle network.
Environmentally-extended input-output (EEIO) model	
+ The model covers the entire life cycle network of a given region.	− The model is based on highly aggregated economy sectors. (i.e., lack of details in data)
+ The United States model is available for free.	
Multi-regional input-output (MRIO) model	
+ Region-specific analysis can be performed.	− Regional data are expensive and challenging to collect.
Integrated hybrid LCA model	
	− Upstream and downstream cutoff flows between value chain process and economy scales need to be identified.
+ The model not only covers the entire life cycle network of a given region but also contains a lot of process details.	− Price for every product needs to be known to connect process data in physical units to economy data in monetary units.

and NG electricity (A^{NG}) can be formulated as follows.

$$A^{coal} = \begin{bmatrix} 1\,\frac{\text{kWh}}{\text{kWh}} & -0.039\,\frac{\text{kWh}}{\text{kg}} & \cdots \\ -0.44\,\frac{\text{kg}}{\text{kWh}} & 1\,\frac{\text{kg}}{\text{kg}} & \cdots \\ \vdots & \vdots & \ddots \end{bmatrix},$$

$$A^{NG} = \begin{bmatrix} 1\,\frac{\text{kWh}}{\text{kWh}} & -0.045\,\frac{\text{kWh}}{\text{m}^3} & \cdots \\ -0.30\,\frac{\text{m}^3}{\text{kWh}} & 1\,\frac{\text{m}^3}{\text{m}^3} & \cdots \\ \vdots & \vdots & \ddots \end{bmatrix}.$$

For instance, the first and second rows of $\underline{\text{A}}^{coal}$ matrix represent an electricity product and a coal product, respectively. Also, the first and second columns of $\underline{\text{A}}^{coal}$ matrix correspond to a coal-fired electricity generation process and a coal mining process, respectively. Then, a_{11} in $\underline{\text{A}}^{coal}$ matrix refers to the amount of electricity generated from the coal-fired electricity generation process. a_{11} has a positive value indicating the electricity generation. Also, a_{21} shows the amount of coal product that is used to produce the a_{11} amount of electricity. a_{21} has a negative value indicating the consumption of coal for electricity generation. $\underline{\text{f}}^{coal}$ and $\underline{\text{f}}^{NG}$ vectors are defined as $\underline{\text{f}}^{coal} = \left[1, 0, \cdots, 0\right]^T$ and $\underline{\text{f}}^{NG} = \left[1, 0, \cdots, 0\right]^T$, respectively.

Also, the intervention equation of process-based LCA model is formulated as follows.

$$\underline{B}\underline{s} = \underline{r},$$

$$\text{where } \underline{B} = \begin{bmatrix} \underline{b}_{11} & \underline{b}_{12} & \cdots & \underline{b}_{1n} \\ \underline{b}_{21} & \underline{b}_{22} & \cdots & \underline{b}_{2n} \\ \vdots & \vdots & \ddots & \vdots \\ \underline{b}_{o1} & \underline{b}_{o2} & \cdots & \underline{b}_{on} \end{bmatrix} = \{\underline{b}_{kj}\} \in \mathbb{R}^{o \times n},\ \underline{s} = \begin{bmatrix} \underline{s}_1 \\ \underline{s}_2 \\ \vdots \\ \underline{s}_n \end{bmatrix},\ \text{and } \underline{r} = \begin{bmatrix} \underline{r}_1 \\ \underline{r}_2 \\ \vdots \\ \underline{r}_o \end{bmatrix}.$$

$\underline{B}$ matrix is referred to by the intervention matrix that includes data about each of the resource use and emissions ($k = 1, 2, \cdots, o$) for each process (j). $\underline{r}$ represents life cycle interventions which are calculated by $\underline{r} = \underline{B}\underline{s} = \underline{B}\underline{A}^{-1}\underline{f}$. For the electricity

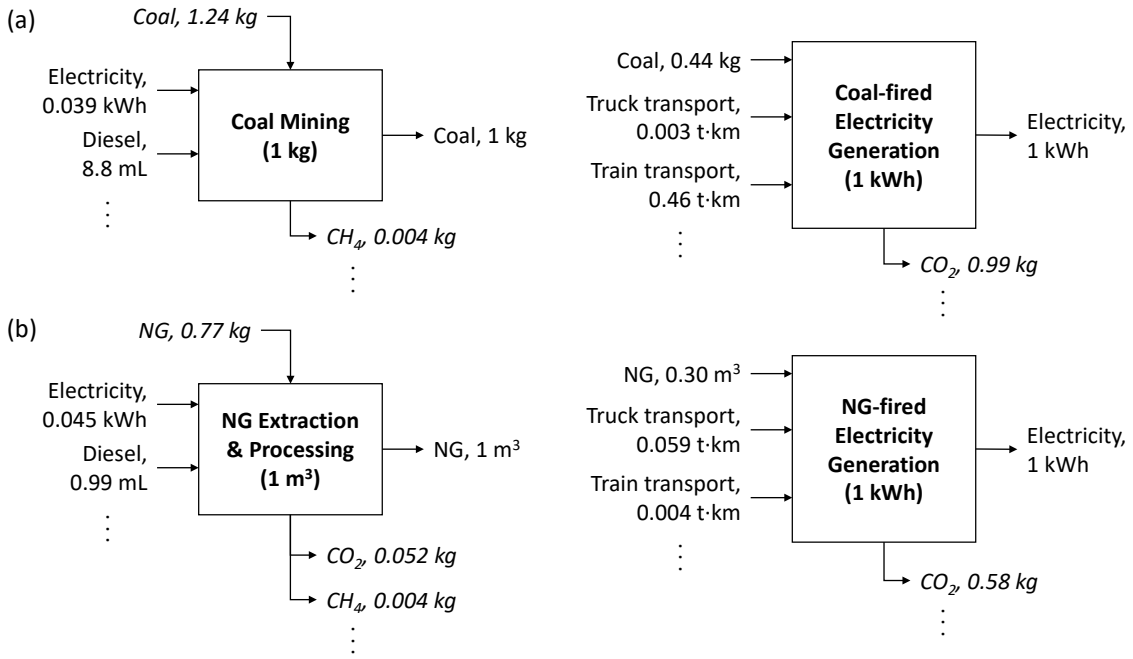

Figure 2.2: Process-based LCA model for coal-fired and NG-fired electricity.

example, $\underline{B}^{coal}$ and $\underline{B}^{NG}$ matrices can be formulated as follows.

$$B^{coal} = \begin{bmatrix} 0.99\,\frac{\text{kgCO}_2}{\text{kWh}} & 0\,\frac{\text{kgCO}_2}{\text{kg}} & \cdots \\ 0\,\frac{\text{kgCH}_4}{\text{kWh}} & 0.004\,\frac{\text{kgCH}_4}{\text{kg}} & \cdots \\ 0\,\frac{\text{kg coal}}{\text{kWh}} & -1.24\,\frac{\text{kg coal}}{\text{kg}} & \cdots \\ 0\,\frac{\text{m}^3\text{ NG}}{\text{kWh}} & 0\,\frac{\text{m}^3\text{ NG}}{\text{kg}} & \cdots \\ \vdots & \vdots & \ddots \end{bmatrix},$$

$$B^{NG} = \begin{bmatrix} 0.58\,\frac{\text{kgCO}_2}{\text{kWh}} & 0.052\,\frac{\text{kgCO}_2}{\text{m}^3} & \cdots \\ 0\,\frac{\text{kgCH}_4}{\text{kWh}} & 0.004\,\frac{\text{kgCH}_4}{\text{m}^3} & \cdots \\ 0\,\frac{\text{kg coal}}{\text{kWh}} & 0\,\frac{\text{kg coal}}{\text{kg}} & \cdots \\ 0\,\frac{\text{m}^3\text{ NG}}{\text{kWh}} & -0.77\,\frac{\text{m}^3\text{ NG}}{\text{kg}} & \cdots \\ \vdots & \vdots & \ddots \end{bmatrix}.$$

In these matrices, $k = 1$ and $k = 2$ correspond to CO_2 emissions and CH_4 emissions, respectively. Therefore, $\underline{b}_{11}$ and $\underline{b}_{21}$ in $\underline{B}^{coal}$ matrix indicate CO_2 emissions and CH_4

emissions, respectively, of the coal-fired electricity generation process ($j = 1$). Also, $k = 3$ and $k = 4$ correspond to coal and NG resource use, respectively. Since these resource use flows are inputs to the processes, $\underline{b}_{32}$ in $\underline{B}^{coal}$ matrix and $\underline{b}_{42}$ in $\underline{B}^{NG}$ matrix have negative signs.

To calculate life cycle impact indicators (i.e., midpoint indicators), LCIA characterization factors are multiplied with life cycle interventions as follows.

$$Q\underline{r} = \underline{h},$$

$$\text{where } Q = \begin{bmatrix} q_{11} & q_{12} & \cdots & q_{1o} \\ q_{21} & q_{22} & \cdots & q_{2o} \\ \vdots & \vdots & \ddots & \vdots \\ q_{p1} & q_{p2} & \cdots & q_{po} \end{bmatrix} = \{q_{lk}\} \in \mathbb{R}^{p \times o}, \ \underline{r} = \begin{bmatrix} \underline{r}_1 \\ \underline{r}_2 \\ \vdots \\ \underline{r}_o \end{bmatrix}, \text{ and } \underline{h} = \begin{bmatrix} \underline{h}_1 \\ \underline{h}_2 \\ \vdots \\ \underline{h}_p \end{bmatrix}.$$

Q matrix is the LCIA characterization factor matrix that contains characterization factors for each intervention flow (k) to calculate midpoint indicators ($l = 1, 2, \cdots, p$). The midpoint indicators are calculated by $\underline{h} = Q\underline{r} = Q\underline{B}\underline{A}^{-1}\underline{f}$. For the electricity example, if $l = 1$ represents global warming potential (GWP), q_{11} and q_{12} correspond to the characterization factors for CO_2 emissions ($k = 1$) and CH_4 emissions ($k = 2$), respectively, to calculate the GWP ($\underline{h}_1$). The GWP has a mass unit of CO_2 equivalent (e.g., $kgCO_2eq$). According to the LCIA characterization factors provided by EPA,[38] $q_{11} = 1$ $kgCO_2eq/kgCO_2$ and $q_{11} = 25$ $kgCO_2eq/kgCH_4$. Therefore, Q can be formulated by

$$Q = \begin{bmatrix} 1\,\frac{\text{kgCO}_2\text{eq}}{\text{kgCO}_2} & 25\,\frac{\text{kgCO}_2\text{eq}}{\text{kgCH}_4} & 0\,\frac{\text{kgCO}_2\text{eq}}{\text{kg coal}} & 0\,\frac{\text{kgCO}_2\text{eq}}{\text{m}^3\ \text{NG}} & \cdots \\ \vdots & \vdots & \vdots & \vdots & \ddots \end{bmatrix}.$$

Thus, the GWPs for coal-fired electricity generation and NG-fired electricity generation can be calculated as follows.

$$\text{GWP}^{coal} = \underline{h}_1^{coal} = Q\underline{B}^{coal}\underline{A}^{coal^{-1}}\underline{f}^{coal} = 1.08 \text{ kgCO}_2\text{eq}$$

$$\text{GWP}^{NG} = \underline{h}_1^{NG} = Q\underline{B}^{NG}\underline{A}^{NG^{-1}}\underline{f}^{NG} = 0.68 \text{ kgCO}_2\text{eq}.$$

One of the strengths for performing the process-based LCA model is that the model includes detailed process data. Therefore, sustainability assessment can be performed on a variety of products and processes if process data along the life cycle are easily available. Sources of LCI data for the process-based LCA model are introduced in Section 2.3. The process-based LCA model, however, does not account for the entire life cycle network since it is technically impossible to collect the tremendous amounts of process data along the life cycle.

2.2.2 Environmentally-Extended Input-Output (EEIO)

EEIO model has been developed to account for the entire life cycle network within the economy of a given region. The EEIO model is the environmentally-extended version of economy input-output (IO) model. The IO model is based on commodity transaction data between economy sectors in monetary units. Unlike the processes in the process-based LCA model, economy sectors are highly aggregated. For example, coal-fired electricity generation and NG-fired electricity generation are two different technologies. In the IO model, however, all electricity generation technologies are assigned to a single economy sector which is the electric power generation sector as shown in Fig. 2.3. This sector can also be further aggregated into the utility sector that includes a water supply system and a NG distribution system as well as the electric power generation. In Fig. 2.3, ellipses, curved arrows, and angled arrows

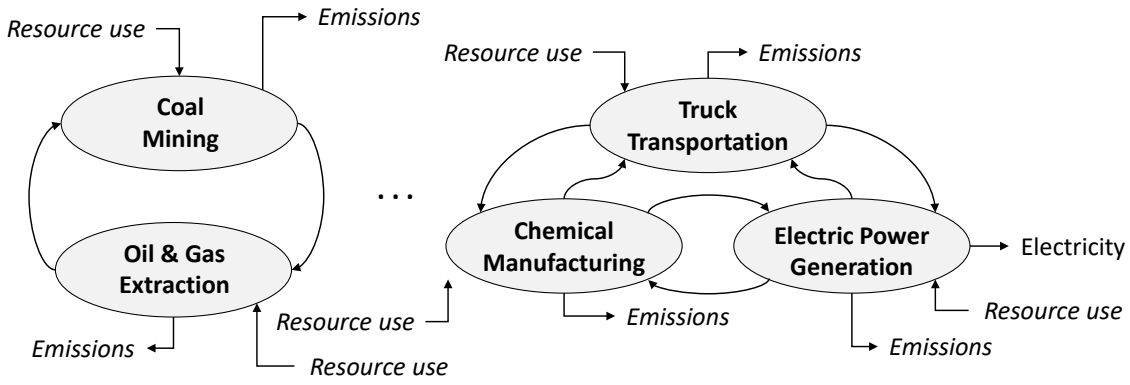

Figure 2.3: EEIO model for electricity generation. Both coal-fired and NG-fired electricity generation technologies are assigned to an electric power generation sector in the EEIO model.

represent economy sectors, commodity flows, and intervention flows, respectively. The commodity transaction between sectors in the IO model is represented by direct requirement ($\overline{A}$) matrix which consists of coefficients about the direct requirement of an input commodity to produce one dollar amount of output commodity. $\overline{A}$ matrix can be obtained from make ($\overline{V}$) and use ($\overline{U}$) matrices. $\overline{V}$ and $\overline{U}$ matrices contain data about commodity outputs from each sector and commodity inputs to each sector, respectively. For example, the aggregated electricity sector in the 2012 U.S. economy supplies 327,938 million dollars of electricity commodity while using 14,900 million dollars of coal mining commodity and 12,825 million dollars of oil and gas extraction commodity. $\overline{V}$ and$\overline{U}$ matrices are combined into the direct requirement matrix ($\overline{A}$) using $\overline{A} = \overline{U}(\overline{V}^T)^{-1}$. Thus, $\overline{A}$ has no unit.

The transaction equation of the EEIO model is formulated as follows.

$(I - \overline{A})\overline{x} = \overline{f}$,

where $\overline{A} = \begin{bmatrix} \overline{a}_{11} & \overline{a}_{12} & \cdots & \overline{a}_{1n'} \\ \overline{a}_{21} & \overline{a}_{22} & \cdots & \overline{a}_{2n'} \\ \vdots & \vdots & \ddots & \vdots \\ \overline{a}_{m'1} & \overline{a}_{m'2} & \cdots & \overline{a}_{m'n'} \end{bmatrix} = \{\overline{a}_{i'j'}\} \in \mathbb{R}^{m' \times n'}$, $\overline{x} = \begin{bmatrix} \overline{x}_1 \\ \overline{x}_2 \\ \vdots \\ \overline{x}_{n'} \end{bmatrix}$, and $\overline{f} = \begin{bmatrix} \overline{f}_1 \\ \overline{f}_2 \\ \vdots \\ \overline{f}_{m'} \end{bmatrix}$.

i''s $(= 1, 2, \cdots, m')$ and j''s $(= 1, 2, \cdots, n')$ refer to commodities and sectors. $\overline{x}$ vector represents the total commodity output (i.e., economic throughput) from each sector, j'. $\overline{x}$ vector is equal to the sum of $\overline{A}\overline{x}$ (the monetary value of every commodity consumed by sectors to produce the final demand) and $\overline{f}$ (the monetary value of final demand that is produced). That is, $\overline{x} = \overline{A}\overline{x} + \overline{f}$. Given that $\overline{f}$ is known, $\overline{x}$ is calculated by $\overline{x} = (I - \overline{A})^{-1}\overline{f}$.

The EEIO model has been developed to conduct the LCA study based on the IO model. Similarly to the process-based LCA, the intervention equation for the EEIO model is formulated as follows.

$\overline{B}\overline{x} = \overline{r}$,

where $\overline{B} = \begin{bmatrix} \overline{b}_{11} & \overline{b}_{12} & \cdots & \overline{b}_{1n'} \\ \overline{b}_{21} & \overline{b}_{22} & \cdots & \overline{b}_{2n'} \\ \vdots & \vdots & \ddots & \vdots \\ \overline{b}_{o1} & \overline{b}_{o2} & \cdots & \overline{b}_{on'} \end{bmatrix} = \{\overline{b}_{kj'}\} \in \mathbb{R}^{o \times n'}$, $\overline{x} = \begin{bmatrix} \overline{x}_1 \\ \overline{x}_2 \\ \vdots \\ \overline{x}_{n'} \end{bmatrix}$, and $\overline{r} = \begin{bmatrix} \overline{r}_1 \\ \overline{r}_2 \\ \vdots \\ \overline{r}_o \end{bmatrix}$.

$\overline{B}$ matrix is the economy scale intervention matrix that represents emissions and resource use $(k = 1, 2, \cdots, o)$ to produce one dollar amount of commodities from each sector (j'). For instance, 6.09 kg of CO_2 is emitted to produce \$1.0 amount of commodities from the electricity sector. If $\overline{B}$ matrix is unknown, it can be obtained by $\overline{B} = \overline{M}\hat{\overline{x}}$. $\overline{M}$ matrix represents total interventions from each sector (e.g., total CO_2 emissions from the electricity sector). $\overline{r}$ is calculated by $\overline{r} = \overline{B}(I - \overline{A})^{-1}\overline{f}$ and represents life cycle interventions for producing the economy scale final demand $(\overline{f})$.

Using the Q matrix, the life cycle impact indicators ($\overline{h}$) are calculated by $\overline{h} = Q\overline{r} = Q\overline{B}(I - \overline{A})^{-1}\overline{f}$. For example, the GWP for producing $1.0 of electricity in the U.S. is calculated to be 6.48 $kgCO_2eq$.

Although the EEIO model includes the entire economy of a given region as a system boundary, the model is based on the aggregated economy sectors. For example, the United States EEIO (USEEIO) model by U.S. EPA has been developed for 388 economy sectors,[39] while the United States LCI (USLCI) by NREL for the process-based LCA model contains inventory data for more than 27,000 processes.[40] Therefore, the EEIO model lacks details in data.

2.2.3 Multi-Regional Input-Output (MRIO)

Process-based LCA and EEIO models are based on average process and economy data, respectively. For example, the USEEIO model represents U.S. average economic activity data, respectively. Thus, those models do not distinguish an activity in one place with the activity in other places. If analysis for multiple regions needs to be performed, however, a multi-regional model that accounts for the regional heterogeneity must be developed. As shown in Fig. 2.4, for instance, region 1 requires more inputs from the coal mining sector for the electric power generation sector than region 2. Also, the electric power generation sector in region 1 needs an inter-regional coal input flow from the coal mining sector in region 2. Moreover, the electric power generation sector in region 1 has larger emissions but requires a smaller water resource to generate electricity than region 2. In this case, the electric power generation in region 1 has different commodity inputs and interventions from region 2. The impacts from emissions and water use in region 1 could be different from the impacts from

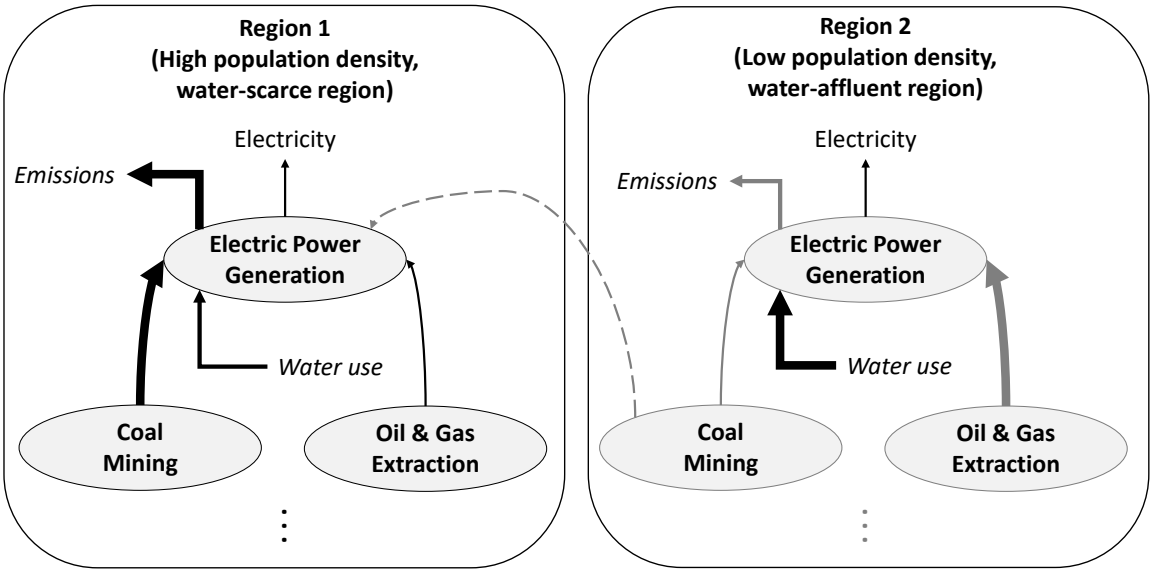

Figure 2.4: MRIO model for electricity generated in two regions.

the same amounts of emissions and water use in region 2 because population density and resource availability are not the same between the regions.[34] In this context, the multi-regional input-output (MRIO) model has been developed to address regional heterogeneity.

The transaction equation for the MRIO model can be formulated as follows.

$$(I - \overline{A}_{MR})\overline{x}_{MR} = \overline{f}_{MR},$$

$$\text{where } \overline{A}_{MR} = \begin{bmatrix} \overline{A}^{11} & \overline{A}^{12} & \cdots & \overline{A}^{1r} \\ \overline{A}^{21} & \overline{A}^{22} & \cdots & \overline{A}^{2r} \\ \vdots & \vdots & \ddots & \vdots \\ \overline{A}^{r1} & \overline{A}^{r2} & \cdots & \overline{A}^{rr} \end{bmatrix}, \overline{x}_{MR} = \begin{bmatrix} \overline{x}^{1} \\ \overline{x}^{2} \\ \vdots \\ \overline{x}^{r} \end{bmatrix}, \text{ and } \overline{f}_{MR} = \begin{bmatrix} \overline{f}^{1} \\ \overline{f}^{2} \\ \vdots \\ \overline{f}^{r} \end{bmatrix}$$

A subscript MR refers to the multi-regional matrix. Superscripts, such as $1, 2, \cdots, r$, represent each region. For example, diagonal elements of $\overline{A}_{MR}$ matrix (i.e., $\overline{A}^{11}, \overline{A}^{22}, \cdots, \overline{A}^{rr}$) represent direct requirement matrices for regions $1, 2, \cdots, r$, respectively. Non-diagonal elements of $\overline{A}_{MR}$ matrix correspond to inter-regional commodity flow matrices. For

instance, $\overline{A}^{12}$ is the matrix for commodity flows from region 1 to region 2. Similarly, $\overline{x}_{MR}$ and $\overline{f}_{MR}$ vectors are, respectively, throughput and final demand vectors for each region.

Also, the multi-regional intervention matrix can be formulated as follows.

$$\overline{B}_{MR}\overline{x}_{MR} = \overline{r}_{MR},$$

$$\text{where } \overline{B}_{MR} = \begin{bmatrix} \overline{B}^{11} & \overline{B}^{12} & \cdots & \overline{B}^{1r} \\ \overline{B}^{21} & \overline{B}^{22} & \cdots & \overline{B}^{2r} \\ \vdots & \vdots & \ddots & \vdots \\ \overline{B}^{r1} & \overline{B}^{r2} & \cdots & \overline{B}^{rr} \end{bmatrix}, \overline{x}_{MR} = \begin{bmatrix} \overline{x}^1 \\ \overline{x}^2 \\ \vdots \\ \overline{x}^r \end{bmatrix}, \text{ and } \overline{r}_{MR} = \begin{bmatrix} \overline{r}^1 \\ \overline{r}^2 \\ \vdots \\ \overline{r}^r \end{bmatrix}.$$

$\overline{B}_{MR}$ is a multi-regional intervention matrix. Diagonal elements of $\overline{B}_{MR}$ matrix correspond to intervention matrices for each region (i.e., region $1, 2, \cdots, r$).

Lastly, the LCIA characterization factor can vary with regions. For example, if region 1's water resource is more scarce than region 2 as shown in Fig. 2.4, the impacts from the same amount of water resource consumption are worse in region 1 than region 2. In such case, the characterization factor for water resource use in region 1 needs to be larger than region 2.[41] Accordingly, the resulting life cycle impact indicators ($\overline{h}_{MR}$) vary with regions as shown below.

$$Q_{MR}\overline{r}_{MR} = \overline{h}_{MR},$$

$$\text{where } Q_{MR} = \begin{bmatrix} Q^1 & 0 & \cdots & 0 \\ 0 & Q^2 & \cdots & 0 \\ \vdots & \vdots & \ddots & \vdots \\ 0 & 0 & \cdots & Q^r \end{bmatrix}, \overline{r}_{MR} = \begin{bmatrix} \overline{r}^1 \\ \overline{r}^2 \\ \vdots \\ \overline{r}^r \end{bmatrix}, \text{ and } \overline{h}_{MR} = \begin{bmatrix} \overline{h}^1 \\ \overline{h}^2 \\ \vdots \\ \overline{h}^r \end{bmatrix}.$$

2.2.4 Integrated Hybrid LCA

As shown in Table 2.2, the process-based LCA model has the opposite characteristics to the EEIO model with respect to the life cycle analysis boundary and the

details in LCI data. Integrated hybrid LCA model has been developed to account for the entire economic activities while employing detailed process data.[12] The excluded activities from the process-based LCA model are included in the hybrid LCA model by connecting corresponding economic activities from the EEIO model to the process-based model. Figure 2.5 shows one example of the hybrid LCA model for NG-fired electricity. In this example, a NG transportation process is excluded from the process-based LCA model. The corresponding economy sector in the EEIO model to the NG transportation process is pipeline transport sector. In the hybrid model, the NG transportation process is substituted by the pipeline transport sector from the EEIO model. In this sense, the hybrid LCA model accounts for the entire life cycle network while keeping the details of process data. However, since the EEIO model covers every economy activity, activities in the process-based model are overlapped by the corresponding activities in the EEIO model. As shown in Fig. 2.5, processes for NG-fired electricity generation and NG extraction & processing in the process-based model are included in sectors for electric power generation and oil & gas extraction in the EEIO model, respectively. To avoid double-counting of those activities, therefore, the EEIO model needs to be disaggregated from the process-based model. In other words, product transaction flows between processes and value chain scale intervention flows from processes need to be removed from the corresponding economy commodity transaction flows and economy scale intervention flows.

The disaggregation of direct requirement matrix ($\overline{A}$) needs to be performed for make ($\overline{V}$) and use ($\overline{U}$) matrices. For the disaggregation of $\overline{V}$ and $\overline{U}$ matrices, value chain scale technology matrix ($\underline{A}$) first needs to be separated into value chain scale make ($\underline{V}$) and use ($\underline{U}$) matrices by $\underline{A} = \underline{V}^T - \underline{U}$. In general, positive and negative

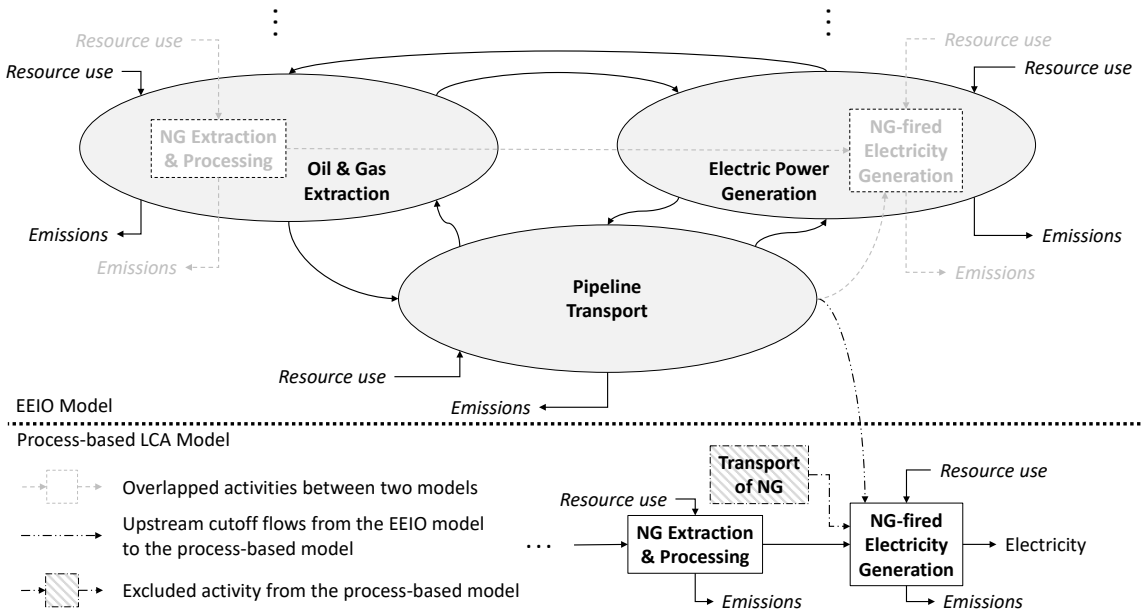

Figure 2.5: Integrated hybrid LCA model for NG-fired electricity.

elements in $\underline{A}$ matrix are assigned to $\underline{V}^T$ and $\underline{U}$ matrices, respectively. Also, the disaggregation of economy scale intervention matrix ($\overline{B}$) needs to be performed for economy scale total intervention matrix ($\overline{M}$). Disaggregation procedures for $\overline{V}$, $\overline{U}$, and $\overline{M}$ matrices are as follows.[13]

1. Construct product-commodity (P_F) and process-sector (P_P) permutation matrices by matching value chain scale products and processes with economy scale commodities and sectors, respectively, as follows.

$$P_F = \{p_{F_{i',i}}\} = \begin{cases} 1 & \text{if value chain product } i \text{ corresponds to the economy commodity } i' \\ 0 & \text{otherwise} \end{cases}$$

$$P_P = \{p_{P_{j,j'}}\} = \begin{cases} 1 & \text{if value chain process } j \text{ corresponds to the economy sector } j' \\ 0 & \text{otherwise} \end{cases}$$

2. Construct a price vector (p) for every value chain scale product to convert the physical amounts of products to the monetary amounts of commodities.

3. Perform the disaggregation of each economy scale matrix by the following equations.

$$\overline{V}^* = \overline{V} - (P_P)^T \underline{V} \hat{p} (P_F)^T$$

$$\overline{U}^* = \overline{U} - P_F \hat{p} \underline{U} P_P - \underline{X}_u P_P - P_F \hat{p} \underline{X}_d$$

$$\overline{M}^* = \overline{M} - \underline{B} P_P$$

The superscript asterisk sign indicates disaggregated economy scale matrices. $\underline{X}_u$ and $\underline{X}_d$ matrices represent the matrices for upstream cutoff flows of economy commodities to the value chain processes and downstream cutoff flows of value chain products to the economy sectors, respectively. $\underline{X}_u$ and $\underline{X}_d$ matrices have $(i' \times j)$ and $(i \times j')$ dimensions, respectively. $\underline{X}_u$ matrix has monetary units while $\underline{X}_d$ has physical units.

The disaggregated direct requirement matrix ($\overline{A}^*$) and economy scale intervention matrix ($\overline{B}^*$) are obtained by $\overline{A}^* = \overline{U}^* \{\overline{V}^{*T}\}^{-1}$ and $\overline{B}^* = \overline{M}^* \hat{\overline{x}}^*$, respectively.

Accordingly, the transaction equation for the integrated hybrid LCA model is formulated as follows.

$$\begin{bmatrix} I - \overline{A}^* & -\underline{X}_u \\ -\underline{A}_d & \underline{X} \end{bmatrix} \begin{bmatrix} \overline{s} \\ \underline{s} \end{bmatrix} = \begin{bmatrix} \overline{y} \\ y \end{bmatrix}.$$

$\overline{x}$ vector in the EEIO model can be represented by an economy scale scaling vector ($\overline{s}$). $\underline{\mathrm{X}}_u$ matrix corresponds to the matrix for upstream cutoff flows from the EEIO model to the process-based model. This upstream cutoff matrix represents economy commodity input flows to the processes. To construct $\underline{\mathrm{X}}_u$ matrix, the physical

amounts of excluded product flows from the process-based model need to be known. The monetary value of products also needs to be known since the EEIO model is based on monetary units. For example, if 0.35 t·km of NG transportation is needed to generate 1 kWh of electricity from the NG-fired electricity generation process as shown in Fig. 2.5, the monetary amount of cutoff flow for the pipeline transportation is obtained by multiplying 0.35 t·km with the price of NG transportation per t·km. Accordingly, the economy scale commodity transaction equation in the hybrid model is shown by $(I - \overline{A}^*)\overline{s} = \overline{y} + \underline{X}_u\underline{s}$. $\underline{X}_u\underline{s}$ represents the demand for upstream cutoff commodities that are needed for value chain processes.

Also, $\underline{A}_d$ matrix corresponds to the matrix for downstream cutoff flows from the process-based model to the EEIO model. The downstream flows of products from the process-based model are included in this downstream cutoff matrix. If downstream activities of the main product do not need to be included in the system boundary of LCA study (i.e., if the study is a cradle-to-gate analysis), by-product and co-product flows in the process-based model can be included in $\underline{A}_d$. To construct $\underline{A}_d$ matrix, economy sectors where downstream products are consumed need to be identified. Then, the physical amounts of downstream cutoff flows need to be normalized by economic throughput from those sectors. That is, $\underline{A}_d$ matrix is obtained by $\underline{A}_d = \underline{X}_d\hat{\overline{x}}$. Accordingly, the product transaction equation in the hybrid model is represented by $\underline{X}\underline{s} = \underline{y} + \underline{A}_d\overline{s}$. $\underline{A}_d\overline{s}$ corresponds to the demand for downstream cutoff products that are consumed by economy sectors.

In the hybrid LCA model, life cycle interventions ($\overline{\underline{r}}$) and midpoint indicators ($\overline{\underline{h}}$) are calculated by the following equations.

$$\begin{bmatrix}\overline{B}^{*} & \underline{B}\end{bmatrix}\begin{bmatrix}\overline{\underline{s}} \\ \underline{s}\end{bmatrix} = \overline{\underline{r}} \quad \text{and} \quad Q\overline{\underline{r}} = \overline{\underline{h}}.$$

Double notations on $\overline{\underline{r}}$ and $\overline{\underline{h}}$ vectors indicate multiple scales that are across economy and value chain process scales.

2.3 Data Sources and Software for LCA Studies

In this section, we introduce various public and commercial sources of LCI data and several software programs to perform the LCA study. LCI analysis, which is the second step in conducting LCA, can be very time-consuming work. Table 2.3 shows various LCI data sources. GREET (The Greenhouse Gases, Regulated Emissions, and Energy Use in Transportation Model) is a public process-based LCA model for U.S. transportation-related activities that include various types of power generation technologies.[42] However, its data are limited to transportation and energy-related activities. NREL USLCI is a public U.S. LCI database for the process-based LCA model.[40] The USLCI database covers diverse activities and includes data on upstream cutoff flows for the extension of the model to the hybrid model. Ecoinvent is a commercial LCI database for the process-based model.[43] The LCI data for various regions (mostly Europe) are available in the Ecoinvent LCI database.

With respect to IO-based LCA models such as EEIO and MRIO models, EPA has developed both EEIO and MRIO models for the U.S. The USEEIO model is a public U.S. EEIO model.[39] This model accounts for the entire U.S. economy in 2013 and includes various environmental intervention data for every economy sector. US state-level MRIO model is a public MRIO model for the 2012 U.S. economy.[33] This model

includes MRIO data for 51 states in the U.S. If a more detailed regional IO model is needed, RIMS II and IMPLAN models are commercial U.S. regional IO models.[45,46] Also, regional interventions data are available in various sources. CAIT Climate Data Explorer has U.S. state-level GHG emissions data for aggregated economy sectors.[48] National Emissions Inventory (NEI) from EPA has U.S. county-level air pollutant emissions data.[49] EnviroAtlas from EPA has U.S. watershed scale water use and nutrient emissions data.[50]

Also, various LCA software programs that use the LCI data collected from Table 2.3 are available. Table 2.4 shows several LCA software programs. OpenLCA is an open-source LCA software program. The LCI data obtained from the USLCI, Ecoinvent, and USEEIO can be directly imported to OpenLCA. SimaPro and GaBi are commercial LCA software programs. Both EIO-LCA (Economic Input-Output Life Cycle Assessment) and Eco-LCA (Ecologically-based Life Cycle Assessment) are

Table 2.3: Various sources of life cycle inventory data.

Source of data	Type of data	Ref.
LCI database for the process-based LCA model		
GREET	U.S. transportation-related process-based LCA model	42
NREL	U.S. LCI data for the process-based model	40
Ecoinvent	Commercial global LCI data for the process-based model	43
LCI database for the EEIO and MRIO models		
EPA	2013 U.S. EEIO model	39
EPA	2012 U.S. state-level MRIO model	33
BEA	U.S. make and use tables for the IO model	44
BEA RIMS II	Commercial U.S. regional IO models	45
IMPLAN	Commercial U.S. regional IO models	46
EPA	U.S. GHG emissions and sinks data for aggregated sectors	47
CAIT	U.S. state-level GHG emissions data for aggregated sectors	48
EPA NEI	U.S. county-level air pollutant emissions data for aggregated sectors	49
EPA EnviroAtlas	U.S. watershed-level water use and nutrient emissions data for aggregated sectors	50

web-based software programs for the U.S. EEIO model while the latter emphasizes the impacts on the ecosystem.

In assessing sustainability, the demand for ecosystem services can be quantified using various established LCA models. Depending on the goal and scope of sustainability assessment study, the choice of models can vary. Besides the models introduced in this section, there have been many advanced sustainability assessment methods developed as well. Most models are based on the LCA approach and mathematical formulation addressed in this section. Using those models, the demand for most provisioning and regulating services can be quantified. However, it is still challenging to quantify the demand for some ecosystem services, such as supporting and cultural services, since such data are not readily available. Moreover, most LCA models do not consider the supply of ecosystem services which also needs to be quantified in assessing sustainability. Therefore, systematic approaches and database construction to quantify the demand for ecosystem services are needed.

Table 2.4: Various LCA software programs.

Program	**Features**	**Ref.**
OpenLCA	Open-source LCA software program	[51]
SimPro	Commercial LCA software program	[52]
GaBi	Commercial LCA software program	[53]
EIO-LCA	Web-based program for the U.S. EEIO model	[54]
Eco-LCA	Web-based program for the U.S. EEIO model with emphasis to ecological impacts	[55]

Chapter 3: Food-Energy-Water Footprints of Households to Explore Consumer Behavior

Households are one of the end-use consumers for many commodities. Each household has different demographic features and consumption behaviors. Little is known about how consumption behaviors affect household environmental impacts. In this study, we assess food-energy-water footprints (FEWprints) of individual households in Columbus, Ohio, U.S.A. to investigate correlations of household FEWprints with demographics and consumption behaviors. FEWprints include carbon, energy, water, and land footprints. We collect household consumption data from grocery and restaurant receipts, utility bills, and transportation mileage records of each household. This data collection method provides high-quality household data and minimizes bias from survey participants compared to the methods employed in other similar studies. The collected consumption data are then categorized into food (meat, non-meat, and restaurant), energy (electricity, NG, ground transportation, and air transportation), and water consumption categories. The Kendall rank correlation coefficients are calculated to obtain insights about FEWprints with respect to specific demographic characteristics and consumption behaviors. For example, we identify gender differences in household consumption behaviors and FEWprints. Males tend to show larger

electricity consumption than females, and thus, they are likely to have a higher carbon footprint. On the other hand, females consume more non-meat than males and show a higher land footprint. We also investigate specific consumption trends that could mitigate household FEWprints. For instance, when households spend more on restaurant consumption than other commodities, they are likely to have lower FEWprints.

3.1 Introduction

Sustainability of human activities relies on goods and services from ecological, social, and economic systems. Social and economic activities rely on ecological benefits provided by ecosystems.[2] For example, freshwater is one of the ecosystem goods that is crucial for social and economic activities. If social and economic systems are managed by neglecting their influences on ecosystems, they may not be sustainable neither socially, economically, nor environmentally.

As shown in Fig. 3.1, environmental sustainability has mainly been addressed by calculating life cycle impact indicators. An economic dimension of environmental sustainability has been studied using sophisticated economic models such as general equilibrium and technology choice models.[6,17,56] Those studies discussed the consequences of price changes and market conditions on environmental sustainability. On the other hand, a social dimension of environmental sustainability has not yet been studied much. Although many studies focused on social indicators, such as human health and social equity-related indicators, by employing social life cycle assessment (SLCA) methodologies,[57] those studies primarily discussed the impacts of technological systems on social sustainability, not the impacts of social systems on

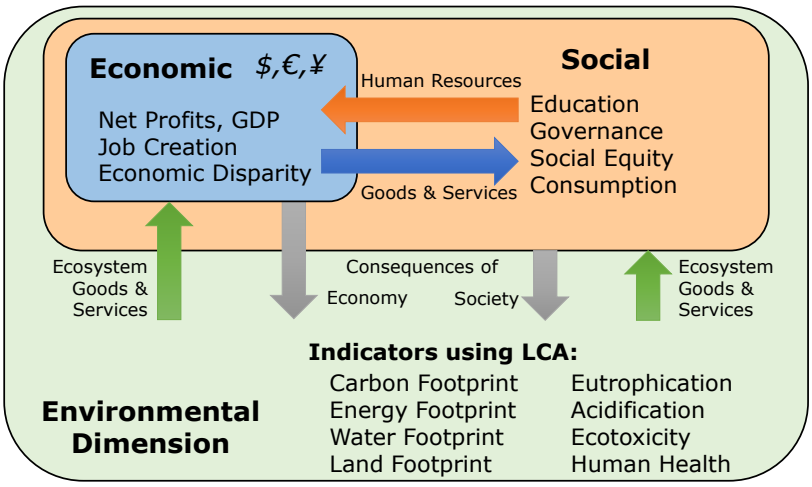

Figure 3.1: Interactions between environmental, economic, and social dimensions for environmental sustainability.[2,3]

environmental sustainability. If we do not account for social impacts on environmental sustainability, solutions from sustainability assessment may result in unexpected outcomes that are attributed to the change in social systems (e.g., human behavior change). The economic rebound effect or Jevons Paradox is one example of such an effect. Therefore, there is a need for a study to understand the consequences of social systems on environmental sustainability.

In this chapter, we focus on household consumption behaviors and their impacts on environmental sustainability. Household consumption has traditionally been conceptualized as having smaller environmental impacts than other sectors, but household consumption choices drive demand for products and services, and hence, all resources are used to create and deliver those products and services. For example, in terms of direct freshwater use in the United States (U.S.), only 1% of water withdrawals

go directly to households.[58] However, more than 20% of direct energy use is residential.[59] Therefore, more than 50% of water withdrawals are attributed to creating food and thermoelectric power that are consumed in households. The indirect impacts of household consumption are likely significant, and household consumption behaviors need to be investigated to reduce the total environmental impacts.

Households consume a variety of resources and commodities, including food, energy, and water. Hence, for comprehensive sustainability assessment, multiple indicators need to be considered to avoid shifting of burdens to other indicators. For instance, improving the energy efficiency of thermoelectric power plants may lead to an increase in water footprints. Such interactions between multiple indicators can be captured by taking account of the food, energy, and water (FEW) nexus for addressing the impact of household consumption.

Table 3.1 summarizes existing studies on the impacts of household consumption. Many such studies assessed indirect impacts on only one or a few impact indicators (mostly carbon footprint), overlooking the multiple environmental impacts associated with FEW consumption. Also, many studies did not capture the full picture of consumption at the household level, focusing mainly on food and dietary consumption. Moreover, most studies employed data obtained from public databases, such as the Consumer Expenditure Surveys of the U.S. Bureau of Labor Statistics, resulting in gross estimates of average household consumption. This approach does not assess consumption at the individual household level but relies on averages, which creates a broad picture of household consumption and its components that lacks important detail. Some studies collected data from individual households through the self-report survey to investigate actual patterns of consumption at the individual household

level. However, they collected individual household consumption data by asking respondents to report the mass of food consumed[60] or by conducting an online survey,[61] which may produce less accurate and low-quality data than observed measures (e.g., purchase data).[62] Self-report and self-selection bias could be associated with such self-report survey methods.[61]

In this work, we collect high-quality FEW consumption data at the individual household level to investigate FEW footprints (FEWprints) of households in Columbus, Ohio, U.S.A. The data are submitted by individual households and include food receipts from grocery stores and restaurants; utility bills including electricity, natural gas, and water; and transportation records by passenger vehicles and public transportation systems. This data collection method is employed to minimize bias from the survey participants compared to the other self-report survey methods.

Table 3.1: Studies on the environmental impacts of household consumption. †FEW: food, energy, and water; CF: carbon footprint; EF: energy footprint; WF: water footprint; LF: land footprint; AP: Acidification potential; EP: eutrophication potential. ‡The sample size (N) represents the number of households who completed the survey.

References	**Environmental sustainability indicators†**	**Household consumption items**	**Household demographics**	**Household data sources‡**
Tilman and Clark, 2014[63]	CF	Food	N	Multiple studies
Poore and Nemecek, 2018[64]	CF, WF, LF, AP, EP	Food	N	Multiple studies
Weber and Matthews, 2008[65]	CF	Multiple commodities	Y	Public data
Druckman and Jackson, 2009[66]	CF	Multiple commodities	Y	Public data
Jones and Kammen, 2011[67]	CF	Multiple commodities	Y	Public data
Long et al., 2019[68]	CF	Multiple commodities	N	Public data
Bozeman et al., 2020[69]	CF, WF, LF	Food	Y	Public data
Carlsson-Kanyama et al., 2003[70]	EF	Food	Y	Survey (N = 10)
Graham et al., 2013[61]	CF	Energy-related	Y	Survey (N = 2,168)
Kennedy et al., 2014[71]	CF	Energy-related	Y	Survey (N = 1,066)
Song et al., 2015[60]	CF, WF, LF	Food	Y	Survey (N = 12,850)
Wa'el A et al., 2017[72]	FEW demand, waste	FEW commodities	Y	Survey (N = 419)
Mackie and Wemhoff, 2020[73]	CF	Food	N	Survey (N = 4,826)
This study	CF, EF, WF, LF	FEW commodities	Y	Survey (N = 24)

To calculate the household FEWprints, the U.S. Environmentally-Extended Input-Output (USEEIO) model that accounts for the entire U.S. economy as the system boundary is employed.[39] FEWprints represent various environmental impact indicators associated with FEW consumption. In this study, carbon, energy, water, and land footprints (CF, EF, WF, and LF) at the household level are quantified.

Household consumption behaviors and their associated FEWprints could vary across demographic characteristics. Also, to address a social dimension of environmental sustainability, it is important to understand how social variables are correlated to environmental indicators. Many environmental sustainability studies lack consideration of social aspects. In this work, we investigate variation in FEW consumption and FEWprints by demographic variables, such as household size; the number of children, males and females; household income; house area (square footage); and the number of vehicles in each household, offering a comparison to previous findings of demographic differences in consumption based on public survey data. We also investigate correlations between specific consumption behaviors (e.g., meat consumption) and FEWprints. This can suggest potential behavior changes to reduce overall household impacts and improve the sustainability of household activities.

This work is a comprehensive study that investigates the life cycle impacts of household activities to address a social domain as well as the nexus of FEW systems. This work could be extended to account for social (human behavior) consequences of sustainability assessment by examining behavioral feedback from households. The challenges and limitations of this work are also addressed.

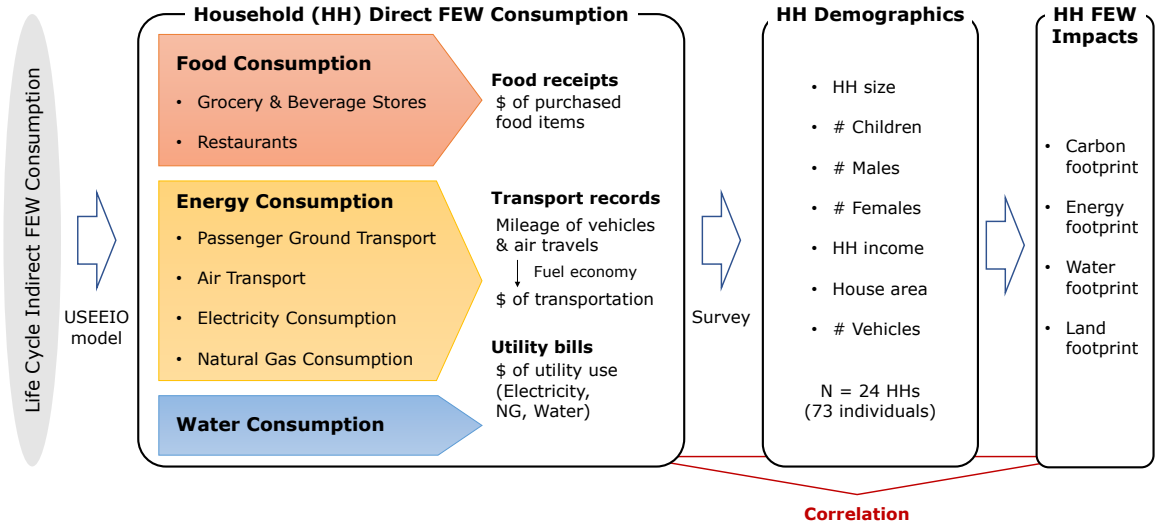

Figure 3.2: The scope of this work to investigate correlations between household consumption behaviors, demographics, and FEW impacts.

3.2 Methods

Figure 3.2 shows the scope of this study. Household demographics and individual households' FEW consumption data are collected from households in Columbus, OH. Life cycle FEW impacts, which include CF, EF, WF, and LF, at the individual household level are calculated by employing the USEEIO model. Then, correlation coefficients between household demographic variables, household FEW consumption behaviors, and household FEWprints are investigated using a statistical approach to get insights about the impacts of social systems on environmental sustainability. Data for household demographics, consumption, and FEWprints are summarized in Table 3.2.

3.2.1 Household Consumption Data Collection

The target population was single family households in the greater Columbus, OH area. For households to be eligible for the study, they had to: (1) pay their own electric/water/gas bills (i.e., home not master-metered); (2) agree to participate in all study activities for 4 or 8 weeks; and (3) have a resident over the age of 18 agree to enroll.

Recruitment Procedures

We used two approaches to recruit, including door-to-door canvassing and online advertising. Trained research assistants conducted door-to-door canvassing in Spring and Summer 2018. During the same time, online advertising took place by posting ads on Craigslist, which instructed interested households to call or email the research team, who fielded inquiries and assessed eligibility criteria via phone or email. For those that met eligibility criteria, we scheduled times when the same trained research

Table 3.2: Data for household demographics, FEW consumption, FEW footprints in this study.

HH ID	Household Demographics							Household FEW Consumption ($)								Household FEW Footprints			
	HH Size	# Chld	# Male	# Female	HH Income ($)	House Area (ft^2)	# Vehicle	Meat	Non-meat	Rest.	Elec.	NG	Ground Tp	Air Tp	Water	Carbon ($kgCO_2eq$)	Energy (GJ)	Water (m^3)	Land (m^2)
1	1	0	0	1	50,000	1550	1	62	79	56	54	74	25	0	27	1254	19	74	1516
2	2	0	1	1	343,000	2478	4	57	147	185	116	127	356	117	53	1747	28	126	970
3	2	0	0	2	33,000	250	1	113	133	85	33	61	87	0	28	1162	17	88	1874
4	4	2	1	3	190,000	1500	2	101	235	0	72	80	288	0	52	1829	29	145	1168
5	2	0	1	1	66,000	850	1	101	214	25	156	45	184	109	36	1894	25	137	1836
6	3	1	1	2	160,000	1300	1	283	315	432	54	45	135	0	65	1771	21	203	4635
7	1	0	1	0	62,649	980	1	105	231	295	77	44	111	0	32	1399	18	155	2062
8	4	2	3	1	175,000	3200	2	115	238	0	212	72	112	0	66	2544	32	191	1880
9	5	3	1	4	250,000	2300	2	189	687	287	109	65	194	0	56	2516	34	290	3043
10	2	0	1	1	140,000	1350	2	15	123	347	64	60	245	1,399	46	2744	54	102	1098
11	5	1	3	2	186,000	2147	1	146	124	36	61	57	25	1,926	36	3145	59	116	2666
12	5	3	1	4	117,000	1200	2	86	241	80	103	32	439	0	51	1485	22	134	2004
13	4	2	1	3	108,000	1700	2	170	352	204	84	73	349	0	68	2101	31	210	2438
14	1	0	1	0	21,313	720	2	55	155	88	61	43	92	0	23	1029	14	83	1246
15	1	0	0	1	0	1100	1	0	183	89	26	51	213	0	31	859	16	82	609
16	2	0	1	1	40,000	650	1	25	77	43	41	49	93	0	34	826	13	57	420
17	4	2	1	3	180,000	1600	2	86	259	374	74	63	321	99	48	1847	29	155	1837
18	2	0	1	1	55,000	1276	2	10	97	72	122	34	164	0	59	1209	16	109	447
19	4	3	2	2	43,000	1300	2	25	116	76	169	38	205	0	102	1647	21	127	545
20	3	1	2	1	255,000	1650	2	105	121	631	164	39	83	0	45	1839	22	159	1261
21	6	4	4	2	85,000	1175	1	226	588	217	133	37	180	0	113	2236	26	298	2849
22	2	0	1	1	50,000	1800	3	166	339	0	63	55	200	0	46	1539	22	189	1990
23	6	3	2	4	125,000	1300	2	127	331	0	91	72	118	0	64	1874	26	177	2049
24	2	0	1	1	88,000	1600	2	109	143	0	73	79	266	0	54	1689	27	111	1615

assistants who canvassed would go to the interested household to meet with a household member to enroll them and provide study materials.

Remind Remind is a cloud-based service that allows real-time, anonymous two-way communication via the Remind mobile application (app), text message, or email. The research team used Remind to: (1) enroll participants in the study; (2) receive electronic copies of food receipts and utility bills; (3) send transportation diary prompts and baseline demographic survey URLs; and (4) deliver submission reminders and incentives. To enroll, participants entered a username of their choice, along with a phone number or email, into the app on the research assistant's phone, thus adding themselves to the study's "group". Participants could opt to receive communications and submit materials to the study team via the Remind app (participants could download to their mobile phones if desired), text, and/or email. Participants could also opt to complete study procedures using paper/pencil by mailing in study materials.

Measures

Households provided FEW consumption data for at least four weeks via submission of grocery receipts, restaurant receipts, and utility bills for electricity, gas, and water usage. They completed weekly transportation diaries and a one-time baseline survey to assess basic demographic information.

Baseline Survey An online baseline survey was hosted on Qualtrics and took approximately 5-10 minutes to complete. We collected participants' demographic information including household size (the number of household members); the number

of children, males, and females; household income; house area (in square feet); and vehicle mileage and fuel efficiency.

Utility Bills Households submitted the most recent copies of their electric, water, and gas utility bills on the day they were recruited. They were asked to submit a second batch of utility bills by their last week of study involvement. For each utility bill, undergraduate research assistants coded utility supplier, billing period, usage (i.e., kWh and CCF), and cost. Total charges are divided by the number of days included in the bills to represent four weeks of utility expenditures.

Food Receipts Households were asked to submit all grocery and restaurant receipts received from every household member each week they participated in the study. For each item on a grocery store receipt, undergraduate research assistants coded item name, item quantity, item cost, and product category code using the North American Industry Classification System (NAICS). For each restaurant receipt, research assistants coded restaurant name, total receipt cost, and type of restaurant using NAICS category codes (i.e., limited-service or full-service restaurants). Restaurant receipts were not coded at an itemized level given the general lack of itemized information and ambiguous names of dishes on these receipts.

Transportation Diaries Households completed a transportation diary (5 minutes) weekly that assessed mileage of all household vehicles as well as the time and distance by which each household member travelled using different modes of transportation (e.g., bus, bike, airplane) over the prior week.

To calculate environmental impacts, we used the USEEIO model. This required transportation data to be in a monetary unit. The fuel economy of participants' vehicles is investigated, and expenditures for passenger ground transportation are estimated using the 2013 retail gasoline price in Ohio.[74] The 2013 price data is used since the USEEIO model calculates the environmental impacts of commodities in 2013 U.S. dollars.[39] For bus transportation, assuming the average passengers per bus are 11.2 persons,[75] bus transportation expenditures are estimated using the average CNG bus fuel economy[76] and the average CNG retail price.[77] Also, expenditures for air and rail transportation are estimated using the 2013 average passenger revenue for air carrier service and commuter rail, respectively.[78] As shown in Fig. 3.2, transportation, electricity consumption, and natural gas consumption are categorized into energy-related household consumption.

Participants

A total of 109 households agreed to participate in the study. Of these households, 37 completed at least the baseline survey and first submission of electric, water, and natural gas utility bills. 24 households (made up of 73 total individuals) completed all the study materials and submitted four weeks of FEW consumption data. Household demographic information is summarized in Table 3.2.

Participant Compensation Participants were sent a $5 e-gift certificate link for completing the baseline survey. E-gift certificate links were administered via Tango Card, which allowed participants to select e-gift certificates from among dozens of retailers, or donate to a range of charities. In addition to baseline survey compensation, households were awarded "points" for each submission of a utility bill, food receipt,

and transportation diary, with the amount of points each submission was worth increasing over time to promote long-term participation. Each point corresponded to $1 in e-gift certificates, and ongoing point totals were shared with participants in their weekly reminder messages. Participants were sent incentive links matching their point totals at the end of the study; those who dropped out were also sent e-gift certificates matching their point totals.

3.2.2 Environmental Sustainability Assessment

The USEEIO model is employed to calculate FEWprints of individual households' FEW consumption.[39] The model is based on the 2013 U.S. average economic transaction and environmental data for 385 economy sectors, which include 43 food-related sectors (11 farm foods, 29 manufactured foods, and 3 food service places), 3 utility sectors (electricity, water, and natural gas), and 3 transportation sectors (passenger ground, air, and rail).

For household food consumption, grocery food expenditures are categorized into their relevant food-related economy sectors. If any grocery expenditures are ambiguous to categorize into these sectors, they are categorized into "311990 all other food manufacturing" sector. Restaurant expenditures are categorized into three sectors of either "722211 full-service restaurants," "722211 limited-service restaurants," or "722a00 all other food and drinking places." In this study, the 43 food-related sectors are further classified into 3 aggregated categories: meat, non-meat, and restaurant. Meat and non-meat consumption represent food-at-home (FAH) consumption while restaurant consumption corresponds to food-away-from-home (FAFH) consumption.

The USEEIO model includes 43 food-related economy sectors: 11 types of farm foods, 29 types of manufactured foods, and 3 types of food services and places.[39] In this study, they are further classified into 3 aggregated food categories as follows.

1. Meat category: 12 animal meat-related food sectors
    - 112120 dairy cattle and milk production
    - 1121a0 beef cattle ranching and farming, including feedlots and dual-purpose ranching and farming
    - 112300 poultry and egg production
    - 112a00 animal production, except cattle and poultry and eggs
    - 114000 fishing, hunting and trapping
    - 311513 cheese manufacturing
    - 311514 dry, condensed, and evaporated dairy product manufacturing
    - 31151a fluid milk and butter manufacturing
    - 311520 ice cream and frozen dessert manufacturing
    - 311615 poultry processing
    - 31161a animal (except poultry) slaughtering, rendering, and processing
    - 311700 seafood product preparation and packaging
2. Non-meat category: 28 non-meat-related food sectors
    - 1111a0 oilseed farming
    - 1111b0 grain farming

- 111200 vegetable and melon farming
- 111300 fruit and tree nut farming
- 111400 greenhouse, nursery, and floriculture production
- 111900 other crop farming
- 311111 dog and cat food manufacturing
- 311119 other animal food manufacturing
- 311210 flour milling and malt manufacturing
- 311221 wet corn milling
- 311225 fats and oils refining and blending
- 31122a soybean and other oilseed processing
- 311230 breakfast cereal manufacturing
- 311300 sugar and confectionery product manufacturing
- 311410 frozen food manufacturing
- 311420 fruit and vegetable canning, pickling, and drying
- 311810 bread and bakery product manufacturing
- 3118a0 cookie, cracker, pasta, and tortilla manufacturing
- 311910 snack food manufacturing
- 311920 coffee and tea manufacturing
- 311930 flavoring syrup and concentrate manufacturing
- 311940 seasoning and dressing manufacturing
- 311990 all other food manufacturing

- 312110 soft drink and ice manufacturing
- 312120 breweries
- 312130 wineries
- 312140 distilleries
- 312200 tobacco product manufacturing

3. Restaurant category: 3 food services and drinking places sectors

- 722110 full-service restaurants
- 722211 limited-service restaurants
- 722a00 all other food and drinking places

Some food expenditures cannot be entirely either meat or non-meat. For example, "311111 dog and cat food manufacturing" and "311990 all other food manufacturing" sectors include both non-meat and meat foods. These sectors only account for 1.39–1.50% of household impacts from food consumption. In this study, we assume these sectors are classified into the non-meat category for the simplicity of analysis.

To account for supporting activities at grocery stores, such as labor and equipment use, we assign total grocery expenditures into the "445000 food and beverage stores" sector. This sector includes the U.S. average farming and food manufacturing activities that are consumed in grocery stores as well as supporting activities in grocery stores. In this study, farming and food manufacturing activities are taken into account by the farming and food manufacturing sectors. To avoid double-counting of these farming and food manufacturing activities, we exclude the impacts of farming and food manufacturing activities from the sector of food and beverage stores.

Accordingly, the sector of food and beverage stores only includes grocery store supporting activities. The impacts from this sector are then allocated between meat and non-meat categories based on the proportion of meat and non-meat expenditures, respectively.

Life cycle impacts for the consumption of the i-th category (h_i) are calculated by the USEEIO model using Equation 3.1.

$$h_i = QB(I - A)^{-1} f_i, \tag{3.1}$$

where I and A are identity matrix and direct requirement matrix, respectively. $(I - A)^{-1}$ is called the Leontief inverse and represents economic multipliers (coefficients) for f_i, a final demand vector for the i-th category. B is intervention matrix, and $B(I - A)^{-1}$ corresponds to life cycle intervention coefficients for f_i. Q is life cycle impact characterization factor matrix, and $QB(I-A)^{-1}$ refers to life cycle impact coefficients for f_i. The life cycle impact coefficients used in this study are available online.[79] Finally, h_i represents life cycle impacts for f_i. For instance, if i is meat category, f_i is meat consumption in a monetary unit, and h_i corresponds to FEWprints for meat consumption.

The USEEIO model is based on economic goods and services in the producer's price, which excludes trade margins by wholesalers and retailers. Household consumption expenditures include those trade margins. In this study, we assume household consumption expenditures to be the demand for goods and services in the producer's price to investigate household impacts using the USEEIO model. Therefore, the household impacts in this work may slightly be overestimated.

Since the USEEIO model is based on the U.S. average economic activities, we assume the U.S. average supply chains for household FEW consumption in Columbus,

Ohio. To perform a region-specific sustainability assessment, a region-specific LCA model and supply chain data to Columbus, Ohio is needed, which is not readily available at this point.

3.2.3 Correlation Coefficient

To understand how social systems are correlated with environmental sustainability, we investigate correlation coefficients between household demographic variables, household FEW consumption (expenditures), and household FEWprints. In this study, we do not have a large sample size due to challenges in collecting many household survey data. Therefore, Kendall's rank correlation method is employed to calculate correlation coefficients for the small sample (N = 24). The Kendall τ coefficient between two variables x and y is calculated by Equation 3.2.

$$\tau = \frac{n_c - n_d}{\frac{1}{2}n(n-1)}, \tag{3.2}$$

where n_c and n_d represent the total number of concordant pairs and the total number of discordant pairs, respectively. When $x_j < x_k$, if a pair of (x_j, x_k) and (y_j, y_k) agrees both $x_j < x_k$ and $y_j < y_k$, it is a concordant pair. Otherwise, it is a discordant pair. Also, n is the sample size, which corresponds to the number of each variable x and y. For example, if correlations between meat consumption (x) and carbon footprint (y) of 24 households are calculated, all of the n, number of x, and number of y are 24. When τ is positive or negative, there is a positive or negative correlation between x and y, respectively. If $\tau = 1$ or 0, there is perfect correlation or no correlation, respectively.

When we investigate correlations between household FEW consumption and FEWprints, the consumption and FEWprint variables are normalized by the total consumption of each household. This is because each household has a different scale of consumption, and FEWprints depend primarily on the scale of consumption. This makes it difficult to investigate the correlations between household consumption and impacts. Therefore, normalized household consumption and normalized FEWprints are calculated as follows:

$$\textit{HH consumption trend}_i = \frac{f_i}{\Sigma_i f_i}, \tag{3.3}$$

$$\textit{HH FEWprint intensities} = \frac{\Sigma_i h_i}{\Sigma_i f_i}, \tag{3.4}$$

where i is each category of FEW commodities (i.e., meat, non-meat, restaurant, electricity, NG, ground transportation, air transportation, and water). A denominator of both equations ($\Sigma_i f_i$) represents the total consumption of each household. The normalized household consumption of the i-th commodity in Equation 3.3 corresponds to the household consumption fraction of the i-th commodity over the total household consumption. These consumption fractions can represent household consumption trends with respect to the i-th commodity if we assume a fixed household budget. For example, one household may have 20% of meat, 30% of non-meat, 30% of electricity, 10% of NG, and 10% of water consumption trends while another household may show 10% of meat, 40% of non-meat, 20% of electricity, 20% of NG, and 10% of water. These two households show different consumption trends from each other. A numerator in Equation 3.4 ($\Sigma_i h_i$) corresponds to FEWprints of each household, and the normalized FEWprints represent FEWprint intensities of each household. For instance, carbon footprint intensity has a unit of CO_2eq/\$. We could obtain insights

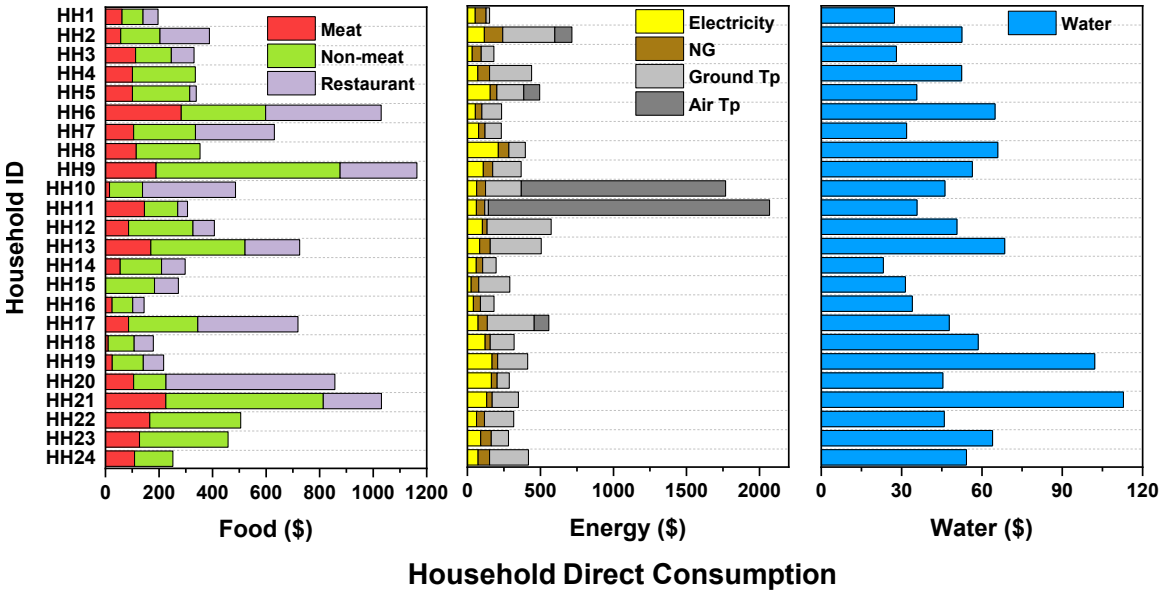

Figure 3.3: Direct FEW consumption (expenditures) of each individual household in Columbus, Ohio, U.S.A.

about the FEW impacts with respect to specific consumption trends within the fixed household budget by investigating the correlations between consumption behavior trends and FEWprint intensities.

3.3 Results and Discussions

3.3.1 Household FEW Consumption and Footprints

Figure 3.3 shows direct FEW consumption (expenditures) of each household in Columbus, Ohio. Each household shows different consumption patterns. For example, some households (IDs 4, 5, 8, 22, 23, and 24) consume mainly non-meat food commodities. Some households (IDs 4, 8, 22, 23, and 24) consume their foods at restaurants less often compared to the other households.

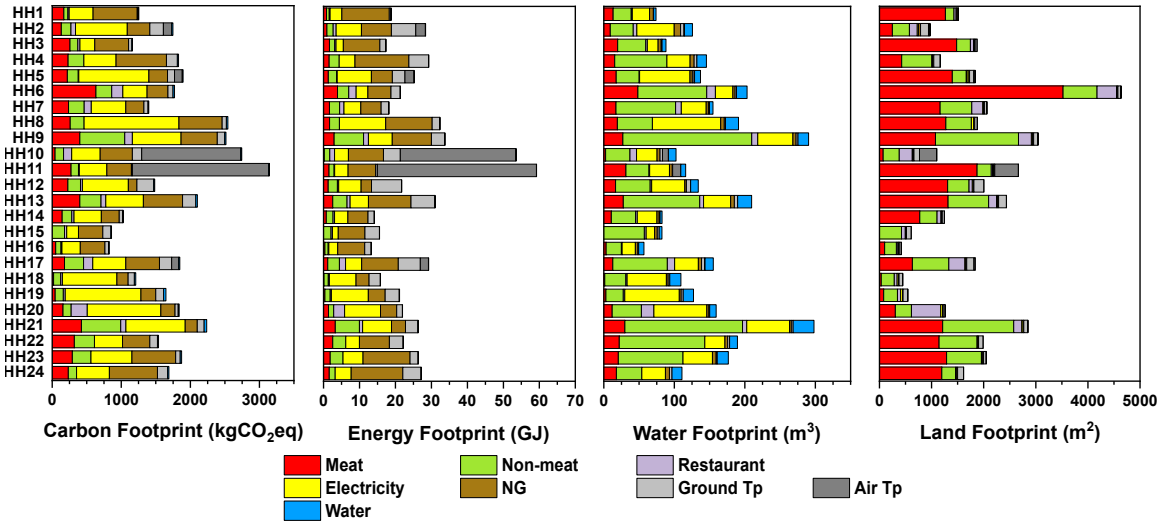

Figure 3.4: Household FEW footprints at the individual household level. Electricity and NG consumption contributes significantly to both carbon and energy footprints. Non-meat and meat consumption is dominant for water and land footprints, respectively.

Figure 3.4 exhibits household FEWprints at the individual household level. The impacts are calculated based on the household direct FEW consumption data using the USEEIO model. Energy-related consumption (electricity and NG) is dominant for carbon and energy footprints. Household electricity and NG consumption account for 36.1% and 26.6% of the total carbon footprint on average, respectively. Also, 23.3% and 38.6% of the total energy footprint are attributed to electricity and NG consumption, respectively. The entire food consumption of households only accounts for 26.4% of the total carbon footprint and 17.8% of the total energy footprint. The results imply that reducing electricity and NG consumption could be the most effective consumption behavior change to mitigate carbon and energy footprints.

When any household members travel very long distances by airplane, air transportation contributes significantly to the carbon and energy footprints as well. Among

the participants, five households (IDs 2, 5, 10, 11, and 17) traveled by air, and only two households (IDs 10 and 11) traveled more than 3,000 miles during the study period. For those two households, air transportation activities are responsible for 52.2–62.7% and 60.0–74.7% of their carbon and energy footprints, respectively.

Household food consumption is the largest contributor to water and land footprints. Specifically, non-meat consumption accounts for 42.6% of the water footprint while meat consumption is responsible for 57.5% of the land footprint on average as depicted in Fig. 3.4. According to the USEEIO model,[39] a sector for sugarcane and sugar beet farming (NAICS: 111900) has the highest water consumption intensity (3.67 m^3/\$) among the food-related sectors, followed by sectors for fresh vegetable farming (NAICS: 111200) and corn farming (NAICS: 1111b0). Also, sectors for cattle ranches (NAICS: 1121a0) and packaged meat manufacturing (NAICS: 31161a) show higher land-use intensities than other food sectors. Therefore, there is a trade-off with respect to water and land footprints depending on whether household food consumption leans toward meat or non-meat diets.

3.3.2 Correlation Between Variables

As mentioned above, every household has a different consumption pattern. Accordingly, they show different FEWprints. The differences are attributed to differences in household consumption patterns and demographic features. To understand the relation between a social dimension (household behaviors) and an environmental dimension (FEWprints), correlations between demographics, consumption patterns, and FEWprints are investigated. In this section, we discuss the Kendall rank correlation coefficients between variables of the demographics, consumption, and FEWprints.

The detailed correlation results including bivariate scatter plots and correlation coefficient values are included in Section 3.3.2.

Correlation Between Household Demographic Variables

Figure 3.5 shows the Kendall rank correlation coefficients (τ) between household demographic variables. Overall, many demographic variables are positively correlated with each other. For instance, household size exhibits strong positive correlations with the number of children, males, and females. Household income, household area, and the number of vehicles are also strongly positively correlated with each other. However, both house area and the number of vehicles are not strongly correlated with variables such as household size, the number of children, males, and females. This indicates that larger households do not necessarily have larger house areas and more vehicles.

Correlations Between Household Demographics and FEW Consumption

Figure 3.6a shows the Kendall rank correlation coefficients (τ) between household demographics and household FEW consumption. Demographic variables such as household size and the number of children, males, and females are positively correlated with FAH (meat and non-meat) and utility consumption variables excluding NG consumption. NG consumption is not significantly correlated with those demographic variables since it does not rely on household size much. NG consumption is more dependent on the house area because the primary use of NG is for the heating of the house. In 2015, more than 70% of household heating systems in the U.S. Midwest employ NG as a main fuel.[80] Governmental survey data for households in the U.S. Midwest also shows the same trends as the results indicated in this study.[80]

Figure 3.5: Kendall rank correlation coefficients between household demographic variables. Larger and darker circles represent greater correlations.

The number of children is especially positively correlated with water consumption. Also, the number of males in the household has a stronger association with electricity and water consumption than females. On the other hand, the number of females is more dependent on non-meat consumption than males. The results imply that males tend to consume more electricity and water than females while females tend to consume more non-meat than males. According to the previous studies, gender differences in energy consumption vary across countries.[81] In the U.S., the studies showed that females have higher pro-environmental behaviors than males.[82,83] Also, the other studies that employed public survey data presented that females are likely to consume more non-meat than males.[84]

Household income is positively correlated with many FEW consumption variables, particularly with electricity consumption, which aligns with the governmental survey

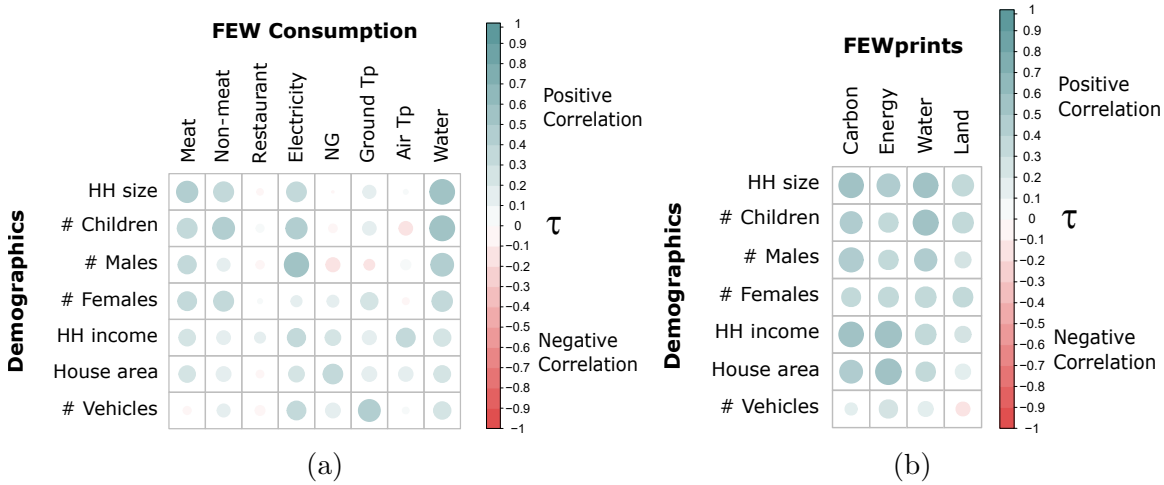

Figure 3.6: Kendall rank correlation coefficients between household demographics and **(a)** household FEW consumption or **(b)** household FEW footprints. Larger and darker circles represent greater correlations. Males tend to have higher carbon and water footprints than females because males consume more electricity. Females tend to have a higher land footprint than males because females consume more non-meat.

results.[80] The number of vehicles is also positively correlated with ground transportation services.

Correlations Between Household Demographics and FEWprints

The Kendall rank correlation coefficients between household demographics and their FEWprints are shown in Fig. 3.6b. Many correlation coefficients between demographic variables and FEWprints are positive. The number of children is strongly positively correlated with water footprint. Also, the number of males shows a stronger positive correlation with carbon footprint than females. This is because males tend to consume more electricity than females as discussed in the previous section. Electricity consumption is the largest contributor to the carbon footprint for many households as shown in Fig. 3.4. The number of females, on the other hand, exhibits a stronger

positive correlation with land footprint than males. As discussed in the previous section, females tend to consume more non-meat than males. Non-meat consumption is the second largest contributor to the land footprint for the households in this study. These results imply that males have a higher carbon footprint than females while females have a larger land footprint than males.

Carbon and energy footprints are positively correlated with household income and house area. As discussed in the previous section, households with larger house areas tend to consume more NG for the heating of the house, and therefore, they have higher carbon and energy footprints. The number of vehicles in each household does not show strong correlations with any of the FEWprints. Figure 3.6a shows that households who own more vehicles tend to use ground transportation services more frequently. However, ground transportation services do not contribute much to any of the FEWprints in this study as shown in Fig. 3.4.

Correlations Between Household FEW Consumption Trends and FEWprint Intensities

In the previous sections, we investigated the dependence of household FEW consumption behaviors and FEWprints on household demographics. To understand the impacts of social behaviors on environmental sustainability, we also need to study how household FEWprints are correlated with consumption behaviors. Figure 3.7a exhibits the Kendall rank correlation coefficients between household FEW consumption trends and FEWprint intensities. As described in Section 3.2.3, correlations between household FEW consumption and FEWprints are difficult to investigate because FEWprints highly depend on the scale of household consumption. Therefore,

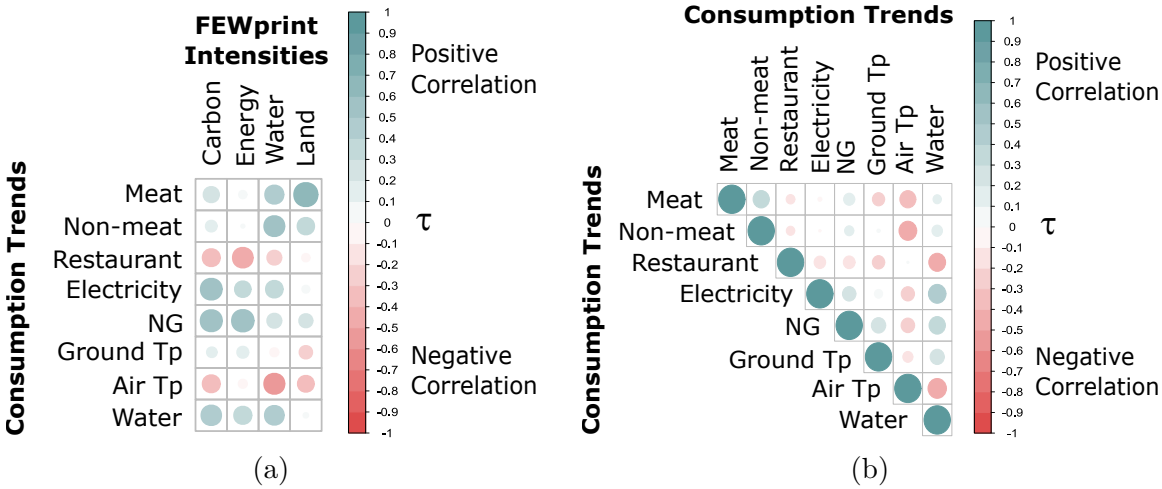

Figure 3.7: Kendall rank correlation coefficients **(a)** between household FEW consumption trends and household FEW footprint intensities and **(b)** between each household FEW consumption trend. Larger and darker circles represent greater correlations. When households spend more on restaurant consumption, lower carbon and energy footprints are expected because they are likely to spend less on other commodities at home.

household FEW consumption and FEWprints are normalized by total household consumption to compare household consumption trends with FEWprint intensities.

With respect to meat and non-meat diets, when households tend to spend more on meat, a higher land footprint is expected. This is because most meat items (e.g., a sector for cattle ranches) require huge land areas. On the other hand, a slightly higher water footprint is expected for households who spend more on non-meat. Non-meat items are identified as the largest contributor to the water footprint as shown in Fig. 3.4. Carbon and energy footprints are not affected much by types of FAH diets (meat or non-meat diets).

If households spend more on restaurants, they are likely to have lower carbon and energy footprints. This could be because FAFH consumption has smaller FEWprint

intensities than FAH consumption. According to the previous study, the carbon footprint intensity (CO_2eq/\$) of FAFH consumption is only half of that of FAH consumption.[73] The study also compared the carbon footprint intensity of FAFH consumption with that of FAH consumption in a unit of CO_2eq/kcal. In that case, the intensity of FAFH (1.26 gCO_2eq/kcal) is slightly smaller than that of FAH (1.32 gCO_2eq/kcal). Also, restaurant consumption trend is negatively correlated with the consumption trends of other FEW commodities as indicated in Fig. 3.7b. This implies that households spend less on other commodities when they spend more on restaurants. This could be attributed to the fact that households with high FAFH consumption do not cook their meals at home much. For instance, more FAFH consumption leads to fewer NG consumption due to less NG use for FAH meal preparation. NG consumption is one of the most significant contributors to the carbon and energy footprints. Therefore, lower carbon and energy footprints are expected from more FAFH consumption.

Electricity and NG consumption trends show positive correlations with carbon and energy footprint intensities. As shown in Fig. 3.4, electricity and NG are responsible for 34.8% and 24.7% of the carbon footprint, respectively. They also account for 23.4% and 35.3% of the energy footprint, respectively. Therefore, households need to spend less on electricity and NG to mitigate their carbon and energy footprints.

Ground transportation services are not likely to affect any FEWprints much since they are not large contributors to the footprints. However, when households spend more on air transportation, their carbon, water, and land footprint intensities become lower. This is because more air travel is correlated with less consumption of other FEW commodities as shown in Fig. 3.7b. This implies that households who traveled by air consume fewer FEW commodities at home than other households with no air

travel. In this study, we did not collect data for utility consumption outside the home (e.g., utility consumption at hotels). If we account for more comprehensive household FEW consumption data, we could obtain better insights about the air travel behavior with respect to the impacts.

Also, households with larger water consumption are likely to show higher carbon, energy, and water footprints. This is not because water consumption has large footprint intensities, but because water consumption trend is positively correlated with electricity consumption trend as shown in Fig. 3.7b. In other words, households with higher water consumption tend to consume more electricity. Electricity consumption has huge carbon, energy, and water footprints as indicated in Fig. 3.4.

Detailed Correlation Results

Additional statistical results including bivariate scatter plots with a fitted line and correlation coefficient values are shown in Figs. 3.8–3.10.

3.4 Conclusions

In this study, we assessed FEWprints at the individual household level by employing a realistic household data collection method. We collected grocery and restaurant receipts, utility bills, and transportation mileage records to obtain individual households' FEW consumption data. This data collection method could provide a better picture of household consumption compared to the other studies, which employed public databases or self-report survey methods. We also collected household demographic data and investigated the Kendall rank correlation coefficients between demographics, consumption behaviors, and FEWprints to understand how social systems (human behaviors) could affect environmental sustainability.

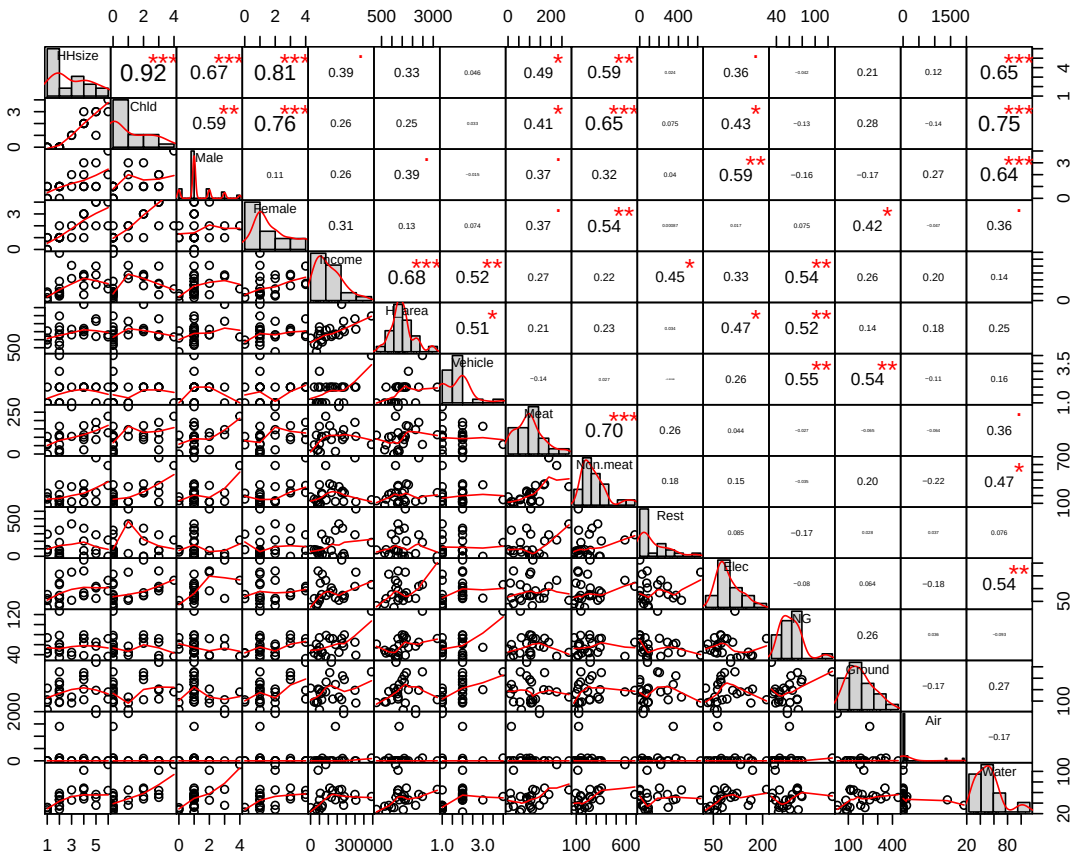

Figure 3.8: Bivariate scatter plots with a fitted line and the Kendall correlation coefficients between household demographics and FEW consumption.

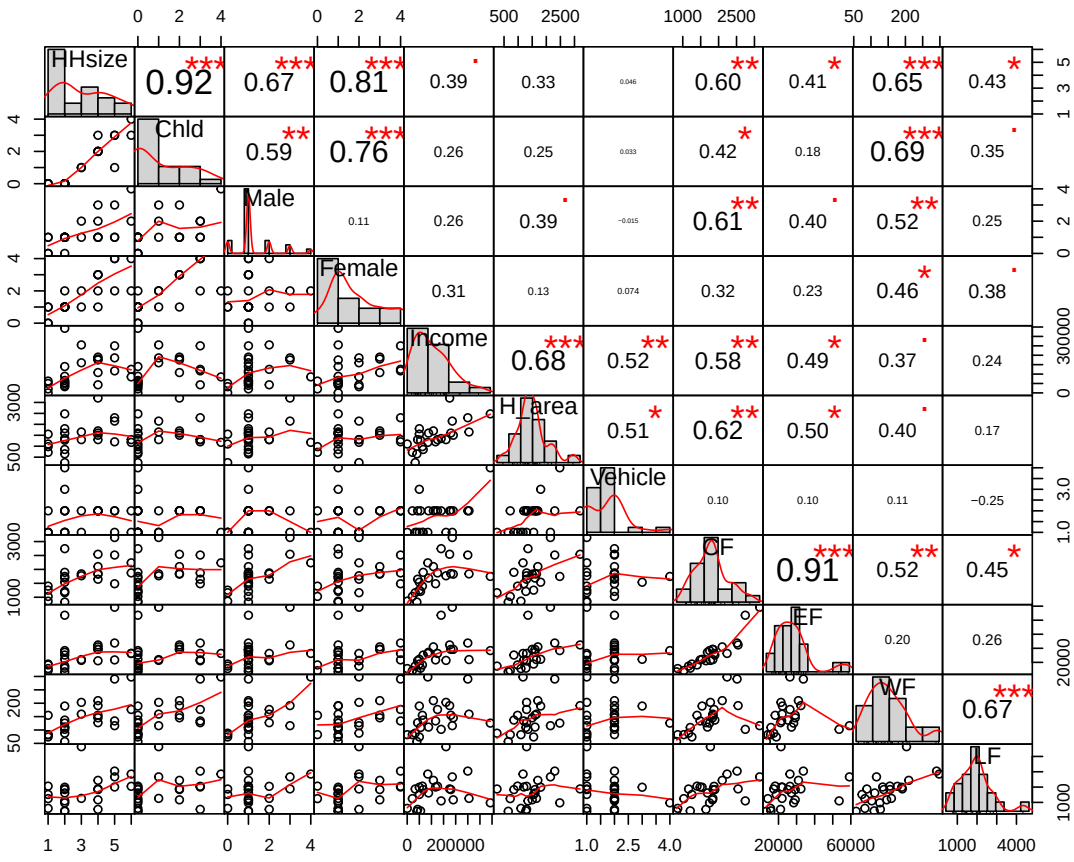

Figure 3.9: Bivariate scatter plots with a fitted line and the Kendall correlation coefficients between household demographics and FEWprints.

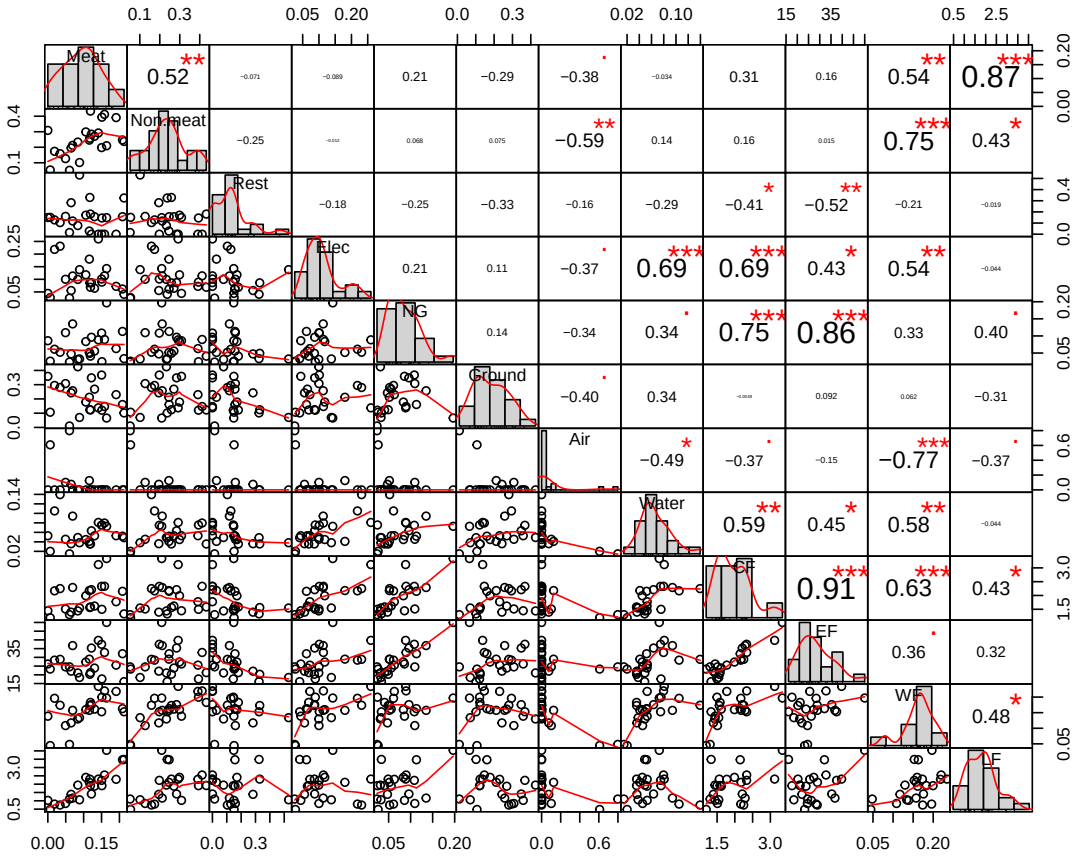

Figure 3.10: Bivariate scatter plots with a fitted line and the Kendall correlation coefficients between household FEW consumption trends and FEWprint intensities.

Correlations between household demographics and their FEWprints were identified. With respect to gender differences in FEWprints, males tend to have higher carbon and energy footprints than females since males consume more electricity, which is one of the largest contributors to the carbon and energy footprints. On the other hand, females are likely to have a higher land footprint because females show larger non-meat consumption, which is one of the most dominant consumption activities for the land footprint. High-income households with large house areas tend to have higher carbon and energy footprints than low-income households with small house areas. This is because high-income households tend to spend more on electricity, and households with large house areas have large NG consumption.

To identify potential behavior changes to mitigate household FEWprints, correlations between household consumption trends and FEWprints were investigated. To lower household carbon and energy footprints, electricity and NG consumption need to be reduced. Household electricity and NG use are the largest contributors to the carbon and energy footprints unless households travel long distances through the air. Males spend more on electricity than females, and thus, households with many male members are likely to have a higher carbon footprint. Also, if households spend more on restaurants (FAFH consumption), they tend to have lower carbon and energy footprints. This is not only because FAFH consumption has smaller footprint intensities than FAH consumption, but also because restaurant consumption reduces the consumption of other FEW commodities at home.

Non-meat and meat consumption are the most dominant household consumption activities for water and land footprints, respectively. Therefore, if households consume more meat or non-meat, they have higher land or water footprints, respectively.

Females consume more non-meat than males, and thus, households with many female members tend to have a large land footprint. Also, households with long-distance air travel have lower FEWprint intensities. Since air transportation contributes significantly to the carbon and energy footprints, they are likely to have large total carbon and energy footprints. However, they have lower total water and land footprints because they do not spend much on the FEW commodities at home during travel.

This study investigated the life cycle impacts of household consumption activities to address a social domain of environmental sustainability as well as the nexus of FEW systems. We employed a data collection method that ensures high quality of data and is less biased by participants' self-selection and lack of awareness. However, many challenges and limitations remain for such studies. First, collecting numerous household data is very demanding work. In this study, 24 households and 73 household individuals completed the survey and submitted their consumption data. However, the sample size is small, and variables in the sample do not always have common distributions. Therefore, Kendall's rank correlation method was employed to investigate the correlations between variables. Moreover, the sample employed in this study represents the upper-middle-class households in Columbus, Ohio. The sample median income is two times higher than the median income in Columbus. If the sample size is larger, we could account for more diverse households, and the analysis could be much more robust and efficient.

Temporal variations in household consumption and footprints also need to be studied. In this work, we only collected four weeks of complete household FEW consumption data. However, household consumption varies with seasons. Thus, if a longer period of consumption data is collected, seasonal variations in household

FEWprints could be investigated. Additionally, there is a region-specific limitation. Columbus is not a place with great public transportation systems. Hence, it is challenging to investigate the effects of using public transportation systems on household FEWprints.

The USEEIO model employed in this study represents the entire U.S. economy in 2013. However, the model is based on highly aggregated national economic data. Thus, it does not account for product-specific and region-specific process and supply chain data. For instance, corn and wheat may have different supply chains from each other. In the USEEIO model, however, they are aggregated into a single grain farming sector (NAICS: 1111b0) that connects to its national average supply chains. If the product-specific and region-specific process and supply chain data are available, a hybrid LCA model could be constructed to perform a more detailed sustainability assessment study.[12]

Finally, this work could be extended to account for human behavioral consequences on environmental sustainability by examining behavioral feedback from households. In this study, we calculated FEWprints at the individual household level. The footprint results could be provided to each household, and its behavioral feedback could be collected. Based on behavioral feedback, an additional footprint analysis could be performed to investigate how household behavior changes could affect FEWprints. A social consequential study is needed to account for the effects of changes in social systems on environmental sustainability. However, long term follow-ups for such a study will be challenging.

Author Contribution Kyuha Lee developed the EEIO model, conducted the footprint analysis, and took the lead in writing the chapter. Nicole Sintov and Ian J. Adams collected and complied data for household consumption in Columbus, OH. Sophie Manaster performed and provided a literature review. Nicole Sintov and Ian J. Adams wrote Section 3.2.1 of the chapter. Nicole Sintov and Bhavik R. Bakshi supervised the project and edited the chapter. All authors provided critical feedback and contributed to the final version of the chapter.

Chapter 4: Carbon Footprint of Biomimetic Carbon Fixation Technologies with RubisCO Immobilization and Adenosine Triphosphate Regeneration

In the Calvin cycle of photosynthesis, ribulose-1,5-bisphosphate carboxylase/oxygenase (RubisCO) catalyzes the conversion of ribulose 1,5-bisphosphate to 3-phosphoglyceric acid (3-PGA) while incorporating atmospheric CO_2 into an organic molecule. Thus, RubisCO is nature's CO_2-sequestering enzyme that is present in chloroplasts. As an effort to mitigate climate change, biomimetic carbon fixation technologies have been developed through RubisCO immobilization into nanostructures to form nanostructure-RubisCO complexes. The technologies mimic the plant cellular environment's ability to convert CO_2 into higher-value products. In this work, a carbon footprint of 3-PGA produced through carbon fixation by the complexes is investigated using the LCA approach. Serine, an amino acid for pharmaceutical applications, is identified as a potential product from 3-PGA. Hotspot processes in terms of the carbon footprint are identified to suggest potential improvements for emerging technologies. Conducting LCA for emerging technologies has many challenges. A sensitivity analysis is performed for uncertain data, and the adenosine triphosphate (ATP) preparation process for the 3-PGA production is identified as a hotspot inventory. We identify that

the carbon footprint to produce 3-PGA can be significantly lowered by integrating carbon fixation technologies with an electrochemical ATP regeneration technology.

4.1 Introduction

In the natural carbon cycle, inorganic CO_2 in the atmosphere is converted to organic hydrocarbons through photosynthesis. However, today's enormous anthropogenic CO_2 emissions along with the increased energy demand make this natural carbon pathway insufficient to close the carbon cycle. Therefore, various CO_2 emissions mitigation strategies are being studied to close this cycle.[85]

One of the strategies is to convert CO_2 into high-value hydrocarbon products such as formic acid, methane, and dimethyl carbonate through chemical conversion processes. Numerous studies have examined the sustainability of such CO_2 conversion technologies.[86] Many of these studies identified environmental effectiveness and technological challenges by conducting life cycle assessment (LCA) studies. Since CO_2 is a stable molecule and requires a huge amount of energy for its activation, CO_2 conversion processes are energy-intensive, and thus, they exhibit positive net CO_2 emissions in many cases.

On the other hand, the carbon cycle of nature (photosynthesis and plant respiration) is closed and attests to the great potential of CO_2 conversion technologies. In the natural carbon cycle, sunlight is a primary energy source for carbon fixation, and it is completely sustainable. To mimic natural photosynthesis, researchers have developed artificial photosynthesis technologies that capture and convert renewable solar energy into high energy density fuels such as hydrogen.[87,88] Renewable energy

sources such as solar and wind power, whose emissions are minimal compared to emissions from conventional fossil energy sources, have been considered to reduce the net carbon footprint of CO_2 conversion technologies as well.[86] Alternatively, whole plants can be grown and their biomass can be processed in biorefineries to generate energy and other valuable products. Since biomass feedstock is prepared through natural photosynthesis, those technologies generally have lower environmental impacts than conventional petrochemical technologies.[89]

More recently, cell-free biomimetic technologies that imitate cellular carbon fixation have been developed.[4] In the Calvin cycle of natural photosynthesis, as shown in Fig. 4.1, cascade reactions to produce 3-phosphoglyceric acid (3-PGA) from ribose-5-phosphate (R-5-P) are catalyzed by three enzymes: phosphoribosyl isomerase (PRI), phosphoribulokinase (PRK), and ribulose-1,5-bisphosphate carboxylase/oxygenase (RubisCO). During these reactions, RubisCO, which is an enzyme present in chloroplasts, catalyzes the conversion of ribulose 1,5-bisphosphate (RuBP) to 3-PGA while incorporating atmospheric CO_2 into the organic molecule.[90] RubisCO has been known as the most abundant enzyme in the world and accounts for most of the biological carbon fixation on earth.[91] The biomimetic carbon fixation technologies produce 3-PGA through CO_2 fixation in cell-free systems.[4] In these technologies, three-dimensional nanoscale structures such as nanotubes and nanofibers are employed as support for enzymes to form CO_2-fixing nanostructure-enzyme complexes.[92,93] The nanostructure-enzyme complexes are comprised of three enzymes (PRI, PRK, and RubisCO) and a nanostructure that supports enzyme immobilization. These complexes enhance the catalytic performance of enzymes for cascade reactions.[4]

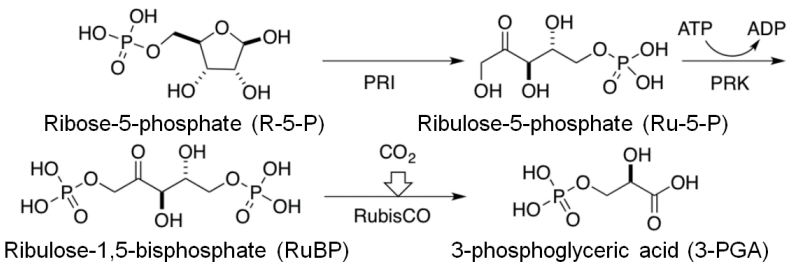

Figure 4.1: Cascade reactions to produce 3-PGA from R-5-P in the Calvin cycle of photosynthesis.

The cell-free in vitro systems have advantages over in vivo biological systems (living cell systems). Higher product yields and lower environmental impacts are expected from the cell-free systems because of their higher product specificity,[94,95] and cell-free systems do not have to divert resources to other life processes. Also, the CO_2-fixing biomimetic technologies do not require CO_2 capture and compression processes as required by chemical CO_2 conversion technologies. Moreover, compared to biorefinery technologies such as biomass conversion, the cell-free biomimetic technologies avoid the extensive land use for biomass growth and do not impact food production.

The LCA approach is employed to examine the environmental impacts of technologies and identify improvement opportunities. LCA accounts for the life cycle of products which ranges from the extraction of upstream resources to the use and disposal of products. In this sense, LCA is also called a cradle-to-grave analysis. LCA estimates total environmental impacts (e.g., carbon footprint) of products by calculating indirect impacts from the upstream and downstream processes as well as

direct impacts. Hotspot inventories that show the highest contribution to the specific impacts could be identified through the LCA study. There are numerous LCA studies on the environmental impacts of chemical CO_2 conversion[86] and biorefinery technologies.[89] However, the environmental effectiveness of cell-free biomimetic carbon fixation technologies remains unknown and the relevant life cycle inventory (LCI) data to such technologies are not readily available from any existing LCI databases. Therefore, challenges and limitations in conducting LCA for such emerging technologies exist and need to be addressed.

In this work, we investigate a carbon footprint of 3-PGA produced through biomimetic carbon fixation by the nanostructure-enzyme complexes using the LCA approach. We investigated two types of nanostructures for the complex as follows: Camptothecin (CPT)-dipeptide nanotubes[4,96] and fluorenylmethyloxycarbonyl (Fmoc) tetrapeptide nanofibers. To examine if the CO_2-fixing 3-PGA has benefits of reducing the footprint, another 3-PGA synthesis route that employs sugar (sucrose) as a carbon source instead of CO_2 is investigated as well.[97] The carbon footprints of three 3-PGA synthesis routes (CPT route, Fmoc route, and sugar route) are compared with each other. To have the life cycle system boundary, the potential use of 3-PGA is investigated, and the life cycle impacts are calculated. The LCA study identifies potential opportunities for technological improvements to reduce the carbon footprint.

Enzymatic processes generally need the presence of coenzymes such as adenosine triphosphate (ATP) and nicotinamide adenine dinucleotide (NAD^+). The CO_2-fixing biomimetic technologies also require the use of ATP as the natural photosynthesis in the Calvin cycle does. However, the preparation of these coenzymes is known to be expensive for industrial applications, and therefore, their regeneration techniques

have been developed for the economic implementation of enzymatic processes.[98,99] Coenzyme regeneration could reduce wastes and improve the circularity of resources in the enzymatic systems. In this study, we examine if the ATP preparation process is environmentally favorable. Then, we investigate the potential impacts and benefits of integrating an electrochemical ATP regeneration technology into biomimetic carbon fixation systems.

4.2 Materials and Methods

4.2.1 Nanostructure-RubisCO Complexes

As shown in Fig. 4.1, RubisCO is nature's CO_2-sequestering enzyme which catalyzes the conversion of RuBP to 3-PGA. To construct cell-free carbon fixation systems, Satagopan et al. have developed nanostructure-RubisCO complexes.[4] The complexes include three enzymes: PRI, RPK, and RubisCO. PRI and form I RubisCO are prepared from the bacterium *Ralstonia eutropha* as described in the report.[100,101] PRK is prepared from the cyanobacterium Synechococcus as described in the report.[102]

Two types of nanostructures are prepared: CPT-dipeptide nanotubes[4,96] and Fmoc tetrapeptide nanofibers. The synthesis procedures for these nanostructures and the nanostructure-RubisCO complexes are described in the report.[4] The nanostructure-RubisCO complexes consist of three enzymes and either CPT-dipeptide nanotubes or Fmoc tetrapeptide nanofibers. Figure 4.2 exhibits an illustration of the complex employing CPT-dipeptide nanotubes. The activity of RubisCO in the complexes has been optimized to its near-native activity levels and the stoichiometric amount of 3-PGA can be produced through these processes.

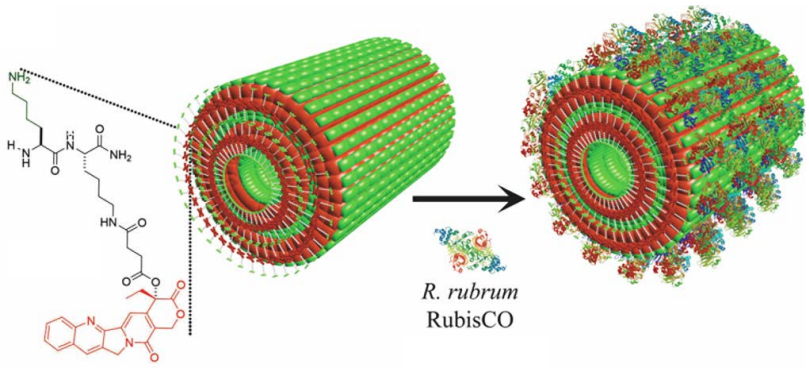

Figure 4.2: An illustration of the nanostructure-RubisCO complex that consists of CPT-dipeptide nanotubes and RubisCO.[4] PRI and PRK enzymes are also mixed into the complex.

4.2.2 Use Phase of 3-PGA

3-PGA is a CO_2-fixed product through the cascade reactions from RuBP in the Calvin cycle as shown in Fig. 4.1. In nature, the Calvin cycle converts 3-PGA to regenerate R-5-P which is converted into ribulose-5-phosphate (Ru-5-P) then RuBP. In the cell-free biomimetic carbon fixation systems, 3-PGA is synthesized by the nanostructure-RubisCO complexes and can be used for industrial applications. According to the report,[103] 3-PGA can be a precursor to synthesize amino acids (serine, cysteine, and glycine) as industrial products for pharmaceutical use. Since serine is a precursor for producing cysteine and glycine, we identify serine as the potential use of 3-PGA in this LCA study.

Serine can be synthesized from 3-PGA through the phosphorylated pathway of serine biosynthesis as shown in Fig. 4.3.[104,105] First, an enzyme 3-phosphoglycerate dehydrogenase (PGDH; *serA*) catalyzes the oxidation of 3-PGA into 3-phosphohydroxypyruvate (3-PHP). NAD^+/NADH is used as a coenzyme for this conversion.

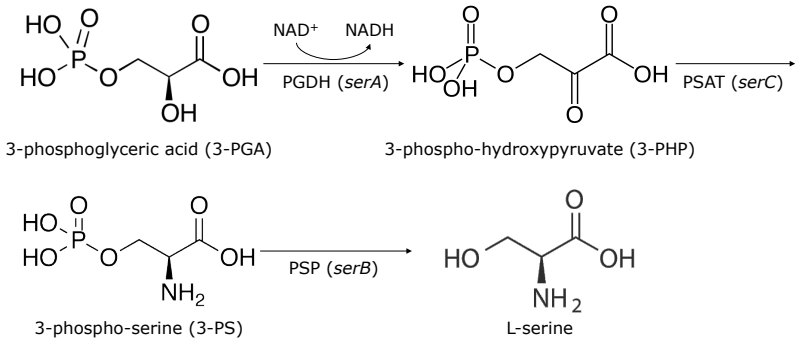

Figure 4.3: Serine biosynthesis from 3-PGA using enzymes *serA*, *serC*, and *serB*.

Then, 3-PHP is converted into 3-phospho-serine (3-PS) by using an enzyme phosphoserine transaminase (PSAT; *serC*) and L-glutamate. Finally, 3-PS is hydrolyzed to L-serine using an enzyme phosphoserine phosphatase (PSP; *serB*) and water.

In this work, the following three 3-PGA synthesis routes are investigated.

- CPT route: CPT-dipeptide nanotubes are used as nanostructure support for RubisCO immobilization in the biomimetic CO_2-fixing processes.
- Fmoc route: Fmoc tetrapeptide nanofibers are used as nanostructure support for RubisCO immobilization in the biomimetic CO_2-fixing processes.
- Sugar route: Sucrose is used as a carbon source instead of CO_2.

3-PGA products from the above routes can be converted into L-serine. Additionally, we examine the conventional L-serine synthesis route. Industrially, serine is synthesized from glycine and methanol by microbial fermentation.[106] The reaction is catalyzed by serine hydroxymethyltransferase (SHMT). Worldwide L-serine production in 2005 was 300 t.[107] Carbon footprints of four serine synthesis routes are investigated using the LCA approach.

4.2.3 ATP Regeneration

In general, enzymatic processes are favorable due to their high selectivity and low environmental impacts. However, many enzymatic reactions require the use of coenzymes such as ATP and NAD^+. The industrial use of coenzymes is impractical because their preparation processes are expensive. Therefore, the regeneration of coenzymes has been the limiting step for their economic utilization.[98,99]

In this study, an electrochemical ATP regeneration technology is considered as a means of reusing coenzymes and reducing environmental impacts. A programmable chemical actuator was created and programmed to control the inorganic phosphate concentration at the electrode surface, condensing ADP to ATP *in situ*. Working and counter electrodes (0.064 cm^2) were prepared from Au wire (0.05 mm diameter) and a 0.064 cm^2 Ag/AgCl reference electrode was prepared with Ag wire (0.01 mm diameter). 253 μg of polypyrrole doped with sodium chloride (PPy(Cl)) was electropolymerized on the working electrode, then programmed for phosphate selectivity in 0.5 M Na_3PO_4. The integration of the ATP regeneration system with the biomimetic CO_2 fixation system means that the same reaction medium is employed for the CO_2 fixation by the nanostructure-RubisCO complexes and for the electrochemical ATP regeneration. The following stoichiometric reaction is assumed for ATP regeneration from ADP and inorganic phosphate:

$$\mathrm{ADP} + \mathrm{H_3PO_4} \rightarrow \mathrm{ATP} + \mathrm{H_2O} \quad (\Delta G^o = 30.5 \text{ kJ/mol.})$$

The PPy($PO_4{}^{3-}$) membrane is prepared through a two part electrochemical process using 0.1 M pyrrole (Py) monomer, 0.1 M NaCl as a dopant, and 0.5 M Na_3PO_4 as an equilibration solution. First, the Py monomer and NaCl are oxidized at the

working electrode, then the polymerization solution is exchanged for the equilibration solution and cyclic voltammetry is performed to form ion-selective pathways in the polymer. ADP is condensed to ATP when the polymer is oxidized, and the concentration of inorganic phosphate is raised at the electrode surface. Polymerization of PPy(Cl), programming of PO_4^{3-} selectivity, and the operation of systems consume 2.92, 0.34, and 25.47 J of energy, respectively. The phosphate actuator has a lifetime of 1,200 cycles before the polymer must be replaced or refreshed.

4.2.4 Life Cycle Assessment

LCA is a tool to assess the environmental impacts of products and processes by accounting for their upstream and downstream life cycle activities. In this study, an open-source LCA software (openLCA)[51] is used to conduct the LCA study. The LCA approach is documented in ISO 14040:2006 and consists of four phases[37] that are described in the context of the selected technology in the following subsections.

Goal and Scope Definition

The goal of the LCA study is to examine how effective biomimetic carbon fixation technologies are to mitigate global warming and to identify how the technologies could be further improved. The analysis boundary is a cradle-to-gate boundary (cradle-to-use phase) which ranges from the raw material extraction to the use phase of 3-PGA. When the same two products with different upstream technologies are investigated, a cradle-to-gate analysis is performed since the downstream activities (use and disposal phases) for the common product are identical to each other. L-Serine is identified as the potential use of 3-PGA. Figure 4.4 shows four types of product systems investigated in this study. As described in Section 4.2.2, CPT and Fmoc routes are the

L-serine synthesis routes from 3-PGA, which is prepared through carbon fixation by nanostructure-RubisCO complexes. Sugar route is the L-serine synthesis route from 3-PGA, which is prepared using sucrose as a carbon source instead of CO_2. The sugar route is included in the study to compare the biomimetic carbon fixation technologies to a non-CO_2-fixing technology. Lastly, the conventional route to L-serine involves the microbial fermentation of glycine and methanol. Accordingly, a function unit is defined as 1 kg of L-serine.

Inventory Analysis

In this work, two existing LCI databases (U.S. LCI database and Ecoinvent) are employed. The U.S. LCI database is prioritized when the desired inventory data is available since the database is based on the U.S. Applying LCA to emerging technologies is challenging because many of their inventory data are difficult to find in any LCI database due to their nascent nature.[108] In such cases, any data that are not available in existing databases are either estimated from laboratory experiments or obtained from literature such as journal articles and patents. If industrial production data is available, it is preferred. Such LCA studies of emerging technologies are likely to have large uncertainty. To account for this uncertainty, a sensitivity analysis is performed on unknown inventory data.

Some data are not available even from the literature. In such a case, the data are estimated by simple fundamental models or ignored in the study. For example, any catalyst inputs are ignored assuming their reusability and small quantity. The manufacture of equipment and the transportation of materials are also excluded unless such data are available from the LCI databases or literature. Moreover, if data for the energy inputs are not provided, they are excluded. This implicitly assumes that

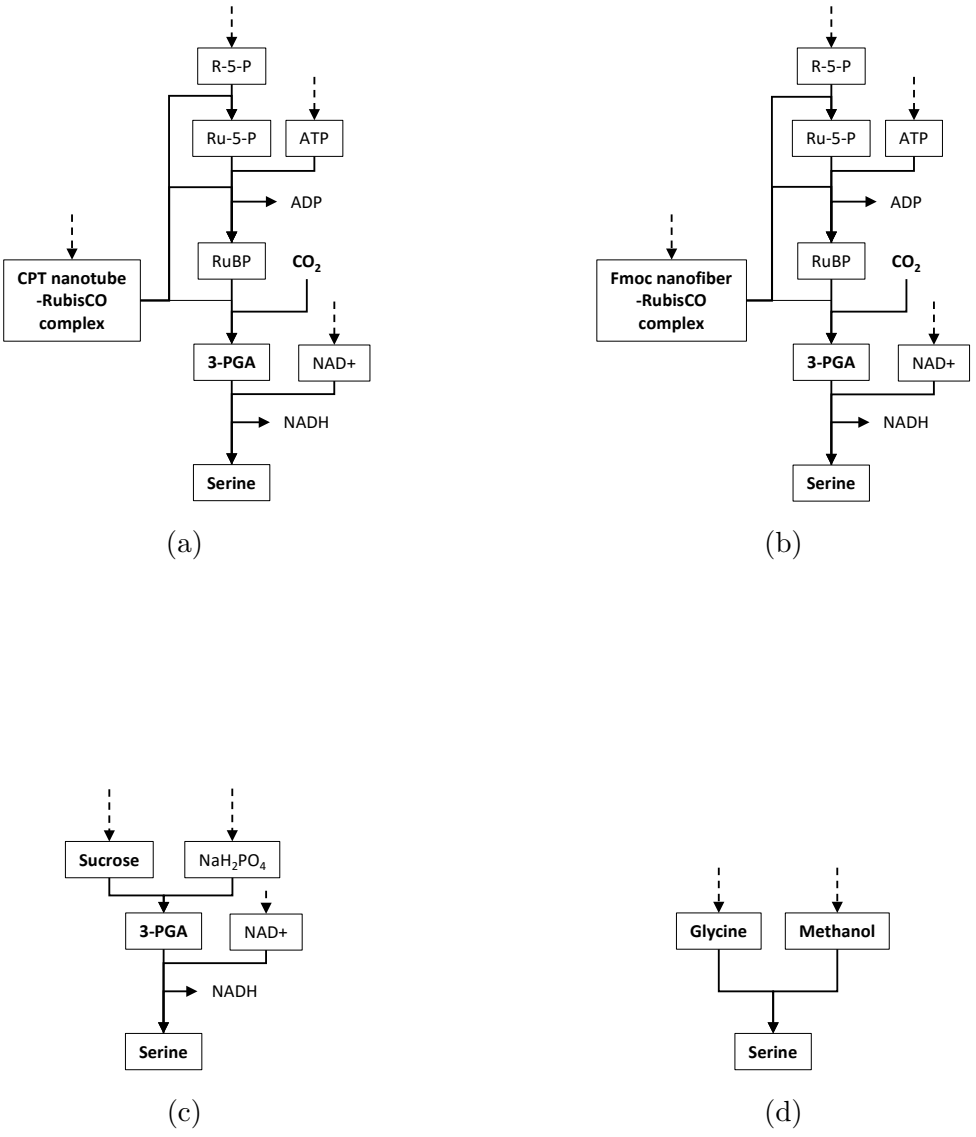

Figure 4.4: Four routes to produce L-serine: (a) CPT route, (b) Fmoc route, (c) sugar route, and (d) conventional route.

these processes occur around room temperature, which is true for most biological processes. Furthermore, product yields are determined by stoichiometric calculation if such data are unknown.

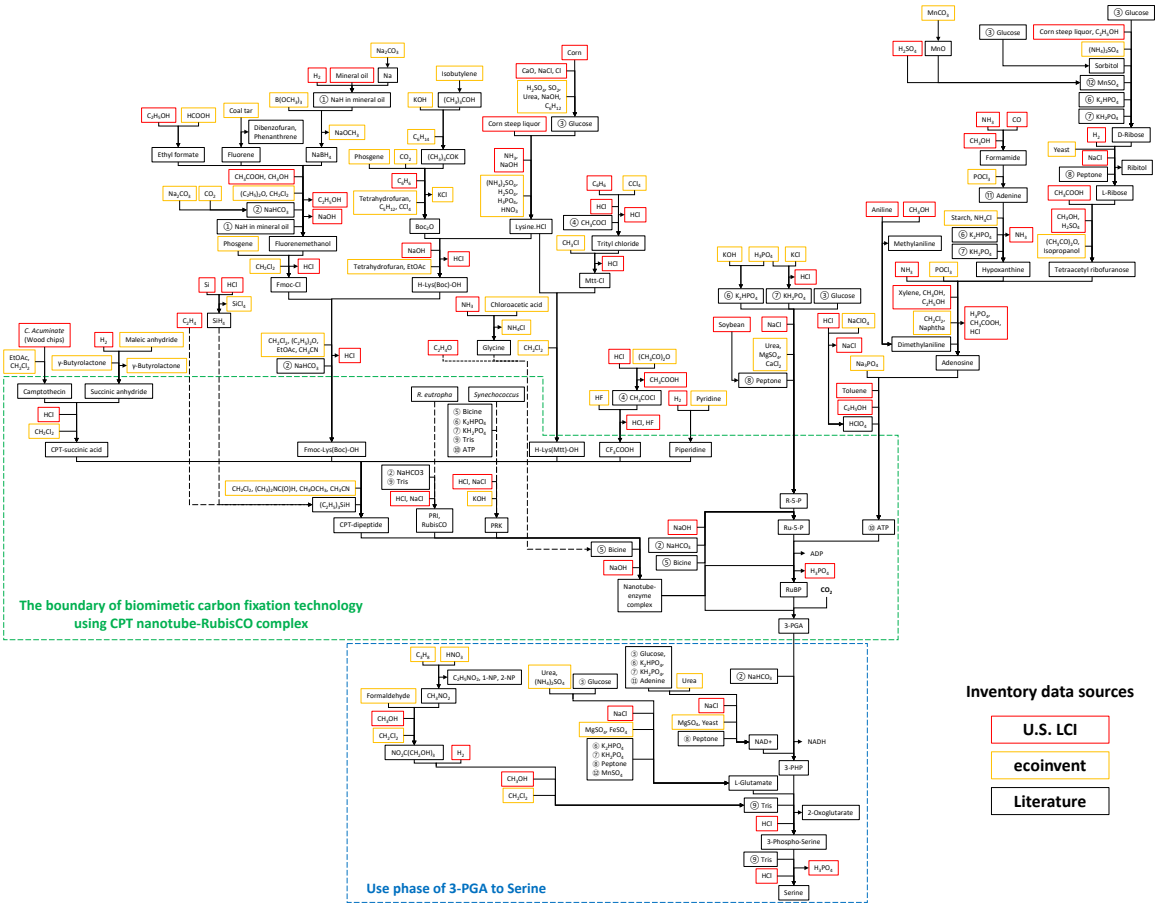

Figure 4.5: Network diagram for the CPT route to produce L-serine.

Figure 4.5 shows a partial life cycle network diagram for the CPT route. The network diagrams for the Fmoc, sugar, and conventional routes are shown in Figs 4.5–4.8. Sources of inventory data are indicated in different colors. The diagram does not show the upstream network for the inventories available in the existing LCI databases. The complexity of the diagram for the CPT route implies difficulties in applying LCA to emerging technologies because their inventory data are difficult to find in any LCI database.

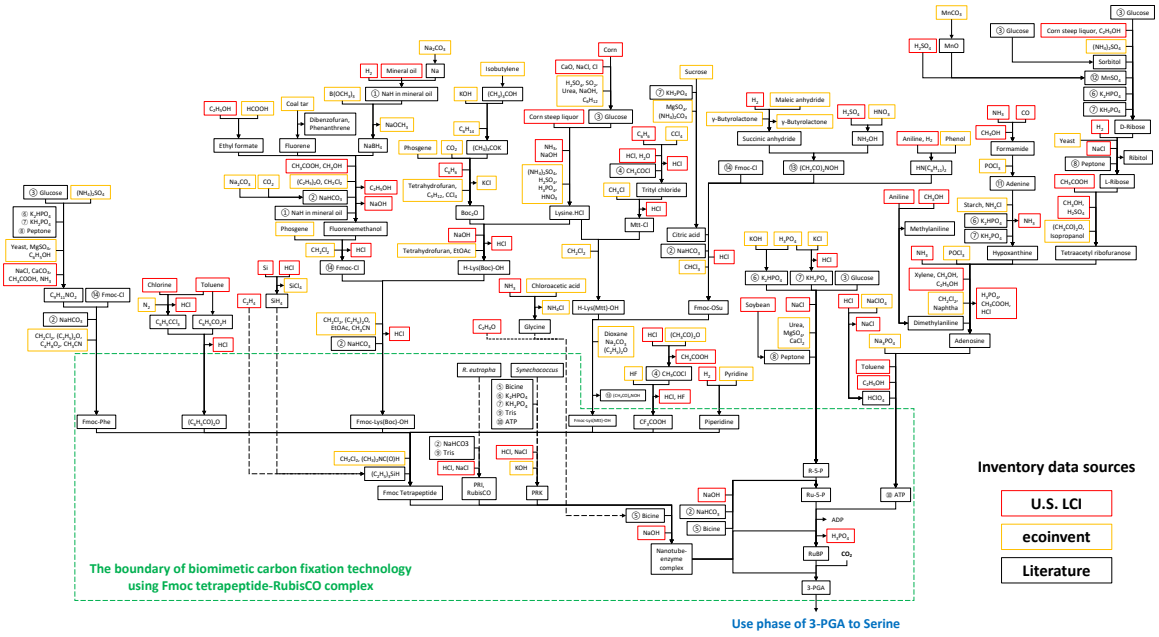

Figure 4.6: Network diagram for the Fmoc route to produce L-serine.

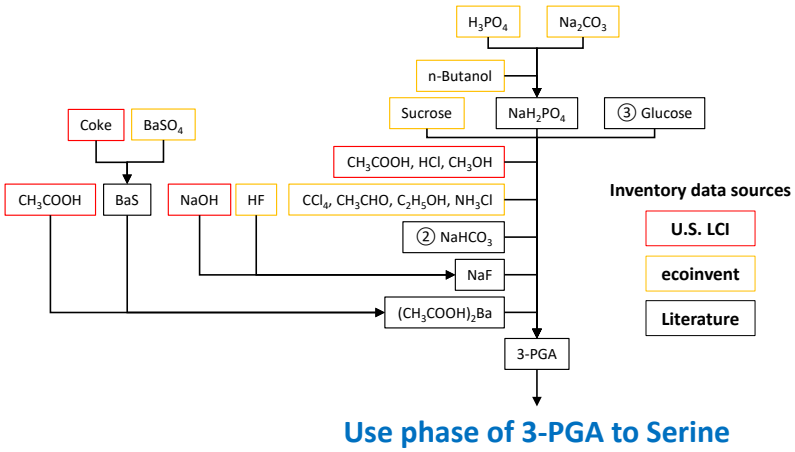

Figure 4.7: Network diagram for the sugar route to produce L-serine.

The green dotted box represents the boundary of biomimetic carbon fixation technology using the CPT nanotube-RubisCO complex. We obtained the inventory data

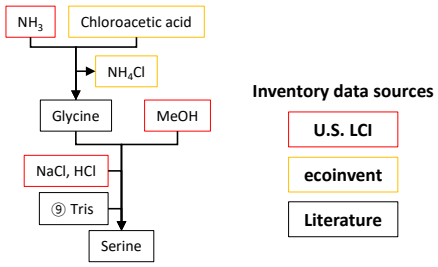

Figure 4.8: Network diagram for the conventional route to produce L-serine.

in the green dotted box from experimental data.[4] The blue dotted box indicates the use phase of 3-PGA to produce L-serine. The same use phase is included among the CPT, Fmoc, and sucrose routes since the 3-PGA products from three routes are identical. The vertical and horizontal input arrows represent reactants and solvent use, respectively. The output arrows indicate products. When more than two products are produced, the main products are shown as the vertical output arrows, while by-products are shown as the horizontal output arrows. Also, adenosine diphosphate (ADP) from the conversion of Ru-5-P to RuBP and NADH from the conversion of 3-PGA to 3-PHP are considered to be waste since these are the cofactors that need to be regenerated into ATP and NAD+, respectively. They also inhibit the reactions using ATP and NAD+ when present in high amounts.

The LCA studies can specify inventories that contribute the most to the impacts in the life cycle system boundary. In this LCA of emerging technologies, the opportunities for technological improvements need to be identified in the green dotted box whose inventories are based on experiments, instead of commercialized processes. The inventories outside the green dotted box are collected from literature and based on

industrial processes. Therefore, either of the following opportunities can be identified in the green dotted box:

- Improving the yield of product or discovering an alternative technology to prepare a reactant, if any reactant inventory is identified as a hotspot inventory.
- Improving the efficiency of solvent use or replacing it with the alternative one that has smaller impacts, if any solvent inventory is identified as a hotspot inventory.

If we consider the integration of electrochemical ATP regeneration technology into the carbon fixation technologies, the analysis boundary needs to include the ATP regeneration process. In such a case, ADP from the cascade reactions is not a waste anymore. Instead, ADP is recycled into ATP through regeneration. Figure 4.9 shows the partial life cycle network diagram for the electrochemical ATP regeneration. The purple dotted box indicates the boundary of ATP regeneration technology. The electrochemical experiments are performed to collect the inventory data in the purple dotted box. PPy(PO_4^{3-}) membrane is prepared from the pyrrole monomer through electrochemical polymerization. ATP is regenerated from ADP through the electrochemical procedure. ADP is provided from the biomimetic carbon fixation, and the regenerated ATP is used in the carbon fixation process.

In many LCA studies on electrolysis in a membrane cell, electrodes and membranes are excluded from the analysis since they are assumed to be reusable.[109] However, the membrane is included in this LCA study since it is known that the polypyrrole membrane can be reused more than 1,200 times.

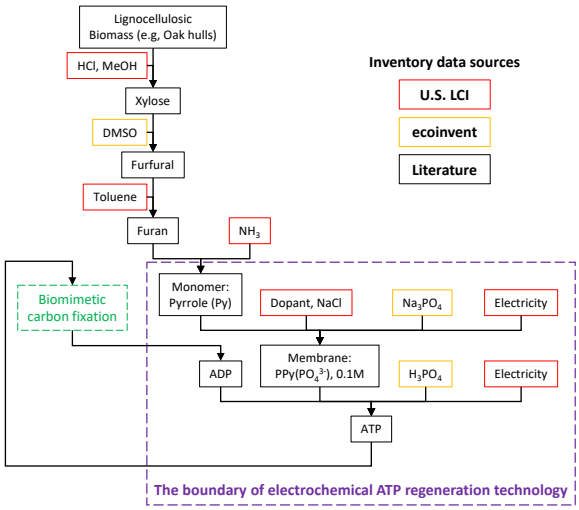

Figure 4.9: Network diagram for the electrochemical ATP regeneration.

Impact Assessment

A carbon footprint of four routes to produce serine is calculated. Life cycle interventions are characterized using TRACI 2.1 life cycle impact assessment (LCIA) method.[110] If by-products and co-products are produced from a certain inventory A, the impacts need to be allocated to the main product. The allocation needs to be performed by either the displacement method or the partitioning method. The former method considers a conventional way of producing those by-products. Then, the by-products are assumed to replace the conventional process. Therefore, the impacts from the conventional process are avoided due to the by-products produced from the inventory A. In the partitioning method, the impacts from the inventory A are partitioned among the main product and by-products based on the ratio of mass, energy, or monetary values. The displacement approach is preferred if conventional process data are available from the LCI databases or literature.

Interpretation

Hotspot inventories (i.e., the largest contributors to the carbon footprint) can be identified through LCIA. Opportunities for technological improvements to reduce the footprint can be discussed. In the following section, we compare the carbon footprint of four serine synthesis routes. Also, we discuss how effectively the coenzyme regeneration technology can reduce the footprint of biomimetic CO_2 fixation technologies.

4.3 Results and Discussions

4.3.1 LCA of Biomimetic Carbon Fixation Without ATP Regeneration

A cradle-to-gate LCA study is performed on biomimetic carbon fixation technologies to investigate a carbon footprint of technologies. These emerging technologies produce 3-PGA product through carbon fixation by nanostructure-RubisCO complexes. In this LCA study, the following two types of nanostructures are investigated: CPT-dipeptide nanotubes and tetrapeptide nanofibers.

In the sensitivity analysis, three cases (lower impact, base, and higher impact) are considered for the ratio of unreacted reactants to be reused, the ratio of fugitive volatile organic compound (VOC) emissions, the number of times of solvent reuse, and the number of times the nanostructure-RubisCO complex is reused. Table 4.1 summarizes three cases considered via the sensitivity analysis. The lower impact case represents a more environmentally beneficial case while the higher impact case refers to the less beneficial case.

80–100% of unreacted reactants are considered to be reused. The unreacted materials that are not reused are assumed to be emitted to the air if they are in the gas

phase at room temperature (e.g., ammonia and phosgene). VOC emissions are the fugitive air emissions from the use of VOCs. They include fugitive emissions from solvents, by-products, and unreacted reactants. 0.5–8% of VOCs are assumed to be lost to the air as fugitive emissions. The VOCs can be classified into three categories based on the boiling point range: VVOC (very VOC), VOC, and SVOC (semi-VOC).[111,112] In this study, the organic compounds are VVOC, VOC, or SVOC, if their boiling points range from the room temperature to 75°C, from 75°C to 250°C, or from 250°C to 400°C, respectively. Every solvent in this study is assumed to be reused 5–20 times through the sensitivity analysis.[113] Also, the nanostructure-RubisCO complexes can be reused numerous times since they show enzymatic behavior. Based on input from the technology developers, the number of times of reuse of this complex is considered to be between 5,000 and 20,000.

Figure 4.10a exhibits the LCIA results of four serine synthesis routes for three sensitivity analysis cases. A total carbon footprint to produce 1 kg of serine is shown at the top of each bar. The carbon footprint for preparing 3-PGA is shown in green bars. The contribution to the footprint from solvent use ($NaHCO_3$, Tris, HCl) and

Table 4.1: Three cases considered via a sensitivity analysis.

Description	Lower impact	Base case	Higher impact
Unreacted reactants to be reused (%)	100	90	80
Fugitive VVOC emissions (%)	2	4	8
Fugitive VOC emissions (%)	1	2	4
Fugitive SVOC emissions (%)	0.5	1	2
Solvents to be reused (times)	20	10	5
Complex to be reused (times)	20,000	10,000	5,000

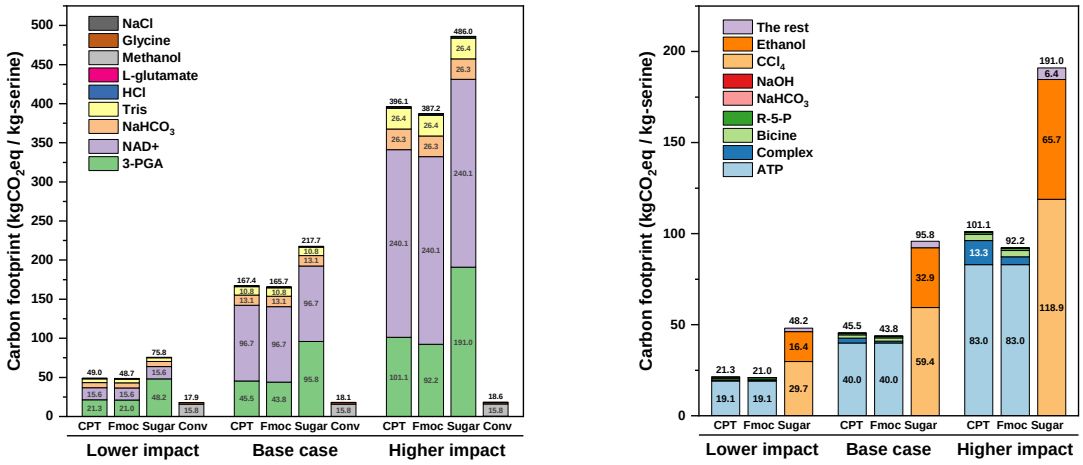

(a) (b)

Figure 4.10: **(a)** Life cycle impact assessment results of four routes to produce serine. A total carbon footprint to produce 1 kg of serine is shown at the top of each bar. Biomimetic CPT and Fmoc routes have lower footprints than the sugar route but higher footprints than the conventional route. **(b)** Detailed LCIA results for 3-PGA production in three serine synthesis routes. ATP inventory shows the largest contribution to the carbon footprint of biomimetic CPT and Fmoc routes.

the other reactant use (NAD+, L-glutamate) for the serine synthesis from 3-PGA is plotted as well.

As shown in Fig. 4.10a, the conventional route exhibits the lowest carbon footprint followed by the Fmoc, CPT, and sugar routes. The sensitivity analysis indicates the results are robust since all sensitivity cases show the same relative results. For each sensitivity case, the footprint from solvent use ($NaHCO_3$, Tris, HCl) and reactant use (NAD+, L-glutamate) is the same among three routes from 3-PGA (CPT, Fmoc, and sugar routes). For instance, the footprint from the use of NAD+ is 96.7 $kgCO_2eq$/kg-serine for those three routes in the base case. This is because those routes share the same use phase of 3-PGA. Also, the impacts of these three routes are very sensitive

to the cases considered in the sensitivity analysis. The footprint from using NAD+ varies from 15.6–240.1 $kgCO_2eq$/kg-serine depending on the sensitivity cases. This is due to the nascent nature of technologies for preparing NAD+ as well as for converting 3-PGA to 3-PHP using NAD+. Since the technologies are not yet fully developed, the inventory data are unavailable from the LCI databases and the impacts of the technologies for industrial scale are uncertain.

In the conventional route, the most dominant inventory in the footprint is methanol which accounts for 85.4–88.4% of the total footprint. Sensitivity analysis shows that uncertainty in the carbon footprint from the conventional route is very small compared to that from the other three routes. This is because, unlike emerging technologies, most of the inventory data for the conventional serine synthesis technology are available from the LCI databases. This indicates that most technologies in the conventional route have already been optimized for commercial scale. Therefore, the impacts of the conventional route do not vary a lot with the sensitivity cases.

The biomimetic carbon fixation technologies in the CPT and Fmoc routes have a lower carbon footprint than the non-CO_2-fixing technology in the sugar route. The CPT and Fmoc routes show 18.5–35.4% and 20.3–35.8% lower footprint than the sugar route, respectively, depending on the sensitivity cases. However, both biomimetic routes show a much higher footprint than the conventional route. These biomimetic technologies are still in development and need to be further improved to be effective in mitigating global warming. The opportunities for improvements can be identified through the LCA study.

Figure 4.10b compares three routes to produce serine from 3-PGA in more detail. A carbon footprint of producing 3-PGA in the CPT, Fmoc, and sugar routes is calculated. For the biomimetic carbon fixation technologies, ATP inventory dominates the carbon footprint. 82.0–89.6% and 89.9–91.3% of the footprint to produce 3-PGA are attributed to the ATP process in the CPT and Fmoc routes, respectively. ATP is used for the phosphorylation of Ru-5-P to RuBP as part of the Calvin cycle. ATP is converted to ADP by providing phosphate to the Ru-5-P molecule.

The Fmoc route has a lower footprint than the CPT route because the CPT-dipeptide nanotubes have a higher footprint than the Fmoc tetrapeptide nanofibers. To prepare CPT-dipeptide, CPT-succinic acid is used. The isolation of CPT is a carbon-intensive process with low yield.[114] Despite the fact that CPT nanotubes have a high footprint, the CPT nanotube-RubisCO complex only accounts for 2.2–13.1% of the footprint to produce 3-PGA. In case of the Fmoc nanofiber-RubisCO complex, it accounts for 1.0–4.8% of the footprint to produce 3-PGA. This small contribution to the footprint is attributed to the complexes' reusability due to their enzymatic behavior in the cascade reactions to produce 3-PGA.

In case of the sugar route, the main contribution to the footprint is the use of carbon tetrachloride (CCl_4), which is one of the major global warming substances. CCl_4 has a 100-year global warming potential of 1,730 $kgCO_2eq/kg\text{-}CCl_4$[115] and is highly toxic. In recent years, its use and emissions have been in decline.[116]

For the base case of the CPT route, the production phase of 3-PGA and its use phase for serine account for 27.4 and 72.6% of the total footprint, respectively, as indicated in Fig. 4.11. The results identify the preparation of coenzymes such as ATP and NAD+ as hotspot inventories with respect to the carbon footprint. In the

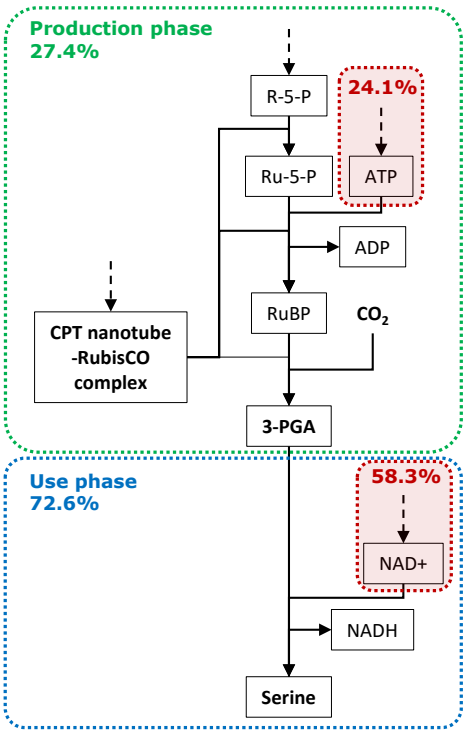

Figure 4.11: Contribution to the total carbon footprint of the CPT route (base case) from the production phase of 3-PGA and the use phase of 3-PGA for serine.

production phase, the ATP preparation process shows the highest contribution to the footprint. In the use phase, the NAD+ preparation process contributes the most to the footprint. Those coenzyme preparation processes have low production yields and require the use of a variety of solvents. Coenzyme preparation has been known as economically expensive.[98,99] The LCA results imply that coenzyme preparation is also environmentally unfavorable.

To improve the biomimetic carbon fixation technologies, the burden of preparing ATP needs to be reduced. Considering that 3-PGA product yield from the cascade reactions is already close to the stoichiometric level, an alternative pathway for preparing ATP needs to be investigated to reduce the footprint of technologies.

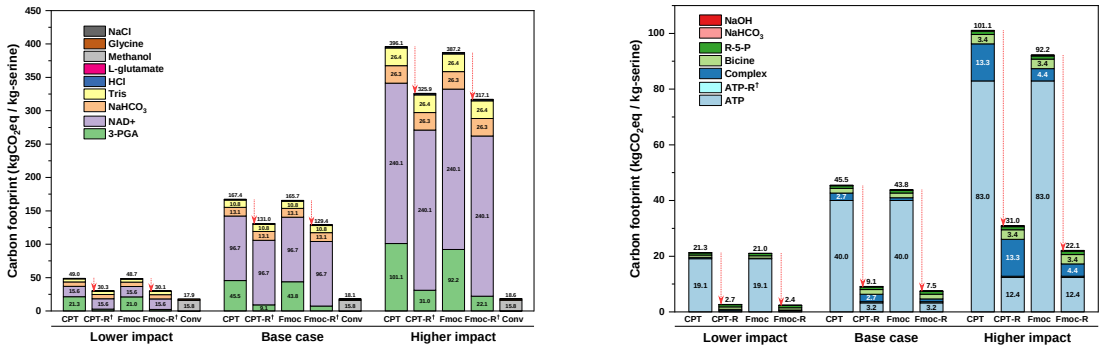

(a) (b)

Figure 4.12: **(a)** Comparison of LCIA results among the CPT, Fmoc, and conventional routes to produce serine. A carbon footprint of biomimetic CPT and Fmoc routes is reduced by integrating ATP regeneration as shown in red-colored dotted arrows. †CPT-R and Fmoc-R refer to the CPT and Fmoc routes, respectively, that include ATP regeneration. **(b)** Detailed LCIA results for ATP-regenerated 3-PGA production between the CPT and Fmoc routes. †ATP-R represents electrochemical ATP regeneration inventory.

4.3.2 LCA of Biomimetic Carbon Fixation Integrating ATP Regeneration

The LCA study in Section 4.3.1 identifies the coenzyme preparation processes to be the main contributors to the carbon footprint of biomimetic carbon fixation technologies. In this section, a carbon footprint of the carbon fixation processes including ATP regeneration is investigated. Figure 4.12a compares the LCIA results between the original systems and the ATP-regenerated systems for the CPT, Fmoc, and conventional serine synthesis routes. A sensitivity analysis is performed for three cases.

Even though ATP is regenerated from ADP, some portions of ATP still need to be prepared from adenosine for the base and higher impact cases because the excess

amount of ATP is required for the biomimetic carbon fixation technologies. In the cascade reactions, one mole of ATP is required to produce two moles of 3-PGA. In the experiments, however, 15 moles of ATP are added in producing 16 moles of 3-PGA. Since the stoichiometric formation of 3-PGA is confirmed in the experiments,[4] 7 moles of ATP can be considered to be unreacted. For the base and higher impact cases, 10 and 20% (0.7 and 1.4 moles) of unreacted materials, respectively, are assumed to be emitted as waste. Hence, even if we consider the stoichiometric regeneration of ATP from ADP, 0.7 and 1.4 moles of additional ATP need to be prepared from adenosine for the base and higher impact cases, respectively.

As shown in Fig. 4.12a, a carbon footprint for producing serine is reduced by 21.7% for the CPT route and 21.9% for the Fmoc route in the base case. In the lower impact case, the ATP-regenerated, CO_2-fixing serine synthesis technologies (CPT-R and Fmoc-R routes) show the most competitive footprint to the conventional serine synthesis technology (conventional route). However, the footprint of the carbon fixation technologies is still higher than the conventional route for every sensitivity case. The main contributor to the footprint of the carbon fixation technologies is the use of NAD+ coenzyme for serine synthesis. This implies that the footprint could potentially be decreased significantly if the NAD+ coenzyme is also regenerated from NADH by employing another chemical actuator. Also, the power to run chemical actuators can be negligible if this comes from renewable sources. In this study, NAD+ regeneration is not considered due to a lack of experimental data. The ATP regeneration reduces the footprint of the ATP inventory by 97.6, 90.8, and 84.6% for the lower impact, base, and higher impact cases, respectively. If we assume a similar reduction in the footprint for the NAD+ regeneration, 13.3–40.0 $kgCO_2$/kg-serine

of the total footprint is expected for the Fmoc route. In the lower sensitivity case, this footprint (13.3 $kgCO_2$/kg-serine) is smaller than the conventional route (17.9 $kgCO_2$/kg-serine).

The detailed LCIA results for ATP-regenerated 3-PGA production between the CPT and Fmoc routes are shown in Fig. 4.12b. ATP regeneration reduces the footprint dramatically since it has a significantly smaller footprint compared to the ATP preparation process from adenosine. Nanostructure-RubisCO complex inventories are identified as new hotspot inventories in terms of the carbon footprint to further improve the carbon fixation technologies. Most of the footprint for the complexes comes from nanostructure supports. Fmoc nanofibers have a smaller footprint than the CPT nanotubes. Other nanostructures as support for enzyme immobilization could be investigated as well. For instance, cellulose nanofibers and chitin nanofibers show high enzymatic activity and stability when they are incorporated with enzymes into the nanostructure-enzyme complex.[117,118] Also, cellulose and chitin are cheaper resources compared to CPT and Fmoc. Further studies are needed for biomimetic carbon fixation to find the most effective nanostructure candidate as support for RubisCO immobilization.

4.4 Conclusions

This work describes the carbon footprint of biomimetic carbon fixation technologies that employ a RubisCO immobilization technique. RubisCO is immobilized into either CPT-dipeptide nanotubes or Fmoc tetrapeptide nanofibers to form the nanostructure-RubisCO complexes. The complexes catalyze cascade reactions from R-5-P to 3-PGA while fixing CO_2 into the organic 3-PGA molecule. 3-PGA then can

be used to synthesize L-serine, an amino acid for pharmaceutical use. The footprint of the technologies was compared with a non-CO_2-fixing technology and the conventional serine synthesis technology. The non-CO−2-fixing technology uses sugar as a carbon source instead of CO_2 to produce 3-PGA. The conventional technology synthesizes L-serine from methanol and glycine, not from 3-PGA.

A sensitivity analysis was performed to account for uncertainty in the inventory data for emerging technologies. The biomimetic carbon fixation technologies showed a lower carbon footprint than the non-CO_2-fixing technology. However, their footprint was much higher than conventional technology. The LCA study identified the preparation processes of coenzymes such as ATP and NAD+ as hotspot inventories in terms of the carbon footprint. ATP is used in the cascade reactions to produce 3-PGA while NAD+ is used to produce serine from 3-PGA.

To reduce the footprint of the carbon fixation technologies, integrated systems of electrochemical ATP regeneration and biomimetic carbon fixation were considered. We performed LCA for the integrated systems. The carbon footprint of emerging technologies to produce serine was decreased by 17.7–38.3% with the regeneration of ATP from ADP. We identified that the carbon footprint of the emerging technologies could potentially be lower than the conventional technology if NAD+ could be regenerated from NADH in a similar manner to the ATP regeneration. The LCIA results for the biomimetic carbon fixation technologies indicated that coenzymes need to be regenerated in order to lower the footprint below that of the conventional process. To further improve the technologies, other types of nanostructures could be examined as support for RubisCO immobilization to see if they lead to better LCIA results.

The analysis boundary of this LCA study was cradle-to-gate (cradle-to-use phase). The nanostructure-RubisCO complexes are assumed to be reusable 5,000–20,000 times. For a more complete LCA study, the disposal phase could be included to account for the impacts of waste treatment. Therefore, we need to investigate how the downstream processes of the complexes affect the overall carbon footprint. Currently, such experimental data are not available. In addition, impacts besides carbon footprint should also be considered.

Given the nascent nature of technologies, many challenges remain in conducting LCA for emerging technologies. Early-stage experimental data will not represent commercialized data since inventory data could highly depend on the production scale. In this study, we performed a sensitivity analysis to account for those uncertain data gaps. However, it is important to perform a robust LCA study using more realistic and data that is closer to the use of mature technologies at an industrial scale.

Author Contribution Kyuha Lee developed the LCA model, conducted the carbon footprint analysis, and took the lead in writing the chapter. Yuan Sun, Sriram Satagopan, and J. Parker Evans performed the experiments for RubisCO immobilization, biomimetic carbon fixation, and electrochemical coenzyme regeneration, respectively, and provided experimental process data for the LCA model. J. Parker Evans wrote Section 4.2.3 of the chapter. Jon R. Parquette, F. Robert Tabita, and Vishnu Baba Sundaresan guided the experimental work. Kyuha Lee, Sriram Satagopan, F. Robert Tabita, Jon R. Parquette, and Bhavik R. Bakshi discussed and proposed the

use phase of 3-PGA. Bhavik R. Bakshi guided the LCA work and edited the chapter. All authors provided critical feedback and contributed to the final version of the chapter. Jon R. Parquette and Bhavik R. Bakshi supervised the project.

Chapter 5: Toward a Framework for Multiscale Consequential Sustainable Process Design: Including the Effects of Economy and Resource Constraints

This chapter is adapted from the following paper: Lee, K., Ghosh, T., and Bakshi, B.R., "Toward Multiscale Consequential Sustainable Process Design: Including the Effects of Economy and Resource Constraints with Application to Green Urea Production in a Watershed." *Chemical Engineering Science* 207, 725–743, 2019.[6]

Decisions made by approaches that only consider the environmental domain could result in unexpected outcomes due to burdens shifting to economic and social domains. These consequences could occur through the entire supply chain at multiple spatial scales. In this work, the process-to-planet (P2P) multiscale modeling framework is integrated with the rectangular choice-of-technology (RCOT) consequential approach. The resulting RCOT-P2P multiscale technology choice modeling framework takes account of market effects, such as economic resource constraints, as a consequential approach for designing engineering systems and their supply chain networks. The integrated modeling framework can represent different stakeholders' interests by considering engineering, environmental, and economic dimensions. The

case study focuses on installation of a new green urea production system in a watershed where there are limited supplies of resources, such as water and land area. We identify how the adoption of new technologies could change and be limited by market constraints, as the urea demand increases. This multiscale consequential framework is useful for modeling substitution effects of emerging technologies while considering market effects.

5.1 Introduction

Existing life cycle approaches for sustainable process design (SPD) aim to develop production systems that have high efficiency, low cost, and low environmental impacts. An implicit assumption in these approaches is that the optimal solution is fully adopted by the market and society such that their environmental and economic benefits are completely realized. Conventional approaches are based on the attributional framework that shows the impacts of technologies and their life cycles on the unconstrained and unchanging economy. In practice, the extent to which a new technology is adopted depends on many non-technological factors such as its effect on market prices, constraints on the availability of raw materials and other resources, and human preferences. Ignoring such factors can result in suboptimal designs and decisions that may result in unintended harm. For example, most of the existing SPD literature like that in[119–122] aims to design engineering processes based on optimizing the trade-off between life cycle environmental and monetary objectives. The process-to-planet (P2P) multiscale modeling framework has been developed to account for the impacts of SPD on economy scale systems by integrating environmentally-extended input-output (EEIO) model.[13] The P2P approach seeks "sustainable" solutions in

designing engineering models in terms of multiple objectives, maximizing profits and minimizing impacts, while considering impacts at all scales.[123,124] The EEIO model has also been employed to capture the impacts of technologies on the global macroeconomic scale.[125] These approaches are also attributional in nature and ignore the consequences of introducing a new technology into the economy and their environmental impacts.

In the real world, however, the market does not always choose the "best" technology, and advanced technologies may not be adopted as much as industry may like or assume because of market constraints. For example, the production of a key feedstock or the capital investment for an advanced technology may not be enough to meet the market demand. Other economic or environmental resources, such as labor, water, minerals, and land area, along with competing alternatives may limit the use of the technology as well. Governmental regulations could also hinder in the adoption of a certain technology. In that case, the market selects among multiple technologies to satisfy the demand and to avoid violating regulations. Moreover, some economic agents may choose sub-optimal decisions for their subjective preferences.[18] Economic rebound may also occur if the more efficient new technology results in increased total resource use when adopted in society. In this sense, there are some gaps between engineering decisions based on technological advances and market decisions based on the economy and human preferences.

Consequential modeling approaches, such as consequential life cycle assessment (CLCA), try to capture the consequences of life cycle modeling decisions on the real world economy to fill those gaps.[19,20] For example, the CLCA modeling approach investigates the change in environmental impacts as a consequence of changes in the

production that is attributed to results from the ALCA approach. Many previous CLCA models are based on marginal data which are about temporal changes in most affected technologies.[21,22] However, the consequences of attributional approaches could be incurred across the entire economy.[23] More recent CLCA approaches utilize models of the economy, such as general or partial equilibrium models, to account for consequences on broader economic systems.[24–26] For process design, the use of economic models has been very limited. Voll et al. integrated market dynamics in designing wood-derived biofuel processes by considering the wood market and its price development using a partial equilibrium model.[126] The equilibrium model has also been applied in designing algal renewable diesel production systems while considering the consequences of design on the life cycle impacts.[127] These approaches are useful for including market price changes as a consequence in the model, but not suitable to assess consequences at a smaller scale because the sectoral or product resolution in the equilibrium models are usually very low.[18] Also, they do not take account of market constraints, such as economic resource constraints, addressed above, and lack a multiscale framework.

The rectangular choice-of-technology (RCOT) model has been developed to account for market constraints and multiple technology uses as a consequence of decisions in analyzing economic systems.[27,28] In the RCOT model, multiple technology options are represented as additional columns in the rectangular shaped commodity transaction matrix. Multiple technologies are chosen when the required amounts of economic resources (also known as economy factors) to satisfy the commodity demand are constrained by their maximum available amounts in the market. For instance, when the demand for an advanced technology is small, the market would only choose

the "best" technology option. However, if the demand is large enough to encounter limits on economy factors for the advanced technology, the market needs to choose a different technology or multiple technologies at the same time because the advanced technology cannot be fully operated to meet the demand. In this sense, the RCOT approach can reflect market effects as a consequence in the model. Also, since the RCOT approach considers multiple technology options and networks of economic activities, this approach can also be employed for supply chain management and design.

Another strength of the RCOT approach is that it could be applied to any spatial scale. One example is the Technology Choice Model (TCM) which applies the RCOT approach at the value chain scale to the process-based LCA model.[18] However, none of the previous studies apply the RCOT framework to multiscale models and to solve engineering design problems. Moreover, the importance of multiscale supply chain modeling and optimization studies has been emphasized to increase the overall profit of systems across spatial scales.[128] Therefore, there is a need for consequential modeling approaches that account for multiple spatial scales.

The importance of considering multiple spatial scales and market effects has been particularly highlighted in assessing environmental sustainability.[9] To avoid unintended harm of solutions for claiming sustainability, sustainability assessment methods must consider the following six necessary, but not sufficient requirements:

1. Consider the demand of ecosystem services (e.g., CO_2 emissions)

2. Consider the supply of ecosystem services (e.g., CO_2 sequestration by vegetation) to avoid ecological overshoot

3. Consider multiple spatial scales to avoid shifting of impacts across scales

4. Consider cross-disciplinary effects to avoid unexpected outcomes from other disciplinary domains

5. Consider temporal dynamics

6. Consider multiple environmental flows to capture their interactions

Most current sustainability assessment methods, such as conventional LCA approaches, account for Requirements 1 and partially 3. Requirement 2 is taken into consideration by the Techno-Ecological Synergy framework.[10,35,129,130] In this work, we will mainly address Requirements 3 and 4 by expanding the spatial system boundary to the planetary scale and by considering market effects and interactions between technological, environmental and economic domains.

To construct the consequential modeling framework that accounts for multiple spatial scales, the RCOT framework is integrated with the P2P multiscale modeling framework.[13,123,124] The integrated RCOT-P2P framework accounts for the market effects and economic resource availability in designing process engineering models. The RCOT-P2P framework gives the flexibility to design process engineering models not only with respect to profits and environmental impacts but also with respect to market conditions and market consequences. The rest of this chapter is organized as follows. In Section 5.2, the background of previous modeling approaches is described. In Section 5.3, we introduce the RCOT-P2P modeling framework in detail. In Section 5.4, the RCOT-P2P framework is applied in designing green urea production systems in the Muskingum River Watershed in Ohio. The recent trend of deglobalization[131] and the potential need for hydrogen storage in ammonia and urea[132,133] are considered

for this case study. Finally, in Section 5.5, we discuss the potential usefulness of RCOT-P2P framework and future research directions.

5.2 Background

Sustainability is a research area that needs to cut across disciplinary boundaries. To avoid shifting of impacts across disciplinary boundaries, as described in Requirement 4 in the previous section, these disciplines need to connect with each other. One of the well-known approaches that shows how sustainability is a comprehensive subject is a triple bottom line approach.[134,135] The triple bottom lines represent economic (e.g., gross profit and market effects), social (e.g., health indicators and human behaviors), and environmental (e.g., pollution and resource depletion) factors. In this approach, those factors need to be accounted for in addressing sustainability. Due to the highly interdisciplinary nature of this subject, therefore, it is crucial to understand the background from different disciplines.

Each discipline often considers different stakeholders and objectives. For instance, engineers have mainly focused on improving the physical efficiency of devices and plant profits within a relatively small system boundary (e.g., a manufacturing site or its supply chain). On the other hand, industrial ecologists have put their efforts into reducing environmental interventions and protecting natural ecosystems. Also, economists have considered a large system boundary, such as the entire economy of a given region. For sustainability research, none of the perspectives should be overlooked not only because every discipline and its associated stakeholder engage in the decision-making process, but also because decisions from each discipline could interact with the decisions of other disciplines. As mentioned in Section 5.1, one

of the requirements for the sustainability assessment methods is to consider multi-disciplinary domains and recognize interactions between them.[9]

In this section, we provide a brief history and background of how existing approaches from various disciplines have been developed and how they satisfy the requirements for sustainability assessment methods. The existing approaches include sustainable process design (SPD), life cycle assessment (LCA), process-to-planet (P2P) multiscale modeling framework, and rectangular choice-of-technology (RCOT) model. Figure 5.1 shows the development flow of each approach and Table 5.1 summarizes how each approach satisfies the requirements for sustainability assessment methods. Two of the six requirements (considering temporal dynamics and considering multiple flows) are excluded from the table since these requirements mostly depend on the scope of study regardless of the approaches selected.

5.2.1 Sustainable Process Design

Traditional process design and supply chain management (SCM) approaches have been studied for decades to enhance productivity by maximizing profits and efficiencies of processes.[136] The main purpose of process design and SCM is to design process systems and their associated supply chain networks by determining process operating conditions and the quantity and location of supply chain components over the network.

To address an environmental dimension to improve the sustainability of process systems throughout the supply chain, sustainable process design (SPD)[137,138] and sustainable supply chain management (SSCM)[139] approaches have been developed.

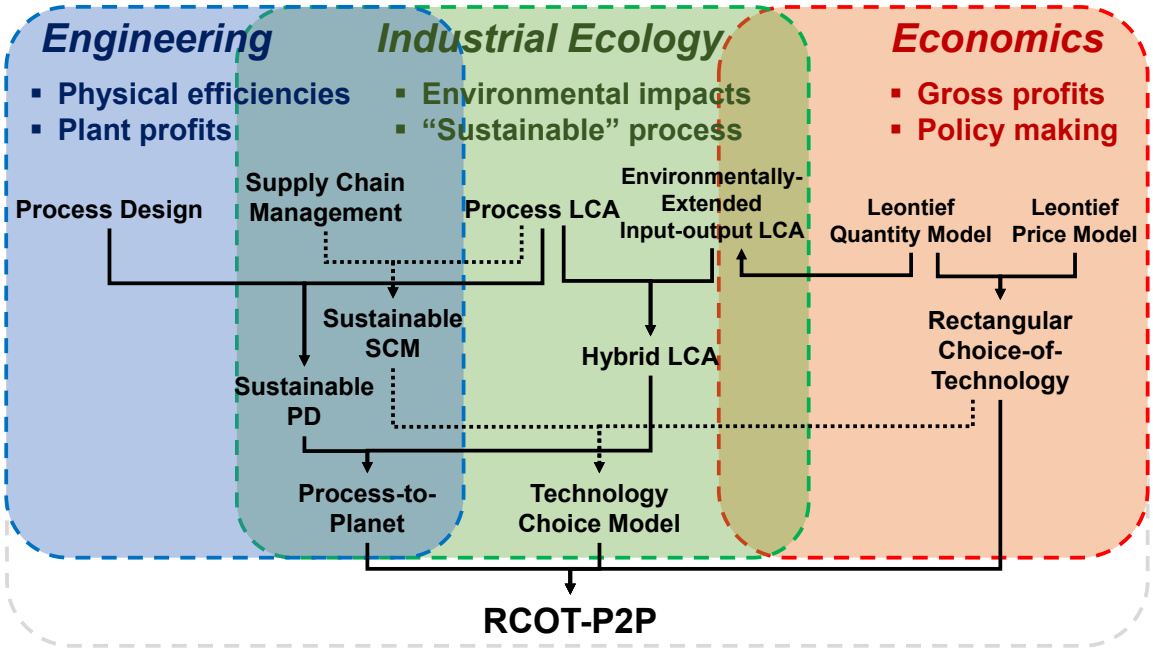

Figure 5.1: Relation between approaches from three disciplines to evaluate sustainability.

These approaches consider environmental impacts from the processes and each supply chain entity by employing LCA-based environmental impact indicators. Many studies consider environmental indicators, such as carbon footprint or other univariate life cycle impact indicators, and profits as a productivity indicator, then identify "sustainable" designs by solving multi-objective optimization problems. However, studies that address an economic dimension in process design still lack an integrated modeling framework that combines engineering, environmental, and economic dimensions. Such a framework needs to be developed to account for market circumstances in designing process systems and supply chain networks.

Since the SPD and SSCM approaches utilize LCA data, the scope of these approaches is analogous to LCA, but this scope is often limited to the activities that

are immediately related to overall profits.[140] Therefore, many SPD and SSCM approaches are economically driven and more related to the field of process systems engineering and operations research than to sustainability science and engineering.

Table 5.1: Characteristics of modeling approaches. [1]Eq: Equipment scale, VC: Value chain scale, E: Economy scale.

Approach	**Goal of the model**	**Objective for decision-marking**	**Requirements for Sustainability Assessment Methods**			
			Demand of ecosystem	**Supply of ecosystem**	**Spatial scale[1]**	**Cross-disciplinary effects**
Process design & supply chain management (SCM)	Design of process systems and supply chains (network, quantity, and location, etc.)	Max profits	-	-	Eq & VC	-
Sustainable process design (SPD) & sustainable SCM (SSCM)	Design of process systems and supply chains with sustainability goals	Max profits Min impacts	Considered	-	Eq & VC	-
Process-based life cycle assessment (P-LCA)	Sustainability assessment	Min impacts	Considered	-	VC	Marginal consequences considered (CLCA)
Environmentally-extended input output LCA (EEIO-LCA)	Sustainability assessment	Min impacts	Considered	-	E	Marginal consequences considered (CLCA)
Hybrid LCA	Sustainability assessment	Min impacts	Considered	-	VC & E	Marginal consequences considered (CLCA)
Process-to-planet (P2P)	Design of process systems with sustainability assessment	Max profits Min impacts	Considered	-	Eq, VC, & E	-
Retangular choice-of-technology (RCOT)	Design of supply chains with factor cost assessment	Min factor costs	Considered	Resource availability considered	E	Market effects considered
Technology choice model (TCM)	Design of supply chains with factor cost assessment	Min factor costs	Considered	Resource availability considered	VC	Market effects considered
RCOT-P2P	Design of process systems and supply chains with sustainability and factor cost assessments	Max profits Min impacts Min factor costs	Considered	Resource availability considered	Eq, VC, & E	Market effects considered

5.2.2 Life Cycle Assessment

LCA approaches are environmentally driven and aim to identify hot-spots in terms of environmental impacts by comparing how two or more product systems differ from each other. Nobel prize-winning economist, W. Leontief has developed the economic input-output (IO) model (also called the Leontief quantity model).[141] This model quantifies the transactions of commodities between economy sectors and accounts for the economy scale. The system boundary of the IO model could be at sub-national, national or global scales. The quantified commodity transaction is represented by the direct requirements matrix ($\overline{A}$) in Table 5.2. The commodity transaction in terms of the economy scale commodity demand ($\overline{y}$) is expressed as $(I - \overline{A})\ \overline{x} = \overline{y}$. $\overline{x}$ refers to the throughput from economy sectors. The environmentally-extended IO (EEIO) model has also been developed for sustainability assessment by adding environmental intervention information to the IO model.[142,143] Since the EEIO model represents the entire economy of a given region, it is also a top-down LCA approach. The intervention data for each economic activity is represented by the economy scale interventions matrix ($\overline{B}$) in Table 5.2. The environmental interventions ($\overline{g}$) are calculated from $\overline{B}\ \overline{x} = \overline{g}$. Details about $\overline{A}$ and $\overline{B}$ matrices, and the mathematical formulation are described in Section 5.3.2. With trade-offs of "completeness" of system boundary in the EEIO models, this model usually lacks data at a fine resolution because it is practically impossible to have all detailed economic transaction data with fine resolution for the entire economy. On the other hand, the process-based LCA (P-LCA) approach has opposite characteristics. The P-LCA model is based on detailed process input and output data that are represented by the technology matrix ($\underline{X}$) and value chain scale interventions matrix ($\underline{B}$) as shown in Table 5.2, but omits some activities

whose impacts are assumed insignificant. This approach is called the bottom-up LCA approach.

The hybrid LCA approach is the integrated LCA model that connects excluded activities from the P-LCA model with the EEIO LCA model.[12] In the integrated hybrid LCA model, the cutoff flows between the P-LCA and EEIO LCA models ($\underline{X}_u$ and $\underline{A}_d$ in Table 5.2) are identified and the EEIO model is disaggregated from the P-LCA model to avoid double-counting of processes of the P-LCA model. Further details about disaggregation are provided in Section 5.3.2.

Many LCA approaches provide retrospective information using average data, and thus, these are attributional LCA (ALCA) approaches. On the other hand, the consequential LCA (CLCA) approach considers the consequences of a decision by including impacts from other domains.[19,20] Many CLCA approaches try to identify marginal technologies that cause changes in impacts.[21,22] Recently, partial and general equilibrium models are combined with the LCA models to include economic consequences (e.g., the elasticity of price) endogenously in the model.[24–26] As mentioned in Section

Table 5.2: Mathematical formulation of LCA-derived modeling approaches. Underbar and overbar notations refer to the value chain scale and the economy scale, respectively. The notation without bar represents the equipment scale. The double bar notation refers to multiple scales.

Model	Transaction equation	Environmental intervention equation
P-LCA	$\underline{X}\,\underline{s} = \underline{y}$	$\underline{B}\,\underline{s} = \underline{g}$
EEIO	$(I - \overline{A})\,\overline{x} = \overline{y}$	$\overline{B}\,\overline{x} = \overline{g}$
Hybrid LCA	$\begin{bmatrix} I - \overline{A}^* & -\underline{X}_u \\ -\underline{A}_d & \underline{X} \end{bmatrix} \begin{bmatrix} \overline{s} \\ \underline{s} \end{bmatrix} = \begin{bmatrix} \overline{y} \\ \underline{y} \end{bmatrix}$	$\begin{bmatrix} \overline{B}^* & \underline{B} \end{bmatrix} \begin{bmatrix} \overline{s} \\ \underline{s} \end{bmatrix} = \overline{\underline{g}}$
P2P	$\begin{bmatrix} I - \overline{A}^*(\{z\}) & -\underline{X}_u(\{z\}) & -X_u^E(\{z\}) \\ -\underline{A}_d(\{z\}) & \underline{X}^*(\{z\}) & -X_u^V(\{z\}) \\ -A_d^E(\{z\}) & -X_d^V(\{z\}) & X(\{z\}) \end{bmatrix} \begin{bmatrix} \overline{s} \\ \underline{s} \\ s \end{bmatrix} = \begin{bmatrix} \overline{y} \\ \underline{y} \\ y \end{bmatrix}$	$\begin{bmatrix} \overline{B}^*(\{z\}) & \underline{B}^*(\{z\}) & B(\{z\}) \end{bmatrix} \begin{bmatrix} \overline{s} \\ \underline{s} \\ s \end{bmatrix} = \overline{\underline{g}}$

5.1, however, equilibrium models are based on aggregated data with low sectoral or product resolution and do not consider economic resource constraints as a consequence of decisions.

5.2.3 Process-to-Planet Multiscale Modeling Framework

In accordance with the multiscale concept of the hybrid LCA approach, the process-to-planet (P2P) modeling framework has been developed to account for multiple spatial scales from the detailed engineering model to the planetary system.[13,123,124] The P2P multiscale modeling framework is based on an integrated model of conventional sustainable process design (SPD) and hybrid LCA. It includes the equipment scale engineering model that has been addressed by the traditional process design approach, the value chain scale process-based LCA model by connecting feedstock inputs of the equipment scale model to upstream value chain scale processes, and the economy scale EEIO LCA model to account for the comprehensive planetary system boundary. Therefore, the P2P model can design engineering systems while assessing sustainability for the entire economy of a given region. The P2P approach meets Requirement 3 of sustainability assessment methods more completely by accounting for multiple spatial scales to avoid shifting of impacts across these scales. It can also provide better designs due to the use of integrated multiscale models, as illustrated in.[123,124] However, it is an attributional modeling approach since it does not consider any consequences from economic or social domains. Thus, designs obtained from the current P2P model are also assumed to fully replace an alternative technology. However, the framework is general enough and may be extended toward consequential modeling, as is done in this work.

5.2.4 Rectangular Choice-of-Technology Modeling Framework

The RCOT modeling framework has been developed to account for market effects as a consequence from the economic domain.[27,28] The RCOT approach has the following three distinct features.

1. Multiple technology choices: In the traditional economy scale IO model, the transaction matrix ($\overline{A}$) that contains commodity exchanges between economy sectors is the square matrix as shown below. That is, the number of commodities (i) is equal to the number of sectors (j). In the RCOT model, the transaction matrix becomes rectangular with additional columns ($\overline{A}'$). The additional third column as shown below ($\{\overline{a}'_{12}, \overline{a}'_{22}, \overline{a}'_{32}, \cdots, \overline{a}'_{i2}\}$) represents an additional technology that produces the same commodity as the second column technology ($\{\overline{a}_{12}, \overline{a}_{22}, \overline{a}_{32}, \cdots, \overline{a}_{i2}\}$) but has a different input structure.

$$\overline{A} = \begin{bmatrix} \overline{a}_{11} & \overline{a}_{12} & \overline{a}_{13} & \cdots & \overline{a}_{1j} \\ \overline{a}_{21} & \overline{a}_{22} & \overline{a}_{23} & \cdots & \overline{a}_{2j} \\ \overline{a}_{31} & \overline{a}_{32} & \overline{a}_{33} & \cdots & \overline{a}_{3j} \\ \vdots & \vdots & \vdots & \ddots & \vdots \\ \overline{a}_{i1} & \overline{a}_{i2} & \overline{a}_{i3} & \cdots & \overline{a}_{ij} \end{bmatrix} \quad \longrightarrow \quad \overline{A}' = \begin{bmatrix} \overline{a}_{11} & \overline{a}_{12} & \overline{a}'_{12} & \overline{a}_{13} & \cdots & \overline{a}_{1j} \\ \overline{a}_{21} & \overline{a}_{22} & \overline{a}'_{22} & \overline{a}_{23} & \cdots & \overline{a}_{2j} \\ \overline{a}_{31} & \overline{a}_{32} & \overline{a}'_{32} & \overline{a}_{33} & \cdots & \overline{a}_{3j} \\ \vdots & \vdots & \vdots & \vdots & \ddots & \vdots \\ \overline{a}_{i1} & \overline{a}_{i2} & \overline{a}'_{i2} & \overline{a}_{i3} & \cdots & \overline{a}_{ij} \end{bmatrix}.$$

2. Market effect consideration: The RCOT approach introduces economy factor flows in the model. Economy factors could be any kind of economic resources that are used by activities. The factors include labor, capital, water, minerals, land, etc. The available amounts of these economy factors depend on geographic location and market conditions. In the RCOT model, market effects are accounted for in a way that economy factor consumption from each activity ($\overline{F}\ \overline{x} = \overline{c}$) is calculated and constrained by their maximum available amounts

(c_{max}). $\overline{F}$ is the economy factor requirement matrix, which contains information about the required amounts of economy factors normalized by each sector's throughput ($\overline{x}$). $\overline{F}$ matrix has a unit of economy factor per dollar (e.g., labor cost/$ and gallons of water/$). From the economy factor equation above, total economy factor consumption ($\overline{c}$) is calculated. It includes the direct and indirect consumption of each economy factor. By constraining the available amounts of economic factors in the market ($\overline{c} \leq c_{max}$), multiple technologies can be chosen simultaneously to satisfy the market demand if the cheapest technology option is not able to meet the demand due to the market constraints.

3. Total factor cost assessment: Total factor costs associated with the final demand are calculated using $Z = \hat{\kappa}\overline{F}\ \overline{x}$. κ is the unit price of each economy factor. Minimizing total factor costs (Z) corresponds to the functional objective of the RCOT approach. Therefore, the RCOT model can design supply chain networks to minimize total factor costs.

The RCOT approach is a consequential approach that considers market constraints in choosing the use of multiple technologies. Since the RCOT approach is based on the IO model, however, the approach is only for the economy scale. The RCOT framework has also been applied to the P-LCA model at the value chain scale.[18] Many case studies based on the RCOT framework have focused on the choice of competing technologies across multiple regions by considering region-specific market constraints.[18,144–146] However, none of the previous studies apply the RCOT framework to multiscale models and solve engineering design problems.

5.3 RCOT-P2P: Multiscale Technology Choice Modeling Framework

In this section, we will introduce the RCOT-P2P multiscale technology choice modeling framework. As shown in Fig 5.1 and Table 5.1, the RCOT-P2P framework integrates P2P, TCM, and RCOT frameworks. This framework enables the design of engineering models with assessing the sustainability of systems while accounting for the entire economy of a given region. At the same time, it designs the supply chain network of process systems for the entire economy and assesses total costs for the economy factor consumption. Therefore, the RCOT-P2P framework contains three distinct categories of decision variables: Engineering, environmental, and economic. Engineering decision variables are from the engineering model, such as profits and net present value (NPV). Environmental decision variables refer to the environmental interventions calculated across all spatial scales. Life cycle impact assessment indicators, such as total greenhouse gas emissions, correspond to this category. Lastly, economic decision variables correspond to the total economy factor costs consumed to produce the required amounts of final demands.

5.3.1 Model and Data Collection

The RCOT-P2P framework needs to be formulated to encompass those decision variables, and thus, it requires various types of data. First, depending on the goal of the study, specific engineering models at the equipment scale are needed. The model could contain detailed nonlinear and complex equations based on mass and energy balance relations. The model only covers the relatively small scale of the engineering

system boundary by including direct inputs (e.g., feedstock and energy flows) and direct outputs (e.g., product, waste, and emission flows).

To include life cycle upstream and downstream activities, the engineering model needs to be connected with LCA models. Figure 5.2 exhibits one example of how the engineering model could be connected with LCA models. The P-LCA model contains value chain scale processes that are connected to the inputs and outputs from the engineering model, while the EEIO model includes the transactions of commodities at the entire scale. The P-LCA model consists of multiple process inventory data. Each inventory contains process input and output data that include product flows between processes and environmental intervention flows from processes. Those physically quantified inventory data can be obtained from existing life cycle inventory (LCI) database, such as the U.S. Life Cycle Inventory Database (USLCI),[40] ecoinvent,[43] etc.

Although the P-LCA model accounts for many life cycle activities, it omits some processes whose impacts are not considered to be significant enough. Also, the existing LCI database often does not have inventory data for some products. For instance, the USLCI database identifies unavailable inventory data as "CUTOFF flows." Thus, the P-LCA model does not reflect the entire economy. Excluded activities from the P-LCA model need to be brought from the EEIO model that reflects the entire economy. The EEIO model consists of two types of data: economy input-output data and environmental intervention data. The input-output data represent monetary transactions between economy sectors in the entire economy of a given region. The number of economy sectors could be varied a lot depending on how much data are aggregated in the database. The U.S. BEA has input-output data for the entire US economy.[44] The environmental intervention data could be found from multiple

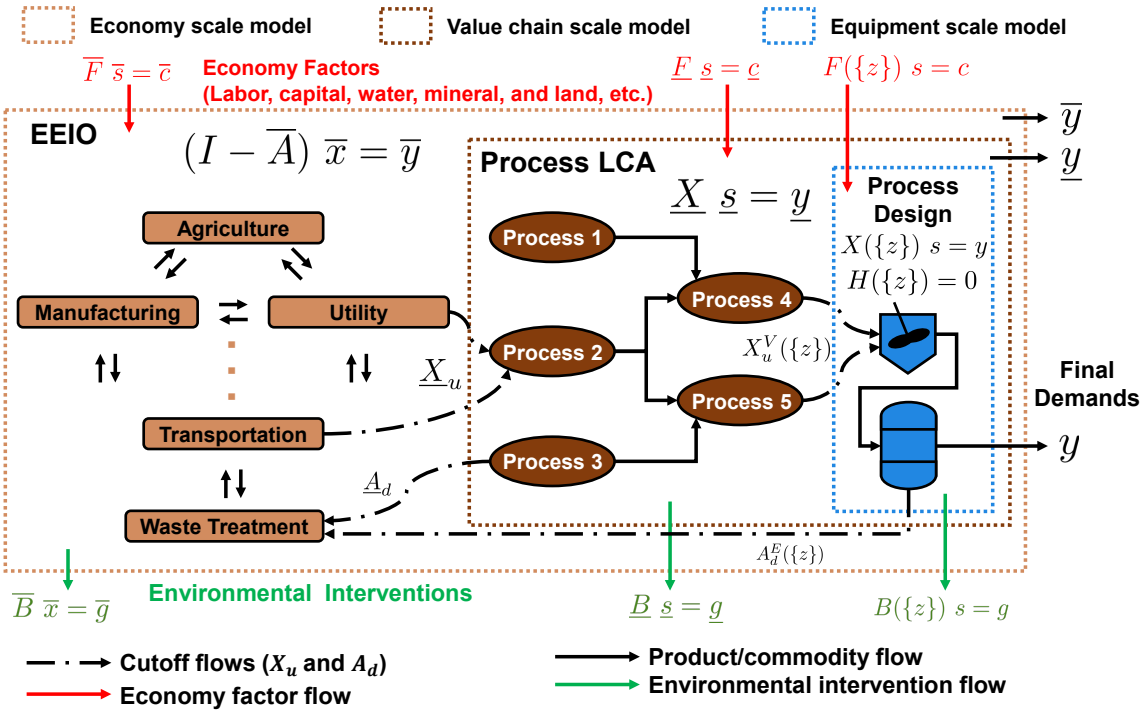

Figure 5.2: Model structure of the RCOT-P2P framework.

sources. For example, the U.S. national greenhouse gas (GHG) emissions and air emissions data are available from government sources.[47,49] Also, the USEEIO model compiles various intervention data from multiple sources for the year 2013.[39]

The RCOT-P2P framework introduces economy factor flows in the model. Therefore, economy factor requirement data need to be collected for every activity in the model. For instance, the U.S. BEA input-output database provides labor costs that are required for each sector to produce commodities.[44] The USEEIO model has data about economic resource uses, such as land, water, minerals, and energy uses.[39] Also, to reflect market constraints to the model as a consequential approach, the maximum

available amounts of economy factors in a given region need to be identified. For example, the land area and water supply for farming activities are not infinite resources in a certain region.

All data in the U.S. BEA input-output database are coded with the North American Industry Classification System (NAICS).[147] Thus, when collecting U.S. economy scale data, such as GHG emissions and labor costs, all data should be classified in the NAICS code.

5.3.2 Mathematical Formulation

Transaction and Intervention Equations

The RCOT-P2P modeling framework is formulated in a fully-quantitative way like most of the LCA-derived methods. One of the compelling strengths in the LCA approach is that each process and activity from multiple spatial scales can be expressed in matrix notation as an integrated model.[12,13] Table 5.2 shows transaction equations and environmental intervention equations for each of the LCA-derived approach. Underbar and overbar notations refer to the value chain scale and the economy scale, respectively. The notation without bar represents the equipment scale. The double bar (underbar and overbar) notation refers to multiple scales.

In the P-LCA model as shown in Table 5.2, $\underline{X}$ is called the technology matrix that contains the physical transaction data of products between value chain scale processes. $\underline{y}$ is a final demand vector in physical units at the value chain scale and $\underline{s}$ is a scaling vector of each value chain scale process to meet the final demand. Thus, the physical balance of value chain scale products can be formulated as $\underline{X}\ \underline{s} = \underline{y}$.

In the EEIO model, on the other hand, $\overline{A}$ represents the commodity-by-commodity direct requirements matrix, which contains data about the direct requirement of

each input commodity to produce each output commodity. $\overline{x}$ is the total monetary throughput from each economy sector. It is equal to the sum of final commodity demands ($\overline{y}$) and other commodity consumption ($\overline{A}\ \overline{x}$) for producing the final demand. Thus, $\overline{x}$ is calculated as $\overline{x} = \overline{A}\overline{x} + \overline{y}$ and the monetary balance at the economy scale is formulated as $(I - \overline{A})\ \overline{x} = \overline{y}$, as shown in Fig. 5.2 and Table 5.2. $\overline{x}$ can be interpreted as the scaling vector of each economy sector in a monetary unit ($\overline{s}$), and thus, $\overline{x}$ and $\overline{s}$ are interchangeable.

The hybrid LCA approach combines the P-LCA model at the value chain scale with the EEIO model at the economy scale.[12] The hybrid LCA approach accounts for the national/planetary system boundary of the EEIO model while employing the details of data from the P-LCA model. In such an integrated LCA model, matrices at different scales are connected with each other via upstream and downstream cutoff flows. The upstream cutoff matrix ($\underline{X}_u$) represents the flows from the economy scale to the value chain scale processes. The upstream cutoff flow corresponds to the product flow whose process inventory data are missing from the P-LCA model. On the other hand, the downstream cutoff matrix ($\underline{A}_d$), which is normalized by the total monetary throughput of each economy sector ($\underline{A}_d = \underline{X}_d\hat{\overline{x}}^{-1}$), represents the flows from the value chain scale to the economy scale sectors. $\underline{A}_d$ is the normalized downstream cutoff matrix and $\underline{X}_d$ is the original downstream cutoff matrix. $\underline{B}$ and $\overline{B}$ matrices are the environmental intervention matrices that contain data about direct interventions from each value chain process and each economy sector, respectively. In the hybrid LCA model, the scaling vectors at each value chain and economy scale ($\overline{s}$, $\underline{s}$) are determined through the transaction equation, as shown in Table 5.2. The total environmental

interventions ($\overline{g}$), which include direct and indirect impacts at the value chain and economy scales, are calculated through the environmental intervention equation.

An asterisk mark on economy scale matrices ($\overline{A}^*$ and $\overline{B}^*$) indicates disaggregated economy scale matrices that remove overlaps between economy and value chain scale models to avoid double counting. The disaggregation of economy scale matrices is necessary for the integration of different scale models because activities at the smaller scales (including product transactions and interventions) are included in the broader system boundary of the economy scale model. Since the commodity-by-commodity direct requirements matrix at the economy scale ($\overline{A}$) has no unit while the technology matrix at the value chain scale ($\underline{X}$) has physical units, the disaggregation needs to be carried out from the economy scale make ($\overline{V}$) and use ($\overline{U}$) matrices whose data for the U.S. are available online.[44] The $\overline{A}$ matrix can be obtained from the $\overline{V}$ and $\overline{U}$ matrices using[148]

$$\overline{A} = \overline{U}(\overline{V}^T)^{-1}. \tag{5.1}$$

The $\overline{V}$ matrix represents the production of commodities from each economy sector, while $\overline{U}$ matrix represents the use of commodities in each sector. The technology matrix at the value chain scale ($\underline{X}$) can also be divided into the value chain scale make ($\underline{V}$) and use ($\underline{U}$) matrices using $\underline{X} = \underline{V}^T - \underline{U}$. Accordingly, the economy scale commodity transaction matrices are disaggregated from the value chain product transaction matrices as follows:[13]

$$\begin{aligned}
\overline{V}^* =& \overline{V} - (P_P)^T \underline{\hat{p}}\,\underline{V}(P_F)^T \\
\overline{U}^* =& \overline{U} - (P_F \underline{\hat{p}}\,\underline{U} P_P + P_F \underline{\hat{p}}\,\underline{X}_d + \underline{X}_u P_P).
\end{aligned}$$

The second term of the right-hand side of above equations corresponds to the overlaps between the economy and value chain scales. $\underline{\hat{p}}$ is a diagonalized price vector for value chain scale products to convert their physical units to the monetary unit. P_P and P_F are permutation matrices to assign value chain processes to the corresponding economy sectors and to relate value chain products to the corresponding economy commodities, respectively. The elements in $P_P(n, j)$ are 1 if value chain process n can be included in the economy sector j. Also, the elements in $P_F(i, m)$ are 1 if value chain product m can belong to the economy commodity i. The other elements in both P_P and P_F are all 0. $\underline{X}_d$ and $\underline{X}_u$ are, respectively, the downstream and upstream cutoff flow matrix between the value chain scale and the economy scale. From the disaggregated $\overline{U}^*$ and $\overline{V}^*$ matrices, the disaggregated $\overline{A}^*$ matrix is obtained using $\overline{A}^* = \overline{U}^*(\overline{V}^{*T})^{-1}$.

Likewise, the economy scale interventions matrix ($\overline{B}$) needs to be disaggregated from the value chain scale interventions matrix ($\underline{B}$). Since $\overline{B}$ has a unit of intervention per dollar while $\underline{B}$ has a unit of intervention, the economy scale total interventions matrix ($\overline{R}$), which has a unit of intervention, needs to be disaggregated from $\underline{B}$ using[13]

$$\overline{R}^* = \overline{R} - \underline{B}P_P, \text{ where } \overline{R} = \overline{B}\hat{\overline{x}}.$$

Accordingly, the disaggregated $\overline{B}^*$ matrix is calculated from $\overline{B}^* = \overline{R}^*\hat{\overline{x}}^{*-1}$. $\overline{x}^*$ is the total throughput from disaggregated economy sectors. In other words, $\overline{x}^*(j) = \sum_i \overline{V}^*(j, i)$, where i's are commodities and j's are sectors.

The P2P multiscale modeling framework is an extended version of the hybrid LCA framework.[13,123,124] It includes the detailed equipment scale engineering model, which is intended to solve process design problems. Process design variables ($\{z\}$) in the equipment scale model are spread out to the larger scale models through the

disaggregation of the larger scale models as follows:[13]

$$\overline{V}^*(\{z\}) = \overline{V} - (P_P)^T \hat{\underline{p}} \underline{V} (P_F)^T - (P_P^E)^T \hat{p} V(\{z\}) (P_F^E)^T$$

$$\overline{U}^*(\{z\}) = \overline{U} - (P_F \hat{\underline{p}} \underline{U} P_P + P_F \hat{\underline{p}} \underline{X}_d + \underline{X}_u P_P) - (P_F^E \hat{p} U(\{z\}) P_P^E + P_F^E \hat{p} X_d^E(\{z\}) + X_u^E(\{z\}) P_P^E)$$

$$\overline{R}^*(\{z\}) = \overline{R} - \underline{B} P_P - B(\{z\}) P_P^E.$$

The third term in the right-hand side of each equation corresponds to the overlaps between the economy and equipment scales. The disaggregated direct requirements matrix ($\overline{A}^*$) and disaggregated interventions matrix at the economy scale ($\overline{B}^*$) are obtained from $\overline{A}^* = \overline{U}^* (\overline{V}^{*T})^{-1}$ and $\overline{B}^* = \overline{R}^* \hat{\overline{x}}^{*-1}$, respectively.

When there are overlaps between value chain and equipment scales, the value chain scale matrices also need to be disaggregated from the equipment scale matrices using[13]

$$\underline{V}^*(\{z\}) = \underline{V} - (P_P^V)^T \hat{p} V(\{z\}) (P_F^V)^T$$

$$\underline{U}^*(\{z\}) = \underline{U} - (P_F^V \hat{p} U(\{z\}) P_P^V + P_F^V \hat{p} X_d^V(\{z\}) + X_u^V(\{z\}) P_P^V)$$

$$\underline{B}^*(\{z\}) = \underline{B} - B(\{z\}) P_P^V.$$

The disaggregated technology matrix at the value chain scale, $\underline{X}^*(\{z\})$, is calculated from $\underline{X}^*(\{z\}) = \underline{V}^*(\{z\})^T - \underline{U}^*(\{z\})$. The detailed procedures for disaggregating the economy scale and value chain scale matrices are described in previous work.[13] The P2P transaction and intervention equations are represented as shown in Table 5.2. Notations for the P2P transaction and intervention equations can be simplified as $\overline{\underline{X}}^*(\{z\})\ \overline{\underline{s}} = \overline{\underline{y}}$ and $\overline{\underline{B}}^*(\{z\})\ \overline{\underline{s}} = \overline{\underline{g}}$, respectively. Through these equations, the P2P approach can solve the process design problems at the equipment scale while accounting for activities at the value chain and economy scales.

Economy Factor Equation

The RCOT-P2P framework in this work is an extension of the aforementioned LCA-derived approaches to account for the economic consequence of the previous approaches. Unlike other approaches, the RCOT-P2P framework requires a third equation, which is the economy factor equation:

$$\begin{bmatrix}\overline{F}^*(\{z\}) & \underline{F}^*(\{z\}) & F(\{z\})\end{bmatrix}\begin{bmatrix}\overline{s}\\ \underline{s}\\ s\end{bmatrix} = \overline{c} \quad \text{or} \quad \overline{\underline{F}}^*(\{z\})\,\overline{\underline{s}} = \overline{\underline{c}}. \tag{5.2}$$

In the same manner as the disaggregation of economy scale matrices from the P2P approach ($\overline{A}^*(\{z\})$ and $\overline{B}^*(\{z\})$), economy factor requirement matrices at the larger scales (e.g., $\overline{F}$) need to be disaggregated from the smaller scales (e.g., $\underline{F}$ and F) to remove the overlaps between multiple spatial scales. When disaggregating the economy scale $\overline{F}$ matrix, the total economy factor requirement matrix at the economy scale ($\overline{Q}$) is used instead of $\overline{F}$. This is because the economy scale $\overline{F}$ matrix has a different unit from the value chain scale $\underline{F}$ matrix and equipment scale F matrix. While the economy scale $\overline{F}$ matrix has a unit of economy factor per dollar (e.g., gallons of water/\$), the value chain scale $\underline{F}$ matrix and equipment scale F matrix have a unit of economy factor (e.g., gallons of water). To disaggregate the economy scale $\overline{F}$ matrix, therefore, the $\overline{F}$ matrix needs to be converted to the total economy factor requirement matrix ($\overline{Q}$), which has a unit of economy factor (e.g., gallons of water). The $\overline{Q}$ matrix contains information about the total direct economy factor consumption from each economy sector. The disaggregation of $\overline{Q}$ matrix is performed using

$$\overline{Q}^*(\{z\}) = \overline{Q} - \underline{F}P_P - F(\{z\})P_P^E, \text{ where } \overline{Q} = \overline{F}\hat{\overline{x}}.$$

The second and third terms of the right-hand side of equation represent the overlaps of economy scale with value chain scale and equipment scale, respectively. After the disaggregation of the $\overline{Q}$ matrix, the disaggregated total economy factor requirement matrix ($\overline{Q}^*(\{z\})$) is normalized by the throughput from disaggregated sectors ($\overline{x}^*$) to obtain the disaggregated economy factor requirement matrix ($\overline{F}^*(\{z\})$), as shown below.

$$\overline{F}^*(\{z\}) = \overline{Q}^*(\{z\})\hat{\overline{x}^*}^{-1}.$$

If there are overlaps between value chain and equipment scales, the value chain economy factor requirement matrix ($\underline{F}$) is also disaggregated from the equipment scale economy factor requirement matrix ($F(\{z\})$), as shown below.

$$\underline{F}^*(\{z\}) = \underline{F} - F(\{z\})P_P^V.$$

As mentioned in Section 5.3.2, the disaggregated matrices from the equipment scale (e.g., $\overline{F}^*(\{z\})$ and $\underline{F}^*(\{z\})$) contain equipment scale design variables.

Rectangular Shape of Matrices

The RCOT framework considers multiple technologies that produce the same product. To account for multiple technology options, additional columns that represent multiple technologies are added to the original square shape of economy scale matrices. Each technology (each column) has a different input structure, consumes different amounts of economy factors, and emits different amounts of emissions. The attributional approach only selects the "best" technology among the technology options. In the RCOT consequential approach, however, the "best" technology may not be able to meet its demand if the economy factors required for the "best" technology

are not sufficient. In that case, the RCOT model chooses multiple technologies simultaneously to satisfy the demand because the economy factor constraints limit the extend to which the "best" technology may be used.[27,28]

In the hybrid LCA and P2P approaches, the square shaped economy scale make ($\overline{V}$) and use ($\overline{U}$) matrices are combined to provide the square shaped commodity-by-commodity direct requirements matrix ($\overline{A}$) using Equation 5.1. Both, rows and columns in the $\overline{A}$ matrix represent the commodity, not the sector or technology. This may cause a problem when applying the RCOT approach to the P2P framework because the $\overline{A}$ matrix will always be of square shape from Equation 5.1, despite the rectangular shape of $\overline{V}$ and $\overline{U}$ matrices. Therefore, the square shape of the commodity-by-commodity direct requirements matrix ($\overline{A}$) needs to be a rectangular shape by dividing one column into two or more columns. The resulting columns that are divided from one column refer to the same commodity produced by different technologies.

When dividing one column into multiple columns, we need to utilize knowledge about multiple technologies that have different input structures, economy factor requirements, and emissions. Each cell ($\overline{a}_{ij}$) in the $\overline{A}$ matrix represents the coefficient about the direct requirement of an input commodity (i) to produce one dollar amount of the output commodity (j). If there are two technologies (j_1 and j_2) that produce the same commodity j, each cell ($\overline{a}_{ij}$) in the column j can be divided into two cells ($\overline{a}_{ij_1}$ and $\overline{a}_{ij_2}$). Otherwise, the coefficient $\overline{a}_{ij}$ in the column j treats both technologies (j_1 and j_2) as single technology. The divided cells ($\overline{a}_{ij_1}$ and $\overline{a}_{ij_2}$) are obtained as

shown below.

$$\overline{a}_{ij_1} = \overline{a}_{ij} \times \frac{\overline{u}_{ij_1}/\overline{x}_{j_1}}{\overline{u}_{ij_1}/\overline{x}_{j_1} + \overline{u}_{ij_2}/\overline{x}_{j_2}} \quad \text{and} \quad \overline{a}_{ij_2} = \overline{a}_{ij} \times \frac{\overline{u}_{ij_2}/\overline{x}_{j_2}}{\overline{u}_{ij_1}/\overline{x}_{j_1} + \overline{u}_{ij_2}/\overline{x}_{j_2}}, \quad \text{where} \quad \overline{a}_{ij} = \overline{a}_{ij_1} + \overline{a}_{ij_2}. \tag{5.3}$$

$\overline{u}_{ij_1}$ and $\overline{u}_{ij_2}$ are components in the rectangular shaped $\overline{U}$ matrix. As shown in Fig. 5.3, they correspond to the use of commodity i in two technologies j_1 and j_2, respectively, and represent different input structures between the two technologies. Also, $\overline{x}_{j_1}$ and $\overline{x}_{j_2}$ correspond to the throughput (total production) from each technology. Therefore, $\overline{u}_{ij_1}/\overline{x}_{j_1}$ and $\overline{u}_{ij_2}/\overline{x}_{j_2}$ represent the use of commodity i per unit of production from technologies j_1 and j_2, respectively. By taking the ratio of these values as a multiplier to the original coefficient ($\overline{a}_{ij}$) as shown in Equation 5.3, new coefficients for each technology ($\overline{a}_{ij_1}$ and $\overline{a}_{ij_2}$) are calculated. The values in Equation 5.3, such as different commodity input structures ($\overline{u}_{ij_1}$ and $\overline{u}_{ij_2}$) and different throughputs ($\overline{x}_{j_1}$ and $\overline{x}_{j_2}$), need to be identified from knowledge about the two technologies or from other data sources.

The resulting $\overline{A}'$ matrix has a rectangular shape, and therefore, the square shape of the identity matrix (I) in the economy scale transaction equation also needs to be rectangular. The following equation shows the rectangular shaped identity matrix (I') when the second column of the original identity matrix (I) is divided into two columns.

$$I = \begin{bmatrix} 1 & 0 & 0 & \cdots & 0 \\ 0 & 1 & 0 & \cdots & 0 \\ 0 & 0 & 1 & \cdots & 0 \\ \vdots & \vdots & \vdots & \ddots & \vdots \\ 0 & 0 & 0 & \cdots & 1 \end{bmatrix} \quad \longrightarrow \quad I' = \begin{bmatrix} 1 & 0 & 0 & 0 & \cdots & 0 \\ 0 & 1 & 1 & 0 & \cdots & 0 \\ 0 & 0 & 0 & 1 & \cdots & 0 \\ \vdots & \vdots & \vdots & \vdots & \ddots & \vdots \\ 0 & 0 & 0 & 0 & \cdots & 1 \end{bmatrix}.$$

Similarly, environmental interventions (k) and economy factor requirements (l) to produce the commodity j also need to be distributed into two technologies (j_1 and j_2),

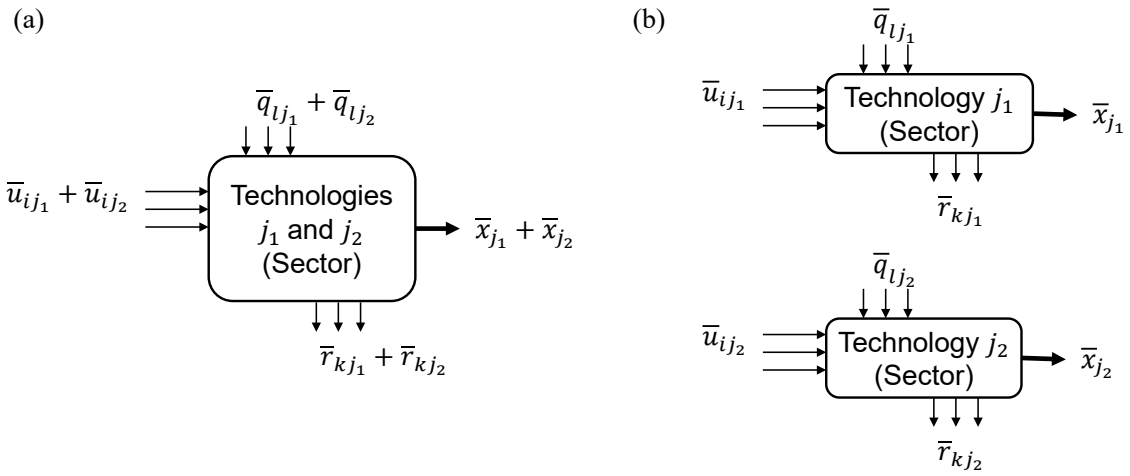

Figure 5.3: Commodity inputs ($\overline{u}_{ij_1}$ and $\overline{u}_{ij_2}$), direct economy factor requirements ($\overline{q}_{lj_1}$ and $\overline{q}_{lj_2}$), direct interventions ($\overline{r}_{kj_1}$ and $\overline{r}_{kj_2}$), and throughput ($\overline{x}_{j_1}$ and $\overline{x}_{j_2}$) from two technologies (j_1 and j_2) that produce the same commodity j, (a) when two technologies are treated as single technology and (b) when each flow is distributed into two technologies.

as shown in Fig. 5.3. While the commodity-by-commodity direct requirements matrix ($\overline{A}$) represents the coefficient of input commodity requirement for output commodity, environmental interventions matrix ($\overline{B}$) and economy factor requirement matrix ($\overline{F}$) refer to the intensities of interventions and economy factor requirements from each sector. That is, each cell ($\overline{b}_{kj}$ and $\overline{f}_{lj}$) in the $\overline{B}$ and $\overline{F}$ matrices represents the intensities and is calculated from $\overline{b}_{kj} = \overline{r}_{kj}/\overline{x}_j$ and $\overline{f}_{lj} = \overline{q}_{lj}/\overline{x}_j$, respectively. $\overline{r}_{kj}$ corresponds to the total direct interventions k from sector j. $\overline{q}_{lj}$ refers to the total direct economy factor requirements l from sector j. Therefore, the interventions ($\overline{b}_{kj_1}$ and $\overline{b}_{kj_2}$) and economy factor requirements ($\overline{f}_{lj_1}$ and $\overline{f}_{lj_2}$) divided for two technologies (j_1 and j_2) are calculated as shown below.

$$\overline{b}_{kj_1} = \overline{r}_{kj_1}/\overline{x}_{j_1}, \quad \overline{b}_{kj_2} = \overline{r}_{kj_2}/\overline{x}_{j_2}, \quad \overline{f}_{lj_1} = \overline{q}_{lj_1}/\overline{x}_{j_1}, \text{ and } \quad \overline{f}_{lj_2} = \overline{q}_{lj_2}/\overline{x}_{j_2},$$

$$\text{where} \quad \overline{q}_{lj} = \overline{q}_{lj_1} + \overline{q}_{lj_2}, \quad \overline{r}_{kj} = \overline{r}_{kj_1} + \overline{r}_{kj_2}, \text{ and } \quad \overline{x}_j = \overline{x}_{j_1} + \overline{x}_{j_2}.$$

The information about different interventions ($\overline{r}_{kj_1}$ and $\overline{r}_{kj_2}$) and different economy factor requirements ($\overline{q}_{lj_1}$ and $\overline{q}_{lj_2}$) needs to be known or obtained from various data sources.[39,40,42–44,47,49]

Economy Factor Constraint

The total economy factor consumption ($\underline{\overline{c}}$) to produce required final demands is calculated by using Equation 5.2. To account for economic consequences in the model, we need to investigate market constraints with respect to economy factors and compare them with $\underline{\overline{c}}$. That is, the amounts of economy factors consumed ($\underline{\overline{c}}$) must not exceed the maximum amounts of economy factors available in the market (c_{max}) as shown below.

$$\underline{\overline{c}} \leq c_{max}.$$

If the amounts of those factors are not constrained in the market, it means we implicitly assume the supply of economic resources are infinite, and we may make wrong decisions based on the unrealistic assumption. In the real-world market, the amounts of those factors always need to be constrained. For example, the land used for farming activities could be limited in a certain region because the total available land area is finite and the farming activities need to compete with other activities in using the limited land area. The supply of labor and capital resources could also be constrained depending on market conditions.

For the value chain and equipment scale activities, the process operating capacity could also be constrained depending on the level of technological development or the preference of stakeholders. For instance, the operating capacity of a certain value chain scale process could be limited if the process is under development. Since the

operation of processes is affected by economy factors (e.g., labor, capital, land, minerals, and water resources), the operating capacity of the value chain and equipment scale processes could be an aggregated economy factor. Kätelhön et al. also consider the operating capacity of value chain scale processes as one of the economy factors.[18]

Environmental Intervention Constraint

Like constraints on economic factors, there may also be constraints on environmental flows. For instance, if a certain region has experienced a serious eutrophication problem, policymakers may want to enact an environmental regulation on nutrient releases that can cause eutrophication. In that case, the maximum allowed emissions are constrained. The amounts of environmental interventions ($\overline{\underline{g}}$) can be constrained by the maximum allowed interventions (g_{max}) as shown below.

$$\overline{\underline{g}} \leq g_{max}.$$

These intervention constraints could also ensure that the region stays within its ecological carrying capacity.

Optimization Formulation

As described at the beginning of Section 5.3, the RCOT-P2P modeling framework contains three categories of decision variables. Therefore, the RCOT-P2P model could have three kinds of functional objectives. The first objective shown as Equation 5.4 in the optimization problem formulation is the conventional engineering objective that maximizes NPV or profits of the engineering model. The engineering model constraints (Equation 5.9) are included to ensure mass and energy balance relations in each unit operation. The second objective (Equation 5.5) is the environmental objective that minimizes environmental interventions across multiple spatial scales.

This objective has been considered in conventional sustainability assessment methods, such as SSCM, SPD, and P2P approaches. The environmental intervention constraints (Equation 5.10) could be included in the model to address environmental regulations, as described in Section 5.3.2. The third objective (Equation 5.6) is the economic objective that minimizes total factor costs across spatial scales. The total factor costs are calculated by multiplying the total economy factor consumption ($\underline{\overline{F}}^*(\{z\})\ \overline{\underline{s}} = \overline{\underline{c}}$) with the unit price of each economy factor (κ). For example, the unit price of land use (κ_{land}) has a unit of \$/(land area). As described in Section 5.3.2, the total economy factor consumption ($\overline{\underline{c}}$) needs to be constrained by the maximum available amounts of economy factors (Equation 5.11) to avoid making unrealistic assumptions, such as an infinite supply of economic resources in the market. The overall optimization formulation of the RCOT-P2P framework can be written as follows:

$$\text{Maximize } Z_{eng} = NPV(\{z\}) \tag{5.4}$$

$$\text{Minimize } Z_{env} = \underline{\overline{B}}^*(\{z\})\ \overline{\underline{s}} \tag{5.5}$$

$$\text{Minimize } Z_{econ} = \hat{\kappa}\underline{\overline{F}}^*(\{z\})\ \overline{\underline{s}} \tag{5.6}$$

$$\text{subject to } \underline{\overline{X}}^*(\{z\})\ \overline{\underline{s}} = \underline{\overline{y}} \tag{5.7}$$

$$\overline{\underline{s}} \geq 0 \tag{5.8}$$

$$H(\{z\}) \geq 0 \tag{5.9}$$

$$\underline{\overline{B}}^*(\{z\})\ \overline{\underline{s}} \leq g_{max} \tag{5.10}$$

$$\underline{\overline{F}}^*(\{z\})\ \overline{\underline{s}} \leq c_{max}. \tag{5.11}$$

5.4 Case Study: Urea Production Systems

In this section, we demonstrate the RCOT-P2P multiscale technology choice modeling framework by applying it to design a urea manufacturing process and its supply chain in a specific watershed with various economic and environmental constraints. We examine how decisions from a conventional SPD approach can be misleading, particularly when the production rate increases, and how the RCOT-P2P framework is able to address this shortcoming. This case study is particularly useful for emerging technologies because business owners usually set up a relatively small pilot scale plant first, then expand the production capacity of the plant as the demand for new technologies increases.

5.4.1 Model Description

The case study is for designing the urea production system and its supply chain network. Urea is a nitrogen fertilizer source for farming activities and is used in the chemical industry as a raw material. Urea contains 46% nitrogen which is the highest nitrogen content among all solid fertilizers. Urea can also be employed as a hydrogen and ammonia storage medium since urea is non-toxic, has a large solubility in water, and a large weight percentage of hydrogen.[132,133] Efficient and safe hydrogen storage technology is one of the biggest challenges in utilizing hydrogen as an alternative fuel. In 2016, the US nitrogen balance between production and consumption was -5 Tg of nitrogen and N demand is expected to grow by 1.3% annually.[8] In accordance with the recent deglobalization trend,[131] we suppose that domestic urea production needs to be increased.

In this case study, a new urea production facility and its immediate resource production facilities are installed in the Muskingum River Watershed (MRW) (hydrologic unit code: 05040004[149]). The MRW is located in Ohio, U.S., as shown in Fig. 5.4. In the MRW, approximately 13 million m^2 of the land area remains barren.[150] Here, we assume $400,000$ m^2 of the barren land is owned by a business owner who wants to build new urea production system in this region. Also, the MRW has limited resource supplies. Available renewable water supply in the MRW is 42×10^6 m^3/y.[41] Available natural gas supplies from conventional and shale wells are 72 and 621 million m^3/y, respectively. Only some portions of the remaining water supply may need to be allocated to the urea facilities due to water rights. In the western U.S., for example, most of the water resources are owned by government agencies to regulate water use, and approximately 90% of the water supply is allocated to farming activities.[151] In Ohio, water use is regulated by the doctrine of riparian water rights and water rights are associated with riparian land ownership.[152] Therefore, it is reasonable to assume that new urea production facilities can utilize partially available resources that are allocated to urea production. The allocation for those resources will be subjective depending on stakeholders' preferences and decisions. In this case study, we assume that approximately 5% of the remaining water supply or 2.2×10^6 m^3/y is allocated to the new urea production facilities. Despite the assumed allocation ratio, it allows us to demonstrate the RCOT-P2P framework effectively. The details for calculating the amounts of available resource supplies are described in Section 5.4.1.

Urea is produced from ammonia and carbon dioxide. Conventionally, the ammonia is manufactured through the steam reforming of NG and the carbon dioxide

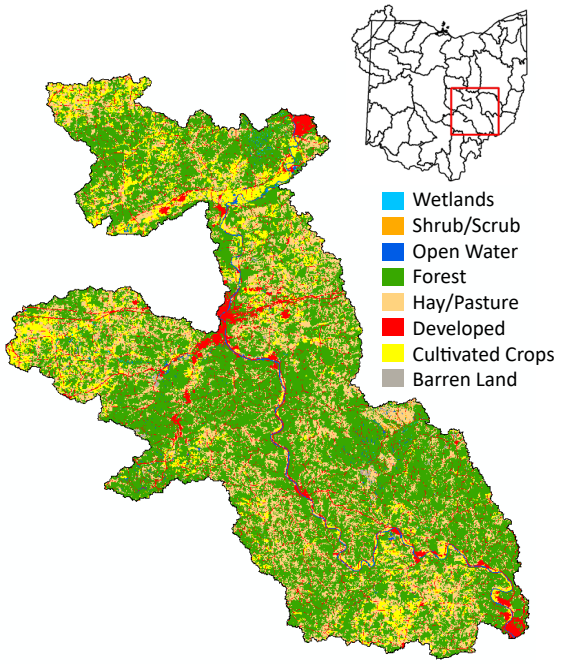

Figure 5.4: Muskingum River Watershed in Ohio, USA

is prepared by CO_2 capture from the ammonia manufacturing process through monoethanolamine (MEA) scrubbing. The urea production facility also requires electricity and natural gas inputs for compressors and flash separators, respectively. The main sources for electricity generation in the MRW are coal and NG.

Urea synthesis is a CO_2 conversion process. In this case study, we suppose the corporation wants to design the urea production systems to have less greenhouse gas emissions. Therefore, we consider employing an emerging "sustainable" ammonia production technology that uses water as a hydrogen source via electrolysis. Also, several renewable sources for power generation (e.g., wind power and solar power) are considered as additional technology options to produce electricity. Accordingly, the following technology options are available for consideration solely or simultaneously.

- NH_3 supply options

    1. Conventional NH_3 via steam reforming of natural gas: The conventional NH_3 production technology uses NG as a hydrogen source and emits more CO_2 (2.06 $kgCO_2eq/kgNH_3$).[42]

    2. "Sustainable" NH_3 via electrolysis of water: The emerging NH_3 production technology requires more electricity and water inputs to provide hydrogen through the electrolysis of water. But, this technology has less CO_2 emissions (0.021 $kgCO_2eq/kgNH_3$).[42]

- Electricity supply options

    1. Fossil fuel electricity: The existing thermoelectric power generation technology requires water for the cooling of turbines and has relatively large CO_2 emissions (0.21 $kgCO_2eq$/MJ of electricity)[153] since it utilizes fossil fuel resources.

    2. Solar photovoltaic electricity: The solar power generation technology requires some water to clean the surface of solar panels. Also, it requires a large land area to install solar panels since the potential solar energy in the MRW is 4445 MJ/m^2.[50] However, it emits less CO_2 from its life cycle (0.013 $kgCO_2eq$/MJ of electricity).[43]

    3. Wind electricity: The water requirement for wind power generation technology is very low. Also, it has the lowest life cycle CO_2 emissions (0.003 $kgCO_2eq$/MJ of electricity)[43] than other power generation options. However, it requires a huge land area to install wind turbines because the

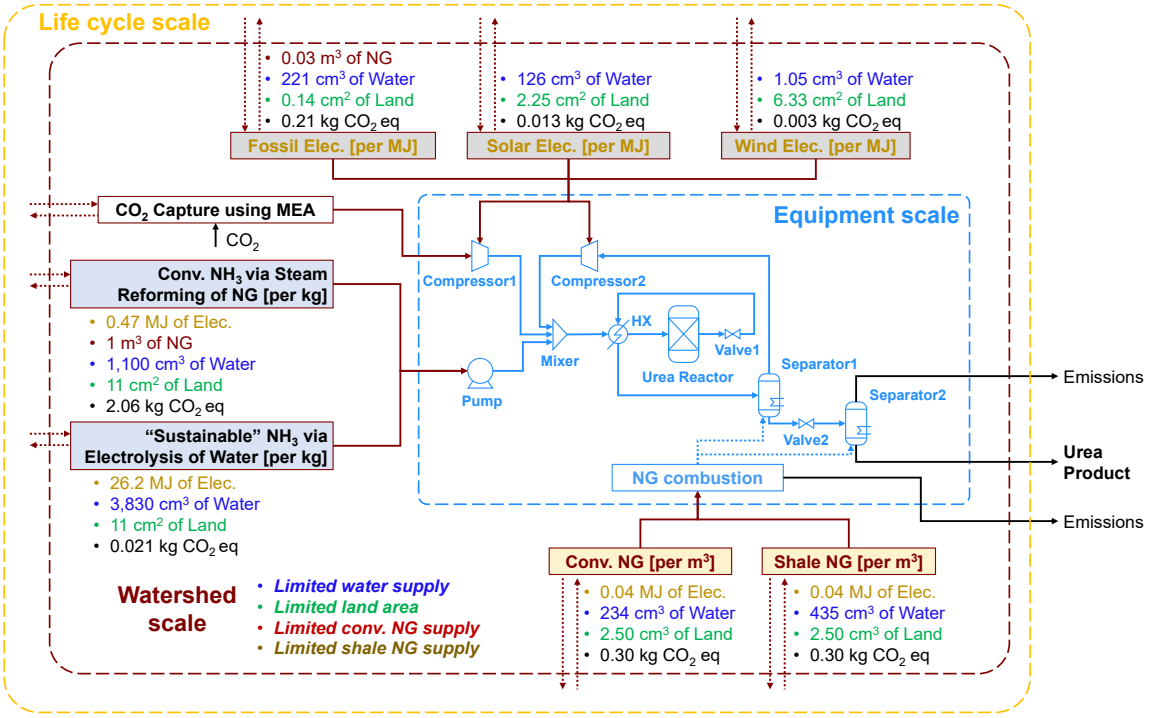

Figure 5.5: Model structure for the urea production systems in the Muskingum River Watershed, Ohio, USA.

potential wind energy in the MRW is 1580 MJ/m^2.[50] The MRW region is not a promising location for generating wind electricity.

- Natural gas supply options:

  1. NG from conventional well: Natural gas is extracted using the traditional way through drilling and pumping operations.

  2. NG from shale well: Natural gas is extracted from shale well via hydraulic fracturing which requires large quantities of water.

The model structure for this case study and the technology options are shown in Fig. 5.5.

As shown in this figure, the nonlinear urea engineering model at the equipment scale is developed based on the process flow diagram from the reports[154–156] and mass and energy balance relations at each unit operation.[157–159] Table 5.3 summarizes key energy balance relations for each unit operation in the urea engineering model. The urea model is simplified to avoid computational difficulties in solving a complex engineering model. Adiabatic conditions are assumed for compressors, expansion valves, a mixer, and a heat exchanger. An isothermal urea synthesis reactor is assumed. The reactor temperature is constrained in the range of 170–220 °C, while fixing the reactor pressure at 180 bar.[160] Also, ideal flash separators based on Raoult's law are assumed.

Value chain scale process data are collected from several life cycle inventory (LCI) databases.[42,43] For instance, 1.44 MJ of energy per 1 kg of CO_2 is required for the CO_2 capture process using MEA. For the existing thermoelectric power generation, its process data is obtained from the local data source,[153] instead of using the national average LCI data. The land use for renewable power generation technologies is estimated from the potential solar and wind energy data for the MRW region.[50]

Table 5.3: Key energy balance relations for each unit operation.

Unit operation	**Key energy balance relation**
Compressor	$T_{out} = T_{in}\ (P_{out}/P_{in})^{(\gamma-1)/\gamma}$
Pump	$T_{out} = T_{in}, \quad P_{out} > P_{in}$
Mixer	$\Delta H = 0$
Heat exchanger	$\Delta H_{cold} = \Delta H_{hot}$
Reactor	$Conv_{CO_2} = -0.287 + 1.09 \cdot exp[-2 \cdot \{(T - 466)/190\}^2]$
Separator	$\xi_i = \alpha_{i/k}\ \xi_k/(1 + (\alpha_{i/k} - 1)\ \xi_k)$ for each component i
Expansion valve	$P_{out} < P_{in}, \quad P_{out} \cdot F_{out} = \sum_i P_{vap,i,out} \cdot fc_{i,out}$

The LCI data used in this case study do not give any information about the interaction with the economy scale (e.g., upstream cutoff flows from the economy scale and downstream cutoff flows to the economy scale). In other words, we do not know the amounts of products or commodities that need to be brought from the economy scale to the value chain or equipment scales. Therefore, we do not consider the economy scale model for this particular case study. More details about data collection and mathematical formulation are described in Section 5.4.1.

In the case study, we only consider land, water, and natural gas resources as economy factors. We assume that other economy factor requirements, such as labor and capital, are similar between different technology options, and thus, they do not affect the choice of technologies. This assumption avoids the need for obtaining labor and capital costs for specific value chain processes, such as "sustainable" NH_3 production via electrolysis of water. Also, the maximum available amounts of labor and capital costs, which mainly depend on the financial situation of the corporation, are unknown. Therefore, we investigate the consequences of land, water, and natural gas resources on process design and supply chain design.

Economy Factor Constraints in the Muskingum River Watershed

To demonstrate the RCOT-P2P multiscale technology choice modeling framework, new green urea production systems are assumed to be installed in the Muskingum River Watershed (MRW) in Ohio. In this case study, four kinds of economy factors are considered as follows: land area, water supply, natural gas supply from conventional wells, and natural gas supply from shale wells. To account for market conditions in the MRW, the maximum available amounts of economy factors are calculated as follows.

1. Maximum available land area: In the MRW, the barren land area is approximately 13 million m^2.[150] Since the corporation that wants to build the new production systems usually owns their area, we assume that the corporation in this case study owns only 400 thousand m^2 of the barren land area in the MRW. This land area is defined as the maximum available land area for the new urea production systems.

2. Maximum available water supply: To calculate the renewable water supply in the MRW, the Available WAter REmaining (AWARE) model,[41] which is based on the Water Global Assessment and Prognosis (WaterGAP) hydrology model,[161] is used. The WaterGAP hydrology model considers the water cycle to calculate the amount of available water. The AWARE model gives how much renewable water is available in the Ohio region (hydrologic unit code: 05[149]). The amount of renewable water in the MRW (hydrologic unit code: 05040004) is estimated by taking the ratio of the MRW area to the Ohio region area. The existing water consumption in the MRW is also investigated from multiple data sources.[42,50,153,162] Finally, the maximum available water supply in the MRW is calculated by subtracting the existing water consumption (2.46×10^7 m^3/y) from the renewable water supply (6.68×10^7 m^3/y). As described previously, approximately 5% of the maximum available water supply (2.2×10^6 m^3/y) is assumed to be available for the new urea production systems.

3. Maximum available NG supply from conventional and shale wells: The remaining amount of NG in reserves in the MRW cannot be defined as the available NG supply because NG is a limited fossil resource and significant amounts of

CO_2 emissions are associated with the burning of NG (1.86 $kgCO_2/m^3$ of NG burning).[163] Ideally, to prevent ecological overshoot from using nonrenewable fossil resources, only the renewable portion of resources (i.e. the formation of fossil resources) needs to be considered as their renewable supplies. However, the rate of NG formation is significantly smaller than the rate of NG production. Therefore, the carbon budget that allows 2°C of global warming above pre-industrial temperatures is considered in defining the maximum available NG supply in this case study.

According to the Intergovernmental Panel of Climate Change (IPCC) report, the rise in global temperature must be limited to 2°C above pre-industrial levels in order to avoid disastrous consequences of climate change.[164] (In 2018, the IPCC has also prepared a special report on the impacts of 1.5°C warming above pre-industrial levels.) The IPCC has calculated the carbon budget that represents the amounts of global CO_2 emissions for keeping the warming under 2°C. The global budget is estimated to be one trillion tonnes of carbon and the remaining budget in 2011 in terms of greenhouse gas (GHG) emissions is 275 billion tonnes of carbon. Since 22 % of total GHG emissions come from the NG use,[165] 61 billion tonnes of carbon can be allocated to the use of NG as the remaining budget at the global scale. By taking the ratio of NG consumption in the MRW (2.615×10^9 m^3 of NG/y in 2014)[153,163] to the global NG consumption,[166] approximately 466 thousand tonnes of carbon per year can be allocated to the NG use in the MRW. (The carbon budget is assumed to be burned for 100 years.) This corresponds to 9.23×10^8 m^3 of NG per year. The amounts of NG in conventional and shale proved reserves in Ohio are 2.29×10^{10}

and 1.81×10^{11} m^3 of NG, respectively, in 2014.[167,168] By multiplying the ratio between conventional and shale proved reserves with the total allowed NG use in MRW (9.23×10^8 m^3 of NG/y), thus, 1.04×10^8 and 8.22×10^8 m^3 of NG per annum can be allowed to be used from conventional and shale wells, respectively. In 2014, 3.2×10^7 and 2.01×10^8 m^3 of NG is produced from conventional and shale wells, respectively.[169,170] To stay within the budget for 100 years, therefore, additional 7.2×10^7 and 6.21×10^8 m^3 of NG can be exploited annually from the conventional and shale wells, respectively.

Data Collection and Mathematical Formulation

Table 5.4 shows value chain scale technology ($\underline{X}$), intervention ($\underline{B}$), and economy factor requirement ($\underline{F}$) matrices and a unit price vector of economy factors (κ). Value chain scale process data for ammonia, carbon dioxide, electricity, and natural gas products are obtained from life cycle inventory databases, such as GREET[42] and ecoinvent,[43] or estimated using regional data sources.[50,153] A unit price of land is also investigated using the U.S. farm real estate value in 2017.[171]

Prices of NG economy factors from conventional and shale wells are assumed to be 0 because we assume there is no monetary value associated with NG economy factors themselves. In general, we do not pay for natural resources themselves but pay for technological and economical inputs to utilize them. Governments may charge rights to extract them in forms of taxes or royalties. In this study, we do not account for the price of NG economy factors due to data availability.

Economy factor flows are different from product flows. NG economy factors do not correspond to either extracted NG products or processed NG products. Therefore, the market price of NG products cannot be considered for the price of NG economy

factors. In the RCOT framework, the unit producer price of products (p) can be determined by the Leontief price, or dual, model as shown in the following equation.[27]

$$p = (I - A^T)^{-1} F^T \kappa,$$

where superscript T represents the transposed matrix. In this equation, the unit producer price of products is equal to the monetary sum of economy factors that are needed for the products. For example, if the production process for NG products needs an electricity input and various economy factors such as labor, capital, water, land, and mineral resources, the unit price of NG products can be determined by the

Table 5.4: Value chain scale matrices and a unit price vector of economy factors for the case study.

Value chain scale technology matrix ($\underline{X}$)

	Conv. NH_3 process [kg][42]	Sust. NH_3 porcess [kg][42]	CO_2 capture process [kg][43]	Fossil power process [MJ][153]	Solar power process [MJ]	Wind power process [MJ]	Conv. NG process [m^3][42]	Shale NG process [m^3][42]	MEA process [kg][43]
NH_3 product [kg]	1	1	0	0	0	0	0	0	0.788
CO_2 product [kg]	0	0	1	0	0	0	0	0	0
Electricity product [MJ]	0.47	26.158	1.44	1	1	1	0.0392	0.0388	1.199
NG product [m^3]	1	0	0.0762	0.0295	0	0	1	1	0.0531
MEA product [kg]	0	0	0.013	0	0	0	0	0	1

Value chain scale interventions matrix ($\underline{B}$)

	Conv. NH_3 process [kg][42]	Sust. NH_3 porcess [kg][42]	CO_2 capture process [kg][43]	Fossil power process [MJ][153]	Solar power process [MJ][43]	Wind power process [MJ][43]	Conv. NG process [m^3][42]	Shale NG process [m^3][42]	MEA process [kg][43]
GHG emissions [$kgCO_2eq$]	2.06	0.0208	0.461	0.21	0.0131	0.00313	0.297	0.297	1.918

Value chain scale economy factor requirement matrix ($\underline{F}$)

	Conv. NH_3 process [kg]	Sust. NH_3 porcess [kg]	CO_2 capture process [kg]	Fossil power process [MJ]	Solar power process [MJ]	Wind power process [MJ]	Conv. NG process [m^3]	Shale NG process [m^3]	MEA process [kg]
Land use [m^2a]	0.00112[43]	0.00112[43]	0.00112[43]	0.000014[43]	0.00022[50]	0.00063[50]	0.0002[43]	0.0002[43]	0.00112[43]
Regional water use [m^3]	0.0011[42]	0.0038[42]	0.03[43]	0.00022[153]	0.00012[42]	0.0000010[42]	0.00023[42]	0.00043[42]	0.0248[43]
Conv. NG use [m^3]	0	0	0	0	0	0	1	0	0
Shale NG use [m^3]	0	0	0	0	0	0	0	1	0

Unit price vector of economy factors (κ)

	Unit price [$]
Land use [m^2a]	0.761[171]
Regional water use [m^3]	0.779
Conv. NG use [m^3]	0
Shale NG use [m^3]	0

monetary sum of every economy factor needed for the NG production process and the electricity generation. Therefore, the price of NG economy factors is considered as a fraction of the market price of NG products. If we set the price of NG economy factors to the market price, we will double count some fractions of the price, which are attributed to the use of other economy factors (land, water, labor, and capital) and the use of upstream commodities such as electricity. In this study, we do not consider economy factors such as labor, capital, and minerals since such data for the processes considered in this case study are not available. Also, we assume the unit price of NG economy factors to be 0. If we have more detailed data, the quality of the case study could be improved.

Urea engineering model at the equipment scale is developed using the General Algebraic Modeling System (GAMS). The GAMS code for urea engineering model is available upon request.

The RCOT-P2P model for the case study is formulated as shown below.

$$\begin{bmatrix} \underline{X} & -X_u^V(\{z\}) \\ 0 & X(\{z\}) \end{bmatrix} \begin{bmatrix} \underline{s} \\ s \end{bmatrix} = \begin{bmatrix} 0 \\ y \end{bmatrix} \tag{5.12}$$

$$\begin{bmatrix} \underline{B} & B(\{z\}) \end{bmatrix} \begin{bmatrix} \underline{s} \\ s \end{bmatrix} = \overline{\underline{g}} \tag{5.13}$$

$$\begin{bmatrix} \underline{F} & F(\{z\}) \end{bmatrix} \begin{bmatrix} \underline{s} \\ s \end{bmatrix} = \overline{\underline{c}} \tag{5.14}$$

$X(\{z\})$ is the equipment scale urea engineering model. $X(\{z\})$ is represented by a urea product output flow from the urea model.

X_u^V is the upstream cutoff flow matrix from the value chain scale to the equipment scale. NH_3, CO_2, electricity, and NG cutoff flows from the value chain scale are

included in X_u^V as follows.

$$X_u^V(\{z\}) = \begin{bmatrix} \text{NH}_3 \text{ feed to the urea model} \\ \text{CO}_2 \text{ feed to the urea model} \\ \text{Electricity inputs to compressors in the urea model} \\ \text{NG inputs to heaters in the urea model} \\ 0 \end{bmatrix}$$

15% of heat loss is assumed for the NG combustion heaters. Also, the last row that represents the MEA input to the equipment scale model is 0. The X_u^V matrix connects value chain scale flows to equipment scale processes.

$B(\{z\})$ and $F(\{z\})$ matrices are the interventions matrix and the economy factor requirement matrix at the equipment scale, respectively, and are formulated as below.

$$B(\{z\}) = \left[\text{CO}_2 \text{ emissions from Separator 2 in the urea model}\right] + \left[\text{CO}_2 \text{ emissions from NG combustion heaters in the urea model}\right]$$

$$F(\{z\}) = \begin{bmatrix} \text{Water inputs required for coolers in the urea model} \\ \text{Land area required for the urea model} \end{bmatrix}$$

In the $F(\{z\})$ matrix, land use data for the urea manufacturing process from the life cycle inventory database[43] is used to estimate the required land area in this study.

In this case study, there are no downstream cutoff flows from the equipment scale to the value chain scale. Also, the urea engineering model at the equipment scale does not belong to any value chain activities in this case study. Therefore, value chain scale matrices do not contain equipment scale design variables ($\{z\}$) because the value chain scale matrices do not need to be disaggregated from the equipment scale.

Scaling vectors ($\underline{s}$ and s) in terms of the final demand (y) are determined using Equation 5.7 and life cycle intervention ($\overline{\underline{g}}$) and economy factor consumption ($\overline{\underline{c}}$) are calculated from Equations 5.13 and 5.14.

5.4.2 Optimization Formulation

As discussed in Section 5.3.2, the RCOT-P2P model can have three distinct decision objectives depending on the disciplines and stakeholders' interests. In this case study, we investigate two cases where total CO_2 emissions are minimized and where total factor costs are minimized.

The RCOT-P2P model for the urea production systems is constructed using the General Algebraic Modeling System (GAMS) to optimize engineering design variables at the equipment scale and technology choice variables at the value chain scale. The nonlinear programming (NLP) problem for this case study is formulated as follows:

$$\text{Minimize } Z_{env} = \overline{\underline{B}}_{CO_2}(\{z\})\ \overline{\underline{s}} \tag{5.15}$$

$$\text{Minimize } Z_{econ} = \hat{\kappa}\overline{\underline{F}}(\{z\})\ \overline{\underline{s}} \tag{5.16}$$

$$\text{subject to } \overline{\underline{X}}(\{z\})\ \overline{\underline{s}} = \overline{\underline{y}} \text{ (Annual urea production)} \tag{5.17}$$

$$\overline{\underline{s}} \geq 0 \tag{5.18}$$

$$H(\{z\}) \geq 0 \tag{5.19}$$

$$\overline{\underline{F}}_{land}(\{z\})\ \overline{\underline{s}} = \overline{\underline{c}}_{land} \leq 4 \times 10^5 \text{ m}^2 \text{ of land} \tag{5.20}$$

$$\overline{\underline{F}}_{water}(\{z\})\ \overline{\underline{s}} = \overline{\underline{c}}_{water} \leq 2.2 \times 10^6 \text{ m}^3 \text{ of water/y} \tag{5.21}$$

$$\overline{\underline{F}}_{convNG}(\{z\})\ \overline{\underline{s}} = \overline{\underline{c}}_{convNG} \leq 7.2 \times 10^7 \text{ m}^3 \text{ of NG/y} \tag{5.22}$$

$$\overline{\underline{F}}_{shaleNG}(\{z\})\ \overline{\underline{s}} = \overline{\underline{c}}_{shaleNG} \leq 6.21 \times 10^8 \text{ m}^3 \text{ of NG/y.} \tag{5.23}$$

Objective functions 5.15 and 5.16 correspond to the environmental objective (case 1) and the economic objective (case 2), respectively. Equation 5.17 makes sure that the designated amount of final demand is produced from the systems. Constraint 5.18 avoids having negative unit sizes for activities in the systems. Constraint 5.19

represents the urea engineering model at the equipment scale by conserving energy and mass balance in the urea engineering model. Constraints 5.20–5.23 correspond to the economy factor (market) constraints. The final demand ($\overline{\underline{y}}$) in this case study is the annual urea production. The resulting GAMS model contains 377 variables, and the CONOPT solver is used to solve the nonlinear problems. In the following two cases, we investigate how technologies could be adopted in the MRW to minimize total CO_2 emissions (case 1) or to minimize total factor costs (case 2) as the urea production capacity increases.

5.4.3 Case 1. Environmental Objective

Figure 5.6 shows the results of the design problem for the environmental objective of minimizing the life cycle greenhouse gas emissions. The results exhibit how technology choices change as the urea production capacity increases and how total CO_2 emissions and total economy factor consumption (e.g., water and land use) changes accordingly. Conventional or attributional LCA determines that green urea production systems have 77.9% less CO_2 emission than the conventional urea production systems that employ conventional technologies. This result is shown by the black dashed line in Fig. 5.6. As discussed in Section 5.1, this result implicitly assumes that the improved efficiency of sustainable urea technologies will be available at larger scales of production as well.

A red dashed CO_2 emission line is calculated from the RCOT-P2P approach, which is the consequential modeling approach. Process scales of each technology in use are shown as the stacked area chart. Even though four kinds of economy factors (water, land, conventional NG, and shale NG) are included in the model, only water

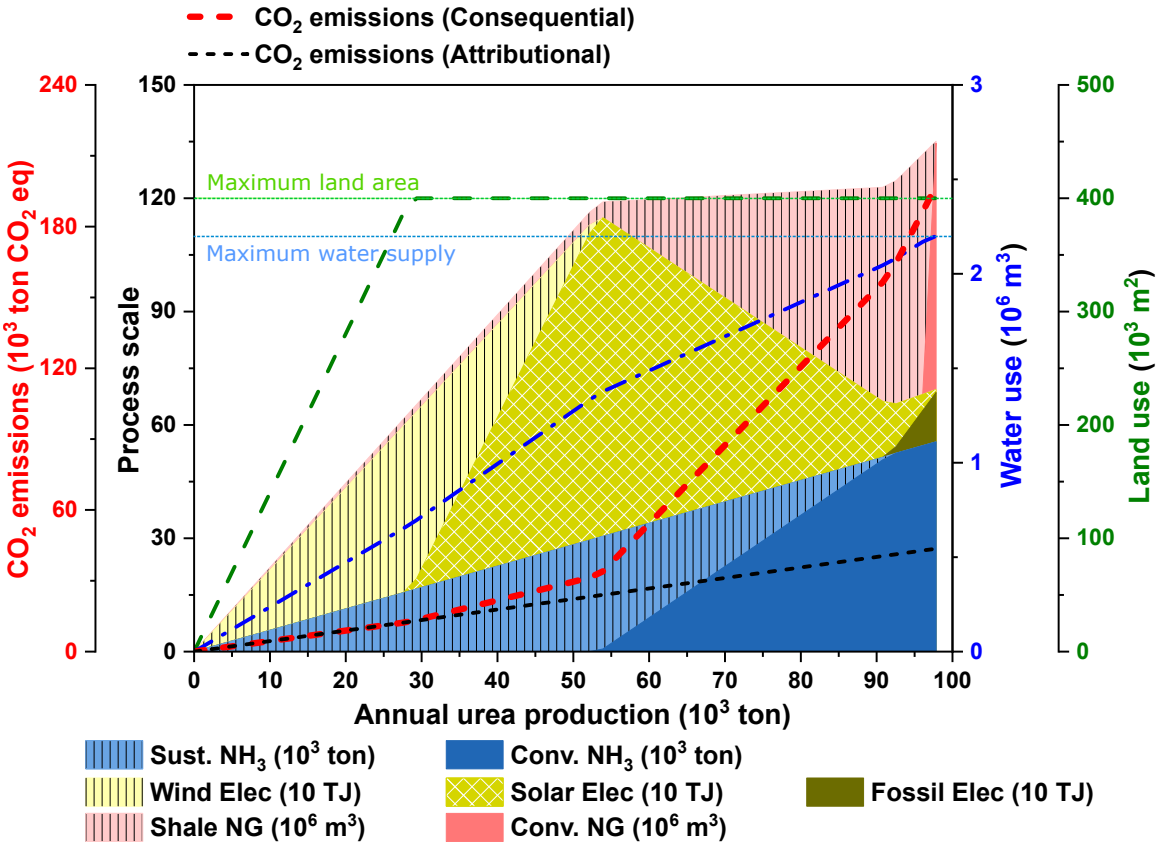

Figure 5.6: Changes in technology choices, total CO_2 emissions, and total water and land use as the urea production capacity increases. The design objective is to minimize total CO_2 emissions.

and land use are shown in Fig. 5.6 because both conventional and shale NG resources are plentiful in the MRW. Constraints 5.22 and 5.23 are never activated in this case study.

Unlike the result of the conventional attributional P2P approach, which identifies only one phase ("sustainable" NH_3, wind energy, and shale NG technologies) at all scales of production, the RCOT-P2P framework identifies five distinct phases due to the activation of various constraints. This is shown in Fig. 5.6.

1. **Nascent phase** (Annual urea production: $0 \sim 28$ thousand tons/y): When the urea production is small, only the "best" technologies are chosen to minimize total CO_2 emissions. As described in the previous section, "sustainable" NH_3 technology through the electrolysis of water, wind power technology, and shale NG technology have lower CO_2 emissions than each competing technology. In this phase, all economy factors in the MRW are plentiful for the technologies chosen to produce urea. This is the phase where the attributional approach is correct as both attributional and consequential CO_2 emission lines completely overlap. Since the attributional approach does not consider market constraints, this approach always leads to the results from this phase regardless of how much urea is produced.

2. **Growth phase** (Annual urea production: $28 \sim 52$ thousand tons/y): As the urea production capacity increases, more electricity is required mostly for the "sustainable" NH_3 production technology that has the huge electricity requirement for the electrolysis of water. Also, land use reaches its maximum limit since the increased wind power generation requires an extensive land area that is not available in this phase. As a result, the solar power generation technology, which requires less land area in the MRW, needs to be used together with the wind power generation to produce the increased amount of urea in this phase. Accordingly, total CO_2 emissions from the RCOT-P2P approach is slightly increased compared to the CO_2 emissions from the attributional approach because the solar power generation has higher CO_2 emissions than the wind power generation.

3. **Mature phase** (Annual urea production: $52 \sim 91$ thousand tons/y): In this phase, the land area constraint takes effect for the solar power generation as well. Therefore, conventional steam reforming NH_3 technology that does not require much electricity needs to be employed simultaneously with the "sustainable" NH_3 technology to reduce the overall electricity consumption. As the urea demand increases, the "sustainable" NH_3 technology is completely replaced by the conventional steam reforming technology to minimize the electricity demand. Also, more NG is consumed for the steam reforming process. As a result, the red-dotted CO_2 emission line for the RCOT-P2P approach diverges noticeably from the black-dotted line for the attributional approach because of the high emissions from the steam reforming and the increased NG demand. This indicates that the benefit in minimizing CO_2 emissions from the attributional approach is a huge overestimate.

4. **Overload phase** (Annual urea production: $91 \sim 98$ thousand tons/y): If the urea production in the MRW continues to increase, fossil power generation technology starts being used instead of solar power generation due to the land area constraint. NG consumption is also increased because additional NG needs to be used for fossil power generation. Total water use in this phase approaches the maximum available amount of water supply since the fossil power generation technology requires a substantial amount of water. Accordingly, the NG production technology changes from shale NG to conventional NG because of less water use for the conventional NG technology. Since fossil power generation technology emits significant amounts of CO_2, total CO_2 emissions determined by the RCOT-P2P approach increase more steeply.

5. **Infeasible phase** (Annual urea production: more than 98 thousand tons/y): In this watershed, the urea production rate cannot exceed 98 thousand tons/y since the water supply and land area become unavailable for any technology option in this case study. In practice, the typical capacity of a urea production facility could be much bigger than 98 thousand tons/y. For example, a urea production facility owned by Dakota Gasification Company can produce 400 thousand tons of urea per annum.[172] Engro Fertilizers Limited has a urea production facility with an annual capacity of 1.3 million tons.[173] The attributional approach would not encounter this infeasible phase because it assumes unconstrained adoption of technologies regardless of market conditions, which can result in incorrect decisions.

As described above, the RCOT-P2P model can address how technology would be adopted as the production capacity increases, by reflecting market constraints in the watershed.

Design of the urea process is also affected by market constraints. One of the most affected unit operations is compressor 2 shown in Fig. 5.5. This unit operation is to compress an NH_3 recycling gas stream flow from separator 1 to increase the flow pressure to the reactor pressure, 180 bar. The optimized electricity requirement for compressor 2 to minimize life cycle CO_2 emissions is 167.9 kJ/kg of urea when less than 28 thousand tons/y of urea production is required. In the growth, mature, and overload phases where more than 28 thousand tons/y of urea need to be produced, however, the optimized electricity requirement is decreased to 151.3, 115.6, and 88.9 kJ/1 kg of urea, respectively. This is because the fossil power generation technology that has much higher CO_2 emissions needs to be used to produce electricity in these

phases due to the land use constraint. To reduce the emissions from fossil power generation, compressor 2 needs to be operated using less electricity. In this sense, the RCOT-P2P approach enables flexible process designs based on accounting for changing market conditions and constraints.

5.4.4 Case 2. Economic Objective

Using the same market constraints 5.20–5.23 in the MRW, total factor costs to produce urea are minimized for the economic decision objective 5.16. As shown in Fig. 5.7, only conventional NH_3 production, fossil power generation, and conventional NG technologies are chosen regardless of how much urea needs to be produced. This is because, unlike case 1, the land and water supply constraints are not activated for the technologies selected in case 2, even though the infeasible phase is identified to be the same as case 1 due to these constraints. Accordingly, the difference between attributional and consequential approaches is not identified in case 2. This is one example of how decisions could change depending on the functional objective and stakeholders' interests.

According to the results in case 2, selected technologies have cheaper cost structures than other competing technologies. Even though some economy factors, such as capital and labor costs, are not considered in this case study, these results are aligned with other reports about the production costs of technologies. Hydrogen production from the electrolysis of water is reported to be about two times more expensive than steam reforming.[174,175] Fossil power generation is also reported to be cheaper than the costs of solar and wind power generation technologies according to the 2013 report that projected the generation costs in the U.S. for 2018.[176] Further projection

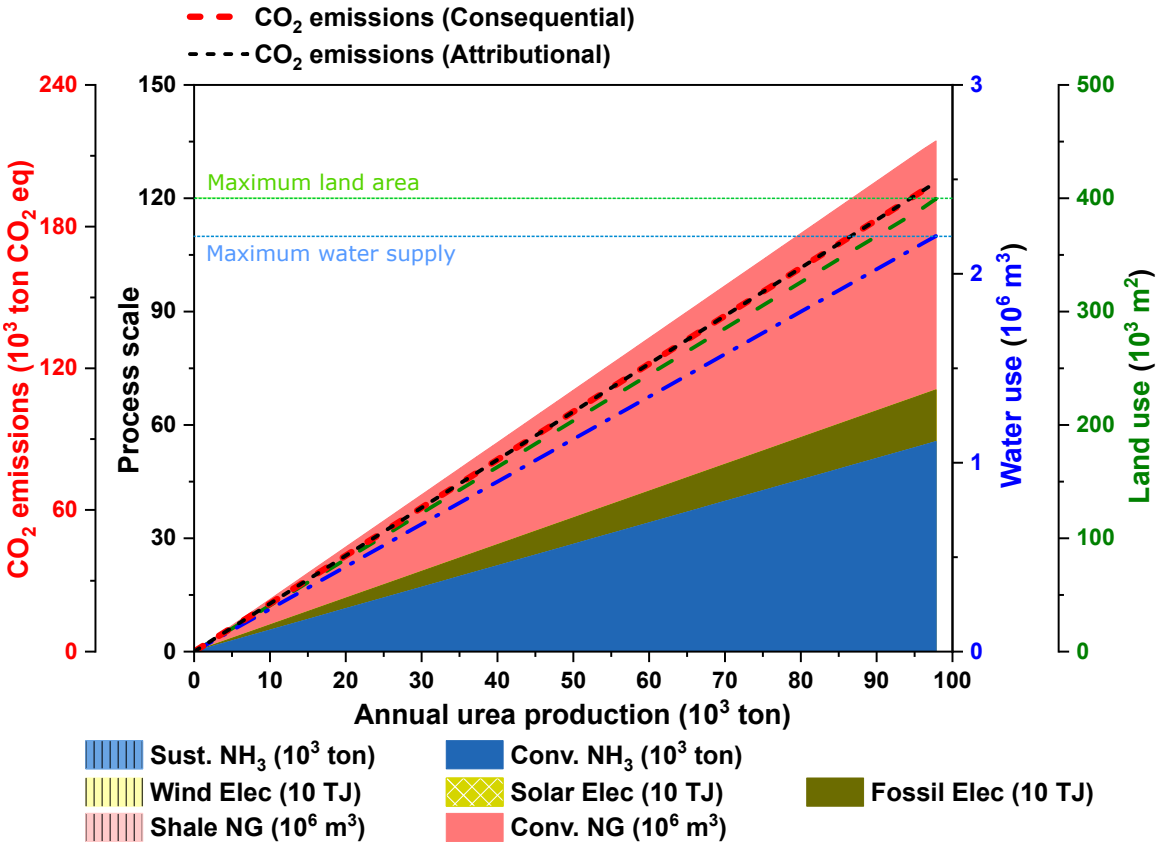

Figure 5.7: Changes in technology choices, total CO_2 emissions, and total water and land use as the urea production capacity increases. The functional objective is to minimize total factor costs.

from a more recent report shows those renewable sources of power generation costs will be much cheaper in 2022.[177] In the U.S., the production cost of shale gas is lower than that of conventional NG.[178] The opposite result is obtained from this case study since we only include water use, land use, and NG use from conventional and shale wells as economy factors. In this case study, the conventional NG technology is identified as a cheaper option because differences between shale NG and conventional NG technologies are negligible in this study except for the larger water use for the shale NG technology.

5.4.5 Multi-Objective Optimization

To identify the design space with respect to multiple objectives, the multi-objective optimization problem is solved using the epsilon-constraint method for engineering and environmental objectives. The multi-objective optimization problem is formulated as follows:

$$\text{Maximize } Z_{eng} = Profit(\{z\}) \tag{5.24}$$

$$\text{Minimize } Z_{env} = \overline{B}_{CO_2}(\{z\})\ \overline{s} \tag{5.25}$$

$$\text{subject to } \overline{X}(\{z\})\ \overline{s} = \overline{y} \text{ (Annual urea production)}$$

$$\overline{s} \geq 0$$

$$H(\{z\}) \geq 0$$

$$\overline{F}_{land}(\{z\})\ \overline{s} = \overline{c}_{land} \leq 4 \times 10^5 \text{ m}^2 \text{ of land}$$

$$\overline{F}_{water}(\{z\})\ \overline{s} = \overline{c}_{water} \leq 2.2 \times 10^6 \text{ m}^3 \text{ of water/y}$$

$$\overline{F}_{convNG}(\{z\})\ \overline{s} = \overline{c}_{convNG} \leq 7.2 \times 10^7 \text{ m}^3 \text{ of NG/y}$$

$$\overline{F}_{shaleNG}(\{z\})\ \overline{s} = \overline{c}_{shaleNG} \leq 6.21 \times 10^8 \text{ m}^3 \text{ of NG/y.}$$

Objective functions 5.24 and 5.25 refer to the engineering objective that maximizes a urea plant profit and the environmental objective that minimize life cycle CO_2 emissions, respectively. As shown in Fig. 5.8, Pareto fronts and technology options selected are identified for different urea production capacities. As discussed in Section 5.4.3, when the urea production capacity is small, only "best" technologies are chosen. The attributional approach can identify only this design space regardless of the production capacity. In the RCOT-P2P consequential approach, however, the feasible design space is reduced as urea production increases because secondary and

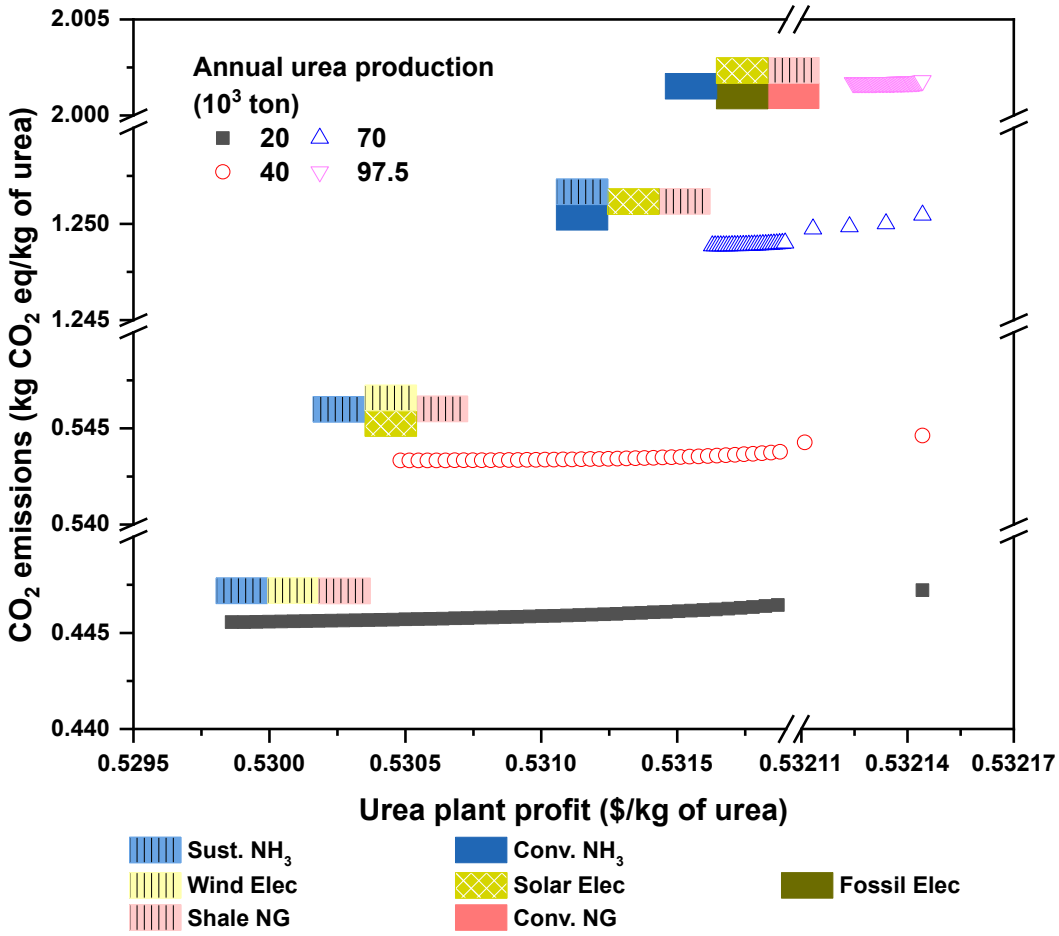

Figure 5.8: Changes in the feasible design space with respect to engineering and environmental objectives as the urea production capacity increases. The technology mix chosen for producing different amounts of urea is shown as rectangular boxes.

tertiary technologies that have higher CO_2 emissions need to be adopted to meet the demand.

5.5 Discussion and Conclusions

The RCOT-P2P multiscale technology choice model integrates models of engineering processes, life cycle, and the economy. It accounts for the interactions between engineering, environmental, and economic domains, while considering the consequences of including new technologies along with economic, environmental, and societal constraints. This consequential multiscale modeling framework advances the method to assess the sustainability of systems in two ways. First, the RCOT-P2P framework combines the benefits from P2P and RCOT approaches, and therefore, it accounts for multiple spatial scales from the equipment to the planetary scale in designing the engineering model and supply chain networks at the same time. To prevent the environmental impacts from shifting outside the system boundary, the consideration of multiple spatial scales is essential.[9] Second, the RCOT-P2P framework is a consequential multiscale modeling approach. The case study in this chapter exhibits the importance of employing the consequential approach by considering market constraints to avoid unexpected outcomes from the attributional approach. Unlike other consequential approaches, the RCOT-P2P framework can account for consequences on multiple spatial scales by considering economy factor constraints that are region-specific. Accordingly, the RCOT-P2P model can be formulated as a general mathematical programming problem, which is very comprehensive in the sense that it accounts for multiple spatial scales that range from the equipment scale to the economy scale in designing processes and supply chains while considering the effects of market constraints across multiple scales. In particular, the framework could be beneficial for modeling the consequences of employing emerging technologies that need to substitute conventional alternatives. The RCOT-P2P model can model the

gradual adoption of emerging technologies in a region and how the adoption affects the entire supply chain across multiple scales.

The RCOT-P2P framework is highly flexible for addressing various types of problems. Since the framework can model decision objectives from three distinct disciplines, it can be employed to represent different stakeholders' interests. The framework can be applied to any complex equipment scale models although computational difficulties in solving such detailed models can be challenging. Also, the framework is capable of designing multiscale supply chain networks. Depending on the data availability and the characteristics of the problem, supply chain options (technology options) could be at the equipment scale, the value chain scale, and/or the economy scale. Moreover, since a variety of economy factors can be included in the RCOT-P2P model, the framework can be used for various purposes. Although we do not consider monetary economy factors in the case study of this chapter, many different forms of monetary factors (e.g., capital, labor, and tax, etc.) could be included as market constraints. The framework could also be useful for regional modeling of specific areas. Since each region has specific regional characteristics, such as different water accessibility, the framework can be used to solve spatial optimization problems for multiple regions by accounting for consequences at a regional scale. Additionally, the framework can be used to address regional environmental regulations.

Although the RCOT-P2P framework has the above strengths, there are several key points that need to be addressed further. First, the role of ecosystem services needs to be included. Even though the RCOT-P2P framework considers the supply of ecosystem goods, such as water supply and mineral supply, it does not take account of ecosystem services, such as CO_2 sequestration and air pollutant removal by

vegetation. To claim absolute sustainability of systems and to avoid ecological overshoots, the supply of surrounding ecosystem services must be quantified and balanced with the corresponding demands for those services (e.g., CO_2 emissions and air pollutant emissions).[9] Recently, Techno-Ecological Synergies in Life Cycle Assessment (TES-LCA) computational framework has been developed to account for the supply of ecosystem goods and services in conducting the LCA,[35,129] which has also been used for sustainable supply chain design with the P2P framework.[179] The consequential approach also needs to account for the consequence of decisions on ecosystems along with effects on economic systems.

Most consequential approaches including this work address the consequences on the economic domain. As described in Section 5.2, however, social consequences also need to be studied. The RCOT-P2P framework could include the macro level of human behaviors, such as job creation and wages, because these social factors could also be one of the economy factors. However, accounting for social consequences is still at a very early stage.

The consequential approach also needs to consider the elasticity of commodity price because the price is determined by the market. The current RCOT-P2P framework does not account for the price elasticity and assumes prices to be fixed. In this work, the change in technology choices as the urea production increases with the engineering decision objective, which is about maximizing plant profits, is not shown because the price of products or commodities is fixed regardless of which technology is selected. Therefore, the profits of urea production at the equipment scale are not affected by technology choices at the value chain scale when profits are maximized. In the real-world market, however, the price of commodities does change due

to technology choices because the most expensive technology in use determines the price.[27] The consequential approach based on the equilibrium model can capture such price elasticity.[24–26] However, its sectoral data resolution is often poor, and thus it is not appropriate for small-scale regional models.[18] The price elasticity could also be accounted for from the duality of Leontief's quantity and price models.[27,180,181] If the RCOT-P2P framework could include the dual price model, it would improve the modeling performance of economic consequences.

In the urea case study, optimal technologies are selected to be employed in the Muskingum River Watershed for each optimization objective. The RCOT-P2P framework can also be applied to larger systems that consist of multiple regions. In such a large-scale analysis, the distribution of technologies could be modeled by considering region-specific market constraints and transportation of products between regions.

Notation

Symbol	Description
P-LCA model	
$\underline{X}$	Technology matrix at the value chain scale
$\underline{s}$	Scaling vector of processes at the value chain scale
$\underline{y}$	Final demand vector of products at the value chain scale
$\underline{B}$	Interventions matrix at the value chain scale
$\underline{g}$	Total interventions at the value chain scale
EEIO model	
I	Identity matrix
$\overline{A}$	Commodity-by-commodity direct requirements matrix at the economy scale
$\overline{x}$	Throughput vector of sectors at the economy scale (analogous to $\overline{s}$)
$\overline{s}$	Scaling vector of sectors at the economy scale
$\overline{y}$	Final demand vector of commodities at the economy scale
$\overline{B}$	Interventions matrix at the economy scale
$\overline{g}$	Total interventions vector at the economy scale
Hybrid LCA model	
$\overline{A}^*$	Disaggregated $\overline{A}$ matrix at the economy scale
$\underline{X}_u$	Upstream cutoff flow matrix from the economy scale to the value chain scale
$\underline{A}_d$	Normalized downstream cutoff flow matrix from the value chain scale to the economy scale
$\overline{B}^*$	Disaggregated $\overline{B}$ matrix at the economy scale
$\overline{\overline{g}}$	Total interventions vector at multiple spatial scales
$\overline{V}$	Make matrix at the economy scale
$\overline{U}$	Use matrix at the economy scale
$\underline{V}$	Make matrix at the value chain scale
$\underline{U}$	Use matrix at the value chain scale
$\overline{V}^*$	Disaggregated $\overline{V}$ matrix at the economy scale
$\overline{U}^*$	Disaggregated $\overline{U}$ matrix at the economy scale
P_P	Value chain scale permutation matrix relating value chain processes to economy sectors
P_F	Value chain scale permutation matrix relating value chain products to economy commodities
$\underline{p}$	Unit price vector of value chain products
$\underline{X}_d$	Downstream cutoff flow matrix from the value chain scale to the economy scale
$\overline{R}$	Total interventions matrix at the economy scale
$\overline{R}^*$	Disaggregated $\overline{R}$ matrix at the economy scale
$\overline{x}^*$	Throughput vector of disaggregated sectors at the economy scale
Process design model	
$\{z\}$	Design variables at the equipment scale
$H(\{z\})$	Engineering model external to $X(\{z\})$
$X(\{z\})$	Technology matrix at the equipment scale
s	Scaling vector of processes at the equipment scale
y	Final demand vector of products at the equipment scale
$B(\{z\})$	Interventions matrix at the equipment scale

Symbol	Description
P2P model	
$\underline{X}_u^E(\{z\})$	Upstream cutoff flow matrix from the economy scale to the equipment scale
$\underline{X}_u^V(\{z\})$	Upstream cutoff flow matrix from the value chain scale to the equipment scale
$\underline{A}_d^E(\{z\})$	Normalized downstream cutoff flow matrix from the equipment scale to the economy scale
$\underline{X}_d^V(\{z\})$	Downstream cutoff flow matrix from the equipment scale to the value chain scale
$\underline{X}^*(\{z\})$	Disaggregated $\underline{X}$ matrix at the value chain scale
$\underline{B}^*(\{z\})$	Disaggregated $\underline{B}$ matrix at the value chain scale
$V(\{z\})$	Make matrix at the equipment scale
$U(\{z\})$	Use matrix at the equipment scale
P_P^E	Equipment scale permutation matrix relating equipment processes to economy sectors
P_F^E	Equipment scale permutation matrix relating equipment products to economy commodities
p	Unit price vector of equipment products
$\underline{X}_d^E(\{z\})$	Downstream cutoff flow matrix from the equipment scale to the economy scale
$\underline{V}^*(\{z\})$	Disaggregated $\underline{V}$ matrix at the value chain scale
$\underline{U}^*(\{z\})$	Disaggregated $\underline{U}$ matrix at the value chain scale
P_P^V	Equipment scale permutation matrix relating equipment processes to value chain processes
P_F^V	Equipment scale permutation matrix relating equipment products to value chain products
$\overline{\underline{X}}(\{z\})$	Transaction matrix at multiple spatial scales
$\overline{\underline{X}}^*(\{z\})$	Disaggregated $\overline{\underline{X}}(\{z\})$ matrix at multiple spatial scales
$\overline{\underline{s}}$	Scaling vector at multiple spatial scales
$\overline{\underline{y}}$	Final demand vector at multiple spatial scales
$\overline{\underline{B}}(\{z\})$	Interventions matrix at multiple spatial scales
$\overline{\underline{B}}^*(\{z\})$	Disaggregated $\overline{\underline{B}}(\{z\})$ matrix at multiple spatial scales
RCOT model	
$\overline{A}'$	Rectangular shaped direct requirements matrix at the economy scale
$\overline{F}$	Economy factor requirement matrix at the economy scale
$\overline{c}$	Total economy factor consumption vector at the economy scale
c_{max}	Maximum available economy factor vector
κ	Unit price vector of economy factors
RCOT-P2P model	
$\overline{F}^*(\{z\})$	Disaggregated $\overline{F}$ matrix at the economy scale
$\overline{Q}$	Total economy factor requirement matrix at the economy scale
$\overline{Q}^*(\{z\})$	Disaggregated $\overline{Q}$ matrix at the economy scale
$\underline{F}$	Economy factor requirement matrix at the value chain scale
$\underline{F}^*(\{z\})$	Disaggregated $\underline{F}$ matrix at the value chain scale
$F(\{z\})$	Economy factor requirement matrix at the equipment scale
$\overline{\underline{F}}(\{z\})$	Economy factor requirement matrix at multiple spatial scales
$\overline{\underline{F}}^*(\{z\})$	Disaggregated $\overline{\underline{F}}(\{z\})$ matrix at multiple spatial scales
$\overline{\underline{c}}$	Total economy factor consumption vector at multiple spatial scales
$\overline{a}_{ij}$	Coefficient about the direct requirement of an input commodity i to produce one dollar amount of the output commodity j
$\overline{u}_{ij}$	Use of commodity i in technology (sector) j
$\overline{x}_j$	Throughput from technology (sector) j
I'	Rectangular shaped identity matrix
$\overline{b}_{kj}$	Intensity of intervention k from technology (sector) j
$\overline{r}_{kj}$	Total direct intervention k from technology (sector) j
$\overline{f}_{lj}$	Intensity of economy factor consumption l from technology (sector) j
$\overline{q}_{lj}$	Total direct economy factor consumption l from technology (sector) j
g_{max}	Maximum allowed interventions vector

Symbol	Description
Case study: Urea engineering model at the equipment scale	
γ	Heat capacity ratio
X_{CO_2}	Conversion yield of CO_2
$P_{vap,i}$	Vapor pressure of component i
F	Total mass flow rate
f_{c_i}	Mass flow rate of component i
a_i	Activity of component i
ξ_i	Overhead split fraction of component i
$\alpha_{i/k}$	Relative volatility of component i with respect to component k

Chapter 6: Climate-Resilient Process Design Using a Flexibility Analysis Approach

6.1 Introduction

Climate change is happening gradually. The impacts of this change can be fatal to current and future generations in various ways. We have seen the increased fluctuation of precipitation and temperature, which induces more frequent natural disasters, such as flooding, drought, severe storms, and even hurricanes. These are the direct impacts of climate change primarily related to the water cycle, which is one of the supporting services from ecosystems.[182] The change in supporting ecosystem services will affect not only other ecosystem services (i.e., provisioning, regulating, and cultural services) that rely on the supporting services but also economic and societal activities that rely on various ecosystem services.[183]

Numerous studies indicated that the knock-on (indirect) impacts of climate change on ecosystems[184,185] and the overall economy[186,187] are significant as well. Shaw et al. (2011) investigated the impacts of climate change on ecosystems in California, U.S.[185] Many ecosystem services are likely to be affected by climate change, including the change in water supply, habitat for biodiversity, forest ecosystems due to the increased frequency and intensity of the fire, and the production of crops and livestock due to

the changing patterns of precipitation. They predicted that the supply and value of ecosystem services are likely to decrease under future greenhouse gas (GHG) emissions trajectories.

Since all economic activities rely on those ecosystem services, their decline could result in a decrease in economic outputs. Martinich and Crimmins (2019) investigated how climate change will affect multiple economy sectors (e.g, human health, infrastructure, and agriculture) of the U.S.[187] The study estimated that the overall economic damages range in the hundreds of billions of dollars annually by 2100 under a high GHG emissions scenario. However, mitigation strategies under a low GHG emissions scenario will result in substantial economic benefits. Also, the Stern Review claimed that the damages from climate change are likely to be large, and therefore, immediate action for reducing GHG emissions is urgent.[186,188]

The climate change impacts will vary with mitigation strategies decided by policymakers. Therefore, various adaptation strategies to climate change have been investigated to enable proper action. For instance, van Vliet et al. (2016)[30] examined the vulnerability of the world's current energy systems to climate change (water availability and temperature), considering the continuing increase in energy demands along with the growing population. Then, they investigated adaptation options (increased plant efficiency and alternative options for fuel and cooling) for sustaining water-energy security.

It is critical that we need to investigate both vulnerability (climate change impacts) and adaptation (alternative options) of technological systems to climate change. Currently, most work has been conducted on agricultural and energy sectors. However, studies on manufacturing systems for climate change are still lacking. Some

analytic work exists regarding the impacts of climate change on manufacturing systems. Mac Dowell et al. (2017)[189] investigated the effectiveness of CO_2 capture and chemical conversion technologies in the context of climate change. They estimated that CO_2 chemical conversion can account for only 1% of the mitigation challenge. Other works investigated the vulnerability of U.S. manufacturing systems to water scarcity.[190,191] Walker et al. (2013) conducted detailed engineering modeling work with respect to the impacts of water scarcity on industrial boiler systems.[192] However, they did not consider climate change scenarios and solve design problems. To the best of our knowledge, no work has been reported that solved detailed engineering design problems in the context of climate change.

Traditional engineering approaches rely on the assumption of stationarity, which means the natural systems fluctuate within an unchanging variability.[193] However, this assumption is not valid anymore since we are experiencing the increasing variability in climate and its impacts. Therefore, designing flexible and resilient manufacturing process systems to climate change is necessary to make them adapt to uncertain climate disturbances and changes in ecosystems and economic markets. Additional costs will be involved with adaptation strategies by showing trade-offs with the benefits of avoiding climate change impacts. In this chapter, we address climate-resilient process design (CRPD) problems using a flexibility analysis (FA) approach.

The main motivation for FA is to guarantee the operability (the capability of feasible operation) of manufacturing processes under uncertain changes and disturbances at the design stage of processes.[194] FA is suitable for exploring CRPD since future climate projections are uncertain. Numerous global climate models (also known as general circulation models or GCMs) have been developed to project future climate

data. Based on these data, future ecosystem provisioning services, such as water supply, can be simulated using hydrological modeling or ecosystem modeling tools.[184,195] For example, water is an important resource for manufacturing systems since it is used for cooling and steam-heating processes. Therefore, the projected climate and simulated water supply data can be considered as uncertain parameters for the FA study to ensure the operability of processes under climate change.

In this chapter, we will explore CRPD approaches using the FA approach. A case study is performed for a simple heat exchanger network (HEN) system. Given that the indirect impacts of climate change could also affect entire manufacturing systems and supply chain networks, CRPD solutions need to account for any changes in supply chains that are attributed to climate change. Therefore, we will conduct another case study for the urea manufacturing systems that include multiple supply chain options for electricity generation and ammonia production. We will discuss how the processes and supply chains need to be designed to maintain productivity and avoid damages under climate change scenarios.

6.2 Methods

6.2.1 Representative Concentration Pathway Scenarios

Representative concentration pathway (RCP) scenarios, which are adopted by the Fifth Assessment Report of the Intergovernmental Panel on Climate Change (IPCC AR5), show future GHG concentration trajectories.[5] According to IPCC AR5, the rise in global temperature must be limited to 2 °C above pre-industrial levels (1850–1900) in order to avoid disastrous consequences of climate change.[164] For the decade 2006–2015, we have already reached to 0.87 °C above pre-industrial levels.[196] In 2018,

IPCC issued the Special Report on the impacts of 1.5 °C above pre-industrial levels in response to the Paris Agreement that we should pursue efforts to hold the increase in global average temperature well below 2 °C above pre-industrial levels and limit the increase to 1.5 °C.[196]

RCP scenarios are labeled after a possible range of radiative forcing values in watts per square meter by 2100 as shown in Fig. 6.1a. RCP 8.5 is a high emissions scenario with no mitigation.[197] This shows the continuous increase in CO_2 concentrations that reach more than 900 ppm in 2100 as shown in Fig. 6.1b and result in approximately 4 °C warming in 2100 above pre-industrial levels. The global coal industry will continue to grow in this scenario. Considering that other types of fuel, such as solar,[177] are increasingly cheaper than coal today, RCP 8.5 represents not a business-as-usual case, but the worst case.

On the other hand, RCP 4.5 exhibits a suppressed increase in CO_2 concentrations due to mitigation strategies applied in the future. This scenario will lead to approximately 2 °C warming above pre-industrial levels by 2100. As shown in Fig. 6.1c. CO_2 emissions in this scenario need to be decreased by around 2045 and mitigated to the stable level by around 2080 to achieve the stable radiative forcing level in 2100.[198] RCP 4.5 represents one of the intermediate cases.

In addition, RCP 1.9 represents a scenario for 1.5 °C warming above pre-industrial levels by 2100. In this work, we only consider RCP 4.5 and 8.5 scenarios since climate modeling data for RCP 1.9 are not yet available from the USGS Geo Data Portal (GDP) database.[199]

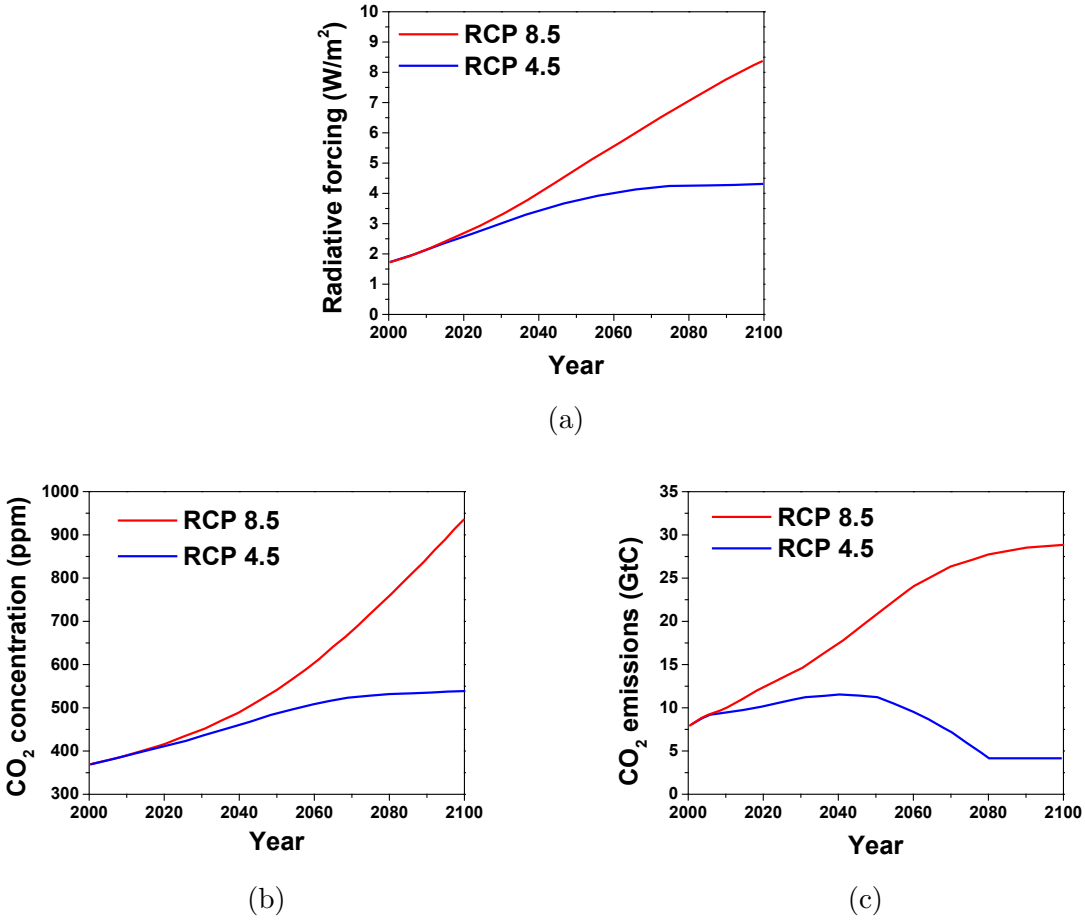

Figure 6.1: Trajectories of **(a)** radiative forcing, **(b)** atmospheric CO_2 concentrations, and **(c)** CO_2 emissions for RCP 8.5 and 4.5 scenarios.[5]

6.2.2 Climate and Hydrological Modeling

To estimate future climate change based on the RCP scenarios, various GCMs have been developed. Since uncertain future climate data are projected from GCMs, multiple GCMs are generally employed for the studies that investigate the impacts of climate change. In this study, we employ five GCMs (CCSM4, GFDL-CM3,

HadGEM2-AO, MIROC5, and MPI-ESM-LR) from the USGS GDP database to account for variance between the models.[199] Those models are from the Coupled Model Intercomparison Project Phase 5 (CMIP5) archive. CMIP5 is a standard experimental protocol for various climate model studies. The GCMs employed in this work are statistically downscaled at a 1/16th degree spatial resolution using LOCA (Localized Constructed Analogs) statistical downscaling technique.[200] The downscaled GCMs estimate future daily minimum/maximum temperature and precipitation in a selected region.

Climate disturbances affect the supply of various ecosystem services[184,185] as mentioned in Section 6.1. Based on the climate data projected from GCMs, hydrological modeling or ecosystem modeling tools can be used to simulate the change in ecosystem services.[184,195] For example, to account for future water scarcity risk, the Soil and Water Assessment Tool (SWAT) model can be employed to simulate total water yield in a selected region using future climate data obtained from the GCMs.[201,202] Water temperature is also an important factor that affects manufacturing processes since they rely heavily on water resources, both for generating steam and cooling the process. Average daily water temperature (°C) is estimated from the average daily air temperature (°C) based on a linear regression method by Equation 6.1.[203]

$$T_{water} = 5.0 + 0.75T_{air}, \tag{6.1}$$

where T_{water} and T_{air} represent average daily water temperature and average daily air temperature, respectively. Equation 6.1 assumes that the lag time between air and water temperatures is less than 1 day.[201]

6.2.3 Flexibility Analysis

FA has mainly been developed by scholars in the field of process systems engineering.[7,194,204–207] To ensure the operability of industrial processes under uncertain changes and disturbances, the processes need to be designed to be flexible to uncertain disturbances. The FA approach considers potential disturbances as uncertain parameters but not as fixed values.

Two approaches have been developed for FA: flexibility test problem and flexibility index problem. The former examines if a given design is flexible over a specified range of unknown parameters by adjusting control variables. The given design refers to the fixed structure and equipment size. On the other hand, the flexibility index problem aims to maximize the flexibility of a specified design with respect to the unknown parameters. In this chapter, we focus on the flexibility index problem since the test problem is nothing but an examination tool to check if the system is flexible or not.

The operability of industrial processes under disturbances needs to be guaranteed at the design stage of processes to avoid unexpected outcomes by such disturbances. Given that future climate data are uncertain, the flexibility of processes with respect to the changing climate can be investigated using the FA approach. The flexibility index (F) was developed to quantitatively measure how much flexibility can be achieved in a given design (d) for the unknown parameters (θ).[194] The flexibility index problem can be formulated as follows.

1. Define uncertain parameters (θ).

   The unknown parameters could include physical properties such as inlet temperatures, pressures, flow rates, and concentrations; and economic properties such as price of resources and demand of products.

2. Define a nominal value (θ^N) and an expected deviation of uncertain parameters ($\Delta\theta^+$ and $\Delta\theta^-$).

   The range of unknown parameters (T) is defined as follows:

$$T(\delta) = \{\theta : \theta^N - \delta\Delta\theta^- \leq \theta \leq \theta^N + \delta\Delta\theta^+\}, \tag{6.2}$$

   where θ^N and δ indicate a nominal value of the unknown parameters and a non-negative scalar variable, respectively. $\Delta\theta^+$ and $\Delta\theta^-$ are an expected deviation of uncertain parameters. While conventional process design approaches only consider the nominal value, FA considers the range of uncertain parameters ($T(\delta)$), which is a function of δ.

   The nominal value and expected deviation need to be known based on knowledge or historical data. For example, if the uncertain parameter is the temperature of input water from the environment, θ^N can be the average water temperature for a certain time period (e.g., the last decades). Also, $\Delta\theta^-$ and $\Delta\theta^+$ can be the historical deviation of water temperature. Then, $\delta\Delta\theta^-$ and $\delta\Delta\theta^+$ represent the deviation of unknown parameters.

3. Calculate the flexibility index (F) for a given design (d).

   F is calculated by solving the following optimization problem:

$$\begin{aligned} F = \ & \max \ \delta \\ \text{s.t.} \quad & \chi(d) = \max_{\theta \in T} \psi(d, \theta) \\ & \psi(d, \theta) = \min_{z} \max_{j \in J} f_j(d, z, \theta) \leq 0 \\ & T(\delta) = \{\theta : \theta^N - \delta\Delta\theta^- \leq \theta \leq \theta^N + \delta\Delta\theta^+\}, \quad \delta \geq 0, \end{aligned} \tag{6.3}$$

   where $\chi(d)$ and $\psi(d, \theta)$ refer to the flexibility function and the feasibility function for a given design d, respectively. $\chi(d) \leq 0$ is a constraint for the feasible

operation over the range of θ (i.e., $T(\delta)$). f_j is the j-th inequality equation (constraint) in the model, and J is the index set for the inequalities. z represents control variables in the model. Maximized δ $(= F)$ in Equation 6.3 represents the maximized range of unknown parameters (i.e., $T(F)$) that ensure the feasible operation. That is, the flexibility of a given design can be calculated by maximizing the range of unknown parameters. $F = 1.0$ represents that a selected design d is most flexible to the expected variation of uncertain parameters. $F < 1.0$ and $F > 1.0$ indicate that a design d is less and more flexible to the expected deviation, respectively.

Equation 6.3 can be converted to the following mixed-integer optimization problem by considering the Karush–Kuhn–Tucker conditions of the function $\psi(d, \theta)$:[7,194]

$$
\begin{aligned}
F = \min_{\delta, \lambda_j, s_j, y_j} \quad & \delta \\
\text{s.t.} \quad & f_j(d, z, \theta) + s_j = 0, \qquad j \in J \\
& \sum_{j \in J} \lambda_j = 1 \\
& \sum_{j \in J} \lambda_j \frac{\partial f_j(d, z, \theta)}{\partial z} = 0 \\
& s_j \leq U(1 - y_j) \\
& \lambda_j \leq y_j \\
& \sum_{j \in J} y_j = n_z + 1 \\
& \theta \leq \theta^N + \delta \Delta \theta^+ \\
& \delta, \lambda_j, s_j \geq 0, \quad y_j \in \{0, 1\},
\end{aligned}
\tag{6.4}
$$

where s_j and λ_j refer to the slack and Lagrange multipliers for the constraints f_j, respectively. U and y_j are a valid upper bound for s_j and the binary variables for s_j and λ_j. If $s_j = 0$ and $\lambda_j \leq 1$, $y_j = 1$. Also, if $0 \leq s_j \leq U$ and $\lambda_j = 0$, $y_j = 0$. n_z is the dimensionality of the control variables (z) in the model. The details of Equation 6.4 are available from the previous studies.[7,194]

4. Calculate F for alternative designs (d').

   Step 3 can be repeated for different design conditions (e.g., different equipment size). Also, by including a cost minimization function and solving a multi-objective optimization problem, a trade-off between flexibility and cost could be identified. Also, optimal designs with desired flexibility and cost could be identified.

6.2.4 Multiscale Consequential Process Design Model

Many studies on the impacts of climate change on energy systems considered adaptation technologies to climate change, such as water-efficient cooling and renewable power generation technologies.[30,208] Also, climate change could affect activities in supply chains. Therefore, multiple supply chain options need to be taken into account to examine how supply chains need to be adapted to climate change.

Multiscale consequential process design model[6] has been developed to conduct process and supply chain design studies while considering resource constraints and multiple technology options. The process-to-planet (P2P) multiscale process design model[13] is integrated with the rectangular choice-of-technology (RCOT) model[27] to construct the RCOT-P2P model, which is the multiscale consequential process design model.

The P2P multiscale model can solve process design problems at the equipment scale while accounting for activities at the value chain and economy scales as shown in Fig. 6.2. The P2P model is formulated by Equations 6.5 and 6.6.[13]

$$\overline{\underline{X}}^*(\{z\})\,\overline{\underline{s}} = \overline{\underline{y}} \quad \text{or} \quad \begin{bmatrix} I-\overline{A}^*(\{z\}) & -\underline{X}_u(\{z\}) & -X_u^E(\{z\}) \\ -\underline{A}_d(\{z\}) & \underline{X}^*(\{z\}) & -X_u^V(\{z\}) \\ -A_d^E(\{z\}) & -X_d^V(\{z\}) & X(\{z\}) \end{bmatrix} \begin{bmatrix} \overline{s} \\ \underline{s} \\ s \end{bmatrix} = \begin{bmatrix} \overline{y} \\ \underline{y} \\ y \end{bmatrix}, \quad (6.5)$$

$$\overline{\underline{B}}^*(\{z\})\,\overline{\underline{s}} = \overline{\underline{g}} \quad \text{or} \quad \begin{bmatrix} \overline{B}^*(\{z\}) & \underline{B}^*(\{z\}) & B(\{z\}) \end{bmatrix} \begin{bmatrix} \overline{s} \\ \underline{s} \\ s \end{bmatrix} = \overline{\underline{g}}. \quad (6.6)$$

Underbar and overbar notations refer to the value chain scale and the economy scale, respectively. The notation without bar represents the equipment scale. The double bar (underbar and overbar) notation refers to multiple scales.

- The commodity transaction equation (Equation 6.5) represents the physical and monetary balance of commodities to produce the demanded amounts of products, which are defined by a vector of final demands ($\overline{\underline{y}}$). $\overline{\underline{X}}^*(\{z\})$ matrix represents the transactions of commodities between processes across multiple scales. $I-\overline{A}^*(\{z\})$ matrix correspond to the commodity transaction matrix at the economy scale. I and $\overline{A}$ are identity and direct requirement matrices, respectively. $\underline{X}^*(\{z\})$ correspond to the product transaction matrix at the value chain scale. $\underline{X}^*(\{z\})$ is also referred to by the technology matrix. $X(\{z\})$ is the engineering model at the equipment scale. Non-diagonal elements in $\overline{\underline{X}}^*(\{z\})$ matrix are upstream and downstream cutoff flows across multiple scales, which are indicated by subscripts u and d, respectively. For instance, $X_u^V(\{z\})$ and $A_d^E(\{z\})$ represent matrices of upstream cutoff flows from the value chain to the equipment scales and downstream cutoff flows from the equipment to the economy scales, respectively. Equation 6.5 determines the scale of each process,

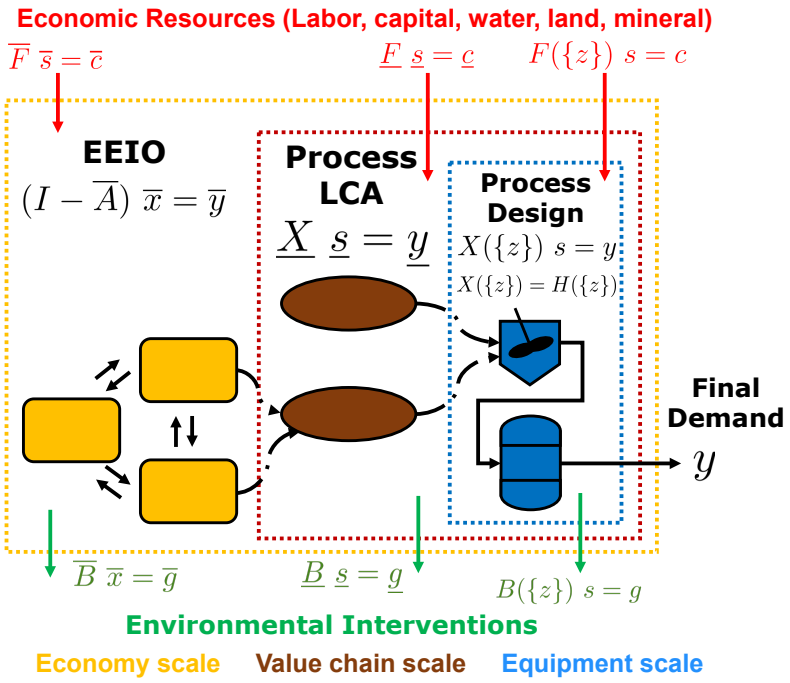

Figure 6.2: RCOT-P2P multiscale consequential process design model structure.[6]

which is defined by a vector of scaling factors ($\underline{\overline{s}}$), to produce the demanded amounts of products ($\overline{\underline{y}}$). The details about P2P model formulation are available from the previous studies.[13,123]

- The intervention equation (Equation 6.6) determines life cycle environmental impacts ($\overline{\underline{g}}$) by scaling the direct intervention from each process ($\overline{\underline{B}}^*(\{z\})$) with the scaling vector ($\underline{\overline{s}}$), which is determined by Equation 6.5.

An asterisk mark on several matrices (e.g., $\overline{A}^*$ and $\overline{B}^*$) in Equations 6.5 and 6.6 indicates the larger scale matrices are disaggregated from smaller scales to remove overlaps between the matrices. The disaggregation of larger-scale matrices is necessary for the integration of multiple scale models because activities at the smaller

scales are included in the larger scale models. The details about disaggregation procedures are available from the previous studies.[13,123] Through the disaggregation, process design variables ($\{z\}$) in the equipment scale model are spread out to the larger-scale models. Through Equations 6.5 and 6.6, the P2P model solves process design problems at the equipment scale while accounting for activities at the value chain and economy scales.

On the other hand, the RCOT model is a consequential technology choice model based on the environmentally-extended input-output (EEIO) model.[27,28] RCOT accounts for market resource constraints and multiple technology options at the economy scale to investigate the consequences of resource availability in the market on the adoption of technologies. The RCOT framework is integrated with the P2P framework to construct a consequential process design model that accounts for multiple spatial scales.[6] The integrated RCOT-P2P framework accounts for market effects and economic resource availability in designing the engineering model while considering value chain and economy scale activities. Moreover, since the RCOT model can select technologies from multiple technology options as a consequence of economic resource constraints, the RCOT-P2P framework solves not only engineering design problems at the equipment scale but also supply chain design problems at the value chain and economy scales.

The RCOT-P2P model has the same equations for commodity transactions (Equation 6.5) and interventions (Equation 6.6) as the P2P model. Also, as shown in Fig. 6.2, the RCOT-P2P model accounts for economic resource constraints by Equation

6.7.

$$\overline{\underline{F}}^{*}(\{z\})\ \overline{\underline{s}} = \overline{\underline{c}} \quad \text{or} \quad \begin{bmatrix}\overline{F}^{*}(\{z\}) & \underline{F}^{*}(\{z\}) & F(\{z\})\end{bmatrix} \begin{bmatrix}\overline{s} \\ \underline{s} \\ s\end{bmatrix} = \overline{\underline{c}}, \tag{6.7}$$

$$\overline{\underline{c}} \leq c^{max}. \tag{6.8}$$

- The economy factor (economic resource) equation (Equation 6.7) calculates the total economic resource consumption ($\overline{\underline{c}}$) to produce the demanded amounts of products ($\overline{\underline{y}}$) using the economic resource requirement data for each activity at multiple scales ($\overline{\underline{F}}^{*}(\{z\})$). A vector of scaling factors ($\overline{\underline{s}}$) is determined by Equation 6.5. For example, total consumption of labor, capital, land, mineral, and water resources can be calculated with respect to $\overline{\underline{y}}$ by Equation 6.7.

- As shown in Equation 6.8, the calculated total economic resource consumption ($\overline{\underline{c}}$) needs to be smaller than the available amount of economic resources (c^{max}). If there are not enough resources available for the best technology option, the RCOT-P2P model selects the secondary and tertiary technology options simultaneously with the best option.

The details about RCOT-P2P model formulation are available in the previous study.[6]

6.2.5 Climate-Resilient Process Design Approach

To design manufacturing systems to be robust and flexible to climate change, multiple models need to be employed since climate change affects not only temperatures and precipitation but also the supply of various ecosystem services. In this work, we explore CRPD approaches by employing various GCMs, a hydrological model (SWAT model), and manufacturing models (FA model and RCOT-P2P model).

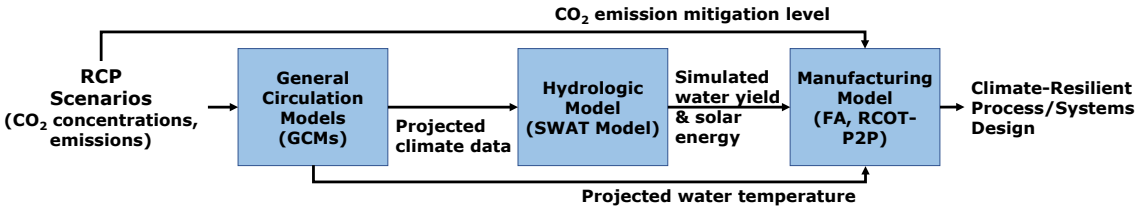

Figure 6.3: A systematic modeling approach for designing climate-resilient processes and supply chains.

Figure 6.3 exhibits a systematic modeling approach to obtain CRPD solutions by employing various models. RCP scenarios give CO_2 emissions trajectories, and statistically downscaled GCMs project daily climate data (temperatures and precipitation) in a selected region up to 2100 for each RCP scenario. Some GCMs give climate data up to 2099. Based on the projected climate data, the SWAT model simulates the supply of ecosystem services such as water yield and solar radiation in the region. In this work, we assume wind speed is not affected by climate change because the WXGEN weather generator in the SWAT model calculates wind speed based on a random number.[201]

The manufacturing engineering model solves CRPD problems with climate change constraints that are defined by the other models. For example, the GHG emission trajectory of RCP scenarios determines CO_2 emission mitigation targets (e.g., the percentage reduction in CO_2 emissions) for manufacturing systems. Mitigation strategies will be needed to satisfy the mitigation levels. Also, water temperature is one of the climate change constraints. As described in Section 6.2.2, water temperature can be estimated from air temperature using Equation 6.1.[203] Water yield and solar radiation simulated from the SWAT model will affect decisions for the manufacturing

process and supply chain design as well. Those climate change constraints can be considered for the manufacturing engineering model to obtain CRPD solutions. The FA approach in Section 6.2.3 can be employed by identifying climate change constraints as uncertain parameters. Also, the RCOT-P2P model in Section 6.2.4 can be constructed with the climate change constraints to account for the consequences of climate change on process and supply chain design.

6.3 Results and Discussion

In this work, we explore CRPD solutions by investigating the consequences of climate change on manufacturing processes and supply chains. Two case studies are conducted for a simple HEN system and urea manufacturing systems in the Muskingum River Watershed (MRW) in Ohio, the United States using the FA approach and the RCOT-P2P model, respectively. All codes for the case studies can be available upon request. Land use of the MRW is shown in Fig. 5.4.

6.3.1 General Circulation Models and SWAT Hydrological Model

Figure 6.4 shows historical and projected climate data in the MRW up to 2099 for both RCP 4.5 (mitigated) and 8.5 (non-mitigated) scenarios. The projected data are obtained from five different GCMs (CCSM4, GFDL-CM3, HadGEM2-AO, MIROC5, and MPI-ESM-LR). The projected average, minimum, and maximum values are plotted in Fig. 6.4. The annual average temperatures are increased for both RCP 4.5 and 8.5 scenarios. The increase for RCP 8.5 (4 °C warming scenario) is much larger than that for RCP 4.5 (2 °C warming scenario).

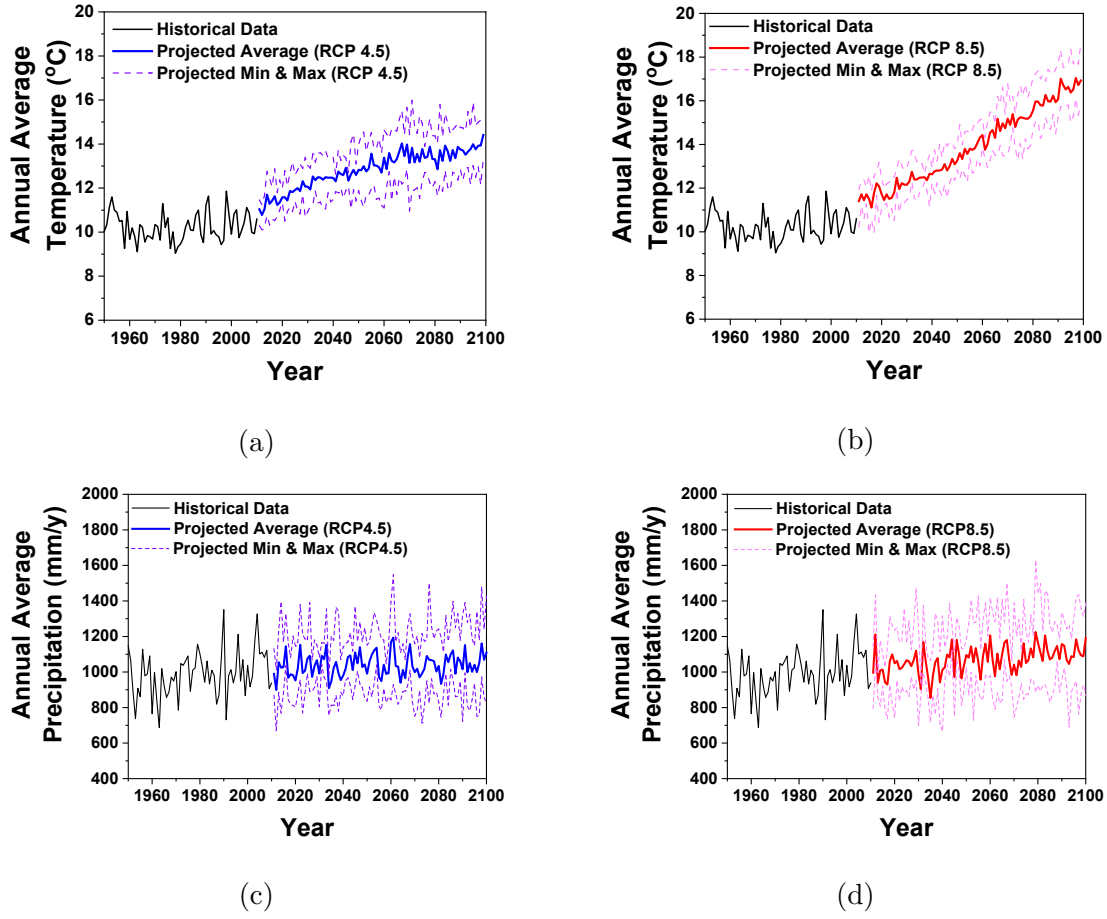

Figure 6.4: Historical and projected climate data in the MRW up to 2099. The projected average, minimum, and maximum values from the five GCMs are plotted with respect to annual average temperatures for **(a)** RCP 4.5 and **(b)** RCP 8.5, and annual average precipitation for **(c)** RCP 4.5 and **(d)** RCP 8.5.

With respect to the annual average precipitation results, the increasing standard deviations of the annual average precipitation over the years are observed for both RCP scenarios as shown in Fig. 6.5a. RCP 8.5 shows a larger increase in the standard deviations than RCP 4.5. Also, Figure 6.6 exhibits box plots of daily precipitation in the MRW for both RCP scenarios. The chance of heavy rainfall (outliers in the plots) tends to increase over time. These results support that the assumption of stationarity

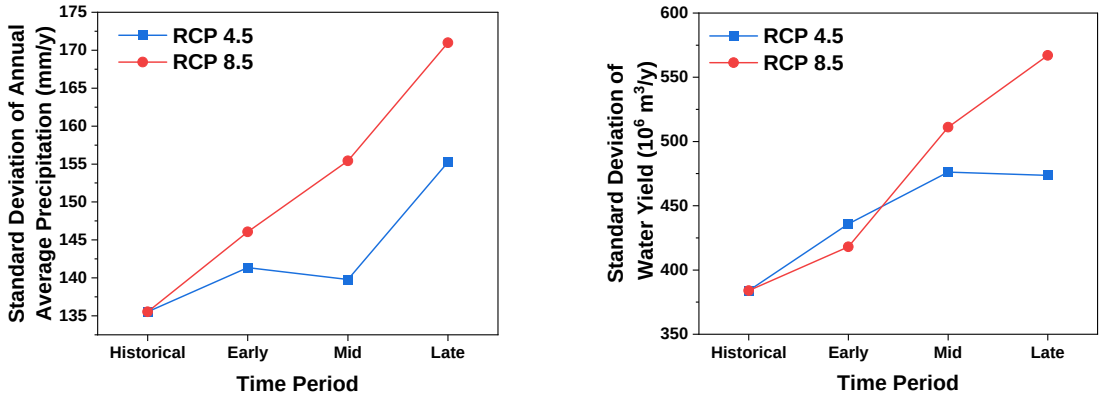

(a) (b)

Figure 6.5: Standard deviation of **(a)** annual average precipitation and **(b)** annual water yield in the MRW for each 30-year period from 1980–2099. Standard deviations of projected data are calculated for multiple data from five GCMs. Historical data represents years 1980–2009. Early-, mid-, and late-century represent years 2010–2039, 2040–2069, and 2070–2099, respectively.

is not valid anymore.[193] Therefore, we need to address CRPD approaches to account for the effect of climate change on design solutions.

Based on the projected climate data from GCMs, the SWAT model calculates water yield in the MRW. Ambient CO_2 concentrations are adjusted for every 30 years from 330 ppm to 660 ppm in the SWAT model to account for the effect of changing atmospheric CO_2 concentrations over the years.[209] Atmospheric CO_2 concentrations in the early-century (2010–2039), mid-century (2040–2069), and late-century (2070–2099) for RCP 4.5 scenario are fixed to 420, 490, and 530 ppm, respectively, by calculating the average concentrations for each time period. Also, atmospheric CO_2 concentrations in the early-, mid-, and late-century for RCP 8.5 scenario are fixed to 430, 580, and 660 ppm. The late-century CO_2 concentrations for RCP 8.5 are 800

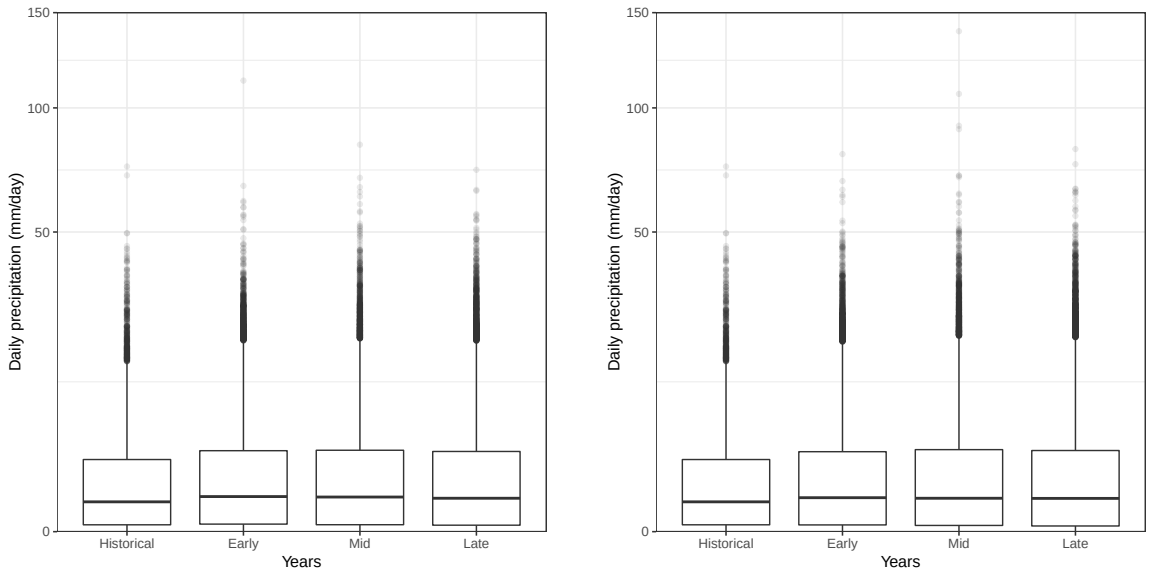

Figure 6.6: Box plots of daily precipitation in the MRW for RCP **(a)** 4.5 and **(b)** 8.5 scenarios.

ppm but are considered to be 660 ppm. This is because the SWAT model simulation is based on the CO_2 concentrations up to 660 ppm.[209]

Figure 6.7 shows the simulated annual water yield for RCP 4.5 and 8.5 scenarios. Both results show large variations in the future annual water yield results since five different GCMs are employed to estimate future climate. The daily variation is likely to be much larger. In both RCP scenarios, these variations are intensified over time due to the increased variability in precipitation. As shown in Fig. 6.5b, RCP 8.5 scenario shows larger standard deviations in water yield than RCP 4.5 scenario in the mid and late centuries.

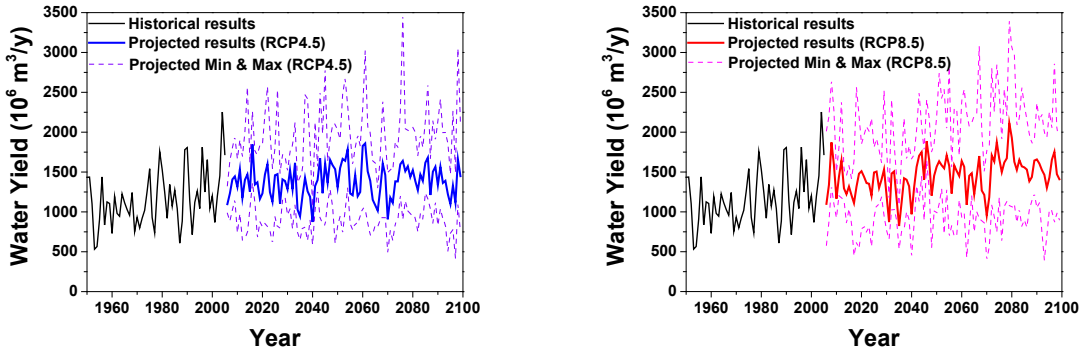

(a) (b)

Figure 6.7: Historical and projected annual water yield in the MRW up to 2099 simulated from the SWAT model for **(a)** RCP 4.5 and **(b)** 8.5 scenarios.

6.3.2 Case Study 1. Heat Exchanger Network

One of the most famous examples for FA is a simple HEN problem as shown in Fig. 6.8.[7,194,205,206] This HEN system consists of three heat exchanger units (H1-C1, H2-C1, and H2-C2) and one cooler unit (H1-W). H1 and H2 are hot process streams, and C1 and C2 are cold process streams. T_1, T_2, $\cdots$, and T_8 correspond to the temperatures of streams across the HEN system. Q_c is the heat load of the cooler unit. In this case study, we modify the HEN model from the previous study[7] to examine the consequences of climate change on design solutions for the HEN system. We define the temperature of cooling water from the environment ($T_{env,wat}$) as an uncertain parameter, θ. Future climate change will affect the water temperature. We explore CRPD solutions for the HEN system in the MRW by investigating the consequences of the change in water temperature.

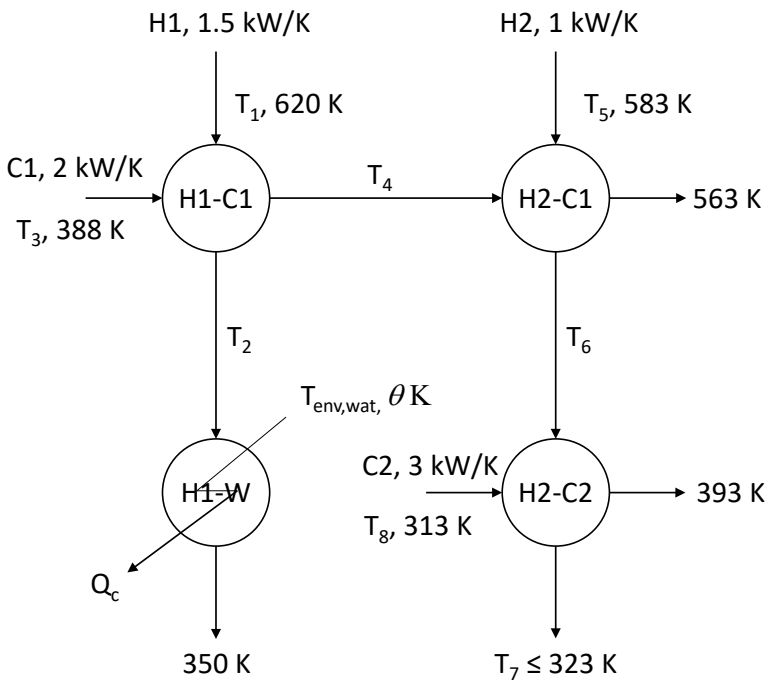

Figure 6.8: Heat exchanger network system.[7]

Flexibility Analysis Model Construction

A flexibility index problem for the HEN example can be formulated as follows. The range of uncertain parameters ($T(\delta)$) is defined by Equation 6.9

$$T(\delta) = \{\theta : \theta \leq \theta^N + \delta\Delta\theta^+\}, \quad \theta = T_{env,wat}, \tag{6.9}$$

where a nominal value (θ^N) and an expected deviation of the uncertain parameter ($\Delta\theta^+$) are obtained from the historical weather data in the past 30 years (1980–2009). In this work, only the positive deviation of water temperature is considered because water is used for cooling in the HEN system of this case study. Equation 6.1 is used to calculate water temperature from the air temperature data shown in Fig. 6.4. The average water temperature during the past 30 years was 12.74 °C. Also, the historical

monthly maximum water temperature was 26.86 °C. This indicates that the positive deviation of water temperature during the past 30 years was +14.12 °C. Conventional engineering approaches that are based on the assumption of stationarity consider the historical range of water temperature.

Then, the flexibility index (F) problem is formulated by Equation 6.10.

$$\begin{aligned} F = \ & \max \ \delta \\ \text{s.t.} \quad & \chi(d) \leq 0 \\ & T(\delta) = \{\theta : \theta \leq 285.89 + 14.12\delta\}, \quad \theta = T_{env,wat}, \\ & \delta \geq 0. \end{aligned} \tag{6.10}$$

Also, the inequality constraints for the HEN system ($f_1, \cdots, f_5$) are shown in Equations 6.11–6.15.[7]

$$f_1 = -0.67Q_c + T_3 - 350 \leq 0, \tag{6.11}$$

$$f_2 = -T_5 - 0.75T_1 + 0.5Q_c - T_3 + 1388.5 \leq 0, \tag{6.12}$$

$$f_3 = -T_5 - 1.5T_1 + Q_c - 2T_3 + 2044 \leq 0, \tag{6.13}$$

$$f_4 = -T_5 - 1.5T_1 + Q_c - 2T_3 - 2T_8 + 2830 \leq 0, \tag{6.14}$$

$$f_5 = T_5 + 1.5T_1 - Q_c + 2T_3 + 3T_8 - 3153 \leq 0, \tag{6.15}$$

where T_1, T_3, T_5, and T_8 are fixed to 620, 388, 583, and 313 K, respectively, to investigate the flexibility of HEN system only for the unknown water temperature. Also, the outlet temperature of cooling water ($T_{out,wat}$) needs to be maintained below 45 °C to avoid excessive fouling. An additional inequality constraint (f_6) is needed for the temperature of cooling water as shown in Equation 6.16.

$$f_6 = \frac{Q_c}{F_W c_p} + T_{env,wat} - 318 \leq 0, \tag{6.16}$$

where F_W and c_p are the flow rate of cooling water and specific heat per unit mass at constant pressure, respectively. Also, $Q_c = F_W c_p(T_{out,wat} - T_{env,wat})$.

The annual cost for HEN system is calculated using Equation 9 in the previous study.[210] This cost includes the utility cost, the fixed charges, and the area cost for heat exchangers and a cooler.

As described in Section 6.2.3, Equation 6.10 can be formulated as a mixed-integer optimization problem. To investigate a trade-off between flexibility (Z_1) and cost (Z_2), a mixed-integer multi-objective optimization problem is formulated as shown in Equation 6.17.

$$
\begin{aligned}
Z_1 = & \min_{\delta,\lambda_j,s_j,y_j} \ \delta \ (= F) \\
Z_2 = & \ \min Cost \\
\text{s.t.} \quad & f_j(d,z,\theta) + s_j = 0, \qquad j = 1,2,\cdots,6 \\
& \sum_{j=1}^{6} \lambda_j = 1 \\
& \sum_{j=1}^{6} \lambda_j \frac{\partial f_j(d,z,\theta)}{\partial z} = 0 \\
& s_j \le 170(1-y_j) \\
& \lambda_j \le y_j \\
& \sum_{j=1}^{6} y_j = 2 \\
& \theta \le 285.89 + 14.12\delta, \quad \theta = T_{env,wat}, \\
& \delta, \lambda_j, s_j \ge 0, \quad y_j \in \{0,1\}.
\end{aligned}
\tag{6.17}
$$

In this case study, the minimized upper bound for s_j is 170 to avoid infeasible solutions. The dimensionality of control variable (the flow rate of cooling water, F_W) is one (i.e., $n_z = 1$).

Consequences of Climate Change on the HEN System

Figure 6.9 shows the flexibility index (F) and cost for the HEN system. A trade-off between F and cost is identified. When the HEN system design is based on the historical climate data, F is equal to 1.00 since the system is most flexible to the expected (historical) variation of water temperature (shown as an orange-dotted vertical line in Fig. 6.9). However, the HEN system needs to have larger flexibility to maintain its operability in the future years due to the increasing variability of water temperature. As shown in Fig. 6.9a, when we assume the average climate trajectory, which is represented by the average temperatures projected from the five GCMs (Fig. 6.4), F of the HEN system needs to be 1.03 and 1.19 in 2099 for RCP 4.5 and 8.5 scenarios, respectively. This is because the HEN system needs to tolerate warmer water temperatures for its feasible operation. According to the average climate results projected from the five GCMs, annual average water temperatures can get warmer than the historical trend by 0.47 °C and 2.67 °C for RCP 4.5 and 8.5 scenarios, respectively. When we assume the worst climate trajectory, which is represented by the warmest temperatures projected from the five GCMs, much larger flexibility is required for the HEN system since the system needs to operate under warmer water temperatures, as shown in Fig. 6.9b. Due to the trade-off identified between F and cost, more expenses are required to have the HEN system with larger flexibility.

Figure 6.10 exhibits the number of operation failure days per year up to 2099 for HEN system design ($F = 1.00$) based on the historical weather data in the past 30 years (1980–2009). As shown in Fig. 6.10a, when the average climate trajectory is assumed, the HEN system from the conventional design approach ($F = 1$) will fail to operate only for 10 days up to 2099 for RCP 4.5 scenario. However, the system

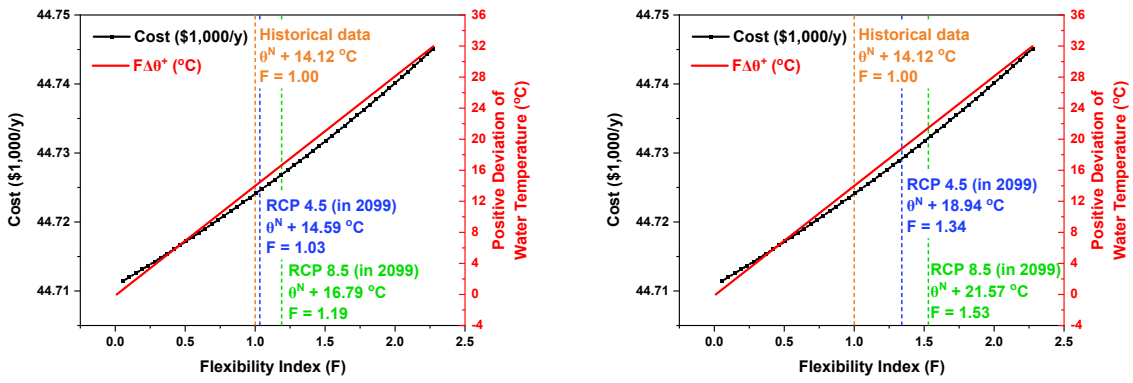

Figure 6.9: A trade-off between flexibility and cost for HEN system when **(a)** the average and **(b)** worst climate trajectories are assumed for the year 2099.

will fail to operate for 26 days on average every year in the late-century (2070–2099) for the RCP 8.5 scenario. If we assume the worst climate trajectory, the number of failure days per year for operating the HEN system will be increased significantly for both RCP scenarios, as shown in Fig. 6.10b. In the late-century, the HEN system will fail to operate for 54 days and 102 days on average every year due to the warmer water temperatures than the historical trend. To maintain the operability of the HEN system, it needs to be designed to be flexible to the warmer water temperatures. As indicated in Fig. 6.9, more expenses will be required for the more flexible HEN system design.

Pros and Cons of Employing the Flexibility Analysis Approach for Climate-Resilient Process Design Problems

The following is a list of pros and cons of employing the FA approach for CRPD studies.

Pros:

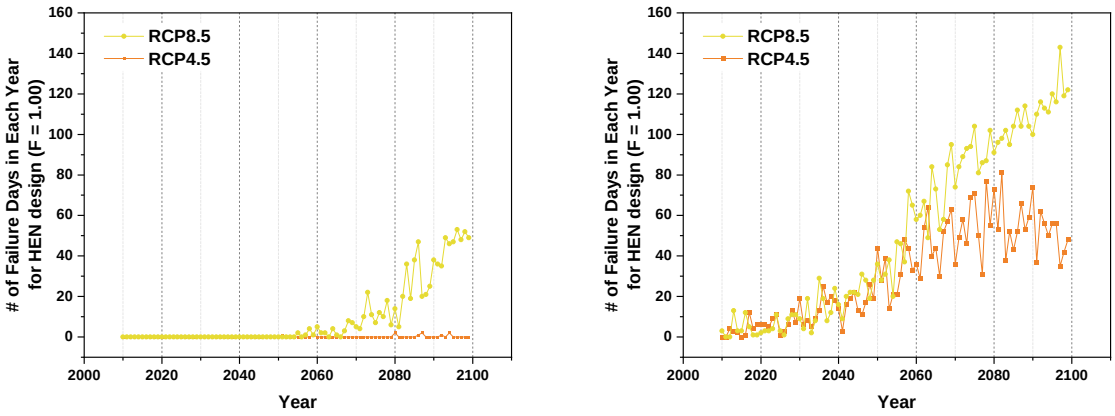

(a) (b)

Figure 6.10: The number of failure days in each year for HEN system design based on the historical weather data, when **(a)** the average and **(b)** worst climate trajectories are assumed.

- FA methodology has been established for decades to address flexible process design problems. Therefore, applying the FA approach for CRPD problems could be readily acceptable and applicable to engineering disciplines.

- Since FA is based on the mathematical engineering model, it can be integrated with other mathematical models such as supply chain models and economic models. Thus, the flexibility of processes can be examined while accounting for supply chain networks and the planetary boundary. Considering that climate change could have indirect impacts on many sectors,[187] incorporating a broad system boundary in the model could be valuable. However, the increased computational challenges will be a trade-off.

- Various methodological developments are available for the FA approach.[194] Some of them could be useful to address the shortcomings described below.

Cons:

- FA addresses the capability of feasible operation in the steady-state. On the other hand, climate change disturbances are dynamic uncertain parameters. FA does not address the dynamic capability to recover from disturbances in a fast and smooth manner. In other words, it does not account for how resilient the processes are to disturbances.

  → The dynamic flexibility index (DF) problem can potentially address the dynamic capability issue.[211] DF represents the maximized flexibility of processes to the worst trajectory of the uncertain parameters that can be tolerated throughout a selected time horizon while maintaining the feasibility of processes.

- FA identifies climate change disturbances as uncertain parameters for process design problems. However, it does not account for uncertainties in future climate change impacts. As pointed out by many studies,[193,212,213] climate change research essentially involves plenty of uncertainties due to the nature of future prediction. Uncertainties could stem from the GHG emissions trajectories of different RCP scenarios, the downscaling of GCMs to specific regions, the response from ecosystems to climate change, and the knock-on effect of climate change on economic and societal systems.

  → Some methodological developments in the FA approach may be useful to address this shortcoming. One work incorporated nonlinear confidence intervals of the uncertain parameters in the FA model.[214] Other works introduced a joint probability distribution function for the range of uncertain parameters to address the stochastic flexibility of processes.[215,216]

6.3.3 Case Study 2. Urea Manufacturing Systems

The HEN system in Section 6.3.2 is partial units in the entire manufacturing plant. As discussed previously, climate change could affect the entire manufacturing systems and supply chains. For instance, alternative technologies such as renewable power generation may need to be adopted to adapt to climate change. In the following case study, we investigate how climate change could affect urea manufacturing processes and supply chain networks in the MRW, by employing the RCOT-P2P multiscale consequential process design model.[6]

Specifically, we examine the effectiveness of technologies that help reduce CO_2 emissions from producing urea to mitigate and adapt to climate change. For example, as shown in Fig. 6.11, green urea production systems could employ water instead of NG as feedstock to provide hydrogen to urea since the electrolysis of water usually has smaller carbon footprints than the conventional steam reforming of methane. Other technology options to mitigate CO_2 emissions include the use of renewable energy sources (solar and wind power) instead of fossil fuels (coal and NG), which are the conventional fuel sources for power generation in the MRW.

In this case study, we account for more comprehensive climate change constraints than the previous case study, which only considers the effect of water temperature. As described in Section 6.2.2, the SWAT model can simulate regional water yield and solar radiation based on the climate data projected from GCMs. The water yield results simulated from the SWAT model for the MRW are shown in Fig. 6.7. As shown in Fig. 6.3, other climate change constraints in this case study include water temperatures projected from GCMs, and CO_2 emission mitigation targets, which are defined by each RCP scenario.

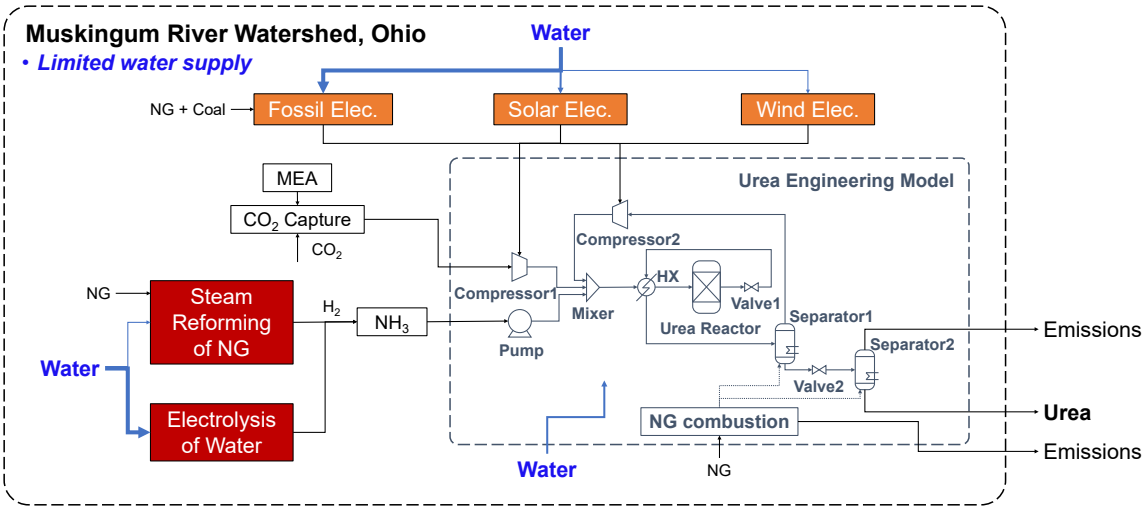

Figure 6.11: Model structure for the urea production systems in the MRW. Alternative technology options are considered as CO_2 emission mitigation strategies.

According to the report,[8] the U.S. nitrogen fertilizer balance was -5 TgN in 2014 but is expected to increase. Also, the global nitrogen fertilizer demand is expected to grow by 1.3% annually, which is driven by population and income growth. In this case study, we assume that urea manufacturing systems are installed in the MRW. The urea production capacity in the MRW is estimated by allocating the U.S. negative nitrogen fertilizer balance (-5 TgN/y) based on the proportion of nitrogen fertilizer consumption in the MRW over the U.S. consumption. Then, we estimate future urea demand in the MRW with the annual increase rate of global nitrogen fertilizer demand (1.3%/y), as shown in Fig. 6.12. We assume that the urea production capacity in the MRW needs to be increased every 30 years (2040, 2070, and 2100) to meet the increased future demand.

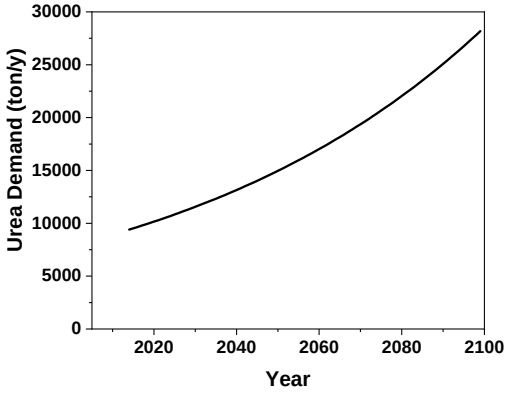

Figure 6.12: Annual urea demand in the MRW estimated with the annual increase rate of global nitrogen fertilizer demand (1.3%/y).[8]

RCOT-P2P Model Construction

Since we investigate the impacts of future resource constraints on process and supply chain design, the RCOT-P2P model in Section 6.2.4 can be employed to account for the consequences of climate change. We can investigate how manufacturing processes and their supply networks could be affected by future changes in climate and how they could adapt to maintain their productivity.

In this case study, we only consider the worst case where the water availability is the lowest and the water temperature is the warmest on an annual basis. Accordingly, the urea RCOT-P2P model is formulated to maximize the urea plant profits

$(Profits(\{z\}))$ as follows:

$$Z = \max Profits(\{z\}), \tag{6.18}$$

$$\text{s.t. } X(\{z\})\ s = y, \tag{6.19}$$

$$H(\{z\}) \geq 0, \tag{6.20}$$

$$T_{env,wat} = \text{Projected water temperature}, \tag{6.21}$$

$$F_{wat}(\{z\})\ s = c_{wat} \leq c_{wat}^{max}, \tag{6.22}$$

$$E_{solar} = \text{Simulated solar radiation}, \tag{6.23}$$

$$B_{CO_2}(\{z\})\ s = g_{CO_2} \leq g_{CO_2}^{max}, \tag{6.24}$$

where X is the commodity transaction matrix between processes across scales. s and y are a scaling vector for processes and a final demand vector, respectively. Constraint 6.19 ensures that the systems produce the demanded amount of urea. As described earlier, the urea demand is expected to increase by 1.3% annually. Constraint 6.20 represents urea engineering model constraints based on mass and energy balance relations. The details about the RCOT-P2P model formulation for the urea manufacturing systems are available in Section 5.4.1.

In this case study, water is not only used for the heater and cooler units in the urea engineering model but also used for power plants in the MRW. The change in water temperatures due to climate change will affect the amount of water consumption in those units and power plants. Therefore, to account for those effects of climate change on the urea manufacturing systems, the urea RCOT-P2P model is modified using Equation 6.16 and equations in the previous study.[29]

Constraints 6.22–6.24 refer to the climate change constraints, which are summarized in Table 6.1. Constraint 6.22 is a constraint for water temperatures projected

from GCMs. F_{wat} in Constraint 6.21 is a matrix of the water resource requirement for each process. Total water consumption (c_{wat}) needs to be smaller than the available amount of water supply in the MRW (c_{wat}^{max}), which is simulated from the SWAT model. In this work, only some portions of the available water supply in the MRW are allocated to the urea manufacturing systems due to water rights.[6] Water use is regulated by the doctrine of riparian water rights in Ohio.[152] The allocation of water supply is performed based on the proportion of U.S. fertilizer manufacturing sector economy outputs to the total U.S. economy outputs.

Constraint 6.23 is a constraint for solar radiation in the MRW (E_{solar}), which is calculated through the WXGEN weather generator in the SWAT model.[217] B_{CO_2} in Constraint 6.24 is a matrix of CO_2 emissions from each process. Total CO_2 emissions from producing urea in the MRW (g_{CO_2}) need to be reduced to satisfy the emission mitigation levels ($g_{CO_2}^{max}$), which are determined by the GHG emission trajectory of RCP scenarios.

Table 6.1: Climate change constraints considered in the case study for the urea manufacturing systems. The worst climate trajectory is considered on an annual basis. RCP 8.5 scenario does not consider emission mitigation strategies. †This represents the percentage of CO_2 emission levels for each RCP scenario compared to the emission level in 2014.

Climate Change Constraints	RCP 4.5			RCP 8.5		
	Early	Mid	Late	Early	Mid	Late
Water Temperature (°C)	18.3	19.5	19.0	18.2	20.4	21.9
Water Availability (1,000 m^3/y)	247.3	240.9	168.4	180.0	171.1	158.2
Solar Radiation (GJ/m^2/y)	4.54	4.58	4.66	4.62	4.69	4.67
Emission Mitigation Targets (%)†	125.4	81.9	38.5	N/A	N/A	N/A

Consequences of Climate Change on the Urea Manufacturing Systems

Figure 6.13 shows the annual profits of the urea manufacturing plant when the profits are maximized for each RCP scenario. When no climate change impacts, such as scarce water availability and warmer water temperatures, are considered (black dotted lines in Fig. 6.13), the plant profits are expected to increase because the production capacity of the urea plant is increased to meet the future urea demand shown in Fig. 6.12. However, when we consider the impacts of climate change on the urea manufacturing systems, the urea plant profits cannot be increased as compared to the previous case, if the conventional technologies (fossil power generation and steam methane reforming) keep being employed in the future (red solid lines in Fig. 6.13). This is because the urea plant in the MRW cannot produce the desired amount of urea due to the increased risk of water scarcity and warm water temperatures. In case of the RCP 4.5 scenario (Fig. 6.13a), the plant profits are expected to decrease in 2070 and 2100 since the urea manufacturing systems cannot meet the GHG emission mitigation levels (Constraint 6.24) with the conventional technologies.

For the GHG emission trajectory defined by the RCP 4.5 scenario, CO_2 emissions need to be regulated, and thus, mitigation strategies are needed for the urea manufacturing systems. In this work, we consider renewable power generation technologies (solar and wind power) and water electrolysis technology as alternatives to fossil power generation and steam methane reforming, respectively, to mitigate the emissions. With mitigation technologies (a blue solid line in Fig. 6.13a), the manufacturing plant can produce more urea. However, the plant cannot manufacture the demanded amount of urea in 2100 due to the other climate change constraints such as scarce water availability.

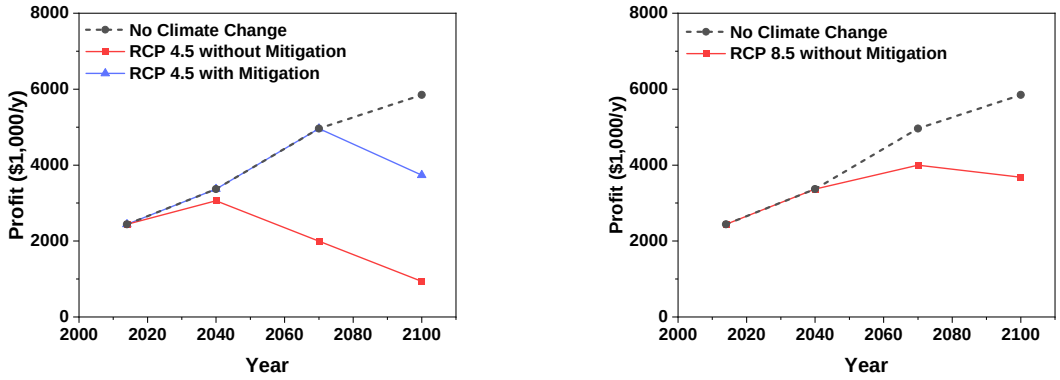

(a) (b)

Figure 6.13: Climate change impacts on the urea manufacturing plant when the urea plant profits are maximized for **(a)** RCP 4.5 and **(b)** RCP 8.5 scenarios. The RCP 8.5 scenario does not consider emission mitigation strategies.

Figure 6.14 exhibits how mitigation strategies for the urea manufacturing systems need to be adopted for the RCP 4.5 scenario. The proportion of each technology in use and the intensity of life cycle CO_2 emissions are shown in stacked pie charts and a line chart, respectively. In 2040, solar power technology needs to replace a third of the conventional fossil power plants to mitigate the total emissions. In 2070, the conventional power plants are entirely replaced by solar power plants, and electrolysis technology needs to be employed with the conventional steam reforming technology. Also, wind power technology is needed to reduce the total water consumption in 2100. This is because wind power plants require less water than solar power plants, which need some water to clean the panels.[218] However, the results in Fig. 6.13a indicate that more advanced adaptation technologies and strategies to climate change are still needed to maintain urea plant productivity in 2100. Considering the IPCC Special

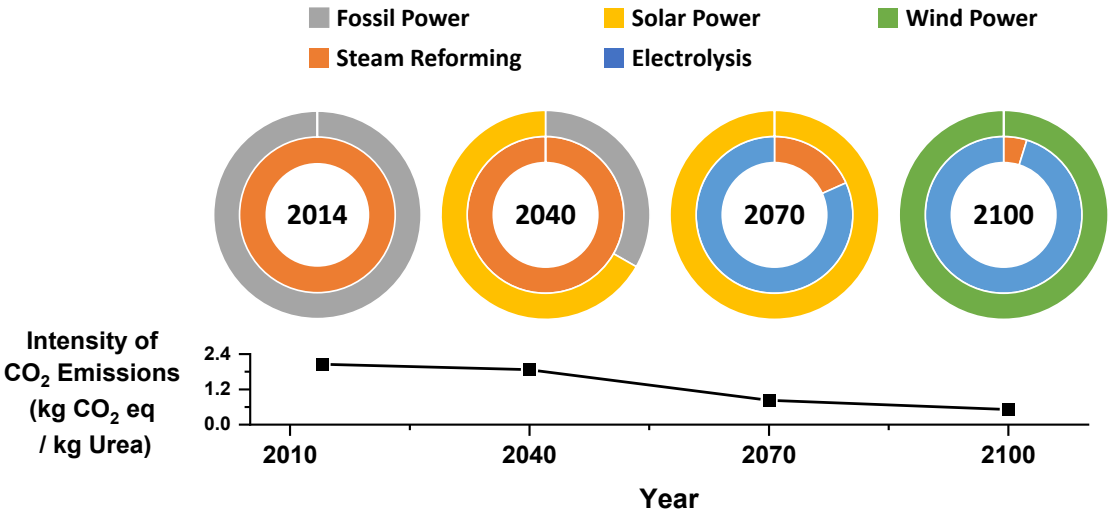

Figure 6.14: The adaptation of supply chains for urea manufacturing to climate change for the RCP 4.5 scenario. The proportion of each technology in use and the intensity of life cycle CO_2 emissions are shown in stacked pie charts and a line chart, respectively. CO_2 emissions from the manufacturing systems are mitigated to satisfy the emission mitigation levels, which are defined by the RCP 4.5 scenario.

Report emphasized the warming should be limited to 1.5 °C, such strategies are indeed needed.[196]

6.4 Conclusions

Climate change could have significant impacts on industrial processes and supply chains, which are traditionally based on the historical weather data while considering the assumption of stationarity.[193] In this work, we explored modeling approaches for designing climate-resilient processes and supply chains and demonstrated them for a heat exchanger network (HEN) system and urea manufacturing systems in the Muskingum River Watershed (MRW) in Ohio, the United States.

Representative concentration pathway (RCP) scenarios define greenhouse gas (GHG) emissions trajectories up to 2100.[5] Various general circulation models (GCMs) have been developed to project future climate data in a selected region for each RCP scenario.[199] In this work, five GCMs were employed to investigate the impacts of climate change on manufacturing systems in the MRW for RCP 4.5 (low emission) and 8.5 (high emission) scenarios. The soil and water assessment tool (SWAT) model was used to simulate future water yield and solar radiation in the MRW using climate data projected from the five GCMs.

To investigate the consequences of climate change on manufacturing systems, a flexibility analysis (FA) approach was employed.[194] FA calculates the flexibility index (F) that measures how much flexibility can be achieved for the specified design to the expected variation in uncertain parameters. Since climate data projected from GCMs are uncertain, the FA approach can be employed to investigate climate-resilient process design (CRPD) solutions.

A case study was performed for the HEN system to examine CRPD solutions employing the FA approach. We considered water temperature as an uncertain parameter and identified that higher expenses are needed to have a more flexible HEN system design. Under future climate change, higher flexibility is required for the HEN system to be adapted to climate disturbances (the increased variation in water temperatures). In this case study, we only considered a single uncertain climate parameter (water temperature). When multiple uncertain climate change parameters are considered, the rectangular or hyper-rectangular feasible space with respect to the range of each uncertain parameter could be determined.

FA methodologies have been established for decades to address flexible process design problems. FA has been employed to identify the operational flexibility of a process network for multiple chemicals,[205,206] a unit commitment problem for electric power systems,[206] and power distribution networks.[207] Although FA has not been applied to investigate the flexibility of manufacturing systems to the climate change impacts, many research opportunities exist to explore CRPD approaches using FA as demonstrated in this work.

Climate change affects not only the HEN system but also entire manufacturing systems including supply chains, ecosystems, and even economic and societal systems. To account for the more comprehensive impacts of climate change on the manufacturing systems, we conducted another case study for the urea manufacturing systems in the MRW. A multiscale consequential process design model for the urea manufacturing systems[6] was employed with various climate change constraints: water temperatures, water availability, solar radiation, and CO_2 emission mitigation levels. We identified that the urea plant will not be able to produce the desired amount of urea due to climate change constraints. Adaptation strategies to climate change, such as employing water-efficient technologies and emission mitigation technologies, will be needed for the urea manufacturing systems to maintain productivity.

The FA approach could be applied for the urea manufacturing systems to explore CRPD solutions while accounting for the impacts of climate change on supply chains. Also, the FA approach could be integrated with sophisticated economic models such as general equilibrium models[56] to obtain CRPD solutions while considering the change in economic systems. For example, the market price of commodities and resources (e.g., water price[219]) will be affected by climate change. Carbon tax and renewable

energy tax credits could be introduced to mitigate climate change. Manufacturing processes and supply chains need to be adapted to such market changes because the optimal design solutions need to create maximum profits. Economic and environmental trade-offs of such designs versus conventional designs that ignore climate change could be discussed.

Also, the impacts of climate change on ecosystem services need to be studied in more detail. In this work, we investigated the change in water provisioning service due to climate change. However, climate change will affect the supply of other ecosystem services as well.[184,185] Considering such ecological consequences of climate change on manufacturing processes could enable us to seek CRPD solutions from different perspectives. For instance, CRPD solutions could include reforestation of barren lands to enhance the supply of carbon sequestration service by forests.

The CRPD approach in this work considers climate change constraints, but it does not address dynamics and uncertainties in climate change scenarios and impacts. To obtain more robust CRPD solutions, dynamics and uncertainties in climate models and manufacturing systems need to be accounted for. For example, multi-period optimization for certain time periods (e.g., 30 years) could be conducted. Real options analysis approach could be incorporated into the CRPD approach to determine the optimal design solutions for each time period to minimize the net cost for every possible climate change scenario.[220–222] Additionally, adaptive pathway analysis approach could be utilized to determine tipping points for each technology option by calculating the temporal distribution of each option that satisfies performance constraints.[223,224] The combined modeling framework could enable us to conduct CRPD studies for manufacturing systems while seeking robust adaptation strategies.

Chapter 7: Techno-Ecologically Synergistic Design Enhances the Nexus of Food-Energy-Water in a Watershed

To avoid unintended shifting of environmental impacts across flows, the assessment of multiple sustainability indicators is required. A concept of the food-energy-water (FEW) nexus accounts for the interactions of FEW flows between various FEW-related activities. In this work, we include waste and ecosystem flows into the traditional FEW nexus approach. The ecologically synergistic FEW nexus approach takes into account more complex interactions between FEW systems and ecosystems than those in the traditional approach. This allows us to evaluate absolute sustainability of FEW-related activities, not just to minimize impacts but to prevent ecological overshoot. The FEW-related activities in this work range from energy-related (mining, power generation, cooling of power plants) and food-related (tillage) activities to waste utilization (CO_2 conversion to hydrocarbons) and ecological activities (forests and wetlands). The case study is performed to explore sustainable management strategies for those activities in the Muskingum River Watershed in Ohio, the U.S. Various technological and agro-ecological alternatives are considered as the management strategies. The environmental effectiveness and economical feasibility of alternatives in improving the overall watershed sustainability are investigated while recognizing trade-offs between multiple sustainability indicators. The results indicate

that internalizing the external benefits of ecosystem services into the market could affect solutions toward sustainability. Also, we identify that common watershed resources (e.g., available lands) need to be distributed properly among the FEW-related activities to improve multiple sustainability indicators simultaneously. The solution could give 'win-win' outcomes in terms of multiple indicators by generating the synergy between alternatives. The ecologically synergistic FEW nexus could give better insights on managing watersheds to help the decision-making process.

7.1 Introduction

The nexus of food-energy-water (FEW) needs to be accounted for in assessing the sustainability of human activities to avoid unintended harm across multiple flows.[9] For instance, maximizing the electricity generation of fossil power plants will increase water consumption and emissions that are positively correlated with power generation. To achieve the sustainability of power generation, those environmental interventions should be minimized in generating electricity. Agriculture also requires the use of water and energy, and releases nutrient emissions in producing food products. It also shows similar trade-offs between improving crop yield versus reducing environmental interventions. In this sense, FEW flows interact with each other within multiple activities. These interactions are represented by the nexus of FEW and must be captured and well understood in assessing sustainability.[225]

In addition to the consideration of the FEW nexus, ecological carrying capacity should be considered not only because the supply of ecosystem services is finite but also because ecosystem flows interact with FEW flows.[15] The Common International Classification of Ecosystem Services (CICES) provides a hierarchical classification

of various ecosystem services, and categorizes them as provisioning, regulating, and cultural services.[182] In the context of the FEW nexus, food production is related to biotic ecosystem provisioning services. Water is an abiotic ecosystem provisioning service. Fossil resources such as coal and natural gas are provided through the geological formation over a very long period. Some work defines such fossil provisioning services as geosystem provisioning services.[226] Ecosystems also provide various regulating services (e.g., climate regulation, air and water quality regulation, and nutrient retention services) that treat anthropogenic emissions. To be sustainable with regards to each ecosystem service, human interventions must be smaller than the available (renewable) amount of ecosystem services. Therefore, the supply of ecosystem services needs to be accounted for and quantified to claim sustainability.[10] If a study omits ecosystem services from the study scope, its conclusions could lead to unintended ecological overshoot. For example, the resulting minimized CO_2 emissions from the study could be still much larger than the supply of its corresponding ecosystem service (i.e., carbon sequestration service from forest ecosystems). Also, the suggested solution (e.g., deforesting area to install solar panels) may deteriorate the supply of ecosystem services, which is likely to result in more severe ecological overshoot. In this work, we address an ecologically synergistic FEW nexus framework that accounts for the flows of various ecosystem services.

There are several existing studies that account for the supply of ecosystem services in addition to the FEW nexus. However, many studies either only considered water provisioning service[227–229] and aquatic ecosystems[230] or did not perform quantitative work.[229–231] Each ecosystem service interacts with other types of ecosystem services. For example, wetland ecosystems provide freshwater provisioning service but

affect climate regulation service as well since wetland ecosystems release methane gas. Therefore, other ecosystem services such as climate regulation and nutrient retention services also need to be considered to grasp complex interactions between ecosystems and FEW systems in a holistic way.

Hanes et al. (2018) addressed local FEW nexus in a quantitative manner while accounting for the supply of various ecosystem services.[15] They considered local biomass conversion processes and several land-use options including farming, solar panels, and wind turbines. However, the study did not address thermoelectric energy industries which are dominant activities in terms of power generation and most of the environmental interventions. To promote sustainable FEW nexus, interactions between numerous nexus components need to be considered. In addition, to gain insight into absolute sustainability of the activities, the analysis needs to consider the serviceshed of relevant ecosystem services.[232] Their study also did not consider the serviceshed for various ecosystem services.

The watershed (drainage basin) scale is particularly suitable for addressing the FEW nexus since water is one of the primary resources for the food and energy sectors. Also, well-established hydrologic watershed modeling tools such as the Soil and Water Assessment Tool (SWAT) can be employed to conduct in-depth FEW nexus studies. The SWAT model is based on drainage scale water stream data, land-use land-cover data, point source data, and data for regional agricultural practices. It can be used to simulate changes in hydrologic and agricultural flows in a watershed for various alternative scenarios.[202]

In a watershed, common resources such as water and other ecosystem services are exploited for multiple human activities. For the sustainable management of the

watershed, therefore, the watershed resources must be distributed sustainably among multilateral stakeholders including energy industries and farmers.[233] In other words, watershed needs to be managed to enhance net gain for the watershed FEW systems in sustaining human communities while staying within ecological limits. Holistic thinking and strategies are needed to implement such plans to provide mutual benefits to all stakeholders.

To improve the sustainability of watersheds, various potential strategies can be considered. With respect to the energy industries, different fuel options, power generation technologies, cooling technologies, and waste utilization technologies can be considered as alternatives to improve the sustainability of power generation. For instance, traditional coal-fired steam turbine (CST) power plants are shutting down and replaced by natural gas-fired combined cycle (NGCC) plants, although there are concerns about the impacts of increasing shale gas development.[234,235] Renewable energy sources such as solar and wind power are emerging as solutions for sustainable power generation. Also, cooling technologies for power plants have been converted to water-efficient technologies such as recirculating cooling and dry cooling. Moreover, to mitigate CO_2 emissions, industries are striving to develop and implement potential CO_2 conversion technologies which will also be likely to require a substantial amount of energy and water. These technological alternatives can be characterized by the Clean Power Plant (CPP) strategy, which aims to contribute to sustainable development by reducing environmental impacts such as greenhouse gas (GHG) emissions and water consumption while meeting the societal demand for affordable electric power.

Apart from the above technological strategies, agro-ecological alternatives can be considered as well to improve watershed sustainability. Agricultural industries could

consider different farming practice options such as converting intensive tillage to no-till practice. Land-use change options could be considered as ecological strategies since ecosystem flows are sensitive to land-use and land-cover change. For example, the available barren land area can be reforested to enhance various forest ecosystem services that include climate regulation and air quality regulation services. Wetlands can be constructed on the barren land area to improve ecosystem services such as water quality regulation and freshwater provisioning.

In this chapter, we will introduce an ecologically synergistic FEW nexus modeling framework that accounts for various ecosystem and waste flows as well as FEW flows. The framework enables us to understand the interactions between FEW systems and ecosystems. Then, we will discuss the effectiveness and feasibility of various strategies from different domains (technological, agricultural, and ecological) for sustainable watershed management. Multiple objectives including environmental and monetary indicators need to be considered to address the nexus of FEW systems and ecosystems. From the perspective of watershed management, solutions should improve multiple indicators to be beneficial for multilateral stakeholders. The case study is performed for the Muskingum River Watershed (MRW) in Ohio, the United States. This work considers various FEW-related activities in the MRW and explores their alternatives to discover the most sustainable solutions. Accounting for ecosystem services in the FEW nexus could identify additional opportunities toward sustainability. The chapter is organized as follows. In Section 7.2, we describe various watershed activities that include FEW systems (agricultural and energy industries) and ecosystems. In Section 7.3.1, the ecologically synergistic FEW nexus is introduced. In Section 7.3.2,

the modeling framework is employed to conduct a case study for the sustainable management of the MRW.

7.2 Methods

To address the FEW nexus, a holistic modeling approach is needed due to the complex interactions of FEW flows between activities. Figure 7.1 summarizes such interactions between multiple activities in the FEW systems and ecosystems, including alternative activities considered in this study. Extensive data need to be collected from numerous databases for such holistic work. Data sources used in this work are described in Section 7.2.7. In this section, we describe the characteristics of various activities in the FEW systems and ecosystems.

Table 7.1 shows a hierarchical classification of technological and agro-ecological alternatives. The table also exhibits qualitative ranks among the alternatives in each category. For example, solar energy is the best alternative in the fuel category with respect to net CO_2 emissions. These ranks summarize the characteristics of alternatives described in this section.

7.2.1 Mining of Fuel Sources

Coal was a fuel source used the most for electricity generation. In the late 1980s, coal accounted for 56% of fuel sources for the U.S. energy sector.[236] However, the mining and use of coal results in huge environmental and health impacts. Coal was responsible for 85% of CO_2 emissions for the U.S. energy sector in the late 1980s[236] and its GHG emission intensity is more than two times larger than NG.[237] Also, air pollutants from the combustion of coal cause a lot of health problems.[238] Therefore,

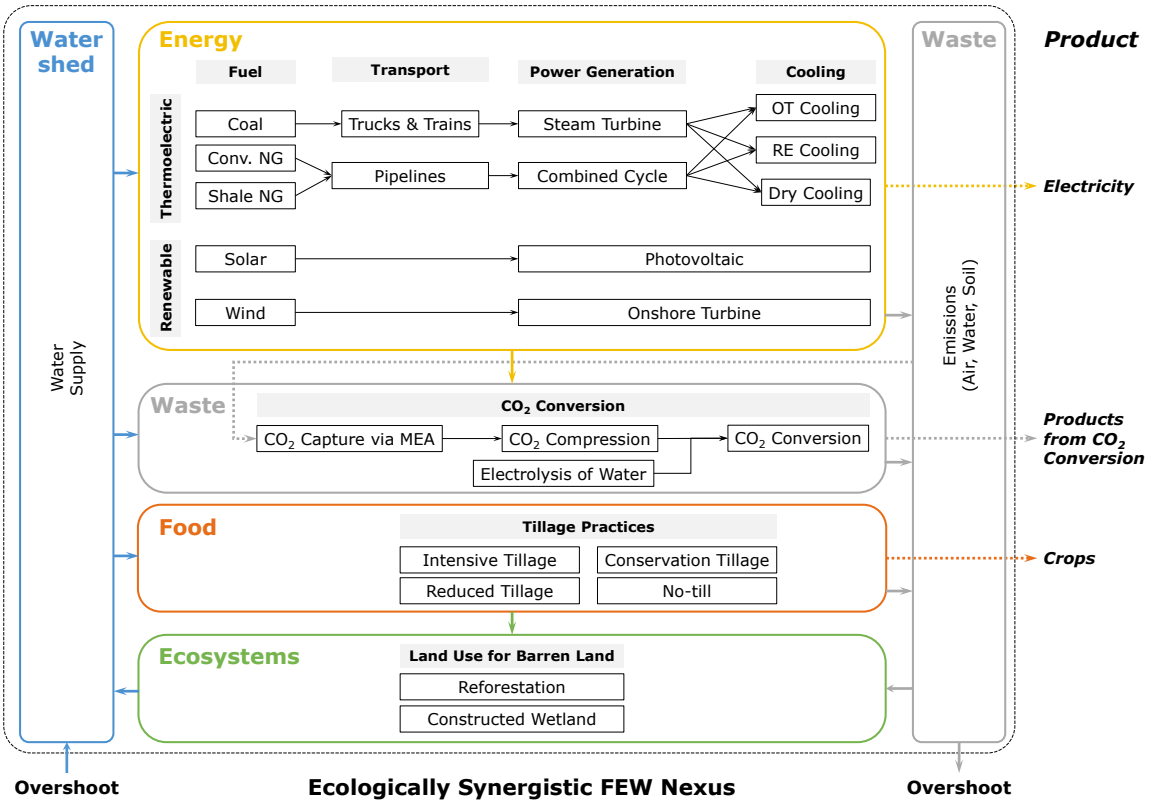

Figure 7.1: Interactions of FEW flows at the ecologically synergistic FEW nexus in this study.

coal has been replaced in many cases by other energy sources such as NG and renewable sources. In 2018, coal accounted for only 32% of fuel sources for the U.S. energy sector.

In contrast to coal, the extraction and use of NG has continued to increase and it accounts for 29% of fuel sources for the 2018 U.S. energy sector.[236] NG accounted for only 10% in the late 1980s. The recent development of shale gas has accelerated NG exploitation. While NG is conventionally extracted by vertical and directional drilling, shale gas is extracted by horizontal drilling and hydraulic fracturing (fracking). For the past five years in the U.S., while the production of conventional NG is reduced by

41%, the production of NG from shale wells has doubled.[239] However, the hydraulic fracturing process uses a large amount of water.[240] Water resources may also be contaminated by the fracking process due to wastewater from shale wells.[234,235]

Fossil fuel resources are transported from the mining sites to the power plants. Coal is transported by diesel-fueled trucks and trains, and thus, its transportation causes GHG and air pollutant emissions. On the other hand, NG is transported through pipelines at high pressure. The leakage of gas from the pipeline transportation results in environmental impacts.

7.2.2 Thermoelectric Power Generation

Since the industrial revolution, fossil resources have been the major power sources. In 2018, thermoelectric power plants account for 61% of electricity in the U.S.[236]

Table 7.1: The qualitative rank between alternatives in each category. The smaller rank indicates better results. [1] CO_2: Net CO_2 emissions, Nut.: Net nutrient runoff, Water: Net water consumption, Water(T): Thermal water pollution, Energy: Net electricity generation, Food: Food productivity, Cost: Monetary cost.

Systems	Nexus elements	Alternative categories	Alternatives	Indicator rank[1]						
				CO_2	Nut.	Water	Water(T)	Energy	Food	Cost
Technological	Energy	Fuel	Coal	5	-	5	-	5	-	5
			Conv NG	3	-	3	-	3	-	4
			Shale NG	3	-	4	-	3	-	2
			Solar	1	-	1	-	1	-	3
			Wind	2	-	2	-	2	-	1
		Cooling	OT	-	-	2	3	1	-	1
			RE	-	-	3	2	2	-	2
			Dry	-	-	1	1	3	-	3
	Waste	CO_2 conversion	No conversion	4	-	2	-	1	-	1
			Methane	3	-	3	-	4	-	3
			Syngas	2	-	3	-	3	-	3
			Formic acid	1	-	1	-	2	-	2
Agro-ecological	Food	Tillage practices	No-till	1	1	1	-	-	4	1
			Conser. tillage	2	2	2	-	-	3	2
			Reduc. tillage	3	3	3	-	-	2	3
			Intens. tillage	4	4	4	-	-	1	4
	Ecosystem	Land use	Reforestation	1	2	2	-	-	-	1
			Wetland	2	1	1	-	-	-	2

However, thermoelectric power generation is also one of the largest contributors to a variety of environmental impacts. In the U.S., thermoelectric activities accounted for 41% of water withdrawals in 2015.[58] They were also responsible for 27% of the 2017 U.S. GHG emissions,[47] 67% of the 2014 U.S. SO_2 emissions, and 12% of the 2014 U.S. NO_X emissions.[49]

Those impacts from power generation depend not only on the type of fuel but also on cooling technologies. In 2018, 34% and 59% of power plants in the U.S. were operating with once-through (OT) and recirculating (RE) cooling technologies, respectively.[153] Both technologies are wet cooling methods. The OT technology withdraws a large amount of water for cooling and discharges most of it to the watershed at a higher temperature. Thus, the OT technology causes thermal water pollution which affects water quality such as the amount of dissolved oxygen content in the water body. Due to the ecological impacts of OT technology, it has been replaced with other cooling technologies. The RE technology withdraws only a small portion of water and recirculates it. However, due to the evaporation from the cooling tower, the RE technology shows larger water consumption than the OT technology. Also, RE technology is more energy-intensive and expensive than OT technology. Loew et al. (2016) reported that the net generation efficiency is decreased by 0.3–1% and the average cost is increased by 0.12–0.27 cents/kWh if the OT technology is converted to the RE technology in the fossil power plants in Texas, U.S.[241]

Dry cooling technology has no use of water since it uses air instead of water for cooling. Approximately 6% of power plants in the U.S. were operating with the dry cooling technology in 2018.[153] However, its energy generation efficiency is smaller and its cost is higher than wet cooling technologies. It was reported that the net

plant efficiency is reduced by 1–4% and the average cost is increased by 0.60–0.63 cents/kWh when the RE technology in the Texas power plants is retrofitted to the dry cooling technology.[241] Also, the low energy generation efficiency results in the increased emissions for generating electricity since more fuel resources need to be consumed.

7.2.3 Renewable Power Generation

To reduce the impacts of utilizing fossil fuels, renewable energy sources such as solar and wind power are considered as alternative power generation technologies. In 2018, 1.5% and 6.5% of electricity were generated from solar and wind resources in the U.S., respectively,[236] and these shares are expected to increase. Renewable technologies require less water and have fewer emissions than the thermoelectric power generation technologies described in Section 7.2.2. For solar power generation, concentrated solar power (CSP) technology needs a similar amount of water as the thermoelectric technologies to generate electricity since the CSP technology requires the cooling of solar panels and steam turbines. In 2018, CSP accounted for only 6% of solar power generation in the U.S.[153] The rest of 94% utilize photovoltaic (PV) technology. Unlike the CSP technology, PV technology does not require the use of much water for generating electricity and it needs only a small amount of water for cleaning the surface of solar panels.[242] Wind power generation technology does not need any water as well. Moreover, solar and wind power generation technologies do not have direct air and water emissions. In addition, since the renewable technologies replace conventional thermoelectric technologies, displacement credits can be given to renewable technologies. That is, upstream life cycle emissions associated with

the thermoelectric generation technologies can be avoided by employing renewable technologies.

Although renewable generation technologies have many strengths in terms of environmental impacts compared to thermoelectric technologies, they also have some shortcomings. One of the biggest challenges is the intermittency of power sources. The available amount of solar and wind power depends on location and time with uncertainties. Therefore, technologies need to be employed with energy storage systems. Also, solar and wind power technologies require a large land area. The renewable generation technologies may compete with other activities for the limited land area. Farming activities for food production and ecological activities (e.g., forests and wetlands) for providing ecosystem services require a huge land area as well.

For renewable generation technologies to be economically feasible, they need to be cheaper than thermoelectric generation technologies. When we do not consider any monetary credits for utilizing renewable power sources, the levelized costs of electricity (LCOE) for newly entering conventional NGCC, solar PV, and onshore wind power plants in 2023 are estimated to be 42.8, 48.8, and 42.8 $/MWh, respectively.[243] If federal tax credits are considered for renewable power sources, the LCOE for solar PV and onshore wind power plants are reported to be 37.6 and 36.6 $/MWh, respectively, which are cheaper than the conventional NGCC plants. Therefore, renewable power generation technologies can be economically feasible if tax incentives are considered.

7.2.4 CO_2 Conversion

To reduce environmental impacts from human activities, waste materials can be utilized by recycling them or converting them to other valuable products. In this

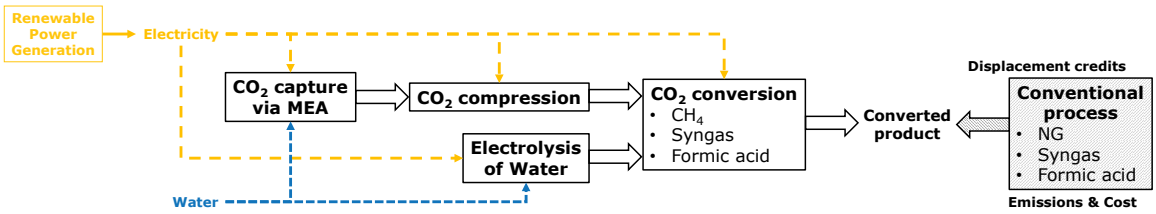

Figure 7.2: Energy- and water-intensive CO_2 capture and conversion processes. The converted products displace the products from conventional processes.

chapter, we focus on CO_2 utilization strategies. To mitigate global warming, various CO_2 utilization pathways and technologies have been studied.[85,244] As one of the pathways, CO_2 can be captured from stationary point sources such as fossil power plants through pre- and post-combustion technologies or from the air by direct air capture technology.[245] The captured CO_2 can be converted to various hydrocarbon products such as methane, synthetic gas, formic acid, urea, and methanol, which can be used for many industrial uses.

As shown in Fig. 7.2, however, these carbon capture and conversion technologies are energy-intensive. The capture process using 15–20% of monoethanolamine (MEA) solution requires 0.4 kWh for 1 kg of CO_2.[109] The captured CO_2 needs to be compressed to a high pressure, which requires the use of electricity as well. Also, many CO_2 conversion processes are highly energy-intensive. For example, CO_2 can be converted to methane through Sabatier reaction as shown in Eq. 7.1.

$$CO_2 + 4H_2 \rightarrow CH_4 + 2H_2O \quad (\Delta_R H^o_{298} = -165\text{kJ/mol}). \tag{7.1}$$

If we consider that hydrogen is provided from water through electrolysis technology, the electrolysis process requires energy as follows:

$$H_2O \rightarrow H_2 + 1/2O_2 \quad (\Delta_R H^o_{298} = 286\text{kJ/mol}). \tag{7.2}$$

As a result, the overall conversion process from the captured CO_2 to methane is described by Eq. 7.3:

$$2H_2O + CO_2 \rightarrow CH_4 + 2O_2 \quad (\Delta_R H^o_{298} = 979\text{kJ/mol}). \tag{7.3}$$

CO_2 can also be used to produce carbon monoxide through the reverse water-gas shift reaction and formic acid (FA) through the hydrogenation of CO_2 as shown in Eqs. 7.4 and 7.5, respectively.

$$CO_2 + H_2 \rightarrow CO + H_2O \quad (\Delta_R H^o_{298} = 41\text{kJ/mol}). \tag{7.4}$$

$$CO_2 + H_2 \rightarrow HCOOH \quad (\Delta_R H^o_{298} = -31.5\text{kJ/mol}). \tag{7.5}$$

CO_2-converted carbon monoxide from Eq. 7.4 can be combined with hydrogen from Eq. 7.2 to produce syngas.

Since these conversion processes need to utilize the electrolysis of water shown in Eq. 7.2, the conversion processes are not only energy-intensive but also water-intensive. Moreover, the carbon capture process requires additional water for cooling.[246] If electricity for the CO_2 capture and conversion processes is provided from conventional thermoelectric power plants, total energy and water consumption including the upstream processes will be significantly large. Therefore, renewable power generation technologies that have smaller emissions and resource consumption need to be considered for providing electricity to the conversion processes,[247] as shown in Fig. 7.2.

The CO_2 capture and conversion processes are also economically expensive. For instance, Pérez-Fortes et al. (2016) estimated that the production cost for CO_2-converted FA is more than 3 times the cost of conventional FA through methyl formate hydrolysis process, primarily because of the large resource and utility consumption

for the conversion processes.[248] Also, Agarwal et al. (2011) discussed that negative net present value for the CO_2-converted FA is estimated over 10 years due to the high capital equipment investment cost.[249] They claimed that the profitability for the CO_2 conversion processes can be improved by technological development.

The CO_2-converted products will replace the products from conventional processes. For example, CO_2-converted methane can displace NG from the fossil fuel extraction process. CO_2-converted CO can be used as synthesis gas by combining with hydrogen. Syngas is produced conventionally through the gasification of coal or the steam reforming of NG.[250] In this chapter, steam reforming of NG is identified as the conventional syngas production process since the production of NG has increased significantly due to the shale gas boom. As shown in Fig. 7.2, environmental impacts and costs for the conventional processes can be avoided and considered as displacement credits to the CO_2 conversion technologies.

Song (2006) estimated the worldwide potential market of CO_2 utilization for chemical conversion to be less than 1×10^{12} kgC/y, since converting this much CO_2 will satisfy the global demand for all hydrocarbon chemicals.[244] Also, they estimated the global liquid fuel production to be 2.1×10^{12} kgC/y. Given that global CO_2 emissions from the combustion of fossil fuels in 2016 are 8.8×10^{12} kgC,[47] therefore, it is important to consider the market demand for CO_2-converted products. With respect to FA, for example, its global production capacity in 2009 was 7.2×10^8 kg.[251] Stoichiometrically, this corresponds to only 1.9×10^8 kg C if FA is produced from the hydrogenation of CO_2. The cost reduction of conversion technologies could expand their potential uses and lead to an increase in market size for the CO_2 conversion.

Unlike other activities described in this section, CO_2 conversion technologies have not been fully commercialized yet. Therefore, it is challenging to obtain reliable data for the conversion processes. Experimental data are available from numerous sources. However, they are based on different process configurations such as different catalyst use, conversion ratio, temperature, and pressure. For instance, while one study was performed by employing 120 bar of CO_2 pressure for converting CO_2 to FA,[252] others employed 30 bar.[253–255] Due to these difficulties, we assume 30 bar of CO_2 pressure for CO_2 conversion reactions for the simplicity of analysis in this work.

7.2.5 Agricultural Activities

Interventions from farming activities depend on weather conditions. If a region suffers from water shortage due to low precipitation, a large amount of water needs to be used for irrigation. Accordingly, water may need to be allocated to the agricultural activities instead of other water-intensive activities such as thermoelectric activities. In such a case, technologies that do not require much water (e.g., dry cooling technology) could be preferred to minimize water consumption. If the other region experiences frequent heavy rainfall, the amount of nutrient runoff from farm fields is increased.

Those interventions also vary with farming practices such as tillage, crop rotation, buffer strips, and crop covers. These practices affect food productivity, water nutrient emissions, soil erosion, and even ecosystem services such as carbon sequestration and soil retention services. For example, tillage practices are performed to improve crop productivity. They are categorized into three practices: intensive, reduced, and conservation tillage. Intensive tillage (also called conventional tillage) has high soil

mixing efficiency (uniformity) and leaves less than 15% of crop residues on the soil. Therefore, it requires large amounts of fertilizers to enhance crop yield. Accordingly, it shows an increased risk of soil erosion and eutrophication due to nutrient runoff. The reduced and conservation tillage practices have 15–30% of crop residues and more than 30% of crop residues on the soil, respectively, and thus, they show smaller soil erosion and nutrient runoff than intensive tillage. On the other hand, no-till practice shows the least risk of soil erosion and nutrient runoff, although it is likely to reduce crop yield. However, the long-term crop yield could be increased due to improved soil fertility. Also, soil carbon sequestration can be enhanced by employing no-till practice instead of tillage practices. For example, a study in Wooster, Ohio, the U.S. shows that the no-till practice can sequester 83 g $C/m^2/y$ more than conventional tillage.[256] Moreover, no-till practice is cheaper than tillage practices since it requires less labor and machinery. Weersink et al. (1992) investigated costs of no-till and various tillage practices, and estimated the average cost of no-till practice to be 7.7% cheaper than the intensive tillage.[257]

7.2.6 Ecosystem Services

Ecosystem services are the basis for the above activities.[183] To avoid ecological overshoot, the supply of ecosystem services must be considered because the interventions could outweigh their corresponding ecosystem services. Techno-Ecological Synergy (TES) modeling framework has been developed to account for the supply of ecosystem services in the modeling work.[10] This TES framework calculates TES sustainability indices (V_k) for each ecosystem flow (k) by Eq. 7.6:

$$V_k = \frac{S_k - D_k}{D_k}, \tag{7.6}$$

where $V_k \geq -1$. S_k and D_k are the supply and demand for ecosystem services, respectively, for the k-th ecosystem service. In terms of CO_2 flow, for instance, S_{CO_2} and D_{CO_2} correspond to carbon sequestration service by vegetation and soil, and CO_2 emissions from human activities. V_k must be positive to avoid ecological overshoot and claim absolute sustainability in the selected region for that ecosystem service.

In calculating V_k metrics, the selection of analysis boundary is important since the scale of beneficiaries (serviceshed) for each ecosystem service depends on its characteristics.[232] For example, the serviceshed for CO_2 flow is defined as global, while the serviceshed for freshwater flow is the watershed. Also, if D_k represents interventions from a specific activity, S_k needs to be allocated to that activity because ecosystem services are beneficial to every activity in the serviceshed.[129] For the holistic modeling work where multiple activities are considered, D_k can be the intervention from every activity in a region. In such a case, S_k needs to represent the whole supply in the region and V_k can be calculated for all activities in the region.

In this chapter, we focus on three types of ecosystem services: freshwater provisioning, climate regulation, and nutrient retention services. The water provisioning service corresponds to the renewable amount of freshwater. This considers various factors in the water cycle such as precipitation, evapotranspiration, infiltration, and surface/subsurface runoff. Several tools are available to estimate the water provisioning service. For example, the SWAT model calculates water yield to streamflow in a watershed.[195] Water Global Assessment and Prognosis (WaterGAP) hydrology model has been developed to calculate the amount of available water on a global scale while accounting for factors in the water cycle.[258] Available Water Remaining (AWARE)

model, which is based on the WaterGAP model, can also be used to calculate the amount of available water.[41]

Ecosystem flows are sensitive to land-use and land-cover. For the water provisioning service, wetlands improve the supply of freshwater by removing water contaminants and excessive nutrients from wastewater. i-Tree Hydro can simulate the effect of land-use change on water provisioning service.[259] Wetlands provide the nutrient retention service as well. Kadlec (2008, 2016) investigated how much nitrogen and phosphorus could be removed by constructed wetlands.[260,261] With respect to climate regulation service, wetlands sequester CO_2 but release CH_4 whose contribution to global warming is 25 times greater than CO_2 emissions. Whiting and Chanton (2001) studied the impacts of wetlands on global warming.[262] They identified that the overall effects of wetlands on climate change vary with geographic location and time horizon.

Forests affect various ecosystem services as well. Forest ecosystems provide climate regulation, air quality regulation, and biomass provisioning services. Regional data can be obtained from various i-Tree tools such as i-Tree County Benefits and i-Tree Landscape.[150] Reforestation strategy (land-use change from barren lands to forests) could enhance those ecosystem services. However, reforestation could decrease water provisioning service. Filoso et al. (2017) reviewed the impacts of reforestation on water yield.[263] They concluded that water yield is reduced in the short term and recovered in the long term due to the improved soil infiltration.

The ecological strategies to improve the supply of ecosystem services could be economically cheap solutions. For example, the USDA's report estimated tree establishment costs for Ohio, the U.S. to be around \$500/ha.[264] The capital costs

for constructed wetlands were estimated to be \$69,000/ha for large wetlands and \$132,000/ha for small wetlands.[261] Also, those ecological strategies do not require many operation and maintenance (O&M) expenses. Non-commercial reforestation only requires \$10/ha/y of O&M cost,[265] and large and small constructed wetlands require \$3,620/ha/y and \$770/ha/y of O&M costs, respectively.[261]

The supply of ecosystem services could be monetized to internalize the benefits of ecosystem services in the economic market. Internalized monetary benefits of ecosystem services are referred to as external cost and public cost. The monetary valuation of ecosystem services varies with the location since each region has a different population, weather, land-use and land-cover, and tree species. Collecting such region-specific data for the valuation of ecosystem services could be time-consuming and expensive. Therefore, the benefit transfer method can be used to monetized regional ecosystem services.[266,267] According to this method, the monetary value (e.g., \$/ha) for the benefits of ecosystem services in a study region can be estimated from the value that has been investigated already for the other region that has similar regional characteristics as the study region. In this study, the value for the benefits of ecosystem services is obtained from the Environmental Valuation Reference Inventory.[268]

7.2.7 Data Sources

In this work, a case study for the ecologically synergistic FEW modeling framework is conducted. Table 7.2 summarizes various data sources used in the case study. Monetary and environmental data for activities and alternatives vary with regions. In this study, regional data for the MRW are used if such regional data are available.

Some regional data such as cost are hard to obtain. In such a case, national data from online sources and literature reports are used.

Table 7.2: Data sources for activities, environmental interventions, and ecosystem services in the Muskingum River Watershed. If the spatial resolution of data is larger than HUC8 scale, the data is allocated to the HUC8 scale based on the ratio of population or area.

Activities	**Data Types**	**Data Sources**	**Spatial Resolution**
Thermoelectric	GHG emissions	EPA eGRID[269]	Facility
	Air pollutants	EPA NEI[49]	County
	Water pollutants	EPA NPDES[270]	Facility
	Thermal water pollution	EIA-923[153]	Facility
	Water withdrawal	EIA-923[153]	Facility
	Water consumption	EIA-923[153]	Facility
	Natural gas consumption	EIA-923[153]	Facility
	Electricity consumption	EIA-923[153]	Facility
	Electricity generation	EIA-923[153]	Facility
	Cost	Multiple sources[178, 241, 243]	-
Mining	GHG emissions	GREET[42]	U.S. average
	Air pollutants	EPA NEI[49]	County
	Water pollutants	NETL[271, 272]	Appalachia average
	Water withdrawal	USGS[162]	Ohio
	Water consumption	GREET[42]	U.S. average
	Natural gas consumption	EIA[163]	Ohio
	Electricity consumption	USLCI[40]	U.S. average
Agricultural & Other Activities (Residential, Commercial, Industrial, Transportation, Wastewater treatment)	GHG emissions	EPA GHGRP[269]	Facility
		EPA NEI[49]	County
	Air pollutants	EPA NEI[49]	County
	Water pollutants	(Agricultural) SWAT[202]	HUC8
		(Other activities) EPA[273]	HUC4
	Water withdrawal	EnviroAtlas[50]	HUC8
	Water consumption	USGS[162]	Ohio
	Natural gas consumption	EIA[163]	Ohio
	Electricity consumption	EIA[274]	Ohio
	Food production	SWAT[202]	HUC8
	Tillage cost	Weersink et al. (1992)[257]	-
Supply of Ecosystem Services	Carbon sequestration	(Vegetation) i-Tree Landscape[150]	HUC8
		(Soil) West and Post (2002)[256]	-
	Air quality regulation	i-Tree Landscape[150]	HUC8
	Water quality regulation	Kadlec (2016),[261] Kadlec (2018)[260]	-
	Water provisioning	SWAT[202]	HUC8
	External benefits	EVRI[268]	-
Alternatives	Renewable power	GREET,[42] EIA[243]	-
	CO_2 conversion	Multiple sources[40, 109, 243, 248, 275]	-
	Land-use change	Multiple sources[259, 264, 265]	-

7.3 Results and Discussion

7.3.1 FEW Nexus Modeling Framework

Figure 7.3a shows a schematic diagram for a traditional FEW nexus framework.[276] Energy and water resources are required to produce food. Water is needed for generating energy. Energy is needed for water supply systems. However, energy requirements for the food and water systems are relatively small compared to other activities such as residential, commercial, and industrial activities. It seems that the interactions between FEW flows are not very strong. Moreover, the framework does not account for the role of ecosystem services, which needs to be considered as described in Section 7.2.6. Therefore, the solution suggested from this framework could result in ecological overshoot.

In this chapter, we develop an ecologically synergistic FEW nexus modeling framework. As shown in Fig. 7.3b, ecosystem and waste flows are included as additional components for the FEW nexus. Ecosystems provide freshwater (i.e., water provisioning service) that can be used for energy and food systems. Ecosystems also provide climate regulation, air and water quality regulation, and nutrient retention services for various emissions from the energy and food systems. If the emissions and water consumption exceed the corresponding ecosystem services, there will be ecological overshoot. Sustained ecological overshoot will result in resource depletion and ecosystem degradation, so to be sustainable for human activities, there should be no overshoot over a selected time period. In this work, we consider the time period to be one year. The food systems also influence ecosystem flows such as water provisioning and climate regulation services, as described in Section 7.2.5. The ecologically synergistic FEW nexus framework shows stronger interactions between FEW flows

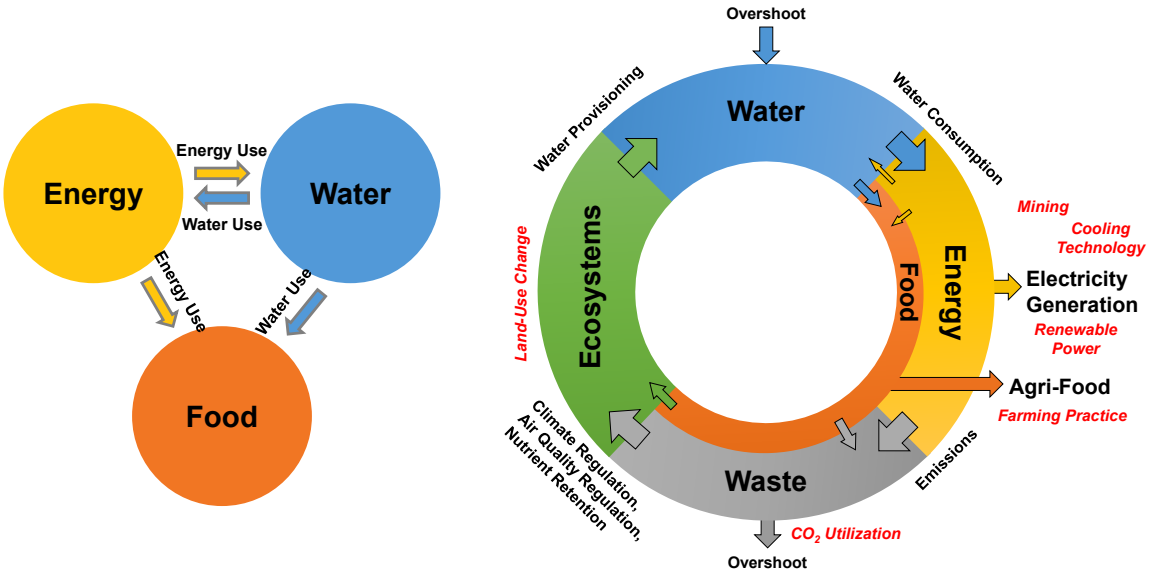

(a) (b)

Figure 7.3: **(a)** Traditional FEW nexus framework. **(b)** Ecologically synergistic FEW nexus framework. Orange, yellow, blue, green, and gray-colored arrows represent food, energy, water, ecosystem, waste flows, respectively. Technological and agroeoclogical options that affect FEW flows and ecosystem flows are shown in red italics.

than the original framework by considering the interactions of FEW systems with ecosystems.

Changes in FEW systems and ecosystems (shown in red italics in Fig. 7.3b) will affect the amount and intensity of each flow. As described throughout Section 7.2, technological options such as the type of fossil fuels and mining activities, cooling technologies, power generation technologies (thermoelectric and renewable technologies), and CO_2 conversion technologies will change the amount of water consumption and emissions in generating electricity. The change in farming practices to produce crops will affect the supply of ecosystem services as well as the amount of water

consumption and emissions. Also, land-use change options such as reforestation and wetland construction will affect the supply of various ecosystem services. These FEW and ecosystem service flows interact with each other as shown in Figs. 7.1 and 7.3b. In the following section, we will discuss how those technological and agro-ecological options will affect multiple flows in the FEW nexus by applying the framework to a case study.

7.3.2 Sustainable Watershed Management Strategies

The case study is performed for the Muskingum River Watershed (MRW) in Ohio, the U.S. Figure 7.4 exhibits a land-use land-cover map for the MRW. The map shows the watershed boundary where the 8-digits of hydrologic unit code (HUC) is 05000405. The Muskingum River in the MRW flows into the Ohio River, which flows into the Mississippi River and eventually drains into the Gulf of Mexico. Water nutrient emissions from the MRW also flow into those downstream rivers.

In 2014, the MRW had five operating thermoelectric power plants. The year 2014 is selected for the case study since some data are not available for the years after 2014 at this point. The Conesville Power Plant is a coal-fired steam turbine (CST) power plant equipped with recirculating cooling systems. This coal power plant is still operating. On the other hand, the Muskingum River Power Plant which was a CST plant with once-through cooling systems was shut down in 2015 due to environmental impacts from its operation. Since the analysis in this case study is for the year 2014, we include the Muskingum River Power Plant in the analysis to maintain consistency of the data. The other three power plants in the MRW (Dresden Energy, Waterford, and Dynegy Washington) are NGCC power plants with recirculating cooling systems.

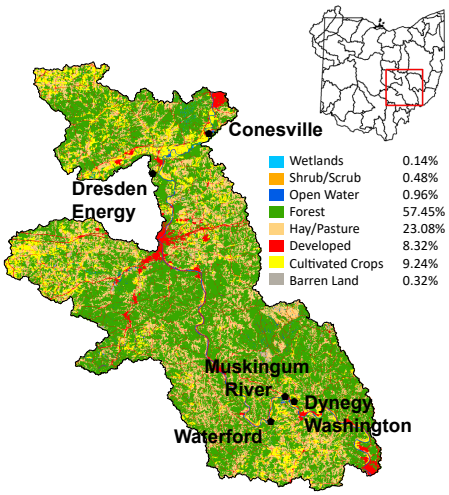

Figure 7.4: Land-use land-cover map for the Muskingum River Watershed (MRW). The MRW is located in the southern east of Ohio, the U.S. (⬟: location of thermo-electric power plants.)

In 2014, 48% of electricity was generated from the CST plants, and the rest 52% was from the NGCC plants.[153]

For renewable energy production, the U.S. EPA's EnviroAtlas shows that solar and wind energy potentials per unit area in the MRW are 1.23 and 0.44 MWh/m^2/y.[50] However, there were no such facilities in this region in 2014. Also, there were no CO_2 conversion facilities.

As shown in Fig. 7.4, the MRW had 3.76×10^8 m^2 of farmland (9.24% of land-use in the MRW). Production of corn and soybean was 2.2×10^5 t/y and 7.2×10^4 t/y, respectively. 57.0% of tillage practices in the MRW were no-till practice, while 22.29%, 20.0%, and 0.11% of the practices were conservation, reduced, and intensive tillage practices, respectively. Wetlands and forests accounted for 0.14% and 57.45% of land-use, respectively. The MRW also had 1.30×10^7 m^2 of barren land (0.32% of land-use).

The case study is conducted as follows. First, we investigate the environmental impacts of activities and benefits of ecosystem services in the MRW for the year 2014 (defined as a base case). The TES sustainability metrics are calculated for CO_2 emissions, air pollutant emissions, N & P runoff, and water consumption. Then, we explore alternative management strategies that are shown in Fig. 7.1 to understand their effect on sustainability of the MRW in the context of the FEW nexus. Two categories of alternative strategies are considered: technological and agro-ecological. The technological strategy is the Clean Power Plant (CPP) which aims to minimize environmental impacts from generating electricity. The CPP also needs to ensure affordable power supply and be cost-effective. In this study, alternative fossil fuels for generating electricity, alternative cooling technologies used by power plants, renewable power generation technologies, and potential CO_2 conversion technologies are considered as parts of the CPP strategy. The agro-ecological strategy includes different types of tillage and land-use change such as restoring barren lands to other ecological land cover types. The environmental effectiveness and economic feasibility of various technological and agro-ecological alternatives are examined.

Multiple objectives need to be considered to perform the FEW nexus study to account for various interactions between FEW flows and ecosystem flows. The radar plots in this case study (Figs. 7.8–7.12) have seven axes: three TES indices (V_{CO_2}, V_N, and V_{water}), marginal net electricity generation, marginal corn production, marginal profits, and marginal external benefits. The marginal values are based on comparison with the base case. Net electricity generation corresponds to the aggregated electricity generation minus aggregated consumption by activities in the MRW. Thus, the

marginal net electricity generation (MNEG) is calculated by Eq. 7.7:

$$\text{MNEG} = (\sum_{i}^{n} \text{EG}_i - \text{EC}) - (\sum_{i}^{n} \text{EG}_{base,i} - \text{EC}_{base}), \tag{7.7}$$

where $i = 1, 2, \cdots, n$ correspond to power plants. EG_i and EC represent electricity generation (the output of the generator) from each power plant i and aggregated electricity consumption in the MRW, respectively. EC includes parasitic loads to generate electricity from the power plants. A subscript *base* means base case values. Similarly, the marginal corn production (MCP) is calculated by Eq. 7.8:

$$\text{MCP} = \sum_{i'}^{n'} \text{CP}_{i'} - \sum_{i'}^{n'} \text{CP}_{base,i'}, \tag{7.8}$$

where $i' = 1, 2, \cdots, n'$ correspond to farms. $\text{CP}_{i'}$ is the amount of corn production from each farm i'.

With respect to two monetary objectives, the marginal profits refer to the change in profits for plant operators by employing alternative options. The marginal profits (MP) are calculated by Eq. 7.9:

$$\text{MP} = \sum_{j}^{m} (p_j \times \text{Prod}_j - \text{Cost}_j) - \sum_{j}^{m} (p_j \times \text{Prod}_{base,j} - \text{Cost}_{base,j}), \tag{7.9}$$

where $j = 1, 2, \cdots, m$ correspond to products, and p_j represents unit price of products j. The market price of products is assumed to be fixed over alternative options in this study. Prod_j and Cost_j correspond to the physical amount of production for products j and the monetary cost for the production, respectively. In case of electricity, Prod_{elec} is equal to $(\sum_i^n \text{EG}_i - \text{EC})$ in Eq. 7.7. On the other hand, the marginal external benefits mean the change in external benefits to society from reducing environmental damages. The marginal external benefits (MEB) are calculated by Eq. 7.10:

$$\text{MEB} = \sum_{k}^{l} \{c_k \times (S_k - D_k)\} - \sum_{k}^{l} \{c_k \times (S_{base,k} - D_{base,k})\}, \tag{7.10}$$

where $k = 1, 2, \cdots, l$ correspond ecosystem flows. c_k represents the unit external cost for society to absorb environmental damages. c_k in this work is obtained from the benefit transfer method.[266,267] If the external costs and benefits are internalized in the market, the marginal change in total profits is equal to MP + MEB.

Monetary and environmental data for activities and alternatives vary with regions. In this study, regional data for the MRW are used if such regional data are available. Some regional data such as cost are hard to obtain. In such a case, national data from online sources and literature reports are used. Data sources used for the case study are identified in Section 7.2.7.

Base Case Results

Figure 7.5 shows environmental impacts from various activities and the supply of ecosystem services in the MRW. GHG emissions, air pollutant emissions, water nutrient runoff, and water use from each activity are plotted in Fig. 7.5 (a), (b), (c), and (d), respectively. The background concentrations of those emissions (e.g., nutrient runoff from the upstream to the MRW) are not included.

Most environmental interventions are mainly attributed to thermoelectric activities except for PM_{10}, CO, N, and P flows. Transportation activities and agricultural activities are the main contributors to the PM_{10} and CO air emissions, and N and P water emissions, respectively. These results in the MRW match the U.S. national average.[47,49,58]

In the MRW, 8.4×10^4 TJ/y of electricity is generated from five thermoelectric power plants. A CST plant with OT cooling systems (Muskingum River Power Plant) and a CST plant with RE cooling systems (Conesville Power Plant) produce 14% and 34% of electricity, respectively. The rest 52% is produced from NGCC plants with RE

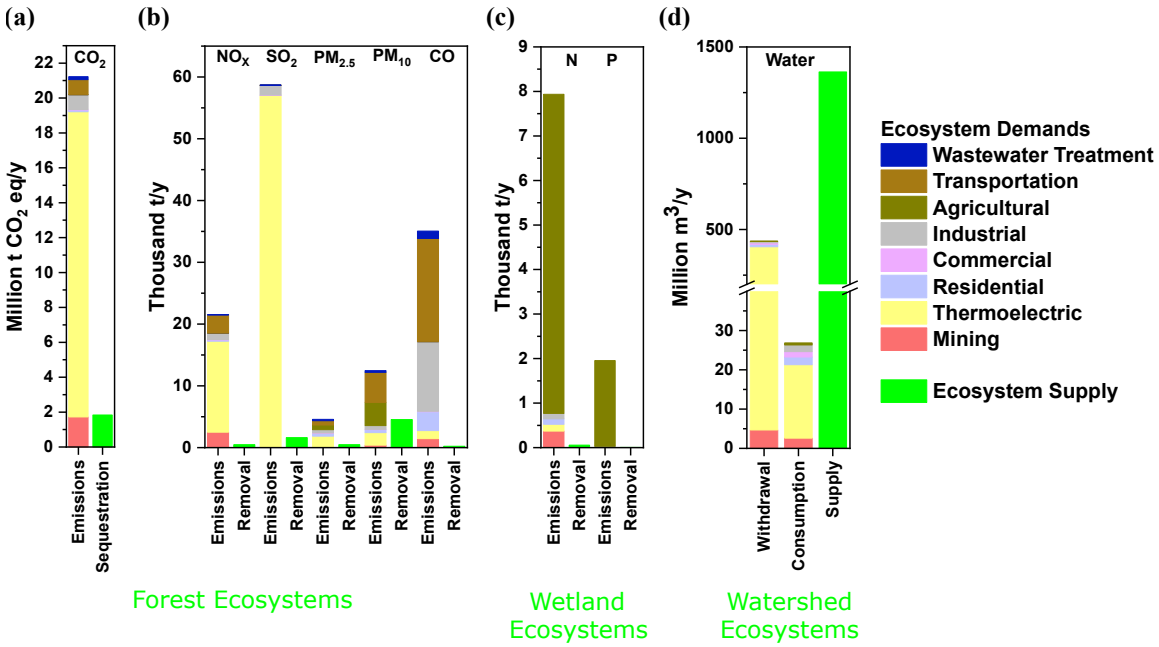

Figure 7.5: Environmental impacts from human activities and the supply of their corresponding ecosystem services for the base case. **(a)** GHG emissions, **(b)** air pollutant emissions, **(c)** water nutrient runoff, and **(d)** water use. All the environmental impacts except for water consumption exceed the supply of their corresponding ecosystem services.

cooling systems. Figure 7.6 exhibits the intensity of various environmental impacts for three types of power plants in the MRW. All values are normalized by total electricity generated in the MRW (TJ_{elec}). Compared to the CST plants, NGCC plants show smaller intensities for every impact category. In comparison between OT and RE cooling technologies, CST with RE shows higher CO_2 and NO_X emissions than CST with OT (Fig. 7.6 (a) and (b)). This is because the RE systems have lower power generation efficiency than the OT systems. With respect to SO_2 emissions, however, CST with RE shows much lower emissions than CST with OT because of the flue gas desulfurization (FGD) systems in the CST plant with RE (Conesville Power Plant)

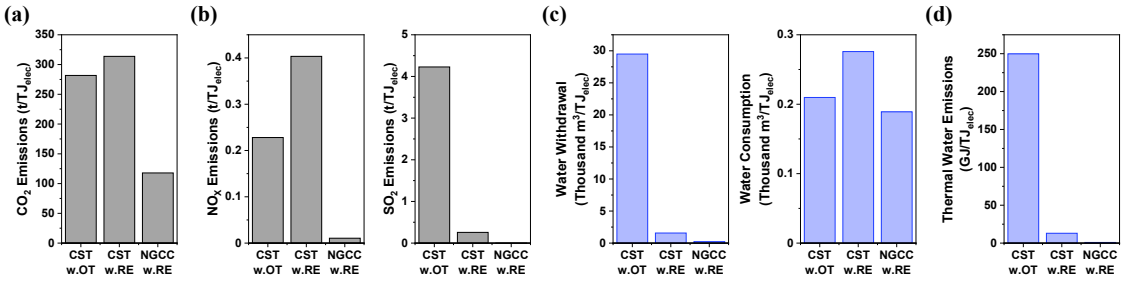

Figure 7.6: Intensity of environmental impacts for a CST plant with OT (Muskingum River Power Plant), a CST plant with RE (Conesville Power Plant), and NGCC plants with RE cooling systems (Dresden Energy, Waterford, and Dynegy Washington Power Plants) in the MRW. **(a)** GHG emissions, **(b)** air pollutant emissions, **(c)** water use, and **(d)** thermal water emissions.

(Fig. 7.6 (b)). The CST plant wit OT (Muskingum River Power Plant) did not equip the FGD systems in 2014 and was one of the largest SO_2 emitters in the nation.[153] Also, CST with OT withdraws more water than CST with RE, while the amount of water consumption is higher for the RE systems than the OT systems due to the evaporation from the cooling tower (Fig. 7.6 (c)). However, the OT systems result in huge thermal water pollution due to the cooling water discharge to the watershed, which leads to damages in the watershed ecosystems.

The TES sustainability metrics (V_k's) are calculated for each intervention (k) in the MRW as described in Section 7.2.6. In terms of water use, the amount of water consumption is considered as the demand for water provisioning service. As shown in Fig. 7.7, every V_k index except for V_{water} is close to negative one (-1). This indicates unsustainable conditions of activities in the MRW in terms of those intervention flows. The positive V_{water} value indicates that this region does not suffer from the water shortage. Therefore, the MRW could be managed by employing alternative strategies

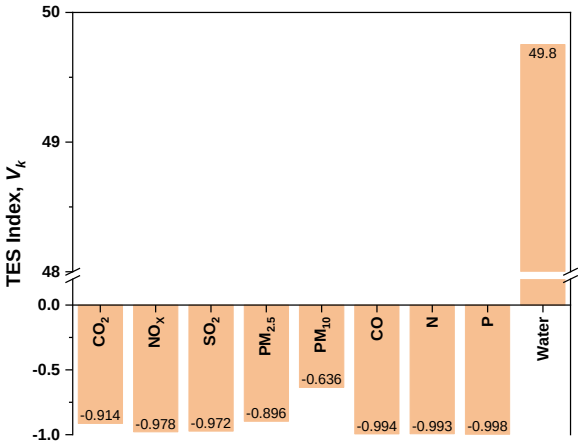

Figure 7.7: TES sustainability metrics are calculated for environmental interventions in the MRW. Activities in the MRW are only sustainable with respect to water consumption.

that are water-intensive to improve the sustainability of the MRW. Alternatives could be considered for thermoelectric and agricultural activities since most interventions are attributed to those activities as shown in Fig. 7.5. Also, land-use change options could be considered to enhance the supply of ecosystem services.

Clean Power Plant Strategy

Thermoelectric power generation is a huge contributor to most of the environmental impacts. In this study, the replacement of coal by NG, water-efficient cooling, renewable power sources, and conversion of CO_2 to hydrocarbons are considered as alternatives for the CPP strategy. For the comparison, 8.4×10^4 TJ/y of annual electricity generation is fixed regardless of alternative options adopted. Among various environmental indicators, we only focus on CO_2 emissions, N runoff, and water consumption indicators. Many air pollution indicators (e.g., NO_X and SO_2) and P indicator are similar to CO_2 and N indicators, respectively, as shown in Fig. 7.5.

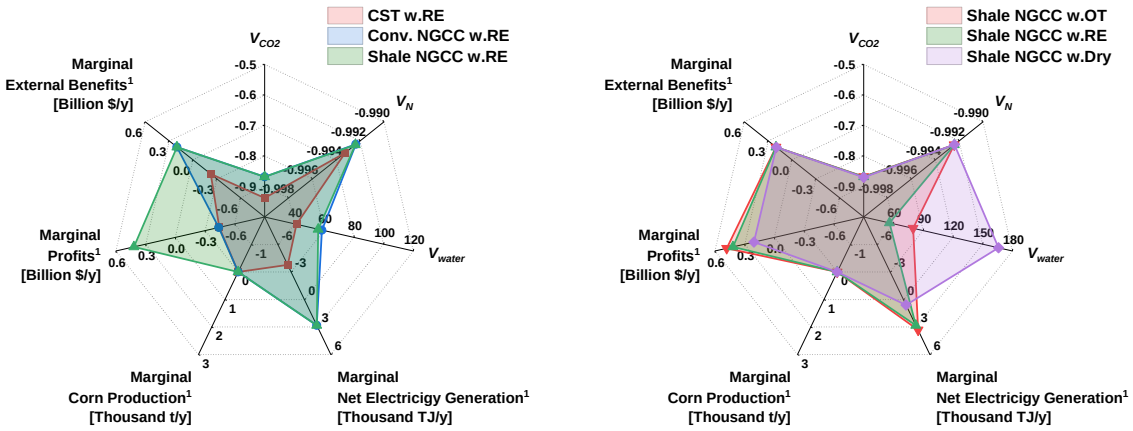

(a) (b)

Figure 7.8: Sustainability indicators for **(a)** different fuel options for generating electricity and **(b)** different cooling technology options for generating electricity. These indicators are defined such that larger values indicate greater sustainability. Note that the scale of V_{water} axis is different in each plot. Shale NGCC with RE and shale NGCC with dry cooling are desirable for water-affluent and water-scarce regions, respectively. [1]Marginal values are based on comparison with the base case.

Therefore, the indicators for air pollutants and P runoff are excluded from further analysis.

Replacement of Coal by NG for Power Generation As shown in Fig. 7.6, coal is a dirty fuel in every way. Therefore, NG could be employed for a fossil power source instead of coal to improve the sustainability of power generation. Figure 7.8a compares various sustainability indicators among coal, conventional NG, and shale NG as fossil power sources. We assume that only one type of fuel is employed for every thermoelectric power plant in the MRW.

By employing NG instead of coal for generating electricity, most indicators except for the corn production indicator can be improved. Using coal is environmentally

inferior to using NG. Economically, coal is much more expensive than shale NG. Comparison between conventional NG and shale NG options shows no significant differences in environmental indicators because mining activities account for relatively small portions of the overall environmental interventions as shown in Fig. 7.5. Fracking for extracting shale gas has been known as having higher water consumption[240] and releasing more water pollutants.[234,235] The study on the NG extraction in Appalachian where the MRW is a part of it reported that nitrogen emissions to water from shale gas extraction are approximately 300 times larger than those from conventional NG extraction.[272] However, the results in this study show that the increased interventions for the shale gas option are relatively insignificant from the perspective of holistic, watershed-scale sustainability. Rather, exploiting shale gas makes sense because it is more cost-effective than the conventional NG[178] as indicated in Fig. 7.8a.

Water-Efficient Cooling Figure 7.6 exhibits that the OT cooling systems have massive thermal water emissions due to the huge amount of water discharged to the watershed at the warmer temperature, although they are energy efficient and economically cheaper than other cooling technologies. We compare three cooling systems (OT, RE, and dry cooling) by assuming that all five fossil power plants in the MRW adopt the same type of cooling systems. As shown in Fig. 7.8b, dry cooling systems can be very effective for improving the TES water sustainability indicator (V_{water}) since they do not require the use of water for cooling. However, dry cooling is more energy-intensive and more economically expensive than wet cooling options. For water-scarce regions that have a negative V_{water} value, the dry cooling technology

could be a good alternative to improve water sustainability. However, for the water-affluent regions such as the MRW, it makes more sense to employ recirculating cooling systems since the dry cooling systems are expensive.

Renewable Power Generation Increasing the use of renewable power sources is one of the primary alternatives for the CPP strategy to minimize the interventions from power generation. The power density of solar PV energy is known to be 20 W/m^2, which is two times higher than that of wind energy (10 W/m^2).[277] Considering solar and wind energy potentials in the MRW, 0.8 and 2.3 m^2 of land area are required on an average for solar and wind power generation to generate 1.0 MWh of electricity, respectively.[50] If we assume that the barren land area (1.30×10^7 m^2) in the MRW can be utilized for those renewable power generation, 58 and 21 TJ/y of electricity can be generated from solar and wind power sources, respectively. These correspond to approximately 90% and 32% of total electricity generated from the fossil power plants in the MRW, respectively.

The previous results in Fig. 7.8 show that the shale NGCC plants with recirculating systems are preferred for the MRW in both environmental and economic aspects. Figure 7.9a exhibits sustainability indicators for adopting solar PV and wind power plants to the available barren lands to replace 90% and 32% of electricity produced from the shale NGCC plants with recirculating systems. Both solar PV and wind power plants have similar intervention intensities (e.g., kg CO_2 emissions per MJ of electricity generation) which are very small compared to the fossil power plants. However, since solar power has a higher energy potential per area than wind power, larger environmental benefits (higher V_{CO_2} and V_{water} indicator values) can be obtained with

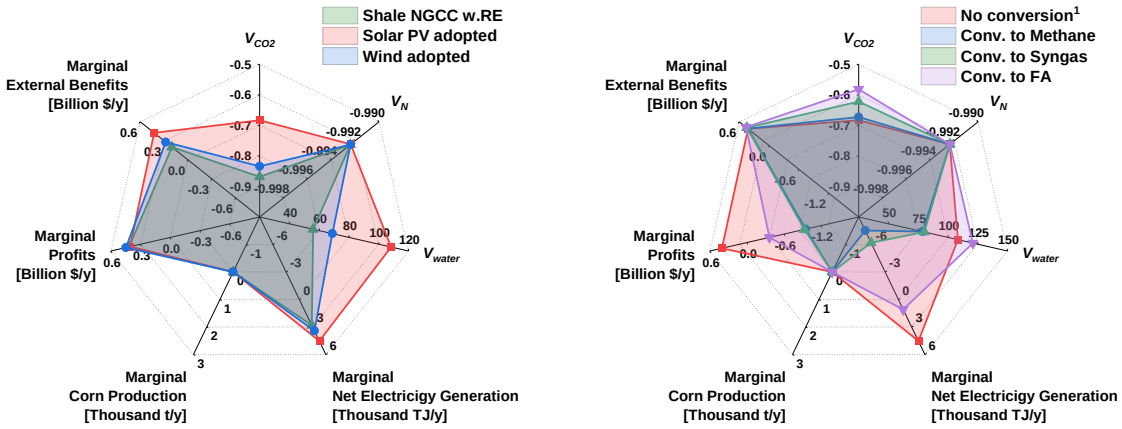

(a) (b)

Figure 7.9: Sustainability indicators for **(a)** adopting renewable power plants (solar PV or wind power) to 1.30×10^7 m^2 of barren lands to replace shale NGCC power plants with recirculating systems and **(b)** employing CO_2 conversion technologies in addition to the solar PV option from (a). Note that the scale of V_{water}, MP, and MEB axes is different in each plot. Environmental indicators can be improved by employing solar PV plants and converting CO_2 into FA, although CO_2 conversion is costly. Internalizing eternal benefits could yield positive profits. [1]The no conversion option from (b) is the same as the solar PV option from (a).

the solar power option. Renewable power plants do not require an electricity input in generating electricity, while fossil power plants have some parasitic energy losses (e.g., NGCC plants with recirculating systems in the MRW require 0.02 J of electricity to generate 1 J of electricity[153]). Thus, renewable options show higher marginal net electricity generation values than fossil options.

With respect to the monetary aspects, the solar PV option is less profitable than the other options since it has a higher LCOE. However, if we consider the environmental external cost, the monetary benefits of avoiding environmental damages for the solar PV option outweigh its lower profits. This implies that internalizing external benefits could change decisions from the monetary point of view. If we only consider

the profits for private sectors, employing the wind power option makes sense due to its lower LCOE. On the other hand, if the external benefits are internalized, the solar power option should be favored to maximize total profits (i.e., the sum of MP and MEB). In this case, sticking to using shale NGCC plants is the most expensive option because of its lower external benefits than the renewable options. The U.S. EIA report also estimates that the LCOE for solar PV and wind power technologies can be cheaper than the NGCC technology if federal tax credits to promote the use of renewable technologies are included.[243]

CO_2 Conversion CO_2 conversion technologies are promising alternatives to mitigate global warming by converting CO_2 into valuable hydrocarbon products. In this case study, we assume that CO_2 emissions from shale NGCC power plants in the MRW are captured through MEA absorption, compressed to 30 bar, and converted to methane, syngas, and formic acid (FA) as shown in Fig. 7.2. Hydrogen for hydrocarbon products is assumed to be provided from water through the electrolysis process. Electricity needed for the capture, compression, electrolysis, and conversion processes is assumed to be provided from the solar PV power plants which are deemed to be the most plausible from the previous results. 500,000 t/y of CO_2 conversion is assumed for the three conversion options. Also, we assume that newly-developed CO_2-converted methane, syngas, and FA products in the MRW displace NG, syngas, and FA that are produced using conventional technologies, respectively.

Figure 7.9b shows sustainability indicators for a no CO_2 conversion option and three conversion options. The no CO_2 conversion option shows the same results as the

solar PV option in Fig. 7.9a. The detailed results of CO_2 emissions, water consumption, electricity consumption, and production costs are shown in Table 7.3. Overall, the FA option shows the most promising results among the conversion options. The V_{CO_2} indicator for the FA option is the highest due to its higher CO_2 credits from displacing the conventional FA manufacturing process (methyl formate hydrolysis). All conversion options are water-intensive processes not only because the CO_2 capture process requires a substantial amount of water[246] but also because water is used to provide hydrogen to hydrocarbons. However, due to the large displacement credits from the conventional process, the FA option exhibits an increase in the V_{water} indicator. Also, the FA option is the least energy-intensive CO_2 conversion option because of its lower energy requirement for the CO_2 conversion process compared to other options.[249] Accordingly, the FA option is more lucrative than the other conversion options. This is not only because the FA conversion option is less energy-intensive, but also because the monetary displacement credits from the conventional FA process are large. In other words, Prod_{elec} in Eq. 7.9 for the FA option is larger than the other options. Also, $\text{Cost}_{formic\ acid}$ in Eq. 7.9 for the FA option is smaller than the other options because of the higher displacement credits.

Due to the limited demand for CO_2 converted products, the production scale of CO_2 conversion is limited. For example, 500,000 t/y of CO_2 conversion to FA corresponds to 75% of the global production capacity for FA in 2013 (697 thousand t).[251] It is less likely to be able to utilize CO_2 to produce FA in the MRW. However, market conditions have been changing over the years. According to the more recent market report,[278] the global production in 2016 was 1,015 thousand t and was expected to increase to 1,217 thousand t by 2022. In case of the methane and syngas options,

they are rarely constrained given the extensive uses of NG and syngas in the market. However, their CO_2-converted products are less profitable than CO_2-converted FA.

The expensive production cost for conversion processes is another constraint to employ the conversion technologies. Figure 7.10 compares marginal profits and marginal external benefits among three conversion options with the varied CO_2 conversion scale. Due to the expensive cost and high energy requirement for CO_2 conversion processes, all the options become less profitable as more CO_2 is converted. When there is no CO_2 conversion, the marginal profits are positive because the solar PV power plants adopted with shale NGCC power plants with recirculating systems are economically beneficial than the base case, which has two coal power plants without any renewable power plant.

Table 7.3: The detailed results for CO_2 conversion options about CO_2 emissions, water consumption, electricity consumption, and production costs. [1]CO_2 conversion includes the electrolysis of water and the compression of CO_2 to 30 bar. Stoichiometric conversion processes are assumed. [2]Displacement credits are shown as negative values.

	CO_2 emissions [Thousand t/y]	**Water consumption [Million m^3/y]**	**Electricity consumption [Thousand TJ/y]**	**Production costs [Billion $/y]**
Methane				
CO_2 capture	396.82	4.33	0.76	0.03
CO_2 conversion[1]	-500.00	0.41	11.33	0.96
Displacement credits[2]	-82.97	-0.12	-0.04	-0.04
Total	-186.15	4.62	12.05	0.96
Syngas				
CO_2 capture	396.82	4.33	0.76	0.03
CO_2 conversion[1]	-500.00	0.41	10.42	1.04
Displacement credits[2]	-830.93	-0.41	-0.47	-0.09
Total	-934.12	4.33	10.71	0.98
Formic acid (FA)				
CO_2 capture	396.82	4.33	0.76	0.03
CO_2 conversion[1]	-500.00	0.20	3.10	0.90
Displacement credits[2]	-1295.71	-5.82	-0.42	-0.28
Total	-1398.90	-1.29	3.44	0.65

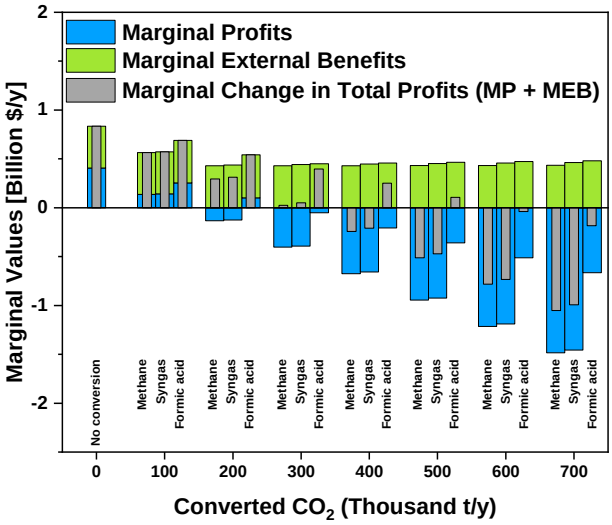

Figure 7.10: Marginal profits and marginal external benefits for CO_2 conversion options along with the different scale of CO_2 conversion. Due to the expensive cost of conversion technologies, profits are decreased substantially, and external benefits are increased slightly as the scale of conversion becomes larger. Marginal change in total profits can be positive when 500 thousand tCO_2 is converted to formic acid.

The marginal profits become negative when 200, 200, and 300 thousand t/y of CO_2 are converted to methane, syngas, and FA, respectively. That is, plant operators will have monetary losses compared to the base case profits when the above amounts of CO_2 are converted. However, if we internalize external benefits from mitigating environmental damages, CO_2 conversion technologies can be more economically competitive. The external benefits are slightly increased as more CO_2 is converted, and marginal change in total profits (MP + MEB) can be positive for 300, 300, and 500 thousand t/y of CO_2 conversion to methane, syngas, and FA, respectively. These results show that the internalization of the external benefits could promote the use

of advanced technologies that mitigate environmental damages but are economically expensive.

Most CO_2 conversion technologies are still in the research and development stage. As depicted in Section 7.2.4, therefore, it is difficult and challenging to compare different CO_2 conversion options whose processes have not been optimized yet. Due to this reason, stoichiometric conversion reactions are assumed in this study. The commercialized conversion processes are likely to have more emissions and resource use. Accordingly, their sustainability indicators will drop to some extent. Nonetheless, we could obtain some important insights into how much the conversion technologies would be effective and which options would make more sense to employ than others.

Technological Solution Overall, the CPP strategy can be a very effective solution for improving the V_{CO_2} indicator and mitigating climate change. In this study, the technological solution includes the replacement of coal by shale gas for generating electricity, recirculating cooling, the adoption of solar power plants in the available lands, and 500,000 t/y of CO_2 conversion to FA. The results for the technological solution are shown in Fig. 7.9b as the FA option. V_{CO_2} for the solution is -0.58 which is improved from -0.91 for the base case. The solution can also improve the V_{water} indicator significantly (from 50 to 121). V_N indicator, however, does not change much for technological alternatives. This is because N runoff is mainly attributed to the agricultural activity as shown in Fig. 7.5. The solution shows trade-offs between environmental objectives (V_k indicators) and an economic objective (MP indicator). However, if the external benefits are included in the market, the solution can result in an increase in total profits.

Depending on the regional characteristics, such as the availability of resources, climate, and market conditions, different technological alternatives may be preferred. For example, if a region has scarce water resources, dry cooling should be prioritized than the other expensive and water-intensive technological alternatives such as CO_2 conversion. Wind power could show more benefits than solar power depending on regional climate conditions. Also, effective CO_2 conversion options and scales could vary with those regional conditions.

Agro-Ecological Strategy

Unlike technological alternatives that only affect to reduce environmental impacts, agro-ecological alternatives such as alternative farming practices and ecological land-use change could enhance the supply of ecosystem services as well. According to the TES sustainability metrics shown in Eq. 7.6, increasing the ecosystem supply (S_k) helps improve the sustainability of human activities. In this section, we discuss the sustainability of agro-ecological alternatives that include various tillage options and land-use change options.

Tillage Practices Figure 7.11a shows sustainability indicators for adopting four different tillage practices: no-till, conservation tillage, reduced tillage, and intensive tillage. Overall, the indicators do not vary drastically with tillage options. No-till practice improves the V_N indicator by reducing nutrient runoff from the farming activity. The no-till practice also improves the V_{CO_2} indicator by enhancing soil carbon sequestration. However, the scale of changes in these indicators is not large.

The no-till practice reduces corn production by 0.5% compared to intensive tillage practice. Accordingly, marginal profits for the no-till option are slightly smaller than

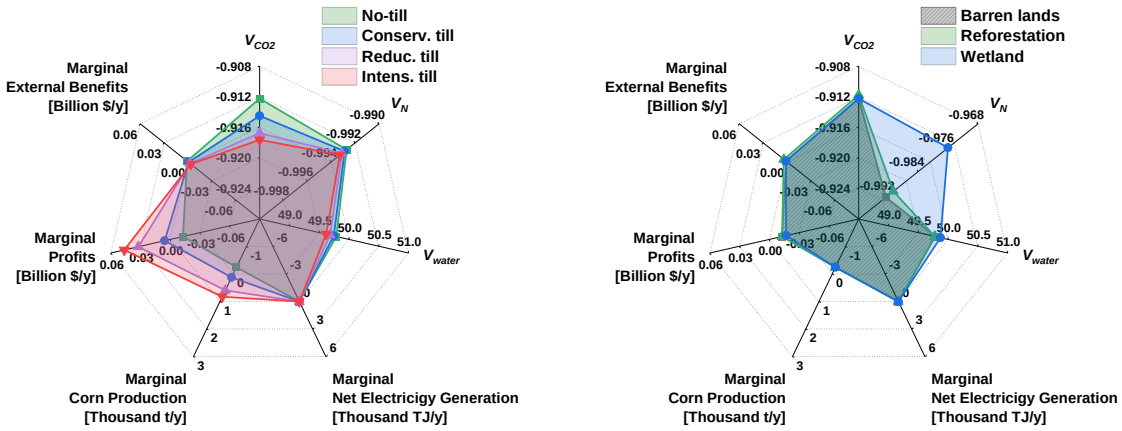

(a) (b)

Figure 7.11: Sustainability indicators for **(a)** employing different tillage practices and **(b)** adopting different land-use change options in addition to the no-till practice. Note that the scale of V_N axis is different in each plot. V_N indicator can be improved by implementing no-till practice and constructing wetlands.

the other tillage options due to the decreased productivity even though the no-till practice is cheaper than the tillage practices. Thus, trade-offs between environmental objectives (V_{CO_2}, V_N) and an economic objective (marginal profits) are observed. That is, fewer nutrient releases from the no-till lead to monetary loss. The nutrient trading scheme could result in a 'win-win' solution by resolving the trade-offs.[279] According to the scheme, other economic entities whose emissions are more expensive to abate than farming could pay farmers for credits to implement agricultural practices that result in lower food production but fewer nutrient emissions. This could yield both economic and environmental benefits.

Land-Use Change The barren land area could potentially be used for various useful ways. The area could be reforested to provide additional forest ecosystem

services, such as carbon sequestration service. Wetlands could be constructed in the area to increase nutrient retention service. These are ecological ways of utilizing the available land area to enhance the supply of ecosystem services.

Figure 7.11b exhibits ecological land-use change options for 1.30×10^7 m^2 of the barren land area in the MRW. Ecological options provide additional ecosystem services such as carbon sequestration service from the reforestation option and freshwater provisioning/nutrient retention services from the wetland option. The reforestation and wetland options improve V_{CO_2} and V_{water} indicators to a small extent, although these options are not as effective as technological options. As depicted in the previous section, technological alternatives, such as installing solar PV plants, are much more effective to improve V_{CO_2} and V_{water} indicators.

Section 7.3.2 shows that most technological alternatives do not improve the V_N indicator effectively. This nutrient runoff indicator can be addressed by ecological land-use change. Reforestation helps to improve the V_N indicator since additional tree cover helps reduce nutrient runoff through soil infiltration. The construction of additional wetlands is the most effective land-use change option to enhance the nutrient runoff indicator among any options in this study. Although the V_N index of the wetland option is still very negative, the index is increased to -0.975 from -0.993 of the base case. The negative index means the nutrient emissions in the MRW exceed the supply of nutrient retention services from the wetlands in the MRW. The excess nutrient emissions will flow into the downstream of the Muskingum River and cause eutrophication.

Synergistic Solution

Watershed should be managed to bring mutual benefits to multilateral stakeholders by improving multiple sustainability indicators. However, watershed resources such as the available land area are limited so that they need to be distributed properly to improve the overall sustainability of watershed activities. Agro-ecological alternatives focus on improving nutrient runoff indicators by both reducing nutrient emissions (no-till practice) and enhancing the supply of nutrient retention service (wetland construction). On the other hand, technological alternatives are effective to reduce air emissions and water consumption and could be economically feasible if the external benefits are internalized in the market. The solution that only concentrates on technological alternatives will overlook the damages of nutrient releases which should not be disregarded from the solution. In the context of sustainable watershed management, the opportunities for improving sustainability (i.e., the available land area, specifically) need to be shared between technological and agro-ecological alternatives. For instance, renewable power plants such as solar PV and wind power plants reduce environmental impacts such as GHG emissions and water consumption by displacing conventional fossil power plants but require a substantial land area. These land-intensive technological options compete with ecological options in the limited land area.

In 2019, Florida Power & Light Co. announced that they have a plan to fill in wetlands to install solar power plants at Kennedy Space Center in Florida, the U.S.[280] However, such action could aggravate water quality and cause eutrophication by eliminating valuable ecosystem services of wetlands. The most plausible sustainable solution could be the combination of solar PV and wetland options by distributing the

land area optimally into the two alternatives. Also, the solar PV panels could be installed in the wetlands and/or farmlands to maximize the synergy between technological systems and agro-ecological systems. In such a case, we need to examine if the installation of solar panels causes any disturbance on the wetland and farmland ecosystems.[281] Recently, there have been studies on agrivoltaic systems where solar panels are placed in croplands.[281–283] The studies identified that the agrivoltaic systems could be very attractive to shade-tolerant crops, such as lettuce. In the MRW, however, most of the farmlands are used for growing corn and soybeans which are not shade resistant crops. In this study, therefore, we consider integrated systems of solar PV panels and wetlands. Some wetland plants, such as sedges, are shade-tolerant or partially shade-tolerant. Currently, there is a lack of studies regarding how the solar PV panel installation would affect wetland ecosystems. Barron-Gafford et al. found that shading by the PV panels could not only improve the productivity of vegetation but also alleviate the heat stress of the panels due to latent heat fluxes between the panels and vegetation.[281] But, the shading may have negative impacts on the performance of wetlands. In this work, we assume that the performance of wetlands and PV panels is maintained in the integrated systems.

Figure 7.12 compares sustainability indicators between the base case, technological solution, agro-ecological solution, and synergistic solution. The technological solution refers to the solution from the CPP strategy in Section 7.3.2, which includes shale NGCC power plants with recirculating cooling systems, solar PV plants for the available land area, and 500,000 t/y of CO_2 conversion to FA. The technological solution is very effective to improve V_{CO_2} and V_{water} indicators, and thus, it gives large external benefits. This solution corresponds to the technology-focused solution since

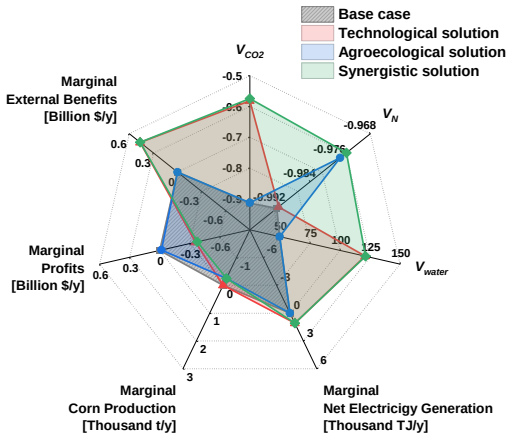

Figure 7.12: Sustainability indicators for the base case, technological solution, agro-ecological solution, and synergistic solution. The available land area is utilized for employing solar PV plants in the technological solution and for constructing wetlands in the agro-ecological solution. The synergistic solution utilizes the land area for both solar PV plants and wetlands to generate synergy between technological and agro-ecological systems.

the available land area is allocated to the solar PV power plants. The agro-ecological solution includes the implementation of no-till practice and the construction of wetlands in the available land area. This solution can improve a nutrient runoff indicator significantly.

The synergistic solution indicates an integrated solution that combines technological and agro-ecological alternatives. In the synergistic solution, solar PV plants and constructed wetlands coexist in the available land area. Solar PV plants replace conventional fossil power plants while wetlands provide an additional nutrient retention service that any technological alternatives fail to improve. That is, the solution includes agro-ecological alternatives (no-till practice and constructed wetlands) as well as various technological alternatives (shale NGCC power plants with recirculating

cooling, solar PV plants, and 500,000 t/y of CO_2 conversion to FA.) The integrated solution generates synergy between technological and agro-ecological alternatives in improving multiple sustainability indicators including a V_N indicator compared to the base case. Two trade-offs between objectives are shown in the solution. No-till practice improves environmental indicators but lowers crop productivity. V_{CO_2} indicator can be enhanced by converting CO_2 to FA, but the conversion technologies are expensive. As discussed in Section 7.3.2, however, the marginal change in total profits (MP + MEB) can be positive if the external benefits of ecosystem services are internalized in the market.

7.4 Conclusions

The FEW nexus must be considered for sustainability assessment to avoid unintended shifting of impacts across multiple flows by capturing the interactions between FEW flows. In this study, the modeling framework for FEW nexus is extended to include ecosystem and waste flows. Ecosystems provide various beneficial services to FEW systems. Watershed ecosystems provide freshwater which is one of the key resources for energy and food systems. Waste flows such as GHG emissions and nutrient releases from the FEW systems are handled by forest and wetland ecosystems to suppress ecological overshoot. In this sense, the ecologically synergistic FEW nexus modeling framework needs to be utilized in assessing the sustainability of holistic systems to capture the complex interactions between FEW systems and ecosystems.

As opposed to the traditional FEW nexus, the ecologically synergistic FEW nexus framework could determine absolute sustainability metrics by calculating TES indicators. The TES indicators measure the absolute extent of ecological overshoot. The

considerations of ecosystem services in the FEW nexus model could result in different solutions and decisions. While the traditional FEW nexus model can only identify opportunities for reducing environmental impacts, the ecologically synergistic FEW nexus model can identify opportunities for improving ecosystem services as well. Moreover, the ecologically synergistic FEW nexus model can estimate the external benefits of ecosystem services and lead to different conclusions if the benefits are internalized in the market. Depending on the case, this may allow a 'win-win' solution for both economical and environmental indicators.

In this work, we focus on watershed-scale FEW systems since water is a primary component in the FEW nexus. Both the energy and food industries largely rely on the sustainable supply of water. To manage watersheds sustainably, common watershed resources such as water supply, available lands, and other ecosystem services must be distributed properly among multilateral stakeholders to enhance overall watershed functions.[233] In this context, sustainable watershed management strategies should not focus on one indicator but multiple ones including climate change, air quality, water quality, water quantity, food production, and monetary profits. In this work, we focus on CO_2, N nutrient, water quantity, corn production, and monetary indicators.

As a case study, various technological and agro-ecological alternatives in the MRW are discussed using the ecologically synergistic FEW nexus modeling framework. Technological alternatives are defined as the CPP strategy which includes diverse alternatives such as NGCC power generation, water-efficient cooling technologies, renewable power generation, and potential CO_2 conversion technologies. Agro-ecological alternatives refer to different tillage farming practices and ecological land-use change options for the available land area. The holistic assessment employing

the ecologically synergistic FEW nexus framework enables us to identify the environmental effectiveness and economical feasibility of those alternatives by understanding the interactions between FEW systems and ecosystems.

Among the options in the CPP strategy, it is identified that converting CST plants to NGCC power plants is essential in improving every sustainability indicator. Assuming that all power plants in the MRW are converted to the shale NGCC plants, employing dry cooling systems is the most effective option in improving water quantity indicator. However, dry cooling systems are very expensive and energy-intensive. Therefore, in regions such as the MRW where water scarcity is not an issue, the recirculating cooling option makes more sense. Renewable power generation technologies such as wind turbines and solar PV panels can displace fossil fuel power plants. While installing wind turbines in the available land area results in larger monetary profits than the other power generation options, solar PV panels could be a more profitable alternative if the external benefits of mitigating impacts are internalized. Also, the solar PV option is superior to the wind option in improving net electricity generation and CO_2 indicators since solar power can displace more capacity of fossil fuel power generation due to its higher energy potential in the MRW. These results might be varied depending on regional solar radiation and wind speed conditions. In addition, for the best CO_2 indicator, CO_2 emissions can be captured and converted to formic acid even though CO_2 conversion processes are highly energy-intensive and expensive. The internalization of external benefits could result in positive profits for a technological solution that includes employing NGCC with recirculating cooling, installing solar PV plants for the available land area, and converting CO_2 into formic acid, while effectively mitigating CO_2 emissions and water consumption.

Unlike technological alternatives, agro-ecological alternatives could enhance sustainability indicators by increasing the supply of ecosystem services. For the best nutrient indicator, the available land area should be allocated to construct wetlands, which provide nutrient retention service. This ecological land-use option competes with technological land-use options, such as installing solar PV panels. The solar PV option is very effective in improving various sustainability indicators except for the nutrient indicator, which can be enhanced primarily by the wetland option. Therefore, the available land area should be distributed between the two land-use alternatives. The best solution could be employing the integrated systems of solar PV panels and wetlands. The synergy between technological and agro-ecological systems could be produced from this solution in improving multiple sustainability indicators. Further research is needed to investigate the impacts of solar panels on wetland ecosystems, and vice versa.

The ecologically synergistic FEW nexus takes account of FEW systems and their interactions with ecosystems. Data collection is a challenging task in such holistic work. In this work, stoichiometric CO_2 conversion processes are assumed since their commercialized process data are not yet available. The robustness of results needs to be evaluated through the sensitivity analysis of uncertain data. Also, activities in the FEW systems and ecosystems vary by season and region. For example, renewable power sources depend on season and weather. Energy storage systems that are not considered in this work may be required for such intermittent renewable power technologies. Thus, seasonal and spatial analyses could be performed to get insights on the seasonal and spatial variations in the FEW nexus. The impacts of climate change on the nexus could also be considered to ensure FEW nexus security

under climate change scenarios. Moreover, a multi-spatial scale FEW nexus model could be constructed to account for different serviceshed scales of ecosystem services. Additionally, nutrient trading between economic entities in the watershed could be considered to examine if it can generate both economic and environmental benefits. For more robust economic analysis, market conditions (e.g., investment budget and labor) and market behavior (e.g., price elasticity) could be accounted for in the FEW nexus modeling work.[17] Use of sophisticated economic models such as the rectangular choice-of-technology model[6] and general equilibrium model[56,126,284] may be needed.

Chapter 8: Computational Framework for Spatially-Explicit Absolute Life Cycle Assessment Based on a Multi-Regional Hybrid Approach

8.1 Introduction

Methodologies for life cycle assessment (LCA) have been developed in various ways to give more reliable sustainability assessment results to decision-makers. For example, a hybrid LCA approach has been developed to represent a more complete life cycle analysis boundary while utilizing detailed inventory data.[12] This approach integrates a process-based LCA (PLCA) model, which is based on detailed process inventory data, with an environmentally-extended input-output (EEIO) model, which accounts for the entire economic activities in a selected region.

Another example of the recent development in LCA methodologies is multi-regional modeling approaches. The conventional LCA models such as PLCA and EEIO are generally national scale models, which are based on national average inventory data.[39,40] These average inventory data ignore region-specific inventory characteristics, such as technologies adopted in a specific region and interventions from those region-specific technologies, by averaging them into a single inventory data. However, such conventional approaches may give inaccurate results to decision-makers,

especially when the study focuses on specific regions or technologies. To account for spatially heterogeneous inventory data, multi-regional modeling approaches have been developed for each of the PLCA[34] and EEIO[33] models. The multi-regional models consist of region-specific intra-regional transaction matrices, inter-regional transaction matrices, and region-specific intervention matrices.

More recently, the PLCA model that accounts for the benefits of ecosystem services has been developed.[129] The supply of ecosystem services needs to be considered for sustainability assessment (e.g., LCA) to calculate absolute sustainability indicators. Otherwise, the solution may cause ecological overshoot that results in resource depletion and ecosystem degradation. The previous study developed a computational framework for techno-ecological synergy in LCA (TES-LCA).[129] This modeling framework quantifies both interventions and the supply of ecosystem services to calculate absolute sustainability indicators. Also, a regionalized TES-LCA model was developed to assess region-specific absolute sustainability indicators.[35] The regionalized TES-LCA model is needed to get accurate insights into the regional benefits of ecosystem services. While some ecosystem services (e.g., climate regulation service) have a global serviceshed scale, other ecosystem services (e.g., air quality regulation) have a regional serviceshed scale. For such ecosystem services, region-specific absolute sustainability indicators need to be calculated using the regionalized TES-LCA model.

In this work, we explore a general computational framework for spatially-explicit absolute LCA (SEA-LCA) by utilizing approaches for regionalized PLCA,[34] multi-regional EEIO,[33] and TES-LCA[35,129] models. SEA-LCA model can represent the

planetary boundary while utilizing detailed local process data, region-specific economic data, and inter-regional supply chain data in calculating spatially-explicit absolute sustainability indicators at each serviceshed scale. For such a comprehensive model, data availability is one of the limiting factors because it is challenging to collect extensive region-specific inventory data. Also, many data sources are often based on different spatial scales (e.g., county scale vs. national scale data). To minimize such time-consuming data collection tasks and utilize various data sources, a hybrid modeling approach that integrates existing databases and models is essential.

There are many previous studies that attempted to integrate models using a hybrid modeling approach to perform a spatially-explicit sustainability assessment. Gibon et al. (2015) integrated PLCA model with global scale multi-regional input-output (MRIO) model to investigate the life cycle environmental impacts of concentrating solar power technology in nine world regions.[285] They employed the ecoinvent PLCA inventory database and EXIOBASE/GTAP MRIO inventory database. They also utilized future energy industry and emission scenarios to assess the impacts of technology in 2050. Agez et al. (2020) constructed a hybrid LCA inventory database using data from the entire ecoinvent PLCA and EXIOBASE MRIO inventory databases.[286] Multiscale input-output models for China were also developed by employing data from Chinese MRIO and global WIOD (World Input Output Database) inventory databases to analyze CO_2 emission flows in China.[287,288]

Those studies constructed multiscale and multi-regional models by employing multiple databases and models that represent different spatial scales. However, they did not propose a general modeling framework that could utilize data at any spatial scale, which could range from local process scale to regional, national, and global economy

scales. Depending on the study, the availability of inventory data varies. Therefore, a general modeling framework is needed to conduct any specialized case studies. Moreover, none of the multiscale and multi-regional modeling work considered the supply of ecosystem services and addressed absolute sustainability indicators.

This work proposes a general modeling framework for SEA-LCA study. The SEA-LCA model in this work could assess the absolute sustainability of activities at various scales (e.g., local, state-level, national, and global scales). Sustainability indicators at different scales are useful in addressing various stakeholder's interests and serviceshed scales of ecosystem services. A case study is performed on county-level corn and soybean production in the Great Lakes (GL) region in the United States. We demonstrate how local process models can be connected to various scales' economic models. We discuss how sensitive to spatial scales the LCA indicators are and why a spatially-explicit assessment needs to be performed to investigate the sustainability of activities in a specific region.

8.2 Background

To develop a general modeling framework for SEA-LCA, approaches for hybrid LCA, multi-regional LCA, and TES-LCA are utilized. Table 8.1 summarizes characteristics of existing sustainability assessment approaches and SEA-LCA approach. In this section, we briefly describe each approach.

8.2.1 Hybrid LCA

Hybrid LCA integrates PLCA model with EEIO model.[12] PLCA model is based on the detailed process data for each type of technologies. For example, PLCA model generally distinguishes coal-fired power generation from NG-fired power generation.

However, PLCA model does not represent the whole life cycle network since it is practically impossible to collect detailed process data for every life cycle inventory. Therefore, PLCA model only focuses on the "important" processes, which in turn could result in inaccurate results. PLCA model could cause shifting of environmental impacts outside its analysis boundary.

EEIO model, on the other hand, accounts for the entire economic activities in a selected region. However, the inventory data of EEIO model is highly aggregated, which makes it challenging to conduct sustainability analysis for specific processes or technologies. For instance, EEIO model often considers all kinds of power generation technologies as a single electricity generation sector.

Figure 8.1a shows a hybrid LCA model structure. Hybrid LCA approach has been developed to account for the complete life cycle boundary of EEIO model while maintaining the detailed process inventory data of PLCA model. In hybrid LCA model, transaction and intervention matrices are formulated as shown in Equations

Table 8.1: Characteristics of existing sustainability assessment approaches and SEA-LCA approach. Spatial scales, level of regional information, whether the approaches account for ecosystem services, and available models for each approach are shown. [1]VC: value chain process scale, Econ: economy scale.

Approaches	**Scales** [1]	**Region**	**Ecosystems**	**Available models**
PLCA	VC	Single	Not included	GREET,[42] USLCI,[40] ecoinvent[43]
EEIO	Econ	Single	Not included	USEEIO[39]
Hybrid LCA[12]	VC + Econ	Single	Not included	-
Regionalized PLCA[34]	VC	Multiple	Not included	-
Multi-regional EEIO	Econ	Multiple	Not included	US state-level MRIO,[33] EXIOBASE[289]
TES-LCA[129]	VC	Single	Included	-
Regionalized TES-LCA[35]	VC	Multiple	Included	-
SEA-LCA (this work)	VC + Econ	Multiple	Included	-

8.1 and 8.2, respectively.

$$\overline{\underline{X}} = \begin{bmatrix} \underline{X} & -\underline{A}_d \\ -\underline{X}_u & I - \overline{A}^* \end{bmatrix}, \tag{8.1}$$

$$\overline{\underline{D}} = \begin{bmatrix} \underline{D} & \overline{D}^* \end{bmatrix}, \tag{8.2}$$

where $\underline{X}$ and $\overline{A}$ represent value chain scale technology and economy scale direct requirement matrices, respectively. The asterisk sign in $\overline{A}^*$ means that the matrix is disaggregated from the models at smaller scales than it to avoid double-counting of overlapped activities between models. In general, $\overline{A}$ includes activities of $\underline{X}$ since EEIO model accounts for the entire economic activities. Therefore, $\overline{A}$ needs to be disaggregated from $\underline{X}$ to represent $\overline{A}^*$ (disaggregated $\overline{A}$), as shown in Fig. 8.1a. Underbar and overbar notations refer to value chain and economy scales, respectively. $\underline{A}_d$ and $\underline{X}_u$ represent downstream and upstream cutoff flows between value chain and economy scales, respectively. Also, $\underline{D}$ and $\overline{D}$ correspond to the intervention matrices at value chain and economy scales, respectively. $\overline{D}$ needs to be disaggregated from $\underline{D}$ to be $\overline{D}^*$ as well. $\overline{\underline{X}}$ and $\overline{\underline{D}}$ are transaction and intervention matrices at multiple spatial scales, respectively.

Transaction and intervention equations of hybrid model are formulated by Equations 8.3 and 8.4.

$$\overline{\underline{X}}\ \overline{\underline{m}} = \overline{\underline{f}}, \tag{8.3}$$

$$\overline{\underline{D}}\ \overline{\underline{m}} = \overline{\underline{r}}, \tag{8.4}$$

where $\overline{\underline{m}}$ and $\overline{\underline{f}}$ represent vectors of scaling factors and final demands at multiple scales, respectively. $\overline{\underline{r}}$ is life cycle interventions that are calculated from the hybrid model. $\overline{\underline{m}}$ is determined by Equation 8.3. Then, $\overline{\underline{r}}$ is calculated by Equation 8.4.

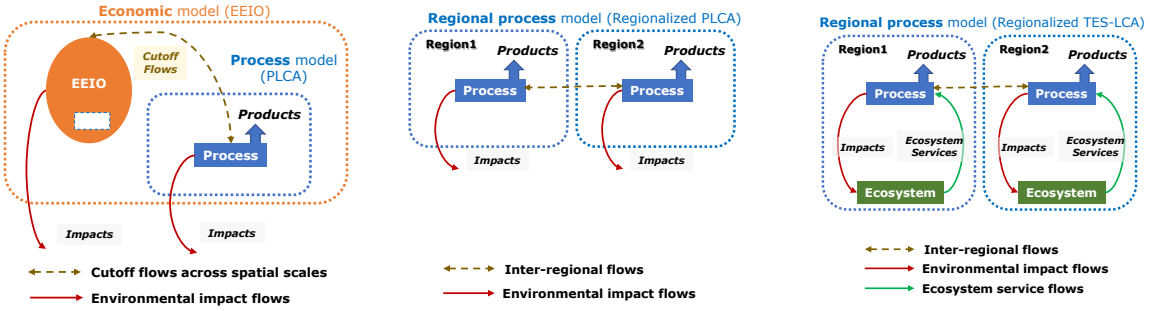

Figure 8.1: Model structures of **(a)** hybrid LCA, **(b)** regionalized PLCA, and **(c)** regionalized TES-LCA models.

8.2.2 Multi-Regional LCA

Multi-regional models are needed to conduct a spatially-explicit sustainability assessment since activities and interventions are different by region. For instance, activities in one region may have different commodity inputs, technological efficiencies, supply chains, and emission coefficients from the other regions. Different demographics by region also require region-specific impact characterization factors.[34]

Multi-regional EEIO model[33] and regionalized PLCA model[34] have been developed. Figure 8.1b exhibits a regionalized PLCA model structure. To account for regional heterogeneity of inventory data, multi-regional transaction and intervention matrices for regionalized PLCA model are formulated by Equations 8.5 and 8.6.

$$\underline{X}_{MR} = \begin{bmatrix} \underline{X}_{11} & \underline{X}_{12} & \cdots & \underline{X}_{1r} \\ \underline{X}_{21} & \underline{X}_{22} & \cdots & \underline{X}_{2r} \\ \vdots & \vdots & \ddots & \vdots \\ \underline{X}_{r1} & \underline{X}_{r2} & \cdots & \underline{X}_{rr} \end{bmatrix}, \tag{8.5}$$

$$\underline{D}_{MR} = \begin{bmatrix} \underline{D}_1 & \underline{D}_2 & \cdots & \underline{D}_r \end{bmatrix}, \tag{8.6}$$

where a subscript MR indicates that the matrix represents multiple regions. Subscripts $1, 2, \cdots, r$ represent each region. Diagonal matrices such as $\underline{X}_{11}, \underline{X}_{22}, \cdots, \underline{X}_{rr}$ are intra-regional transaction matrices at each region. Non-diagonal matrices correspond to inter-regional transaction matrices between regions.

Accordingly, life cycle interventions are calculated by Equations 8.7 and 8.8.

$$\underline{X}_{MR}\ \underline{m}_{MR} = \underline{f}_{MR}, \tag{8.7}$$

$$\underline{D}_{MR}\ \underline{m}_{MR} = \underline{r}_{MR}, \tag{8.8}$$

where $\underline{m}_{MR}$ and $\underline{f}_{MR}$ refer to vectors of multi-regional scaling factors and multi-regional final demands, respectively. Also, $\underline{r}_{MR}$ indicates life cycle interventions calculated for each region.

8.2.3 Techno-Ecological Synergy in LCA

Another effort to advance the LCA methodology is to include the supply of ecosystem services in the PLCA model. Techno-ecological synergy in LCA (TES-LCA) model[129] and its regionalized model[35] have been developed to account for ecosystem services in calculating absolute sustainability indicators at the value chain scale. The TES-LCA modeling approach can be applied to EEIO model as well by quantifying the supply of ecosystem services at the economy scale.

Figure 8.1c represents a model structure of regionalized TES-LCA. Regional ecosystem services need to be quantified in addition to the regional environmental impacts. TES-LCA model can be formulated by Equation 8.9.

$$\left[\begin{array}{c:c} \underline{X} & \underline{C} \\ \hdashline \underline{D} & \underline{S} \end{array}\right] \left[\begin{array}{c} \underline{m} \\ \hdashline \underline{m}_e \end{array}\right] = \left[\begin{array}{c} \underline{f} \\ \hdashline \underline{f}_e \end{array}\right], \tag{8.9}$$

where $\underline{C}$ and $\underline{S}$ represent management and ecosystem matrices, respectively. The management matrix includes inputs flows from technological systems to the ecosystems. The ecosystem matrix includes the supply of ecosystem services (e.g., climate regulation service). It has the opposite sign to $\underline{D}$ matrix. In other words, the supply of climate regulation service is represented by negative values in $\underline{S}$ matrix because GHG emissions in $\underline{D}$ matrix are represented by positive values. $\underline{m}_e$ and $\underline{f}_e$ refer to an ecosystem scaling vector and an ecosystem final demand vector, respectively.

In TES-LCA, absolute sustainability indicators are calculated by Equations 8.10 and 8.11.

$$\underline{X}\ \underline{m} + \underline{C}\ \underline{m}_e = \underline{f}, \tag{8.10}$$

$$\underline{D}\ \underline{m} + \underline{S}\ \underline{m}_e = \underline{f}_e. \tag{8.11}$$

Assuming that $\underline{X}$, $\underline{C}$, $\underline{D}$, and $\underline{S}$ matrices are known, $\underline{f}_e$ can be calculated by specifying $\underline{m}_e$ to be 1, when the absolute sustainability of certain products needs to be calculated. The calculated $\underline{f}_e$ values correspond to the net intervention values (e.g., net carbon footprint and net water footprint). If we fix $\underline{m}_e$ to be 1, it means that $\underline{S}$ matrix represents the total supply of ecosystem services in a selected region, not coefficient values.

According to the techno-ecological synergy (TES) framework,[10] the absolute sustainability index (V_k) for k-th flow can be quantified by Equation 8.12.

$$V_k = \frac{S_k - D_k}{D_k}, \tag{8.12}$$

where S_k and D_k are the supply and demand for ecosystem services for k-th flow, respectively. The positive and negative V_k index values indicate absolutely sustainable and unsustainable conditions of activities in a specific spatial scale, respectively.

In TES-LCA, V_k metrics for k-th flow can be calculated by Equation 8.13.

$$V_k = \frac{-\underline{S}_k \ \underline{m}_e - \underline{D}_k \ \underline{m}}{\underline{D}_k \ \underline{m}}. \tag{8.13}$$

A negative sign is needed for $\underline{S}_k \ \underline{m}_e$ term since $\underline{S}$ has the opposite sign to $\underline{D}$ in TES-LCA model. For example, the supply of carbon sequestration service is represented by a positive value in Equation 8.12, but a negative value in Equation 8.13.

One additional aspect that needs to be addressed in TES-LCA is that ecosystem services need to be allocated to specific activities. In Equation 8.11, the demand for ecosystem services ($\underline{D} \ \underline{m}$) corresponds to the environment interventions with respect to specific activities in a selected region. It does not represent the entire interventions from every activity in a region. Therefore, the supply of ecosystem services ($\underline{S}_k \ \underline{m}_e$) also needs to be the supply with respect to specific activities. Since ecosystem services present their benefits to every human activity, the supply of ecosystem services in a selected region needs to be allocated to the specific activities. Allocation can be performed based on the proportional values of demand for ecosystem services, population, and land areas, etc. as shown in Equation 8.14.

$$\underline{\tilde{S}} = \underline{S} \circ \underline{W}, \tag{8.14}$$

where $\underline{W}$ represents a matrix of weighting factors that allocate the supply of ecosystem services to specific activities. $\underline{\tilde{S}}$ indicates the allocated supply of ecosystem services based on $\underline{W}$. For instance, a total quantity of carbon sequestration service from the ecosystems in a certain region ($\underline{S}_{CO_2}$) can be allocated to fossil power plants in the region based on the ratio of GHG emissions from the power plants to the total GHG emissions in the region. In this case, $\underline{W}$ can be defined by Equation 8.15.

$$\underline{W} = \frac{\underline{D}_{CO_2,PP}}{\Sigma_i \underline{D}_{CO_2,i}}, \qquad i = 1, 2, \cdots, n. \tag{8.15}$$

A numerator in Equation 8.15 ($\underline{D}_{CO_2,PP}$) corresponds to the GHG emissions from the power plants (PP), while a denominator ($\Sigma_i \underline{D}_{CO_2,i}$) represents the total GHG emissions from every activity (i's) in the region.

Liu et al. (2019) also developed a regionalized TES-LCA model, which is formulated by Equation 8.16.[35]

$$\left[\begin{array}{c:c} \underline{X}_{MR} & \underline{C}_{MR} \\ \hdashline \underline{D}_{MR} & \underline{S}_{MR} \end{array}\right] \left[\begin{array}{c} \underline{m}_{MR} \\ \hdashline \underline{m}_{e,M} \end{array}\right] = \left[\begin{array}{c} \underline{f}_{MR} \\ \hdashline \underline{f}_{e,M} \end{array}\right], \tag{8.16}$$

where a subscript MR represents multi-regional matrices and vectors. TES absolute sustainability indices (V_k) for k-th flow can be calculated for each region.

8.3 Spatially-Explicit Absolute Life Cycle Assessment

In this section, we will describe a modeling framework for SEA-LCA. To conduct a spatially-explicit sustainability assessment study, region-specific data and multi-regional models are needed. Also, to utilize detailed process data while representing the complete life cycle system boundary, a hybrid modeling approach is necessary. In this work, we integrate the existing sustainability assessment modeling approaches including PLCA, EEIO, MRIO, hybrid LCA, and TES-LCA to develop the SEA-LCA model. The integration of multiple models enables LCA practitioners to conduct LCA studies for various purposes. Also, SEA-LCA is a general computational model that is applicable to diverse case studies.

8.3.1 Transaction Matrix

Equation 8.17 exhibits transaction matrix for SEA-LCA model ($\underline{\overline{X}}_M$).

$$\underline{\overline{X}}_M = \left[\begin{array}{c|c|c|c} (1)\ \underline{X}_L & (2)\ -\underline{A}_{d,LR} & (3)\ -\underline{A}_{d,LN} & (4)\ -\underline{A}_{d,LG} \\ \hline (5)\ -\underline{X}_{u,RL} & (6)\ I_R - \overline{\underline{A}}^*_R & (7)\ -\overline{\underline{A}}^*_{d,RN} & (8)\ -\overline{\underline{A}}^*_{d,RG} \\ \hline (9)\ -\underline{X}_{u,NL} & (10)\ -\overline{\underline{A}}^*_{u,NR} & (11)\ I_N - \overline{\underline{A}}^*_N & (12)\ -\overline{\underline{A}}^*_{d,NG} \\ \hline (13)\ -\underline{X}_{u,GL} & (14)\ -\overline{\underline{A}}^*_{u,GR} & (15)\ -\overline{\underline{A}}^*_{u,GN} & (16)\ I_G - \overline{\underline{A}}^*_G \end{array}\right], \tag{8.17}$$

where subscripts L, R, N, and G represent local, regional, national, and global scales, respectively. Matrices and vectors with a subscript M are the multiscale and multi-regional matrices and vectors for SEA-LCA model, respectively. Diagonal elements in the matrix (elements 1, 6, 11, and 16) correspond to local scale technology, regional scale commodity transaction, national scale commodity transaction, and global scale transaction matrices, respectively. Non-diagonal elements represent cutoff flows across spatial scales. For example, element 2 ($\underline{A}_{d,LR}$) represents downstream cutoff flows of local scale products to the regional scale sectors. Also, element 5 ($\underline{X}_{u,RL}$) represents upstream cutoff flows of regional scale commodities to the local scale processes. Depending on the scope of study and the availability of data, the model could include some portions of elements in $\underline{\overline{X}}_M$. For example, a hybrid LCA model that integrates PLCA and USEEIO models includes elements 1, 3, 9, and 11. The integrated model of PLCA and global MRIO includes elements 1, 4, 13, and 16. Figure 8.2 shows a model structure of SEA-LCA model. Any scale models could be multi-regional models if multi-regional inventory data are available. Each element in Equation 8.17 is shown in italics in Fig. 8.2.

When the detailed process data are available, technology matrix (element 1) can be included in the transaction matrix. This could be national average process data, county-level average process data, or facility-level process data depending on the

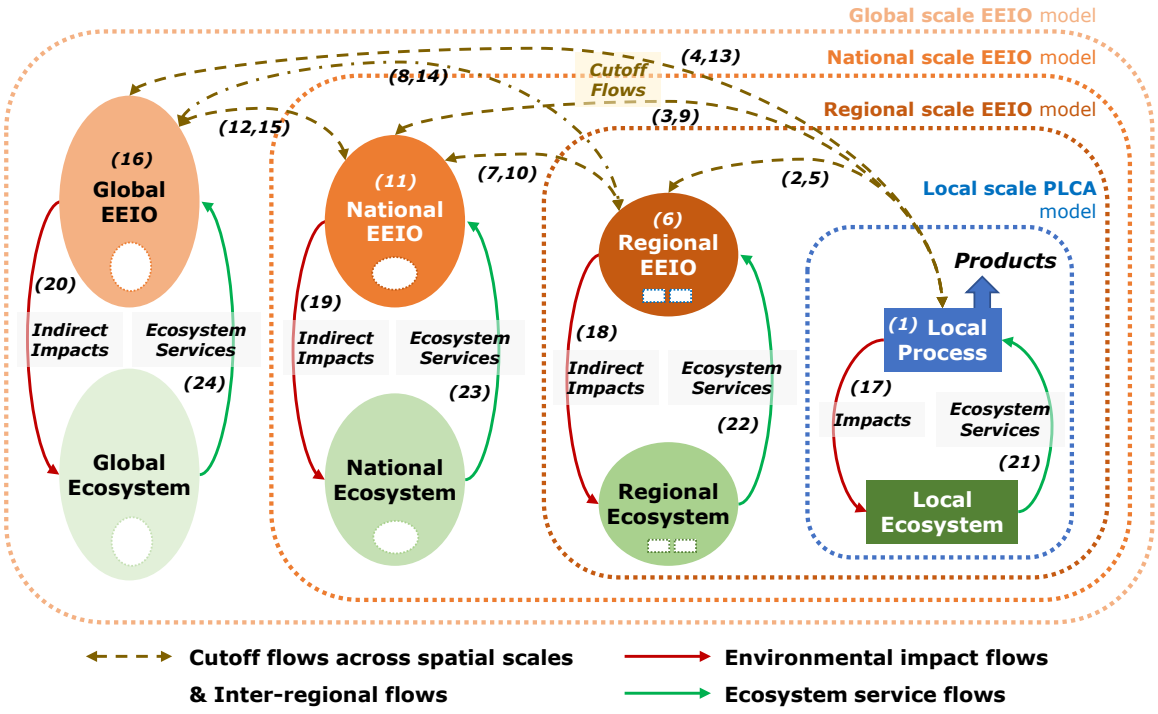

Figure 8.2: Model structure of SEA-LCA model. Any scale models could be multi-regional models if multi-regional inventory data are available. Each element in Equations 8.17, 8.35, and 8.40 is shown in italics. Management matrix is ignored from the figure by assuming that ecosystem management flows are negligible.

study scope and data availability. If multiple regions are considered, this technology matrix could be a multi-regional technology matrix.[34] Here, we define the scale of process data to be local. If any local process data are not easily available at fine scales, EEIO data can be employed to represent the complete life cycle boundary. In the literature, different scales of EEIO models are available. U.S. EPA has published the U.S. state-level multi-regional EEIO model[33] (element 6) and the national scale USEEIO model[39] (element 11). Also, global MRIO models (element 16), such as EXIOBASE,[289] are available.

Elements 2, 3, and 4 correspond to downstream cutoff flows of local scale products to the regional, national, and global economy sectors, respectively. These downstream cutoff matrices include the physical amount of local scale products that is normalized by the throughput of corresponding economy sectors. Elements 5, 9, and 13 represent upstream cutoff flows of regional, national, and global economy commodities to the local scale processes in a monetary unit, respectively.

When different scales of EEIO models are integrated, downstream and upstream cutoff flows are considered as inter-regional flows between multiple regions. For instance, when elements 11 and 16 correspond to the USEEIO model and global scale multi-regional EEIO model, respectively, elements 12 and 15 represent flows between the U.S. and global economy. Since the global scale EEIO model includes commodity transaction data in the USEEIO model, the global scale model needs to be disaggregated from the USEEIO model. Then, the disaggregated global scale EEIO model (element 16) does not have any overlaps with the USEEIO model (element 11). In other words, the disaggregated global scale EEIO model accounts for commodity transactions between countries except for the United States. In this context, elements 7, 8, 10, 12, 14, and 15 refer to the inter-regional flows between regions as well.

Disaggregation of larger scale matrices from the smaller scale matrices

When multiscale models are formulated, large scale models should be disaggregated from smaller scale models to remove overlaps between models. For example, global scale EEIO model (element 16) includes commodity transactions in the national scale EEIO model (element 11). To avoid double-counting of commodity transaction data in the national scale model, the global scale EEIO model needs to be disaggregated from the national scale EEIO model. The disaggregation of global scale direct

requirement matrix ($\overline{A}_G$) can be performed using global and national scale make ($\overline{V}_G$, $\overline{V}_N$) and use ($\overline{U}_G$, $\overline{U}_N$) matrices as shown in Equations 8.18 and 8.19.

$$\overline{V}_G^* = \overline{V}_G - (\overline{P}_{P,NG})^T \overline{V}_N (\overline{P}_{F,GN})^T - (\overline{P}_{P,NG})^T \overline{V}_{d,NG} - \overline{V}_{u,GN} (\overline{P}_{F,GN})^T, \quad (8.18)$$

$$\overline{U}_G^* = \overline{U}_G - \overline{P}_{F,GN} \overline{U}_N \overline{P}_{P,NG} - \overline{P}_{F,GN} \overline{U}_{d,NG} - \overline{U}_{u,GN} \overline{P}_{P,NG}. \quad (8.19)$$

$\overline{P}_{P,NG}$ and $\overline{P}_{F,GN}$ are permutation matrices to permute national scale sector information to the global scale sector information and permute global scale commodity information to the national scale commodity information, respectively. If the global scale multi-regional EEIO model is disaggregated from the national scale EEIO model (e.g., USEEIO[39]), $\overline{V}_N$ in Equation 8.18 represents production flows within the country of the national scale EEIO model. $\overline{V}_{d,NG}$ and $\overline{V}_{u,GN}$ correspond to the export (from national to global) and import (from global to national) production flows, respectively. The information of $\overline{V}_N$, $\overline{V}_{d,NG}$, and $\overline{V}_{u,GN}$ needs to be removed from $\overline{V}_G$ matrix to avoid double-counting of those production data.

Also, the national scale direct requirement matrix can be disaggregated from the regional scale direct requirement matrix by Equations 8.20 and 8.21.

$$\overline{V}_N^* = \overline{V}_N - (\overline{P}_{P,RN})^T \overline{V}_R (\overline{P}_{F,NR})^T - (\overline{P}_{P,RN})^T \overline{V}_{d,RN} - \overline{V}_{u,NR} (\overline{P}_{F,NR})^T, \quad (8.20)$$

$$\overline{U}_N^* = \overline{U}_N - \overline{P}_{F,NR} \overline{U}_R \overline{P}_{P,RN} - \overline{P}_{F,NR} \overline{U}_{d,RN} - \overline{U}_{u,NR} \overline{P}_{P,RN}. \quad (8.21)$$

The disaggregation of regional scale direct requirement matrix from the local scale technology matrix can be performed by Equations 8.22 and 8.23.

$$\overline{V}_R^* = \overline{V}_R - (\underline{P}_{P,LR})^T \underline{V}_L \, \underline{\hat{p}} (\underline{P}_{F,RL})^T, \quad (8.22)$$

$$\overline{U}_R^* = \overline{U}_R - \underline{P}_{F,RL} \, \underline{\hat{p}} \underline{U}_L \underline{P}_{P,LR} - \underline{P}_{F,RL} \, \underline{\hat{p}} \underline{X}_{d,LR} - \underline{X}_{u,RL} \underline{P}_{P,LR}. \quad (8.23)$$

$\underline{\hat{p}}$ is a price vector for local scale products to convert the physical information of local scale model to the monetary information. $\underline{X}_{d,LR}$ includes the information about

downstream cutoff flows of local scale products to the regional scale economy sectors in physical units. The detailed procedures about the disaggregation of direct requirement matrix from the technology matrix are described in the previous studies.[6,13] Disaggregated matrices are shown as the matrices with the asterisk sign.

Larger scale cutoff matrices also need to be disaggregated from the smaller scale cutoff matrices when overlaps of cutoff flows between different scale matrices exist. Equations 8.24 and 8.25 perform the disaggregation of national–regional scale consumption cutoff matrices ($\overline{U}_{d,RN}$ and $\overline{U}_{u,NR}$) from the national–local scale consumption cutoff matrices ($\underline{X}_{d,LN}$ and $\underline{X}_{u,NL}$).

$$\overline{U}^{*}_{d,RN} = \overline{U}_{d,RN} - \underline{P}_{F,RL}\ \underline{\hat{p}}\underline{X}_{d,LN}, \tag{8.24}$$

$$\overline{U}^{*}_{u,NR} = \overline{U}_{u,NR} - \underline{X}_{u,NL}\underline{P}_{P,LR}, \tag{8.25}$$

Also, Equations 8.26 and 8.27 perform the disaggregation of global–regional scale consumption cutoff matrices ($\overline{U}_{d,RG}$ and $\overline{U}_{u,GR}$) from the global–local scale consumption cutoff matrices ($\underline{X}_{d,LG}$ and $\underline{X}_{u,GL}$).

$$\overline{U}^{*}_{d,RG} = \overline{U}_{d,RG} - \underline{P}_{F,RL}\ \underline{\hat{p}}\underline{X}_{d,LG}, \tag{8.26}$$

$$\overline{U}^{*}_{u,GR} = \overline{U}_{u,GR} - \underline{X}_{u,GL}\underline{P}_{P,LR}, \tag{8.27}$$

The national–regional and global–regional scale production cutoff matrices ($\overline{V}_{d,RN}$, $\overline{V}_{u,NR}$, $\overline{V}_{d,RG}$, and $\overline{V}_{u,GR}$) do not need to be disaggregated from the national-local and global–local scale production cutoff matrices, respectively, since the product/commodity cutoff flows across local scale technology matrix (elements 2, 3, 4, 5, 9, and 13 in Equation 8.17) are represented only by consumption cutoff flows.

The disaggregation of global–national scale production ($\overline{V}_{d,NG}$ and $\overline{V}_{u,GN}$) and consumption ($\overline{U}_{d,NG}$ and $\overline{U}_{u,GN}$) cutoff matrices from the global–regional scale production ($\overline{V}_{d,RG}$ and $\overline{V}_{u,GR}$) and consumption cutoff matrices ($\overline{U}_{d,RG}$ and $\overline{U}_{u,GR}$) is performed by Equations 8.28–8.29 and 8.30–8.31, respectively.

$$\overline{V}^*_{d,NG} = \overline{V}_{d,NG} - (\overline{P}_{P,RN})^T \overline{V}_{d,RG}, \tag{8.28}$$

$$\overline{V}^*_{u,GN} = \overline{V}_{u,GN} - \overline{V}_{u,GR} (\overline{P}_{F,NR})^T, \tag{8.29}$$

$$\overline{U}^*_{d,NG} = \overline{U}_{d,NG} - \overline{P}_{F,NR} \overline{U}_{d,RG}, \tag{8.30}$$

$$\overline{U}^*_{u,GN} = \overline{U}_{u,GN} - \overline{U}_{u,GR} \overline{P}_{P,RN}. \tag{8.31}$$

Finally, the disaggregated make and use matrices at regional, national, and global scales from Equations 8.18–8.23 and the disaggregated production and consumption cutoff matrices from Equations 8.24–8.31 are converted to the multiscale direct requirement matrix by Equation 8.32.

$$\begin{aligned}
&\left[\begin{array}{c|c|c} \overline{U}^*_R & \overline{U}^*_{d,RN} & \overline{U}^*_{d,RG} \\ \hline \overline{U}^*_{u,NR} & \overline{U}^*_N & \overline{U}^*_{d,NG} \\ \hline \overline{U}^*_{u,GR} & \overline{U}^*_{u,GN} & \overline{U}^*_G \end{array}\right] \left\{ \left[\begin{array}{c|c|c} \overline{V}^*_R & \overline{V}_{d,RN} & \overline{V}_{d,RG} \\ \hline \overline{V}_{u,NR} & \overline{V}^*_N & \overline{V}^*_{d,NG} \\ \hline \overline{V}_{u,GR} & \overline{V}^*_{u,GN} & \overline{V}^*_G \end{array}\right]^T \right\}^{-1} \\
&= \left[\begin{array}{c|c|c} (8.23) & (8.24) & (8.26) \\ \hline (8.25) & (8.21) & (8.30) \\ \hline (8.27) & (8.31) & (8.19) \end{array}\right] \left\{ \left[\begin{array}{c|c|c} (8.22) & \overline{V}_{d,RN} & \overline{V}_{d,RG} \\ \hline \overline{V}_{u,NR} & (8.20) & (8.28) \\ \hline \overline{V}_{u,GR} & (8.29) & (8.18) \end{array}\right]^T \right\}^{-1} \\
&= \left[\begin{array}{c|c|c} \overline{A}^*_R & \overline{A}^*_{d,RN} & \overline{A}^*_{d,RG} \\ \hline \overline{A}^*_{u,NR} & \overline{A}^*_N & \overline{A}^*_{d,NG} \\ \hline \overline{A}^*_{u,GR} & \overline{A}^*_{u,GN} & \overline{A}^*_G \end{array}\right].
\end{aligned} \tag{8.32}$$

The multiscale direct requirement matrix is converted to the elements in Equation 8.17 as follows:

$$
\begin{aligned}
I - &\left[\begin{array}{c|c|c} \overline{A}^*_R & \overline{A}^*_{d,RN} & \overline{A}^*_{d,RG} \\ \hline \overline{A}^*_{u,NR} & \overline{A}^*_N & \overline{A}^*_{d,NG} \\ \hline \overline{A}^*_{u,GR} & \overline{A}^*_{u,GN} & \overline{A}^*_G \end{array}\right] \\
&= \left[\begin{array}{c|c|c} (6)\ I_R - \overline{A}^*_R & (7)\ -\overline{A}^*_{d,RN} & (8)\ -\overline{A}^*_{d,RG} \\ \hline (10)\ -\overline{A}^*_{u,NR} & (11)\ I_N - \overline{A}^*_N & (12)\ -\overline{A}^*_{d,NG} \\ \hline (14)\ -\overline{A}^*_{u,GR} & (15)\ -\overline{A}^*_{u,GN} & (16)\ I_G - \overline{A}^*_G \end{array}\right].
\end{aligned}
\tag{8.33}
$$

8.3.2 Management Matrix

Equation 8.34 shows management matrix for SEA-LCA model ($\underline{\overline{C}}_M$).

$$
\underline{\overline{C}}_M = \left[\begin{array}{c|c|c|c} \underline{C}_L & \underline{C}_{d,LR} & \underline{C}_{d,LN} & \underline{C}_{d,LG} \\ \hline \underline{C}_{u,RL} & \underline{\overline{C}}^*_R & \underline{\overline{C}}^*_{d,RN} & \underline{\overline{C}}^*_{d,RG} \\ \hline \underline{C}_{u,NL} & \underline{\overline{C}}^*_{u,NR} & \underline{\overline{C}}^*_N & \underline{\overline{C}}^*_{d,NG} \\ \hline \underline{C}_{u,GL} & \underline{\overline{C}}^*_{u,GR} & \underline{\overline{C}}^*_{u,GN} & \underline{\overline{C}}^*_G \end{array}\right]. \tag{8.34}
$$

This matrix contains information about product flows from technological processes and commodity flows from economy sectors to the ecological modules. Technological and economic inputs to the ecosystems are generally negligible. Also, such data are relatively hard to obtain. In the previous studies,[35,129] therefore, it was assumed that management matrix has zero values. When any technological or economic data for ecosystem management are identified, the management matrix includes negative values for such data. Also, if there is any overlap between management matrices at different scales, larger scale matrices need to be disaggregated from the smaller scale matrices (e.g., $\overline{C}^*_R$, $\overline{C}^*_N$, and $\overline{C}^*_G$).

Non-diagonal elements in the $\underline{\overline{C}}_M$ matrix correspond to the downstream and upstream management cutoff matrices between different spatial scales. Downstream management cutoff matrices ($\underline{C}_d$) could be non-zero and negative if products/commodities at smaller scales are used for the management of ecosystems at larger scales. Also,

if commodities at larger scales are used for the management of ecosystems at smaller scales, upstream management cutoff matrices ($\underline{C}_u$) include negative values.

8.3.3 Intervention Matrix

Equation 8.35 shows intervention matrix for SEA-LCA model ($\overline{\underline{D}}_M$).

$$\overline{\underline{D}}_M = \begin{bmatrix} (17)\ \underline{D}_L & 0 & 0 & 0 \\ 0 & (18)\ \overline{D}^*_R & 0 & 0 \\ 0 & 0 & (19)\ \overline{D}^*_N & 0 \\ 0 & 0 & 0 & (20)\ \overline{D}^*_G \end{bmatrix}. \tag{8.35}$$

For the intervention matrix, non-diagonal elements are all zeros. That is, there are no intervention cutoff flows between different scales because interventions are embedded in each of the processes and economy sectors. For example, CO_2 emissions and water consumption for fossil power plants in a certain region at a certain scale are only attributed to the power plants in that region at that scale.

Also, the disaggregation of larger scale intervention matrices from the smaller scale matrices need to be performed to avoid double-counting of smaller scale interventions. Equations 8.36–8.38 show the disaggregation of regional, national, and global scale total intervention matrices ($\overline{M}_R$, $\overline{M}_N$, and $\overline{M}_G$) from the smaller scale matrices.

$$\overline{M}^*_R = \overline{M}_R - \underline{D}_L \underline{P}_{P,LR}, \tag{8.36}$$

$$\overline{M}^*_N = \overline{M}_N - \overline{M}_R \overline{P}_{P,RN}, \tag{8.37}$$

$$\overline{M}^*_G = \overline{M}_G - \overline{M}_N \overline{P}_{P,NG}. \tag{8.38}$$

The disaggregated total intervention matrices then need to be normalized by the throughput of economy sectors as shown in Equation 8.39.

$$\begin{aligned}&\left[\begin{array}{c|c|c} \overline{M}_R^* & 0 & 0 \\ \hline 0 & \overline{M}_N^* & 0 \\ \hline 0 & 0 & \overline{M}_G^* \end{array}\right]\left[\begin{array}{c|c|c} \overline{x}_R^* & 0 & 0 \\ \hline 0 & \overline{x}_N^* & 0 \\ \hline 0 & 0 & \overline{x}_G^* \end{array}\right]^{-1} \\ &= \left[\begin{array}{c|c|c} (18)\ \overline{D}_R^* & 0 & 0 \\ \hline 0 & (19)\ \overline{D}_N^* & 0 \\ \hline 0 & 0 & (20)\ \overline{D}_G^* \end{array}\right],\end{aligned} \tag{8.39}$$

where $\overline{x}_R^*$, $\overline{x}_N^*$, and $\overline{x}_G^*$ are the throughput of regional, national, and global economy sectors that are disaggregated from the smaller scale models, respectively.

8.3.4 Ecosystem Matrix

Equation 8.40 shows ecosystem matrix for SEA-LCA model ($\underline{\overline{S}}_M$).

$$\underline{\overline{S}}_M = \left[\begin{array}{c|c|c|c} (21)\ \underline{S}_L & 0 & 0 & 0 \\ \hline 0 & (22)\ \overline{S}_R^* & 0 & 0 \\ \hline 0 & 0 & (23)\ \overline{S}_N^* & 0 \\ \hline 0 & 0 & 0 & (24)\ \overline{S}_G^* \end{array}\right]. \tag{8.40}$$

Same as the intervention matrix, non-diagonal elements in ecosystem matrix are all zeros because ecosystem services are embedded in specific ecosystem modules (e.g., forest and wetland modules) that are located in a certain region at a certain scale. Some may argue that the benefits of ecosystem services are not limited to the region and scale where ecosystem modules are located. The effective scale of ecosystem services is determined by identifying the scale of serviceshed.[232] This will be addressed in Section 8.3.5.

Also, the total supply of ecosystem services in a certain region must be allocated to specific technological processes and economy sectors in the model as described in Section 8.2.3. The allocation of ecosystem services can be performed based on the ratio of the interventions from processes and sectors. For instance, if CO_2 emissions

of fossil power plants in a certain region are 40% of the total CO_2 emissions in that region, 40% of carbon sequestration service in the region can be allocated to the fossil power plants.

The disaggregation of larger scale ecosystem matrices from the smaller scale matrices needs to be performed to remove overlaps between different scales by Equations 8.41–8.43.

$$\overline{S}_R^* = \overline{S}_R - \underline{S}_L \underline{P}_{E,LR}, \tag{8.41}$$

$$\overline{S}_N^* = \overline{S}_N - \overline{S}_R \overline{P}_{E,RN}, \tag{8.42}$$

$$\overline{S}_G^* = \overline{S}_G - \overline{S}_N \overline{P}_{E,NG}, \tag{8.43}$$

where $\underline{P}_{E,LR}$, $\overline{P}_{E,RN}$, and $\overline{P}_{E,NG}$ matrices are the permutation matrices that permute local, regional, and national scale ecosystem module information to the regional, national, and global scale ecosystem module information, respectively.

8.3.5 SEA-LCA Model Formulation

SEA-LCA model can be formulated as shown in Equation 8.44.

$$\left[\begin{array}{c:c} \overline{X}_M & \overline{C}_M \\ \hdashline \overline{D}_M & \overline{S}_M \end{array}\right] \left[\begin{array}{c} \overline{m}_M \\ \hdashline \overline{m}_{e,M} \end{array}\right] = \left[\begin{array}{c:c} (8.17) & (8.34) \\ \hdashline (8.35) & (8.40) \end{array}\right] \left[\begin{array}{c} \overline{m}_M \\ \hdashline \overline{m}_{e,M} \end{array}\right] = \left[\begin{array}{c} \overline{f}_M \\ \hdashline \overline{f}_{e,M} \end{array}\right]. \tag{8.44}$$

$\overline{m}_M$ and $\overline{f}_M$ are vectors of multiscale and multi-regional scaling factors and final demands, respectively. $\overline{m}_{e,M}$ and $\overline{f}_{e,M}$ represent vectors of multiscale and multi-regional ecosystem scaling factors and ecosystem final demands, respectively.

TES absolute sustainability indicators (V_k) for k-th flow are calculated by Equations 8.45–8.47.

$$\overline{\underline{X}}_M \overline{\underline{m}}_M + \overline{\underline{C}}_M \overline{\underline{m}}_{e,M} = \overline{\underline{f}}_M, \tag{8.45}$$

$$\overline{\underline{D}}_M \overline{\underline{m}}_M + \overline{\underline{S}}_M \overline{\underline{m}}_{e,M} = \overline{\underline{f}}_{e,m}, \tag{8.46}$$

$$V_k = \frac{-\overline{\underline{f}}_{e,M,k}}{\overline{\underline{D}}_{M,k} \overline{\underline{m}}_M}, \tag{8.47}$$

where $\overline{\underline{f}}_{e,M,k}$ and $\overline{\underline{D}}_{M,k}$ are the ecosystem final demand vector and intervention matrix for k-th flow in SEA-LCA model.

The scale of serviceshed depends on the type of ecosystem flows. For example, the serviceshed scale of climate regulation service is global, while that of air quality regulation service is regional. Therefore, TES absolute sustainability indicators also need to be calculated for each serviceshed scale ($i = L, R, N, G$) as shown in Equations 8.48–8.49.

1. Global scale serviceshed (e.g., climate regulation)

$$V_{G,k} = \frac{\sum_i^G \overline{\underline{f}}_{e,i,k}}{\sum_i^G \overline{\underline{D}}^*_{i,k} \overline{\underline{m}}_i}, \tag{8.48}$$

$$\begin{aligned}
\text{where } \sum_i^G \overline{\underline{f}}_{e,i,k} &= \overline{f}_{e,G,k} + \overline{f}_{e,N,k} + \overline{f}_{e,R,k} + \underline{f}_{e,L,k} \\
&= (\overline{D}^*_{G,k} \overline{m}_G + \overline{S}^*_{G,k} \overline{m}_{e,G}) + (\overline{D}^*_{N,k} \overline{m}_N + \overline{S}^*_{N,k} \overline{m}_{e,N}) \\
&\quad + (\overline{D}^*_{R,k} \overline{m}_R + \overline{S}^*_{R,k} \overline{m}_{e,R}) + (\underline{D}_{L,k} \underline{m}_L + \underline{S}_{L,k} \underline{m}_{e,L}).
\end{aligned}$$

2. Regional scale serviceshed (e.g., air quality regulation)

$$V_{R,k} = \frac{\sum_i^R \overline{\underline{f}}_{e,i,k}}{\sum_i^R \overline{\underline{D}}^*_{i,k} \overline{\underline{m}}_i}, \tag{8.49}$$

$$\begin{aligned}
\text{where } \sum_i^R \overline{\underline{f}}_{e,i,k} &= \overline{f}_{e,R,k} + \underline{f}_{e,L,k} \\
&= (\overline{D}^*_{R,k} \overline{m}_R + \overline{S}^*_{R,k} \overline{m}_{e,R}) + (\underline{D}_{L,k} \underline{m}_L + \underline{S}_{L,k} \underline{m}_{e,L}).
\end{aligned}$$

The vectors of ecosystem scaling factors ($\overline{\underline{m}}_e$) can be 1 by definition to calculate $\overline{\underline{f}}_e$. If $\overline{\underline{m}}_e = 1$, $\overline{\underline{S}}_M$ represents the total supply of ecosystem services in the selected region. In this case, we need to allocate the total supply of ecosystem services to specific processes and economy sectors by using weighing factors as shown in Equation 8.14. If the allocation of ecosystem services is performed based on the proportional values of corresponding demand for ecosystem services, weighting factors can be defined as shown in Equation 8.15.

Special Case of Multiscale Model Integration

Smaller scale models generally have more detailed data than larger scale models as shown in Fig. 8.3a. For example, PLCA model contains detailed process-level data, while EEIO model is based on the aggregated economy sector data. In rare cases, larger scale models contain more detailed data than the smaller scale models as shown in Figs. 8.3b and 8.3c. For example, U.S. EPA has released the USEEIO model that is based on 385 economy sectors.[39] U.S. EPA, however, has also developed the state-level multi-regional EEIO model that is based on 15 sectors for each state. These two EEIO models could potentially be integrated to utilize regional scale EEIO data with high-detailed national scale EEIO data. Since there are overlaps between two EEIO models, disaggregation procedures that are described previously need to be performed. However, in this case, the disaggregation should not be performed in the same way.

If a larger scale model has higher details (e.g., corn and soybean sectors) than the smaller scale model, the smaller scale low-detailed data (e.g., aggregated agricultural sector) need to be allocated between the corresponding high-detailed data at the

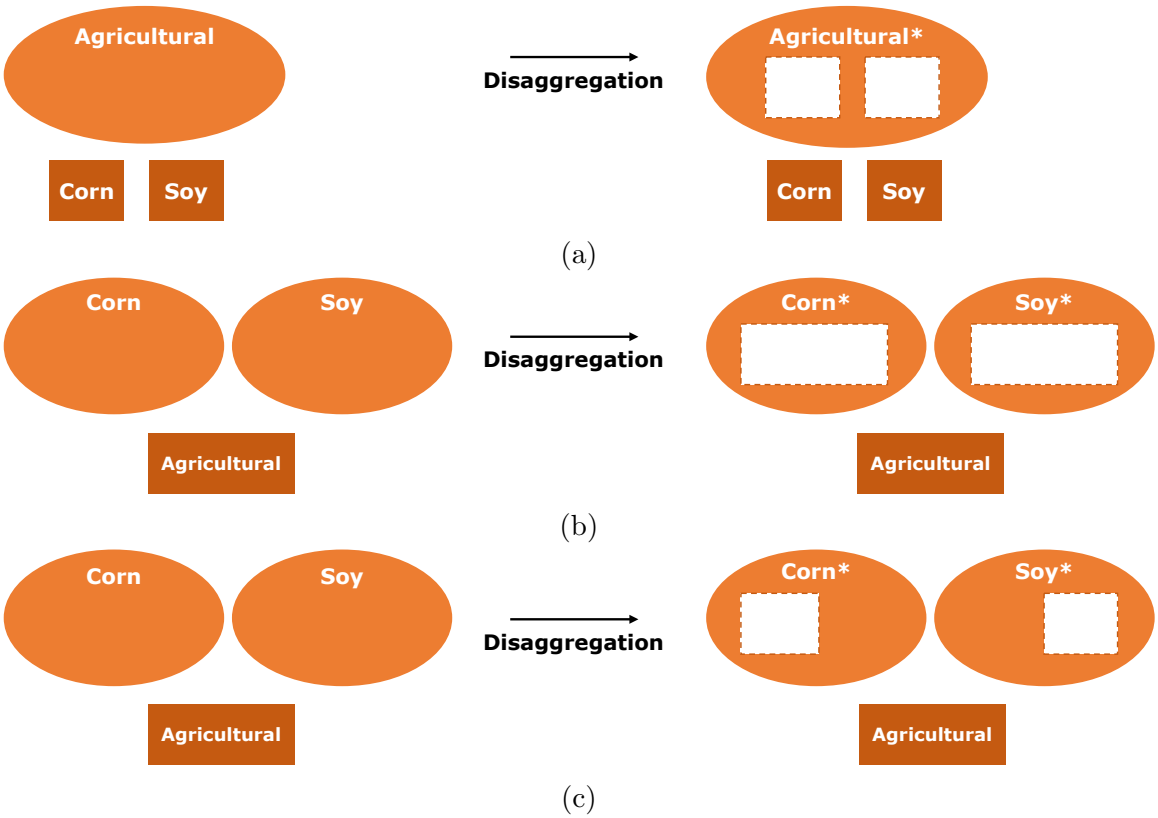

Figure 8.3: **(a)** Disaggregation of a larger scale agricultural sector from smaller scale corn and soybean sectors. **(b, c)** Disaggregation of larger scale corn and soybean sectors from a smaller scale agricultural sector **(b)** without and **(c)** with the allocation of smaller scale data. To avoid the excessive disaggregation of larger scale high-detailed data, the smaller scale low-detailed data needs to be allocated into each larger scale data.

larger scale. Otherwise, the larger scale model is disaggregated excessively as shown in Fig. 8.3b.

The allocation of low-detailed data needs to be performed whenever the low-detailed industry or commodity information is permuted to high-detailed industry or commodity information by using permutation matrices (P_P and P_F). For instance, let us consider a case where a national scale high-detailed 5×5 $\overline{V}^N$ matrix needs to be

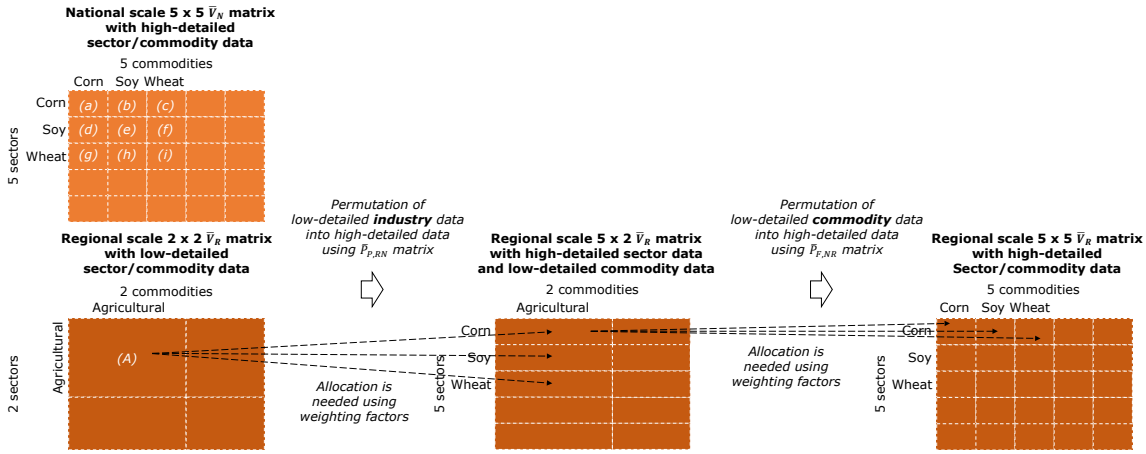

Figure 8.4: The allocation of regional scale low-detailed data into the national scale high-detailed data is needed when the regional scale data is permuted to the national scale date.

disaggregated from the regional scale low-detailed 2×2 $\overline{V}^R$ matrix as shown in Fig. 8.4. Then, we need to permute the regional scale low-detailed sector and commodity information into the high-detailed sector and commodity information at the national scale. When smaller scale low-detailed industry information is permuted into larger scale high-detailed industry information, the allocation of low-detailed agricultural data (A) into corn, soybeans, and wheat sectors can be performed as follows.

$$\begin{aligned}
\text{Agricultural} \;\rightarrow\; \text{Corn sector:} &\qquad A \times \frac{a+b+c}{a+b+\cdots+i}, \\
\text{Agricultural} \;\rightarrow\; \text{Soybean sector:} &\qquad A \times \frac{d+e+f}{a+b+\cdots+i}, \\
\text{Agricultural} \;\rightarrow\; \text{Wheat sector:} &\qquad A \times \frac{g+h+i}{a+b+\cdots+i}.
\end{aligned}$$

The fractional parts (e.g., $\frac{a+b+c}{a+b+\cdots+i}$) correspond to the weighting factors for regional scale data permuted using $\overline{P}_{P,RN}$. The excessive disaggregation of national scale data can be avoided through the allocation of regional data using the weighting factors.

More generally, the weighting factors ($W_{\overline{V}_R}$) for industry-permuted regional scale $\overline{V}_R$ matrix can be formulated by Equation 8.50.

$$W_{\overline{V}_R} = \frac{\overline{V}_N \overline{P}_{F,NR}}{(\overline{P}_{P,RN})^T \overline{P}_{P,RN} \overline{V}_N \overline{P}_{F,NR}}. \tag{8.50}$$

The numerator term represents the national scale industry outputs from high-detailed sectors with respect to each low-detailed commodity (e.g., $a+b+c$ in Fig. 8.4). The denominator term corresponds to the national scale aggregated industry outputs from aggregated sectors with respect to each low-detailed commodity (e.g., $a+b+\cdots+i$ in Fig. 8.4).

After permuting the regional scale sector information of $\overline{V}_R$ matrix into the national scale information, the regional scale commodity information of $\overline{V}_R$ matrix also needs to be permuted into the national scale information. The additional allocation is needed using another set of weighting factors to avoid the excessive disaggregation of $\overline{V}_N$. For the case shown in Fig. 8.4, the additional allocation can be performed as follows.

$$\begin{aligned}
&\text{Agricultural} \rightarrow \text{Corn commodity:} && \left(A \times \frac{a+b+c}{a+b+\cdots+i}\right) \times \frac{a}{a+b+c}, \\
&\text{Agricultural} \rightarrow \text{Soybean commodity:} && \left(A \times \frac{a+b+c}{a+b+\cdots+i}\right) \times \frac{b}{a+b+c}, \\
&\text{Agricultural} \rightarrow \text{Wheat commodity:} && \left(A \times \frac{a+b+c}{a+b+\cdots+i}\right) \times \frac{c}{a+b+c}.
\end{aligned}$$

The last fractional parts (e.g., $\frac{a}{a+b+c}$) correspond to the weighting factors ($W'_{\overline{V}_R}$) for the additional allocation of regional scale data permuted using $\overline{P}_{F,NR}$. These weighting factors can be formulated by Equation 8.51.

$$W'_{\overline{V}_R} = \frac{\overline{V}_N}{\overline{V}_N \overline{P}_{F,NR} (\overline{P}_{F,NR})^T}. \tag{8.51}$$

$W'_{\overline{V}_R}$ can also be used for national–regional scale upstream cutoff matrix ($\overline{V}_{u,NR}$) when its regional scale commodity information is permuted into national scale commodity information. Also, weighting factors ($W''_{\overline{V}_R}$) for national–regional scale downstream cutoff matrix ($\overline{V}_{d,RN}$) when its regional scale industry information is permuted into national scale industry information are shown in Equation 8.52.

$$W''_{\overline{V}_R} = \frac{\overline{V}_N}{(\overline{P}_{P,RN})^T \overline{P}_{P,RN} \overline{V}_N}. \tag{8.52}$$

The weighting factors for $\overline{U}_R$ and $\overline{M}_R$ matrices when their regional scale industry or commodity information is permuted into national scale information can also be formulated in a similar way by Equations 8.53–8.55 and 8.56, respectively.

$$W_{\overline{U}_R} = \frac{\overline{U}_N (\overline{P}_{P,RN})^T}{\overline{P}_{F,NR} (\overline{P}_{F,NR})^T \overline{U}_N (\overline{P}_{P,RN})^T}, \tag{8.53}$$

$$W'_{\overline{U}_R} = \frac{\overline{U}_N}{\overline{U}_N (\overline{P}_{P,RN})^T \overline{P}_{P,RN}}, \tag{8.54}$$

$$W''_{\overline{U}_R} = \frac{\overline{U}_N}{\overline{P}_{F,NR} (\overline{P}_{F,NR})^T \overline{U}_N}, \tag{8.55}$$

$$W_{\overline{M}_R} = \frac{\overline{M}_N}{\overline{M}_N (\overline{P}_{P,RN})^T \overline{P}_{P,RN}}. \tag{8.56}$$

Accordingly, if the USEEIO model (385 sectors) needs to be disaggregated from the U.S. state-level multi-regional EEIO mdoel (15 sectors for 51 regions), Equations 8.20, 8.21, and 8.37 need to be modified using weighting factors ($W_{\overline{V}_R}$, $W'_{\overline{V}_R}$, $W''_{\overline{V}_R}$, $W_{\overline{U}_R}$, $W'_{\overline{U}_R}$, $W''_{\overline{U}_R}$, and $W_{\overline{M}_R}$) as follows.

$$\begin{aligned} \overline{V}^*_N =& \overline{V}_N - [\{W_{\overline{V}_R} \circ ((\overline{P}_{P,RN})^T \overline{V}_R)\}(\overline{P}_{F,NR})^T] \circ W'_{\overline{V}_R} \\ & - W''_{\overline{V}_R} \circ ((\overline{P}_{P,RN})^T \overline{V}_{d,RN}) - (\overline{V}_{u,NR} (\overline{P}_{F,NR})^T) \circ W'_{\overline{V}_R}, \end{aligned} \tag{8.57}$$

$$\begin{aligned} \overline{U}^*_N =& \overline{U}_N - [\{W_{\overline{U}_R} \circ (\overline{P}_{F,NR} \overline{U}_R)\} \overline{P}_{P,RN}] \circ W'_{\overline{U}_R} \\ & - W''_{\overline{U}_R} \circ (\overline{P}_{F,NR} \overline{U}_{d,RN}) - (\overline{U}_{u,NR} \overline{P}_{P,RN}) \circ W'_{\overline{U}_R}, \end{aligned} \tag{8.58}$$

$$\overline{M}^*_N = \overline{M}_N - (\overline{M}_R \overline{P}_{P,RN}) \circ W_{\overline{M}_R}. \tag{8.59}$$

Figure 8.5: Great Lakes study region.

8.4 Case Study: Farming in the Great Lakes Region

A case study is conducted to investigate the spatially-explicit absolute sustainability of county-level farming activities (corn and soybean production) in the GL region (Fig. 8.5), which includes five U.S. Midwest states: Illinois, Indiana, Michigan, Ohio, and Wisconsin. We focus on GHG emission indicators in 2012. The year 2012 is selected due to the availability of data. In this case study, SEA-LCA model consists of three spatial scale data: national scale U.S. EEIO data, regional scale state-level multi-regional EEIO data, and local scale county-level PLCA data. Also, data for ecosystem services are collected for each spatial scale. Figure 8.6 shows a model structure of the SEA-LCA model for this case study.

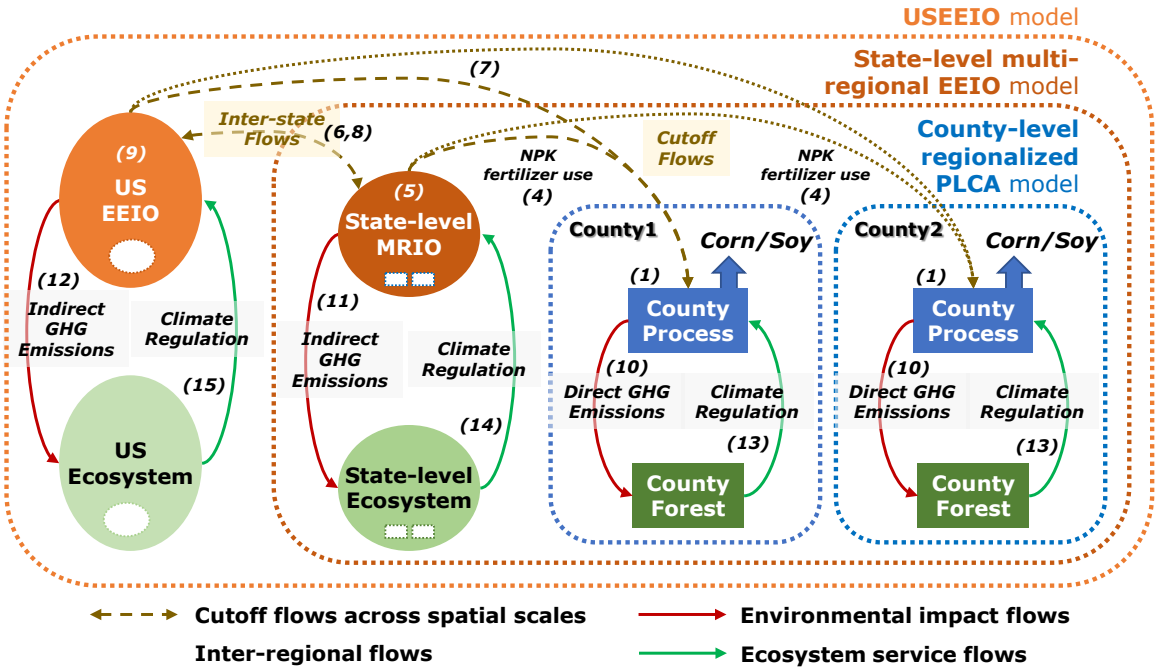

Figure 8.6: Model structure of SEA-LCA model for the case study. Each element in Equations 8.62–8.64 is shown in italics.

8.4.1 Multiscale and Multi-Regional Model Construction

The USEEIO model[39] is used for the national scale EEIO model. This model is based on 385 economy sectors for the 2007 U.S. economy and includes various environmental data. Since a more recent IO data is available from the U.S. BEA website,[44] we modify the USEEIO model using detailed IO data for the 2012 U.S. economy. Procedures for updating the USEEIO model are as follows:

1. According to the 2012 BEA IO data, the number of industries (405 industries) is larger than the number of commodities (402 commodities). Therefore, 405 industries of the 2012 IO data are adjusted to 401 industries. For example,

sectors for "S00101 federal electric utilities" and "S00102 other federal government enterprises' are aggregated into one sector. The number of industries after adjustment (401 industries) is smaller than the number of commodities (402 commodities) since the commodity data includes "S00401 scrap" commodity, which will be adjusted later.

2. BEA has updated classifications for some commodities and sectors in November 2018.[290] The updated BEA IO table has data for 402 commodities and 401 sectors. The USEEIO model, on the other hand, has data for 386 commodities and 385 sectors. The additional adjustment is performed to convert the BEA IO data for 402 commodities and 401 industries to the IO data for 386 commodities and 385 industries.

3. Scrap adjustment is performed as described in the BEA report.[148] The scrap-adjusted IO data has data for 385 industries and 385 commodities.

4. Intervention matrix ($\overline{D}_N$) in the USEEIO model is calculated using the 2007 BEA IO data and the 2013 total intervention data ($\overline{M}_N$). Therefore, the intervention matrix (intervention coefficients, $\overline{D}_N$) also needs to be updated using the 2012 BEA IO data by Equations 8.60 and 8.61.

$$\overline{M}_N = \overline{D}_N \hat{\overline{x}}_N, \tag{8.60}$$

$$\overline{D}'_N = \overline{M}_N \hat{\overline{x}}'^{-1}_N, \tag{8.61}$$

where $\hat{\overline{x}}_N$ and $\hat{\overline{x}}'_N$ are diagonalized vectors for the throughput of 2007 and 2012 economy sectors, respectively. $\overline{D}'_N$ represents the updated intervention matrix using the 2012 BEA IO data.

Also, national scale data for the supply of climate regulation service are obtained from EPA's GHG Inventory report.[47]

In this case study, regional scale EEIO data for five states are obtained from the state-level U.S. multi-regional EEIO model.[33] The model includes intra- and inter-state commodity transaction data between 15 sectors in each state. Also, state-level data for GHG emissions and climate regulation service are obtained from WRI's CAIT Climate Data Explorer database.[48] National scale data are disaggregated from the state-level data by using Equations 8.42, 8.57, 8.58, and 8.59.

Cutoff flows between national and regional scale models are identified from the state-level U.S. multi-regional EEIO model. Since the state-level EEIO model has inter-state transaction data between 51 regions (50 states and District of Columbia), inter-regional flows between five states and the rest of the U.S. can be obtained from the state-level EEIO model. The USEEIO model is based on high-detailed 385 sectors, while the state-level EEIO model is based on low-detailed 15 sectors. Therefore, the permutation of low-detailed industry and commodity information of the state-level EEIO model into the high-detailed information of the USEEIO model is needed. The allocation of state-level low-detailed data into the national scale high-detailed data needs to be performed as described in Section 8.3.5.

County-level corn and soybean production data are obtained from USDA's NASS Quick Stats database.[291] Since the USEEIO and state-level EEIO models represent the 2012 U.S. economy, the 2012 production data are obtained. State-level price data for corn and soybeans are obtained from the NASS Quick Stats database as well.[291] Price data are needed to disaggregate the state-level EEIO model from the county-level PLCA model as shown in Equations 8.22 and 8.23.

For corn and soybean production, nitrogen, phosphorus, and potassium (NPK) fertilizers are needed. Since it is difficult to identify county-level fertilizer production process data, fertilizer consumption flows are included in the SEA-LCA model as national–local and regional–local upstream cutoff flows. County-level data for NPK fertilizer consumption are estimated using data from the NASS Quick Stats database[291] and USDA's ERS database[292] as follows.

1. USDA's NASS Quick Stats database provides county-level data for the harvested area of corn and soybeans in acres (A).

2. USDA's ERS database provides state-level data for NPK fertilizers applied for corn and soybean farming in acre% (B) and lb/acre (C).

3. USDA's ERS database provides national average NPK fertilizer price data (D).

4. The monetary amount of NPK fertilizers applied for corn and soybean production in each county (E) is estimated by $E = A \times B \times C \times D$.

Also, to identify the origin state of fertilizer production for farming, state-level data for fertilizer transportation are obtained from BTS's Commodity Flow Survey (CFS) database.[1] National–local scale fertilizer upstream cutoff flows include regional–local scale fertilizer upstream cutoff flows. The disaggregation of national–local scale upstream cutoff matrix is performed by using Equation 8.25.

County-level GHG emissions from corn and soybean production are estimated from national average data[42] since county-level GHG emission data for farming are not readily available. Also, county-level data for climate regulation service from forests are obtained from i-Tree County Benefits tool.[293] The disaggregation of regional scale

state-level intervention and ecosystem data from the local scale county-level data are performed as shown in Equations 8.36 and 8.41, respectively.

8.4.2 Mathematical Formulation

Equation 8.62 represents multiscale and multi-regional transaction matrix of SEA-LCA model in this case study.

$$\overline{\underline{X}}_M = \left[\begin{array}{ccc:ccc:c} (1)\ \underline{X}_{L_{11}} & \cdots & 0 & (2)\ 0 & \cdots & 0 & (3)\ 0 \\ \vdots & \ddots & \vdots & \vdots & \ddots & \vdots & \vdots \\ 0 & \cdots & \underline{X}_{L_{cc}} & 0 & \cdots & 0 & 0 \\ \hdashline (4)\ -\underline{X}_{u,R_1L_1} & \cdots & -\underline{X}_{u,R_1L_c} & (5)\ I-\overline{\underline{A}}^*_{R_{11}} & \cdots & -\overline{\underline{A}}^*_{R_{1s}} & (6)\ -\overline{\underline{A}}_{d,R_1N} \\ \vdots & \ddots & \vdots & \vdots & \ddots & \vdots & \vdots \\ -\underline{X}_{u,R_sL1} & \cdots & -\underline{X}_{u,R_sL_c} & -\overline{\underline{A}}^*_{R_{s1}} & \cdots & I-\overline{\underline{A}}^*_{R_{ss}} & -\overline{\underline{A}}_{d_{R_s}N} \\ \hdashline (7)\ -\underline{X}_{u,NL_1} & \cdots & -\underline{X}_{u,NL_c} & (8)\ -\overline{\underline{A}}^*_{u,NR_1} & \cdots & -\overline{\underline{A}}^*_{u,NR_s} & (9)\ I-\overline{\underline{A}}^*_N \end{array}\right], \tag{8.62}$$

where subscripts $1, \cdots, c$ in element 1 and $1, \cdots, s$ in element 5 correspond to each county and each state in the GL region, respectively. For instance, $\underline{X}_{u,R_1L_1}$ matrix in element 4 includes data for upstream cutoff flows from state 1 at the regional scale to county 1 at the local scale. Each element in Equation 8.62 is shown in italics in Fig. 8.6. Elements 1, 5, and 9 correspond to local scale county-level regionalized technology, regional scale state-level multi-regional transaction, and national scale transaction matrices, respectively. Non-diagonal components in element 1 are zeros because there are no transaction flows between county-level corn and soybean processes in this case study. Also, elements 4, 7, and 8 refer to regional–local, national–local, and national–regional scale upstream cutoff flows, respectively. Elements 2, 3, and 6 are regional–local, national–local, and national–regional scale downstream cutoff flows, respectively. Values in elements 2 and 3 are all zeros because there are

no downstream cutoff flows of county-level corn and soybean products considered in this case study.

Ecosystem management flows are not considered in this case study, and therefore, $\overline{C}_M = 0$. Also, $\overline{D}_M$ and $\overline{S}_M$ matrices are formulated as shown in Equations 8.63 and 8.64, respectively.

$$\overline{D}_M = \left[\begin{array}{ccc|ccc|c} (10)\ \underline{D}_{L_1} & \cdots & \underline{D}_{L_c} & (11)\ \overline{D}^*_{R_1} & \cdots & \overline{D}^*_{R_s} & (12)\ \overline{D}^*_N \end{array} \right], \tag{8.63}$$

$$\overline{S}_M = \left[\begin{array}{ccc|ccc|c} (13)\ \underline{S}_{L_1} & \cdots & \underline{S}_{L_c} & (14)\ \overline{S}^*_{R_1} & \cdots & \overline{S}^*_{R_s} & (15)\ \overline{S}^*_N \end{array} \right]. \tag{8.64}$$

$\overline{S}_M$ represents the total supply of ecosystem services in each region at each scale. As described in Section 8.3.4, $\overline{S}_M$ needs to be allocated to processes and sectors in the model. In this case study, the allocation of ecosystem services is performed using weighting factors, which are based on the ratio of GHG emissions from relevant processes and sectors in a certain region to the total GHG emissions from every activity in that region. The weighting factors for each scale can be formulated by Equations 8.65–8.67.

$$\overline{W}_N = \frac{\overline{D}^*_N}{\overline{M}^*_N}, \tag{8.65}$$

$$\overline{W}_{R_i} = \frac{\overline{D}^*_{R_i} + \sum_{L_j \in R_i} \underline{D}_{L_j}}{\overline{M}_{R_i}}, \tag{8.66}$$

$$\underline{W}_{L_j} = \overline{W}_{R_i} \text{ such that } L_j \in R_i, \tag{8.67}$$

$$\text{where } i = 1, 2, \cdots, s, \text{ and } j = 1, 2, \cdots, c.$$

i and j are each state and each county in the GL region, respectively. Numerators of the equations correspond to the GHG emissions from processes and sectors in each region. For example, $\overline{D}^*_N$ in Equation 8.65 is the indirect GHG emissions from the national scale sectors outside the GL region. $\overline{D}^*_{R_i}$ and $\sum_{j \in i} \underline{D}_{L_j}$ in Equation 8.66

represent the GHG emissions from regional scale sectors and local scale processes in i-th state, respectively. The sum of those two terms corresponds to the total GHG emissions from corn and soybean production in i-th state. Denominators of the equations correspond to the total GHG emissions from every activity in each region. For instance, $\overline{M}_N^*$ and $\overline{M}_{R_i}$ are the total GHG emissions from every activity outside the GL region and in i-th state, respectively. The weighting factor for j-th county ($\underline{W}_{L_j}$) is the same as the weighting factor for i-th state ($\overline{W}_{R_i}$) if j-th county is a part of i-state. This is because we do not know the total GHG emissions from every activity in each county at this point. Therefore, we cannot calculate the weighting factors for each county.

The allocated supply of ecosystem services is calculated by Equation 8.68.

$$\underline{\tilde{\overline{S}}}_M = \underline{\overline{S}}_M \circ \left[\begin{array}{ccc|ccc|c} \underline{W}_{L_1} & \cdots & \underline{W}_{L_c} & \overline{W}_{R_1} & \cdots & \overline{W}_{R_s} & \overline{W}_N \end{array} \right], \tag{8.68}$$

where $\underline{\tilde{\overline{S}}}_M$ is the allocated supply of ecosystem services. Accordingly, the total demand ($\underline{\overline{D}}_M \ \underline{\overline{m}}_M$) and supply ($\underline{\tilde{\overline{S}}}_{e,M} \ \underline{\overline{m}}_{e,M}$) of ecosystem services with respect to corn and soybean production in the GL region are calculated from Equation 8.69.

$$\left[\begin{array}{c|c} \underline{\overline{X}}_M & 0 \\ \hline \underline{\overline{D}}_M & \underline{\tilde{\overline{S}}}_M \end{array} \right] \left[\begin{array}{c} \underline{\overline{m}}_M \\ \hline 1 \end{array} \right] = \left[\begin{array}{c} \underline{\overline{f}}_M \\ \hline \underline{\overline{f}}_{e,M} \end{array} \right], \tag{8.69}$$

where the final demand vector ($\underline{\overline{f}}_M$) corresponds to the corn and soybean production in each county. Scaling factors for each process and sector ($\underline{\overline{m}}_M$) are calculated from Equation 8.69. Then, ecosystem final demands ($\underline{\overline{f}}_{e,M}$) are calculated. The serviceshed scale of climate regulation service is global. Since the global scale model is not considered in this case study, national scale life cycle TES absolute CO_2 indicators are calculated for each county's corn and soybean production in the GL region using

Equation 8.70.

$$V_{N,GHG} = \frac{\sum_i^N \overline{f}_{e,i,GHG}}{\sum_i^N \overline{D}^*_{i,GHG}\overline{m}_i}, \tag{8.70}$$

$$\text{where } \sum_i^N \overline{f}_{e,i,GHG} = \overline{f}_{e,N,GHG} + \overline{f}_{e,R,GHG} + \underline{f}_{e,L,GHG}$$

$$= (\overline{D}^*_{N,GHG}\overline{m}_N + \overline{\tilde{S}}^*_{N,GHG}) + (\overline{D}^*_{R,GHG}\overline{m}_R + \overline{\tilde{S}}*_{R,GHG}) + (\underline{D}_{L,GHG}\underline{m}_L + \underline{\tilde{S}}_{L,GHG}).$$

If regional scale state-level and local scale county-level indicators need to be known, the indicators can be calculated by Equations 8.71 and 8.72, respectively.

$$V_{R,GHG} = \frac{\sum_i^R \overline{f}_{e,i,GHG}}{\sum_i^R \overline{D}^*_{i,GHG}\overline{m}_i}, \tag{8.71}$$

$$\text{where } \sum_i^R \overline{f}_{e,i,GHG} = \overline{f}_{e,R,GHG} + \underline{f}_{e,L,GHG}$$

$$= (\overline{D}^*_{R,GHG}\overline{m}_R + \overline{\tilde{S}}*_{R,GHG}) + (\underline{D}_{L,GHG}\underline{m}_L + \underline{\tilde{S}}_{L,GHG}),$$

$$V_{L,GHG} = \frac{\underline{f}_{e,L,GHG}}{\underline{D}^*_{L,GHG}\underline{m}_L}, \tag{8.72}$$

$$\text{where } \underline{f}_{e,L,GHG} = (\underline{D}_{L,GHG}\underline{m}_L + \underline{\tilde{S}}_{L,GHG}).$$

In this case study, Python v3.7 is used to construct the SEA-LCA model. All the codes for the procedures and mathematical formulation described above can be available upon request.

8.4.3 Results and Discussion

Spatial Scale of Sustainability Assessment

Multiscale and multi-regional SEA-LCA model developed in this case study integrates various models such as regionalized PLCA, state-level multi-regional EEIO, and national scale EEIO. The integrated model can calculate spatially-explicit absolute sustainability indicators for various regions and scales. This is useful because

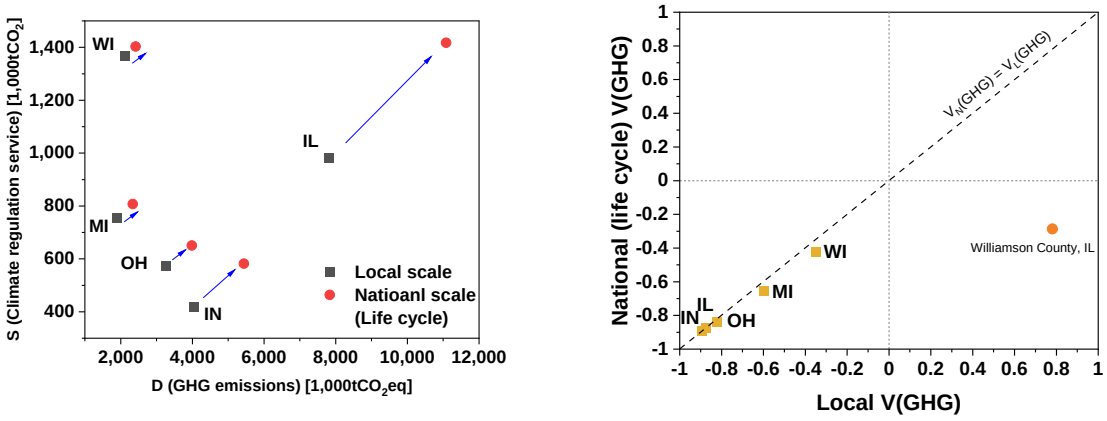

(a) (b)

Figure 8.7: **(a)** Local and national scale demand and supply of climate regulation service and **(b)** TES absolute sustainability indicators with respect to climate regulation service for corn and soybean production in the Great Lakes region. National scale values correspond to the life cycle values.

different serviceshed scales need to be considered for each type of ecosystem service. For example, calculating global scale indicators is appropriate for climate regulation service since its serviceshed scale is global. However, depending on the scope of study and stakeholder's interests, various scale and region's sustainability indicators could still need to be calculated.

Figure 8.7a exhibits the local and national scale demand and supply of climate regulation service with respect to corn and soybean production in the GL region. National scale values correspond to the life cycle values. The local scale demand for climate regulation service corresponds to the direct GHG emissions from corn and soybean production in the GL region, while the national scale life cycle demand represents the total GHG emissions from corn and soybean production across regions and scales. Also, the local scale supply of climate regulation service refers to the

supply, which is from local scale forests and allocated to local scale corn and soybean production activities, while the national scale life cycle supply corresponds to the total supply, which is allocated to relevant activities across spatial scales to the corn and soybean production. Since the SEA-LCA model includes regionalized process and EEIO data, GHG emissions and their corresponding climate regulation service can be calculated for each county and state. Also, farming in each county requires the different amount of NPK fertilizers, and the supply chain data for the fertilizers vary with states. Therefore, national scale life cycle values depend on region-specific data for fertilizer consumption and fertilizer supply chains.

Illinois has larger total GHG emissions at both local and national scales than other states in the GL region because corn and soybean production in Illinois is the largest among the five states as shown in Figs. 8.8a and 8.8b. On the other hand, Wisconsin has a much larger local scale supply of climate regulation service than other states. This is because Wisconsin has a huge supply of carbon sequestration service from forests at the local scale compared to the other states as shown in Fig. 8.8c.

Each state's total GHG emissions and climate regulation service at the national scale are larger than those at the local scale since indirect GHG emissions and carbon sequestration service across scales are included in the national scale life cycle values. The national scale life cycle demand and supply values for Illinois are particularly larger than the local scale demand and supply values. This implies that Illinois has regional and national scale supply chain networks that have larger impacts than other states.

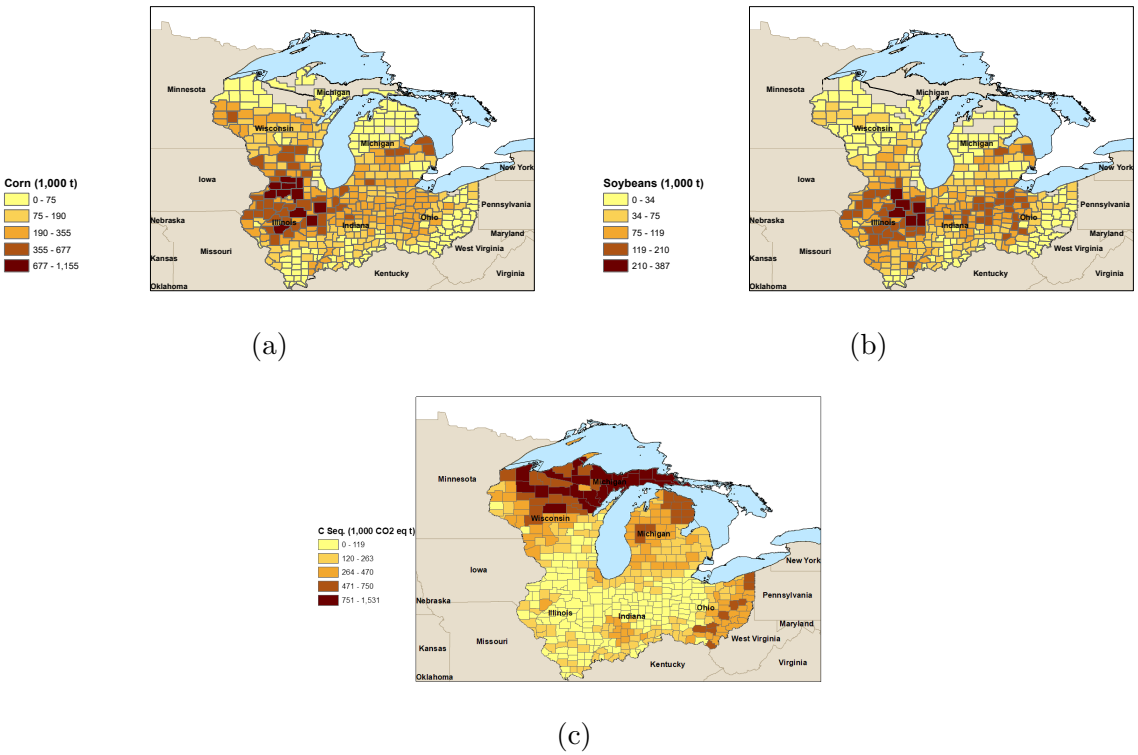

Figure 8.8: **(a)** Corn and **(b)** soybean production in each county of the Great Lakes region in 2012. **(c)** The supply of carbon sequestration service from forests in each county of the Great Lakes region.

National and local scale TES absolute sustainability indicators with respect to climate regulation service are shown in Fig. 8.7b. The national scale life cycle indicators for Michigan and Wisconsin are smaller than their local scale indicators, whereas the national and local scale indicators are similar to each other for the other three states. Depending on the location, differences between national and local scale indicators could be large. For instance, the national and local scale indicators for corn and soybean production in Williamson County, IL are -0.29 (unsustainable)

and 0.78 (sustainable), respectively, as shown in Fig. 8.7b. This is because the monetary amount of fertilizers applied for a unit amount of corn production in Williamson County ($171/t-corn) is much larger than Illinois's average ($55/t-corn) and the GL region's average ($47/t-corn). Thus, the indirect GHG emissions from regional and national scale supply chain activities for Williamson County's corn production are large. These results highlight the importance of accounting for the proper spatial scale when assessing the absolute sustainability of activities.

Spatially-Explicit Emission and Ecosystem Service Intensities

Figures 8.9a and 8.9b show the intensities of national scale life cycle GHG emissions and climate regulation service for corn production in each county of the GL region. The intensity values are calculated by normalizing values of national scale life cycle GHG emissions and climate regulation service for corn production in each county by the amount of corn production in each county. Given that the national average direct GHG emission intensity value is employed for every county's corn production in the GL region, spatially-varying emission intensity results are attributed to the different supply chain networks by states. Some counties do not have intensity values since there are no corn and soybean production activities as indicated in Figs 8.8a and 8.8b. Counties in Illinois have larger GHG emission intensities than other regions. These results indicate that those counties have less sustainable supply chain networks than the other regions. In this case study, NPK fertilizer consumption flows are considered as the upstream cutoff flows from the regional and national scale economy to the local scale farming activities. Thus, indirect GHG emissions from manufacturing NPK fertilizers are attributed to data from the state-level multi-regional EEIO model and the USEEIO model. Table 8.2 exhibits the GHG emission

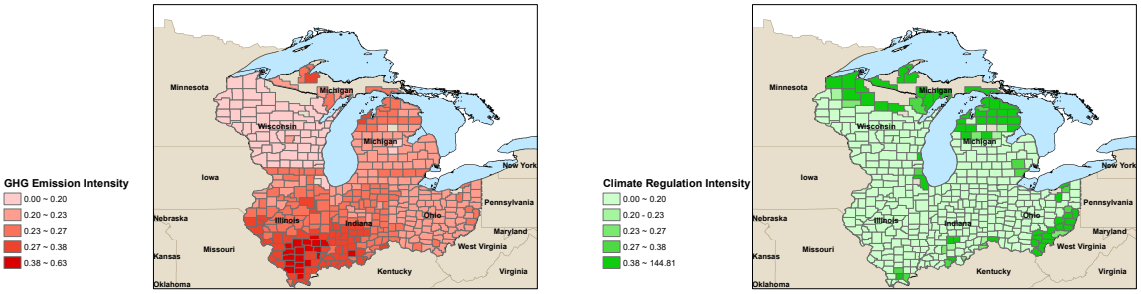

(a) (b)

Figure 8.9: Intensities of national scale life cycle **(a)** GHG emissions and **(b)** climate regulation service (gCO_2eq/g-Corn).

intensities for fertilizer production by regions. Among the five states in the GL region, fertilizer production in Illinois has the lowest emission intensity. Fertilizer production outside the GL region has a higher emission intensity than the states in the GL region. As shown in Table 8.2, 82% of NPK fertilizers for corn production in Illinois are produced outside the GL region, while only 12% of fertilizers are provided from Illinois. If more fertilizers could be produced in Illinois and used for corn production, Illinois' GHG emission intensities for corn production could be significantly lower.

According to Fig. 8.9a, Wisconsin has relatively lower GHG emission intensities for corn production than other regions. This is because almost half of the fertilizers needed for corn production in Wisconsin come from Illinois which has the lowest emission intensity for fertilizer production as indicated in Table 8.2.

With respect to the intensities of climate regulation service, counties in northern Wisconsin, northern Michigan, and southeastern Ohio have larger intensities than other regions. As shown in Fig. 8.8c, those areas have a large supply of climate regulation service from forests. Climate regulation service is provided not only from

forests but also from other types of land areas such as grasslands, wetlands, and farmlands, etc. The supply of climate regulation service by other types of land areas is included in the model at the regional scale as indicated in Fig. 8.6. In the GL region, 99.7% of climate regulation service is provided from forests, and the rest of 0.3% is provided from other types of land areas. Therefore, the reforestation of available land areas could be a very effective solution to improve the absolute sustainability indicators with respect to climate regulation service.

In this case study, the state-level multi-regional EEIO model for the GL region is based on low-detailed 15 sectors for each state. In the state-level EEIO model, fertilizer production is part of the aggregated "31G manufacturing" sector. On the other hand, the USEEIO model is based on high-detailed 385 sectors, which include "325310 fertilizer manufacturing" sector. That is, the USEEIO model is superior to the state-level EEIO model with respect to the details of sector data. However, the USEEIO model is based on the national average sector data, while the state-level

Table 8.2: GHG emission intensities for NPK fertilizer production in each region and the share of fertilizer supply chain regions for corn production in each state of the Great Lakes region. †State-level data for fertilizer transportation are obtained from CFS database.[1] ‡There is no fertilizer production in Wisconsin.

Region of NPK fertilizer production	**Emission intensity for fertilizer production [$kgCO_2eq/\$$]**	**Share of fertilizer supply chain regions for corn production in each state†**				
		Illinois	**Indiana**	**Michigan**	**Ohio**	**Wisconsin**
Illinois	0.51	12%	0%	0%	0%	44%
Indiana	1.42	0%	0%	0%	0%	0%
Michigan	0.88	0%	0%	2%	1%	0%
Ohio	0.95	6%	45%	41%	62%	28%
Wisconsin‡	-	-	-	-	-	-
Rest of the U.S.	1.97	82%	55%	56%	37%	28%

EEIO model has state-specific sector data. Therefore, there is a need for developing a high-detailed and multi-regional EEIO model for a more robust state-level spatially-explicit study.

Spatially-Explicit Absolute Sustainability Assessment

Figure 8.10 shows national scale life cycle spatially-explicit absolute CO_2 indicators ($V_{N,GHG}$) with respect to corn and soybean production in each county. Total GHG emissions and climate regulation service with respect corn and soybean production are shown as bar plots for each county. Many counties in Ohio, Indiana, and Illinois show negative $V_{N,GHG}$ indicators due to large total GHG emissions from corn and soybean production in these regions. On the other hand, $V_{N,GHG}$ indicators of counties in northern Wisconsin, northern Michigan, and southeastern Ohio are positive not only because there are no many farming activities in those counties, but also because the supply of climate regulation service in those counties is larger than other regions.

Depending on the scope of study and stakeholder's interests, local scale sustainability indicators might need to be investigated. Figure 8.11 exhibits local scale spatially-explicit absolute CO_2 indicators ($V_{L,GHG}$) with respect to corn and soybean production in each county. Differences between national and local scale indicators are identified for some counties since national scale life cycle results include indirect GHG emissions and climate regulation services at regional and national scales.

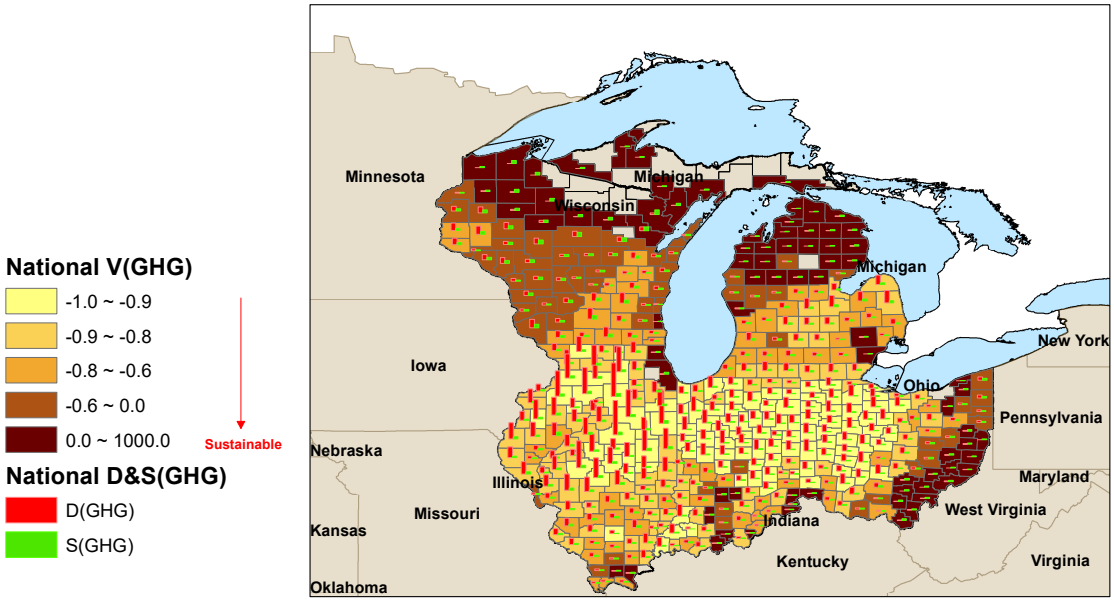

Figure 8.10: National scale life cycle spatially-explicit absolute CO_2 indicators (V^N_{GHG}) with respect to corn and soybean production in the Great Lakes region.

8.5 Conclusions

To best inform sustainability assessment outcomes, a sustainability assessment framework needs to account for regional heterogeneity since activities and their impacts vary with regions. Also, we need to assess the impacts not only from the local scale activities but also from the national and global scale economy while considering inter-regional flows. Moreover, the absolute sustainability of activities needs to be assessed by accounting for the supply of ecosystem services, which also vary with regions. This allows us to identify the opportunities for improvement from both reducing the impacts and improving the ecosystem services. The appropriate scale of absolute sustainability assessment depends on the scale of serviceshed.

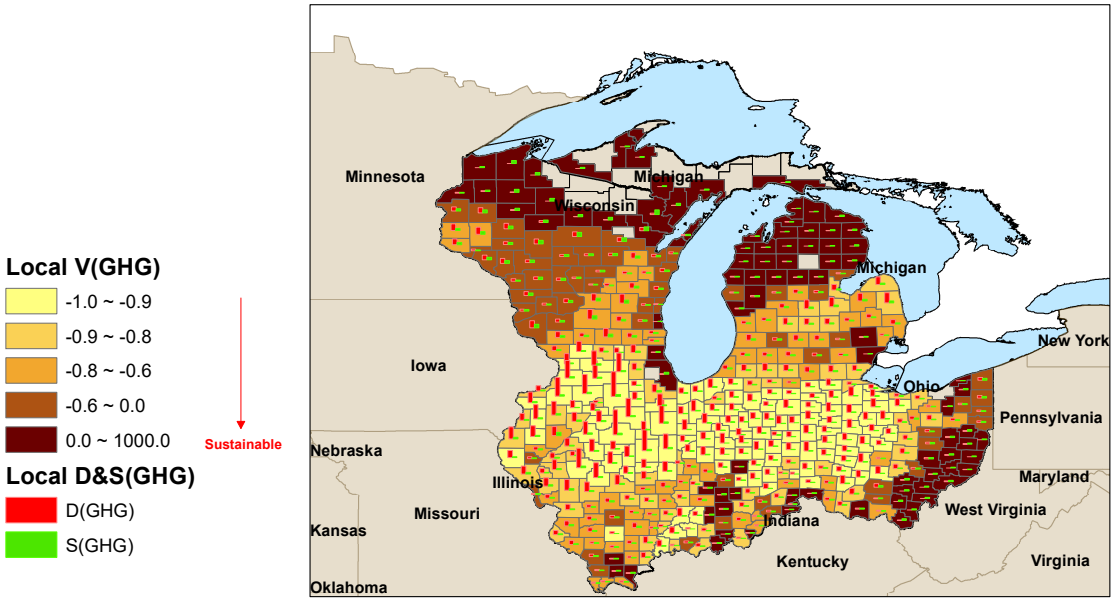

Figure 8.11: Local scale spatially-explicit absolute CO_2 indicators (V_{GHG}^{L}) with respect to corn and soybean production in the Great Lakes region.

In this work, we developed a general computational framework for multiscale and multi-regional absolute sustainability assessment. The framework integrates various existing models including regionalized PLCA,[34] multi-regional EEIO,[33] and TES-LCA.[35,129] The framework can account for not only local processes but also regional, national, and global economies. The framework also considers regional ecosystems that provide various services to technological and economic systems at multiple scales. Spatially-explicit absolute life cycle assessment (SEA-LCA) can be conducted by constructing such an integrated model. The mathematical formulation for SEA-LCA model was described in detail.

We performed a case study for corn and soybean production in the GL region, where includes five states in the U.S. Midwest: Illinois, Indiana, Michigan, Ohio, and Wisconsin. We investigated the absolute sustainability of corn and soybean production with respect to climate change impacts. In this case study, local scale county-level regionalized PLCA, regional scale state-level multi-regional EEIO, and national scale EEIO models were integrated to conduct a SEA-LCA study. County-level crop production data were collected from public databases,[291,292] and EPA's state-level EEIO[33] and USEEIO[39] models were employed. NPK fertilizer consumption flows for corn and soybean farming[1] were identified as regional–local and national–local upstream cutoff flows. Also, the supply of climate regulation service from ecosystems is included in the case study model. County-level data for carbon sequestration service from forests and state-level/national scale service data were collected from various publicly available data sources.[47,48,293]

We discussed how sensitive to spatial scales the sustainability assessment results are. With respect to climate change impacts, the global serviceshed scale needs to be considered. Since we did not include the global scale model in this case study, we compared national scale life cycle indicators with local scale indicators. We identified that the results can be significantly different for certain regions depending on the scale of sustainability assessment.

Regionally heterogeneous sustainability results were obtained for each county's corn and soybean production. Differences in the results by regions are attributed to region-specific crop productivity, supply chain networks (different locations of NPK fertilizer production) for each region's farming, and climate regulation service. Many

counties in Illinois have larger corn and soybean production than other regions. Accordingly, those counties show larger GHG emissions than other regions. Most of the NPK fertilizers for corn production in Illinois are produced outside the GL region, instead of from Illinois. Given that fertilizer production in Illinois has a lower GHG emission intensity than other regions, GHG emissions of corn production in Illinois could be significantly reduced, if fertilizers can be supplied more from Illinois. Also, enhancing the supply of climate regulation service through the reforestation of available land areas could be an alternative solution in improving the absolute sustainability of farming activities.

This case study can be further improved by addressing the following aspects. First, county-level data for livestock farming could be included to account for fertilizer consumption for livestock and calculate its associated environmental impacts. Also, transportation of fertilizers to each farm can be included as additional upstream cutoff flows to the county-scale farming processes from the regional and national economy. Moreover, county-level data for power generation and electricity use for farming can be included in the local scale regionalized PLCA model. Power generation is one of the largest contributors to global warming. If such county-level data are included, more insights into spatially-explicit sustainability results could be obtained. In addition, a global scale multi-regional EEIO model, such as EXIOBASE,[289] can be integrated into the SEA-LCA model of this case study. Since the serviceshed scale of climate change impacts is global, a more complete sustainability assessment study can be performed by including the global scale model.

Sustainability assessment studies that only utilize national average models such as PLCA and USEEIO cannot address spatially-explicit results depicted in this work

because impact intensities for every region will be the same. Also, the studies that only employ a multi-regional EEIO model cannot conduct a robust spatially-explicit sustainability analysis unless detailed process data are included in the model through a multiscale and multi-regional modeling approach in this work.

SEA-LCA modeling framework can potentially be applied to conduct various case studies. For instance, the spatially-explicit impact results for various farming practices (e.g., no-till vs. conventional tillage practices) can be examined by incorporating an agricultural modeling tool, such as SWAT,[202] into the study. Multiple sustainability indicators (e.g., water quantity, water quality, air quality, and land footprint) can be assessed by including additional intervention data at each scale of the model. Also, ecosystem (land use) design problems can be addressed by defining the unit of ecosystem scaling factors as an area unit (e.g., ha). A vector of ecosystem scaling factors ($\overline{m}_{e,M}$) will be design variables, and landscape design problems can be solved with constraints of available land areas in minimizing the final demands of ecosystems ($\overline{f}_{e,M}$). If technological systems in the SEA-LCA model also include design variables (e.g., multiple technology and supply chain options[6]), techno-ecologically synergistic design solutions that minimize the impacts of technological systems and maximize the benefits of ecosystems could be explored.

In addition, SEA-LCA framework can be integrated with equipment scale engineering models to solve region-specific process design problems. An approach for the process-to-planet (P2P) multiscale model,[13] which integrates an equipment scale engineering model with value chain scale PLCA and economy scale EEIO models, can be employed to develop SEA-P2P model.

Through model integration, the SEA-LCA model advances sustainability assessment methodology by accounting for three aspects: multiple spatial scales, spatial heterogeneity, and ecosystem services. Additional aspects can be considered as well to advance the method further. One could be the consideration of cross-disciplinary effects of market changes and social behavioral changes on the sustainability indicators. The temporal dynamics of inventory data also need to be taken into account. A dynamic computable general equilibrium model and behavioral change model could be potentially integrated with the LCA model to address such additional aspects.

Chapter 9: Conclusions and Future Work

9.1 Conclusions

Research works described in this dissertation have improved approaches for sustainability assessment, sustainable process design, and sustainable supply chain design by addressing the following additional aspects that need to be accounted for to obtain sustainable solutions while preventing unexpected outcomes. First, market constraints were considered for sustainable process and supply chain design problems as a consequential multiscale modeling approach to avoid unintended outcomes due to cross-disciplinary effects.[6] Also, to avoid the disastrous consequences of climate change on manufacturing systems, a climate-resilient process design approach was developed by employing the flexibility analysis approach,[194] which is one of the traditional process systems engineering approaches. General circulation models (GCMs) and the SWAT (soil and water assessment tool) model were employed to project future climate constraints. The SWAT model was also used to study the nexus of food-energy-water (FEW) systems and ecosystems.[294] To avoid unintended shifting of environmental impacts across flows, the interactions between multiple flows must be understood. The ecologically synergistic FEW nexus framework was developed to account for the benefits of ecosystem services for FEW systems. In addition, a

multiscale and multi-regional FEW nexus framework for spatially-explicit absolute life cycle assessment (SEA-LCA) was developed to account for regional heterogeneity at multiple spatial scales.

To avoid unintended outcomes and false implications from sustainability modeling studies, all the aspects that were addressed in each topic (i.e., multiple spatial scales, market effects, climate change effects, FEW nexus, and ecological carrying capacity) need to be accounted for in one modeling framework through approaches such as integrated assessment modeling (IAM). For instance, climate change will affect economic systems (e.g., market resource availability and commodity price) and ecosystems (various ecosystem services). Also, the economic and ecological effects of climate change will affect manufacturing systems design and the nexus of FEW systems. Therefore, multiple aspects including climate change, resource constraints, benefits of ecosystems, and the FEW nexus need to be considered to understand their effects on developing sustainability solutions. Developing such an integrated modeling framework will be a huge breakthrough. In this dissertation, market resource effects, climate change effects, and the nexus of FEW systems and ecosystems are addressed separately to advance the systems modeling approaches for obtaining sustainable solutions. This work will contribute to the foundation toward IAM approach.

The summary of conclusions for each research topic in the dissertation is as follows. In Chapter 3, FEW footprints of individual households in Columbus, Ohio were assessed using an environmentally-extended input-output (EEIO) model to address a social domain of environmental sustainability. Correlations between household demographics (e.g., gender), consumption behaviors, and FEW footprints were

investigated to understand how specific consumption behaviors affect household environmental impacts. This work could potentially be extended to account for social (human behavioral) consequences on environmental sustainability by examining behavioral feedback from households. In Chapter 4, a carbon footprint of biomimetic carbon fixation technologies that employ the RubisCO immobilization technique[4] was investigated by constructing a process-based LCA (PLCA) model. RubisCO is nature's CO_2-sequestering enzyme and converts atmospheric CO_2 into the organic carbon molecule, 3-phosphoglyceric acid (3-PGA). The adenosine triphosphate (ATP) preparation process for the 3-PGA production was identified as a hotspot inventory. The carbon footprint to produce 3-PGA can be significantly lowered by integrating carbon fixation technologies with an electrochemical ATP regeneration technology.

Conventional sustainability assessment methods such as EEIO and PLCA were employed in Chapters 3 and 4. To obtain sustainable solutions while avoiding unintended shifting of burdens across space, time, flows, and disciplines,[9] the methodologies need to further be developed. In Chapter 5, a framework for multiscale consequential sustainable process design was developed to account for the consequences of economic constraints, such as the availability of economic resources, on designing engineering systems and their supply chain networks. The framework integrated the rectangular choice-of-technology model[27] with the process-to-planet (P2P) multiscale process design model.[13] The case study was performed for the urea production systems in the Muskingum River Watershed (MRW), Ohio to examine how the adoption of technologies could be limited by market constraints as the demand increases.

In Chapter 6, the consequences of climate change on manufacturing systems were examined. The operability of manufacturing systems needs to be ensured in terms

of the increasing variability of climate since the assumption of stationarity is not valid.[193] The flexibility analysis approach[194] is employed to maximize the flexibility of manufacturing processes to the uncertain climate parameters. Climate-resilient design solutions can be obtained by employing climate constraints estimated by GCMs and the SWAT model.

Sustainability assessment methods also need to capture the interactions between FEW flows to prevent impacts from shifting across flows. Ecosystems also interact with FEW systems. In Chapter 7, to account for the interactions between food-energy-water-ecosystem flows, the ecologically synergistic FEW nexus framework was developed. The framework evaluates the absolute sustainability of FEW activities, not just to minimize impacts but to prevent ecological overshoot. The case study was conducted for various technological and agro-ecological alternatives to improve the sustainability of MRW. The synergy between technological and agro-ecological alternatives can be best for 'win-win' outcomes in terms of multiple indicators.

In Chapter 8, to account for flows across multiple regions at multiple scales, a modeling framework for multiscale and multi-regional absolute sustainability assessment was developed. This framework integrates various existing LCA-derived approaches to conduct a SEA-LCA study and can evaluate absolute sustainability indicators at various serviceshed scales. The case study was performed for corn and soybean production in the Great Lakes region of the U.S. Midwest to investigate spatially-explicit absolute CO_2 indicators. SEA-LCA enables us to identify the region-specific opportunities for improvement from both technological and ecological aspects.

9.2 Future Work

One of the main purposes of sustainability assessment is to help the decision-making of businesses and policymakers toward sustainability. To prevent unintended harm that could be caused by the assessment results, the sustainability assessment methods can be further improved by considering the following aspects.

9.2.1 Accounting for Economic, Ecological, and Social Consequences

A more sophisticated economic model that accounts for price elasticity needs to be integrated with the multiscale consequential sustainable process design model in Chapter 5. For example, the change in commodity prices by the market can be modeled by using the computable general equilibrium (CGE) model.[24–26] The consequential modeling framework in Chapter 5 assumes prices to be fixed. If the framework could be integrated with the CGE model, the price changes due to technology choices and their consequences on environmental sustainability could be investigated, and the modeling performance of economic consequences could be improved.

Also, the economic consequences of climate change on manufacturing systems could be investigated using economic models such as CGE. Climate change could affect not only the physical properties of resources but also the economic properties of resources such as price. For example, the price of water is likely to increase if the water resource becomes scarce by drought under future climate change. The integrated assessment model has also been widely used to address the consequences of climate change by comparing the cost and benefits of mitigating CO_2 emissions.[295,296] By employing such models, the effectiveness of CO_2 emission regulations, such as

carbon tax policy and renewable energy tax credits, on industrial processes could be examined.

Future climate projections show that we may have an increased risk of water scarcity. Climate change could affect not only technological systems but also ecosystems.[184,185] Climate change could affect land use and land cover, such as type of vegetation, and accordingly, cause changes in the supply of various ecosystem services. The consequences of such ecological changes on technological systems need to be understood to avoid potential damages to the technological systems.

Moreover, social consequences on environmental assessment need to be studied. In Chapter 3, FEW footprints of individual households were calculated. The footprint results could be provided to each household, and its behavioral feedback could be examined to account for the consequences of human behavioral changes on environmental sustainability. However, long term follow-ups for such a study will be challenging.

9.2.2 Accounting for Uncertainties and Dynamics of Inventory Data and Models

Many topics in this dissertation integrated existing sustainability assessment models, which rely on extensive data. Also, many studies were based on some assumptions due to lack of data. For example, stoichiometric reactions for potential CO_2 conversion technologies were assumed for the FEW nexus study in Chapter 7 since data for commercialized technologies are not available at this point. GCMs also show large variability in projected climate data depending on the model and climate change scenarios. Moreover, the interventions from technological systems and the supply of ecosystem services vary over space and time. Therefore, uncertainties in such data

need to be addressed through either sensitivity analysis or statistical uncertainty analysis by examining probability distributions of uncertain data (e.g., Monte Carlo analysis). The robustness of results should be evaluated through such approaches.

The temporal dynamics of data also need to be addressed. Many activities of technological systems and the supply of ecosystem services vary with seasons. Therefore, a seasonal analysis could be performed to account for such temporal dynamics of data. Also, since future climate projections show the increasing variability over time, climate-resilient process design problems in Chapter 6 need to account for long-term temporal dynamics. Moreover, the flexibility analysis approach in Chapter 6 does not address uncertainties in climate change scenarios and the impacts associated with each scenario. Considering the longevity of equipment, multi-period optimization for certain time periods (e.g., 30 years) could be conducted. Real options analysis approach could be employed to determine the optimal design solutions for each time period to minimize the net cost for every possible climate change scenario.[220–222] Additionally, adaptive pathway analysis approach could be utilized to determine tipping points for each technology option by calculating the temporal distribution of each option that satisfies performance constraints.[223,224]

9.2.3 Accounting for Projections of Emerging Technologies

In Chapter 4, the carbon footprint of emerging carbon fixation technologies was investigated. Due to the nascent nature of technologies, it was very challenging to collect inventory data. Early-stage experimental data will not represent commercialized data since inventory data could highly depend on the production scale. Learning

curve theory could be employed for the LCA study to estimate changes in the environmental impacts and cost as emerging technologies become mature.[297,298]

Also, technological development needs to be considered for the case study under climate change scenarios. For instance, future NGCC power plants may have fewer emissions than the current NGCC plants due to technological development. Future energy industry and emission scenarios could be utilized to assess the impacts of technologies for the future years. Regression models could be used to estimate the trend in emission levels during the past 10–20 years and extrapolate it to the future.[285]

9.2.4 Additional Considerations for Sustainability Assessment of Regional FEW Systems

In Chapter 7, the sustainability of regional FEW systems was examined by investigating the interactions between FEW systems and ecosystems for various technological and agro-ecological alternatives. In addition to the technological and agro-ecological solutions, economic solutions based on nutrient trading schemes could be explored to avoid adverse impacts on water quality. According to the Ohio EPA report,[279] abating nonpoint source agricultural nutrient loadings is much cheaper than abatement at the regulated point sources. For example, a point source, such as coal-fired power plants, could pay farmers for credits to implement agricultural practices that result in lower food production but fewer nutrient emissions. In doing so, coal-fired power plants can release as many nutrients as they pay for credits. A carbon trading scheme can also be studied in a similar sense. These economic solutions could yield both economic and environmental benefits.

Also, the impacts of climate change on the nexus of food-energy-water-ecosystem need to be examined to ensure FEW nexus security under climate change.[209] Figure

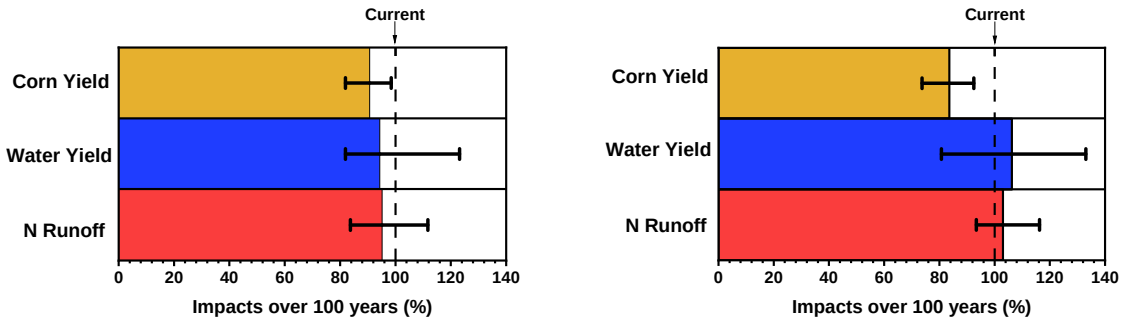

(a) (b)

Figure 9.1: Preliminary results about the impacts of climate change on corn yield, water yield, and nitrogen runoff in the MRW for RCP **(a)** 4.5 and **(b)** 8.5 scenarios.

9.1 shows the preliminary results about the consequences of climate change on corn yield, water yield, and nitrogen runoff in the MRW for RCP 4.5 (2 °C warming) and 8.5 (4 °C warming) scenarios. Five GCMs and the SWAT model are employed as described in Chapter 6. In this preliminary work, farming practices and technologies are assumed to be constant up to 2100 to investigate the impacts of climate change on currently adopted practices and technologies in the MRW. Corn yield is the most vulnerable to climate change, while water yield and nitrogen runoff show large variations. The results imply that climate change should be mitigated to protect food security in the future. As discussed in Chapter 7, the largest contributing activity to GHG emissions in the MRW is fossil power generation. To sustain agricultural systems, therefore, mitigation strategies such as the clean power plant strategy in Chapter 7 are needed.

For the SEA-LCA model in Chapter 8, a global scale multi-regional EEIO model such as EXIOBASE[289] could be included to represent the planetary system boundary in investigating spatially-explicit absolute sustainability indicators. In the case study

in Chapter 8, only GHG indicators of each region were investigated. Other indicators, such as water quantity, water quality, and air quality, could be examined to account for the interactions between multiple flows and investigate trade-offs between indicators. Also, landscape design problems could be solved using the SEA-LCA framework by having ecosystem scaling vectors as design variables. This will allow us to obtain techno-ecologically synergistic design solutions for FEW systems.

9.2.5 Additional Model Integration

The SEA-LCA framework in Chapter 8 can be integrated with equipment scale engineering models. The resulting model will be a spatially-explicit process-to-planet (SEP2P) model, which is the integrated model of SEA-LCA and P2P. The SEP2P model can perform spatially-explicit sustainable process design studies. Since the equipment scale processes are included in larger scale models such as PLCA and regional/national/global EEIO, the larger scale models need to be disaggregated from the equipment scale model. Increased computational difficulties will be a trade-off.

The multiscale technology choice model (RCOT-P2P model) in Chapter 5 integrated the multiscale P2P model with the rectangular choice-of-technology (RCOT) model. Economic resource constraints were considered in the RCOT-P2P model to conduct a consequential sustainable process design study. In addition, market constraints could be considered for multiple regions, and the RCOT model could be integrated with the multiscale and multi-regional SEA-LCA model. Since the SEA-LCA model includes ecosystem modules, the resulting integrated model will be an ecologically synergistic spatially-explicit choice-of-technology (ESSECOT) model. This

model could investigate the optimal distribution of multiple technology options across regions to maximize absolute sustainability indicators.

Appendix A: Life Cycle CO_2 Emissions of the Coal-to-Liquids Process

A life cycle assessment study was conducted to estimate life cycle CO_2 emissions of proposed coal-to-liquids (CTL) processes and to compare them with appropriate conventional processes. To account for the emissions burden of by-products, various allocation methods were employed and compared to each other. The proposed liquefaction process showed lower CO_2 emissions than the conventional process. The CO_2 emissions of jet fuel from the proposed hydrotreating process were higher than those of conventional jet fuel, but lower than those of Fischer-Tropsch (FT) jet fuel from coal, that uses the same feedstock as the proposed processes.

A.1 Objectives

The goals of this work are to, 1) estimate the life cycle CO_2 emissions of synthetic crude oil from the liquefaction part and jet fuel from the hydrotreating part of the CTL process, and 2) compare the life cycle CO_2 emissions of the CTL process with appropriate conventional processes for obtaining both products (synthetic crude and jet fuel).

A.2 Approach

The approach of Life Cycle Assessment (LCA)[37] was applied to calculate the CO_2 emissions to produce synthetic crude oil and jet fuel. Relevant process inventory data, which include material resources, electricity, natural gas for heating, transportation of materials, main products, by-products, and emissions, were provided by Battelle. GREET models[42] were used to obtain the life cycle data of each inventory and the obtained data were implanted in openLCA software[51] to develop life cycle models. The LCA study has four phases as follows: a) goal and scope definition, b) inventory analysis, c) impact assessment, and d) interpretation.

A.2.1 Goal and Scope Definition

Battelle has developed the CTL processes that produce 220,095 tonnes/y of synthetic crude oil from coal and 186,043 tonnes/y of jet fuel from synthetic crude oil. To compare the life cycle CO_2 emissions of the proposed CTL processes with those of conventional processes, four different functional units were identified as follows: a) 220,095 tonnes/y of synthetic crude oil product from the proposed liquefaction process, b) 186,043 tonnes/y of jet fuel product from the hydrotreating process, c) 220,095 tonnes/y of synthetic crude oil product from the conventional process, and d) 186,043 tonnes/y of jet fuel product from the conventional process. The LCA accounts for environmental impacts of a product or a process throughout its entire life-cycle, which ranges from the extraction of the most upstream raw materials to the disposal. In this work, the boundary of analysis is limited to the cradle-to-gate, which does not include the disposal phases of products.

A.2.2 Inventory Analysis

The life cycle CO_2 emissions data of each inventory were obtained from GREET models that correspond to each inventory and were summarized in Table A.1. If multiple GREET models correspond to a single inventory, the most appropriate model that can be used in Ohio or United States was selected. In case of the proposed liquefaction process, only 80% of the CO_2 emissions from biosolvent, which is developed by Battelle, was included. This is because 20% of the rest of CO_2 emissions are attributed to the use of bio derived products, such as pine tree products and paper pulp, that is assumed to be carbon neutral. Monoethanolamine (MEA) is used to capture CO_2 and to produce compressed CO_2 from the hydrotreating process. However, since the GREET model for MEA does not exist, process inventory data to produce MEA were obtained from ecoinvent v2.2 life cycle inventory database[43] and the GREET models that correspond to these inventory data were used to obtain the life cycle CO_2 emissions data of MEA. Also, any catalyst inputs were excluded from the inventory analysis because it is assumed that they can be reused multiple times, which in turn cause small environmental impacts. The appropriate GREET models for the conventional processes were identified as well. In terms of the conventional jet fuel product, three GREET models were considered as follows: conventional jet fuel from crude oil, Fischer-Tropsch (FT) jet fuel from coal, and FT jet fuel from natural gas.

Since several by-products are produced from the proposed CTL processes, the emissions burden needs to be allocated between a main product and by-products. To make the analysis robust, three different allocation methods were employed in this study. First, the emissions burden was allocated by partitioning based on the

mass ratio of products or the exergy ratio of products. In these two partitioning allocation approaches, the main product and by-products carry the emissions burden together. Also, the system expansion approach was employed to account for by-products. In this approach, the main product carries all burdens, while by-products do not carry any. Instead, credit is given to the main product for the by-products that are displaced by other conventional processes to produce these by-products. For this displacement method, GREET models that correspond to by-products were identified as well and included in the analysis. However, some by-products, such as centrifuge solids and compressed CO_2, were excluded from the analysis by the displacement method because of the difficulties in identifying conventional processes that produce these by-products and because their corresponding GREET models do not exist. To compare the cases where each allocation method is employed, only one

Table A.1: Life cycle inventory analysis for the proposed liquefaction and hydrotreating processes and conventional processes. The life cycle CO_2 emissions data of each inventory were obtained from GREET models.

Process	Inventory type	Inventory	Amount	Unit	GREET model	CO_2 emissions	Unit
Liquefaction	Input - Resource	Coal (Mined Bituminous)	328,500	tonne/y	Bituminous Coal Mining and Cleaning	18.80	gCO_2eq/kg
	Input - Resource	Biosolvent	118,259	tonne/y	-	0.26	$kgCO_2eq/kg$
	Input - Resource	Coal tar distillate	32,850	tonne/y	Residual Oil (Petroleum) from Crude Oil	0.40	$kgCO_2eq/kg$
	Input - Resource	Digester gas	23,561	tonne/y	Animal Waste Anaerobic Digestion to Natural Gas as an Intermediate Fuel	1.89	$kgCO_2eq/kg$
	Input - Resource	Water	25,363	tonne/y	-		
	Input - Resource	Limestone	7,745	tonne/y	Limestone Mining	2.08	gCO_2eq/kg
	Input - Utility	Electricity	37,843	MWh/y	Electricity Distributed - RFC Mix	0.59	$kgCO_2eq/kWh$
	Input - Utility	Natural gas	1,521	tonne/y	NA NG from Shale and Regular Recovery	0.22	$kgCO_2eq/kg$
	Input - Transport	Fuel use locomotive, endloader, dump truck 43.5 gal/hr, daylight	635	tonne/y	Conventional Diesel from Crude Oil for US Refineries	0.57	$kgCO_2eq/kg$
	Output - Main product	Syncrude oil (<500C)	220,095	tonne/y	-		
	Output - By-product	500C+ Heavy oil	101,327	tonne/y	Pet Coke from Crude for Use in U.S. Refineries	0.34	$kgCO_2eq/kg$
	Output - By-product	Centrifuge solids	108,823	tonne/y	-		
	Output - Waste	Waste disposal	73,324	tonne/y	-		
	Output - Emission	CO_2 emissions	72,294	tonne/y	-		
Hydrotreating	Input - Resource	Syncrude oil (<500C)	220,095	tonne/y	-		
	Input - Resource	Water	81,633	tonne/y	-		
	Input - Resource	Limestone	3,947	tonne/y	Limestone Mining	2.08	gCO_2/kg
	Input - Resource	Monoethanolamine (MEA)	56	tonne/y	-		
	Input - Utility	Electricity	91,196	MWh/y	Electricity Distributed - RFC Mix	0.59	$kgCO_2/kWh$
	Input - Utility	NG for shift and heating	30,286	tonne/y	NA NG from Shale and Regular Recovery	0.22	$kgCO_2/kg$
	Output - Main product	Jet fuel	186,043	tonne/y	-		
	Output - By-product	Switch engine fueling	212	tonne/y	Conventional Diesel from Crude Oil for US Refineries	0.58	$kgCO_2/kg$
	Output - By-product	Ammonia	2,570	tonne/y	Ammonia Production	2.43	$kgCO_2/kg$
	Output - By-product	Compressed CO_2	37,000	tonne/y	-		
	Output - Credit	Reformer tailgas credit for heating	26,943,132	MJ/y	NA NG from Shale and Regular Recovery	0.22	$kgCO_2/kg$
	Output - Waste	Waste disposal	13,578	tonne/y	-		
	Output - Emission	CO_2 emissions	109,036	tonne/y	-		
Conventional processes	Output - Product	Syncrude oil	220,095	tonne/y	Synthetic Crude Oil as intermediate fuel	1.02	$kgCO_2/kg$
					Conventional Jet Fuel from Crude Oil	0.40	$kgCO_2/kg$
	Output - Product	Jet fuel	186,043	tonne/y	Fischer-Tropsch Jet Fuel from Coal	4.58	$kgCO_2/kg$
					Fischer-Tropsch Jet Fuel from NA NG	1.12	$kgCO_2/kg$

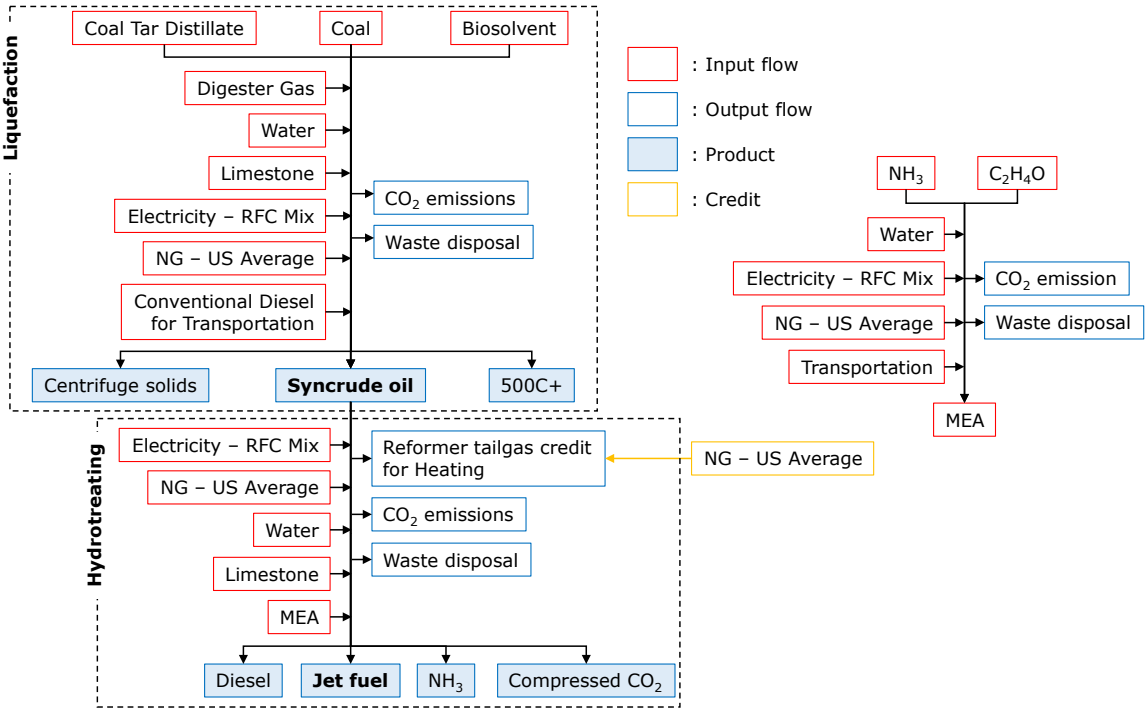

Figure A.1: A network diagram of the proposed CTL processes for the partitioning method based on mass.

type of allocation method was used for each case. In case of the partitioning method based on mass, however, reformer tailgas credit for heating was given to the main product, which is jet fuel, by the displacement method, because it doesn't have a mass unit. Figure A.1 shows a network diagram of the proposed CTL processes for the partitioning method based on mass.

A.3 Results and Discussion

A.3.1 Impact Assessment and Interpretation

The emissions burden of the proposed liquefaction process was divided into three products, synthetic crude oil, 500C+ heavy oil, and centrifuge solids by the partitioning method based on mass, and their life cycle CO_2 emissions were 97,401, 44,841, and 48,159 tonnes CO_2/y, respectively. Figure A.2a shows that the liquefaction process was the highest contributor to the emissions, followed by digester gas and biosolvent. In case of the hydrotreating process, the life cycle CO_2 emissions of jet fuel, switch engine fueling, ammonia, and compressed CO_2, were 219,974, 250, 3,039, and 43,748 tonnes CO_2/y, respectively. As shown in Fig. A.2b, the hydrotreating process was the most dominant contributor. The life cycle CO_2 emissions of conventional processes to synthetic crude oil and jet fuel were obtained from corresponding GREET models. The CO_2 emissions of synthetic crude oil from the conventional process were 224,497 tonnes CO_2/y, which are significantly higher than those from the liquefaction process. The CO_2 emissions of FT jet fuel from coal were 852,079 tonnes CO_2/y, which are higher than those from the hydrotreating process. However, the CO_2 emissions of conventional jet fuel from crude oil and FT jet fuel from natural gas were lower than those from the hydrotreating process, showing 74,417 and 208,369 tonnes CO_2/y, respectively.

Figure A.3 shows the life cycle CO_2 emissions of products when different allocation methods were employed. The results of the displacement method show higher emissions that those of other partitioning methods. However, actual emissions of the displacement method may be lower because credits from some by-products weren't included in the analysis by the displacement method. In case of the partitioning

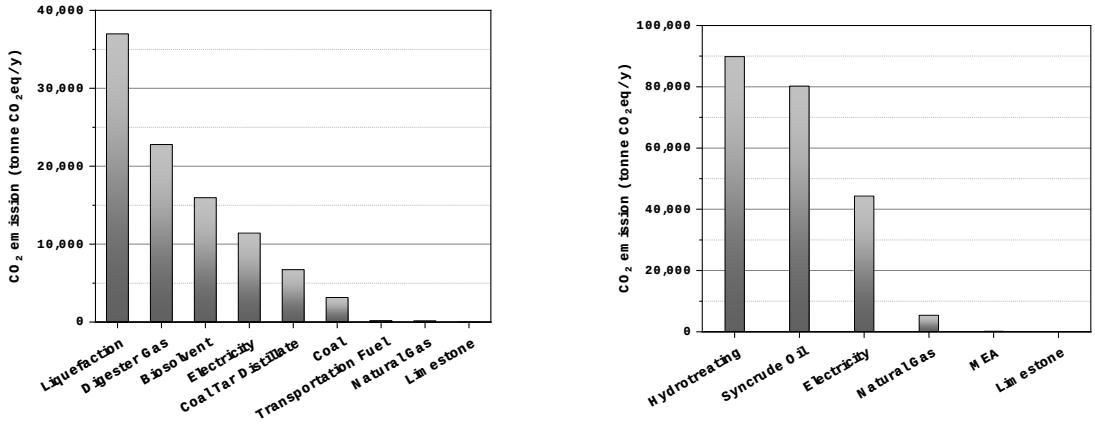

(a) (b)

Figure A.2: The life cycle CO_2 emissions of each inventory in **(a)** the liquefaction process and **(b)** the hydrotreating process when the partitioning allocation based on mass was employed.

method based on exergy, the CO_2 emissions of synthetic crude oil from the liquefaction process were not calculated since the chemical composition of by-products, which are 500C+ heavy oil and centrifuge solids, is unknown, and therefore, exergy values of those by-products are hard to calculate. Regardless of which allocation method was selected, the CO_2 emissions of synthetic crude oil from the liquefaction process were much lower than those from the conventional process. That is, about 43.7% reduction of the CO_2 emissions is expected to produce synthetic crude oil by employing the proposed liquefaction process. Also, regardless of the allocation methods, the CO_2 emissions of jet fuel from the hydrotreating process were higher than those of conventional jet fuel from crude oil and FT jet fuel from natural gas, but were 68.6% lower than those of FT jet fuel from coal, which uses coal as feedstock, the same as the hydrotreating process.

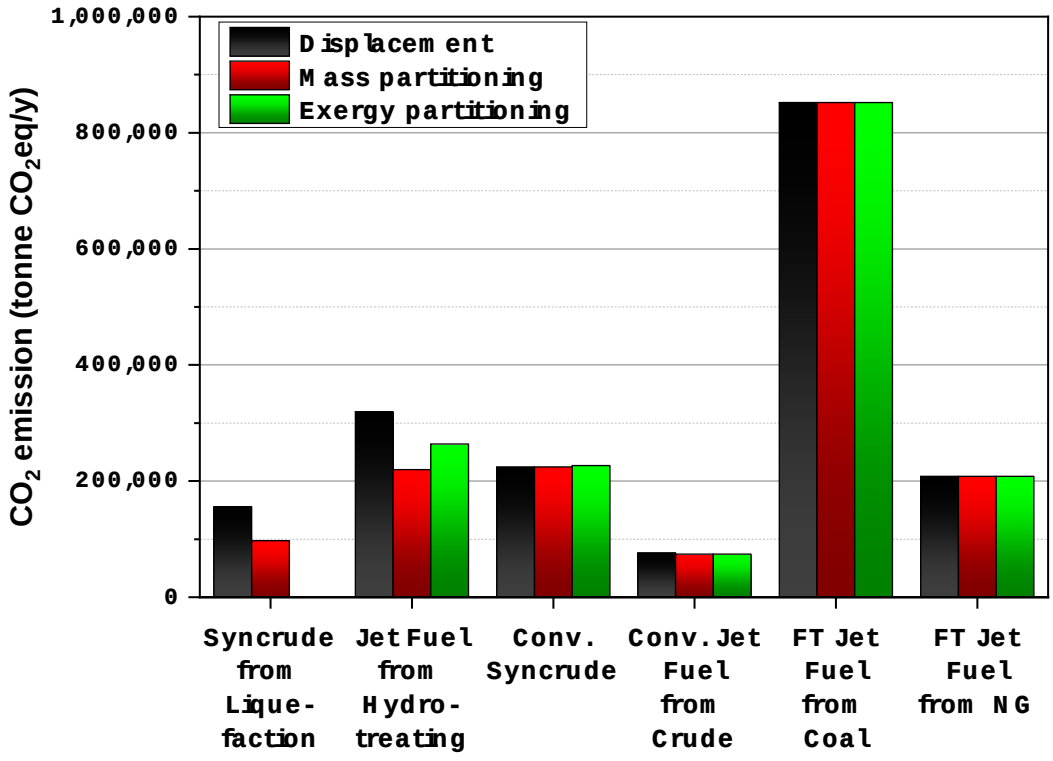

Figure A.3: The life cycle CO_2 emissions of products when each allocation method was employed.

A.4 Conclusions

The life cycle CO_2 emissions of the proposed CTL processes were estimated and compared with those of conventional processes. Three different allocation methods was employed in the analysis to make the results robust. The overall results did not change much regardless of the allocation methods selected. About 43.7% reduction of the CO_2 emissions is expected to produce synthetic crude oil by employing the proposed liquefaction process instead of the conventional process. The CO_2 emissions of jet fuel from the proposed hydrotreating process were higher than those of

conventional jet fuel from crude oil, but 68.6% lower than those of FT jet fuel from coal. Also, the most dominant contributors to the emissions in both liquefaction and hydrotreating processes were liquefaction process and hydrotreating process, respectively. Therefore, if the proposed CTL processes could be optimized further, it is expected that their CO_2 emissions can be decreased further.

A.5 Homework Problem

In this section, we provide an example problem, which is related to the production systems in this chapter. This problem is developed as a homework problem to learn about LCA databases and models (GREET[42] and USEEIO[39]).

Note: You need to download and install the GREET®.Net software to solve this problem. The software is available at this link. The software can only be installed on Windows OS with Microsoft .Net Framework 4.5 already installed. You may need to install GREET on computers in the computer lab in CBEC.

Suppose coal is converted to liquid fuels through the following CPL process in Ohio. The dry crushed coal is mixed with organic biosolvent and coal tar distillate, and liquefied to a synthetic crude oil product through the liquefaction process. The liquefaction process input and output data are shown in Fig. A.4.

The liquefaction process produces two by-products, centrifuge solids and 500C+ heavy oil. These by-products have their own use for some applications. In such a case, the life cycle impacts need to be allocated among the products. The allocation can be performed based on mass, energy value, or monetary value ratios. For example,

the mass-based allocation can be performed for two products A (a kg) and B (b kg) as follows:

$$\text{The impacts for A: } x \times a/(a+b)$$

$$\text{The impacts for B: } x \times b/(a+b),$$

where x is total impacts calculated.

Using the GREET software, calculate the life cycle (well-to-use) greenhouse gas (GHG) emissions to produce 1 kg of synthetic crude oil through the CTL process. Also, compare it to the life cycle (well-to-use) GHG emissions of conventional crude oil. Summarize your conclusion with respect to global warming mitigation.

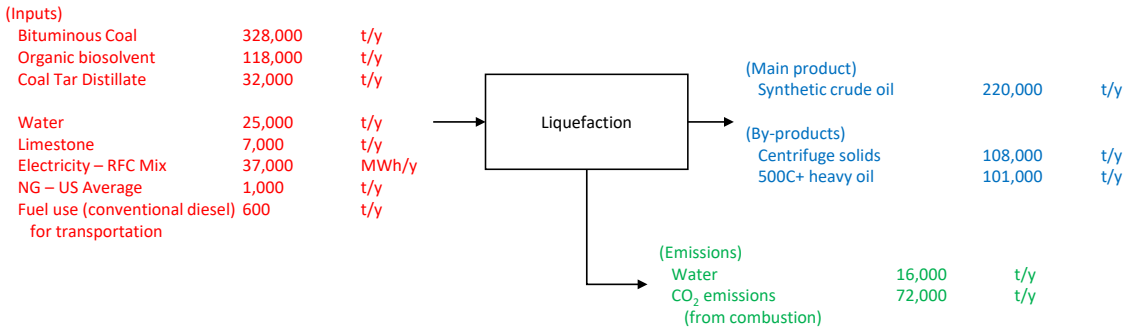

Figure A.4: CTL process to produce synthetic crude oil from coal.

Hint: Table A.2 identifies relevant GREET model data. You may not be able to find relevant data for some flows from GREET. In such a case, use the USEEIO model instead. Assume the price for those flows is \$0.5/kg. In practice, the correct or approximate price needs to be known. For instance, we do not know what organic

biosolvent is. The relevant economy sector in the EEIO model with organic biosolvent can be "325190/other basic organic chemicals."

Table A.2: Relevant data from GREET/USEEIO models and life cycle GHG emissions.

Inventory type	Inventory	Amount	Unit	Relevant GREET model data	Well to Use GHG emissions	Unit
Input - Product	Bituminous coal	328,000	t/y	Bituminous Coal Mining and Cleaning		t CO_2eq/y
Input - Product	Organic biosolvent	118,000	t/y	None (Relevant USEEIO sector: 325190/other basic organic chemical)		t CO_2eq/y
Input - Product	Coal tar distillate	32,000	t/y	None (Relevant USEEIO sector: 325190/other basic organic chemical)		t CO_2eq/y
Input - Product	Limestone	7,000	t/y	Calcium Carbonate (Limestone: CaCO3) Production		t CO_2eq/y
Input - Utility	Electricity - RFC Mix	37,000	MWh/y	Electricity Mix: Non Distributed - RFC Mix		t CO_2eq/y
Input - Utility	Natural Gas - US Average	1,000	t/y	NA NG from Shale and Regular Recovery		t CO_2eq/y
Input - Transport	Fuel use (conventional diesel) for transportation	600	t/y	Conventional Diesel from Crude Oil for US Refineries		t CO_2eq/y
Input - Resource	Water	25,000	t/y	n/a		t CO_2eq/y
Emissions - Water	Water	16,000	t/y	n/a		t CO_2eq/y
Emissions - Air	CO_2 emissions	72,000	t/y	n/a		t CO_2eq/y
Output - Product	Synthetic crude oil	220,000	t/y	n/a		t CO_2eq/y
Output - Product	Centrifuge solids	108,000	t/y	n/a		t CO_2eq/y
Output - Product	500C+ heavy oil	101,000	t/y	n/a		t CO_2eq/y
Conventional Product	Conventional crude oil	220,000	t/y	Conventional Crude Oil		t CO_2eq/y

A.6 Solution

Table A.3 shows the relevant GREET model data for each of the inputs, emissions, and outputs. It also shows well-to-use GHG emissions. For some inputs such as organic biosolvent and coal tar distillate, it is hard to identify relevant GREET model data. In such a case, their GHG emissions data can be estimated from the USEEIO model.

Table A.3 exhibits relevant USEEIO sectors. (Relevant economy sectors can be identified from the NAICS website at this link). Since the USEEIO model is based on the economic model in a monetary unit, the physical data needs to be converted to the monetary data. By assuming the price is \$0.5/kg, the GHG emissions for organic

biosolvent and coal tar distillate can be estimated as follows:

$$\text{Organic biosolvent: } 118,000 \text{ t/y} \times \$500/\text{t} \times 1.30 \text{ kgCO}_2\text{eq}/\$ = 76,700 \text{ tCO}_2\text{eq/y},$$

$$\text{Coal tar distillate: } 32,000 \text{ t/y} \times \$500/\text{t} \times 1.30 \text{ kgCO}_2\text{eq}/\$ = 20,800 \text{ tCO}_2\text{eq/y}.$$

Accordingly, total GHG emissions for the liquefaction process are calculated to be 232,693 $\text{tCO}_2\text{eq/y}$ by adding up all associated GHG emissions.

Since this process has two additional by-products, the life cycle GHG emissions need to be allocated among the products. The life cycle GHG emissions for synthetic crude oil can be calculated using the mass-based allocation method as below:

$$232,693 \text{ tCO}_2\text{eq/y} \times \frac{220,000 \text{ t/y}}{220,000 \text{ t/y} + 108,000 \text{ t/y} + 101,000 \text{ t/y}} = 119,330 \text{ tCO}_2\text{eq/y}.$$

Therefore, the life cycle GHG emissions to produce 1 kg of synthetic crude oil through the CTL process are 0.54 kgCO_2.

The relevant GREET model data for conventional crude oil is identified as shown in Table A.3. Its life cycle GHG emissions to produce 1 kg of crude oil are 0.27 kgCO_2 which is smaller than the CTL process. Therefore, producing synthetic crude oil from coal through the CTL process has higher global warming potential than producing conventional crude oil when the mass of production is equivalent.

Table A.3: Relevant data from GREET/USEEIO models and life cycle GHG emissions.

Inventory type	Inventory	Amount	Unit	Relevant GREET model data	Well to Use GHG emissions	Unit
Input - Product	Bituminous coal	328,000	t/y	Bituminous Coal Mining and Cleaning	42,125	t CO_2eq/y
Input - Product	Organic biosolvent	118,000	t/y	None (Relevant USEEIO sector: 325190/other basic organic chemical)	76,700	t CO_2eq/y
Input - Product	Coal tar distillate	32,000	t/y	None (Relevant USEEIO sector: 325190/other basic organic chemical)	20,800	t CO_2eq/y
Input - Product	Limestone	7,000	t/y	Calcium Carbonate (Limestone: CaCO3) Production	72	t CO_2eq/y
Input - Utility	Electricity - RFC Mix	37,000	MWh/y	Electricity Mix: Non Distributed - RFC Mix	20,178	t CO_2eq/y
Input - Utility	Natural Gas - US Average	1,000	t/y	NA NG from Shale and Regular Recovery	405	t CO_2eq/y
Input - Transport	Fuel use (conventional diesel) for transportation	600	t/y	Conventional Diesel from Crude Oil for US Refineries	413	t CO_2eq/y
Input - Resource	Water	25,000	t/y	n/a	0	t CO_2eq/y
Emissions - Water	Water	16,000	t/y	n/a	0	t CO_2eq/y
Emissions - Air	CO_2 emissions	72,000	t/y	n/a	72,000	t CO_2eq/y
Output - Product	Synthetic crude oil	220,000	t/y	n/a	119,330	t CO_2eq/y
Output - Product	Centrifuge solids	108,000	t/y	n/a	58,580	t CO_2eq/y
Output - Product	500C+ heavy oil	101,000	t/y	n/a	54,783	t CO_2eq/y
Conventional Product	Conventional crude oil	220,000	t/y	Conventional Crude Oil	60,015	t CO_2eq/y

Appendix B: Carbon Footprint of the Solar Panel Facility in the Columbus Zoo Parking Lot

B.1 Objective

A carbon footprint is total greenhouse gas emissions that have a CO_2 equivalent mass unit. The goal of this work is to calculate the carbon footprint of the solar panel facility in a 5-acre VIP parking lot to examine its effectiveness and environmental impacts.

B.2 Approach

The approach of Life Cycle Assessment (LCA) is employed to evaluate the carbon footprint per year of a proposed strategy.[37] The LCA accounts for environmental impacts of a system throughout its entire life-cycle, which ranges from the extraction of the most upstream raw materials to the disposal, and thus, the LCA is called a cradle-to-grave analysis. The solar panel facility that covered the 5-acre VIP parking lot is defined as the final demand of this study, and its relevant life cycle inventory data are collected from the National Renewable Energy Laboratory (NREL) U.S. life cycle inventory database[40] and ecoinvent global life cycle inventory database.[43] The inventories of this study include polysilicon solar panels, steels to support the

panel structures, electric conduits, water collection pipes, underground water tanks and invertors, pump house for water distribution, and vertical gardens on the side of panel structures. From this study, some relevant inventories, such as green roofs and water pipes to nearby golf courses, and the disposal phase of the solar panel facility are excluded. Also, the effects of the shading of vehicles and the reduction of snow removal by the solar panels on the footprint are not considered in this study. A professional and open source LCA software, openLCA, is used to perform the LCA.[51] To account for the benefits of this strategy, savings in the footprint due to not using electricity and water from their conventional supply facilities, such as the electricity grid in Ohio, are considered. Table B.1 shows the life cycle inventory list for this study and their data sources.

B.3 Results and Discussion

The results are shown in Figs. B.1 and B.2. As shown in Fig. B.1, the footprint of a proposed strategy, which corresponds to the footprint of the solar panel facility

Table B.1: Life cycle inventory analysis for the solar panel facility in the 5-acre VIP parking lot.

Type	Inventory	Amount	Unit	Data source
Input	Solar panel (multi-Si)	1.1	MW	ecoinvent v2.2
	Steel for the construction to support the panels	409,200	lb	NREL
	Electrical cable	970	ft	ecoinvent v2.2
	High denstiy polyethylene (HDPE) for water pipes	7,368	lb	NREL
	Water tank, 600 L	2	unit	ecoinvent v2.2
	Water pump, 40 W	2	unit	ecoinvent v2.2
	Water pump station	1	unit	ecoinvent v2.2
	Vertical gardens	5	unit	calculated by Urban Blooms
Output	Solar panel facility	1.1	MW	-
	Electricity generated from the facility	1,298,000	kWh/y	NREL
	Water collected from the facility	3,358,847	gal/y	ecoinvent v2.2

without considering the savings in electricity and water from the conventional facilities, is 2.49 million $kgCO_2eq$. On the other hand, the footprint of a conventional strategy, which corresponds to the footprint when electricity and water are obtained from the conventional facilities, is 0.93 million $kgCO_2eq$. The footprint of the conventional strategy corresponds to the amount of savings in the footprint of the proposed strategy. Hence, the total carbon footprint equals to the footprint of the proposed strategy minus the footprint of the conventional strategy. The results show that the VIP parking lot has a positive total carbon footprint during the first year from the initial installation of the solar panel facility. Figure B.1 also shows that the most dominant positive contribution to the footprint comes from the solar panel manufacturing process. If we investigate the further upstream of the solar panel, the silicon production process for PV is the most dominant positive contributor.

The change in the total carbon footprint over time is calculated and shown in Fig. B.2. It is assumed that any maintenance activities are not required for 30 years. The results show that the total carbon footprint of the facility turns into a negative value within 3 years from its initial installation and the value of the total footprint decreases over time.

B.4 Conclusions

A calculation of the carbon footprint of the solar panel facility in the 5-acre VIP parking lot has been performed to examine its effectiveness and environmental impacts. The results show that the facility will become carbon negative within three years from the initial installation of the solar panel facility. If the proposed strategy could be employed for the entire parking lot at the Columbus Zoo, the reduction in

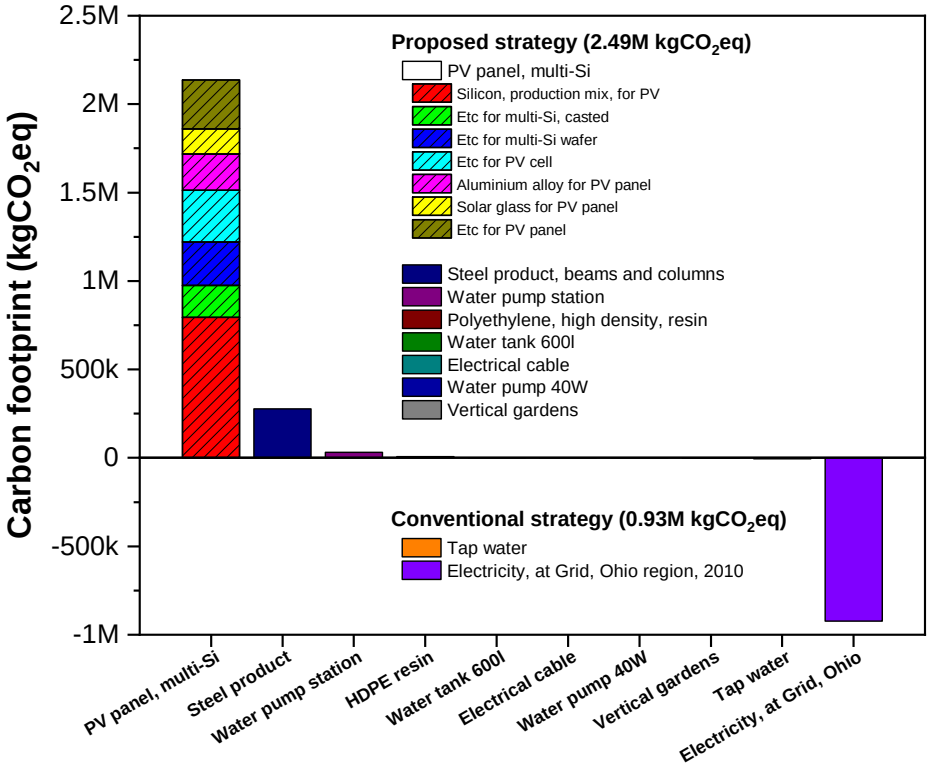

Figure B.1: The carbon footprint of proposed and conventional strategies. The total carbon footprint equals to the footprint of the proposed strategy minus the footprint of the conventional strategy.

the footprint could be enhanced almost in proportional to the area of the parking lot because the amount of solar panels, which have the most dominant contribution to the footprint, will be almost linearly scaled up from the 5-acre parking lot to the entire parking lot.

The carbon footprint might be decreased even further if we could employ solar panels that have higher efficiency or smaller carbon footprint in their manufacturing because the most dominant positive contributor to the footprint is the solar panel

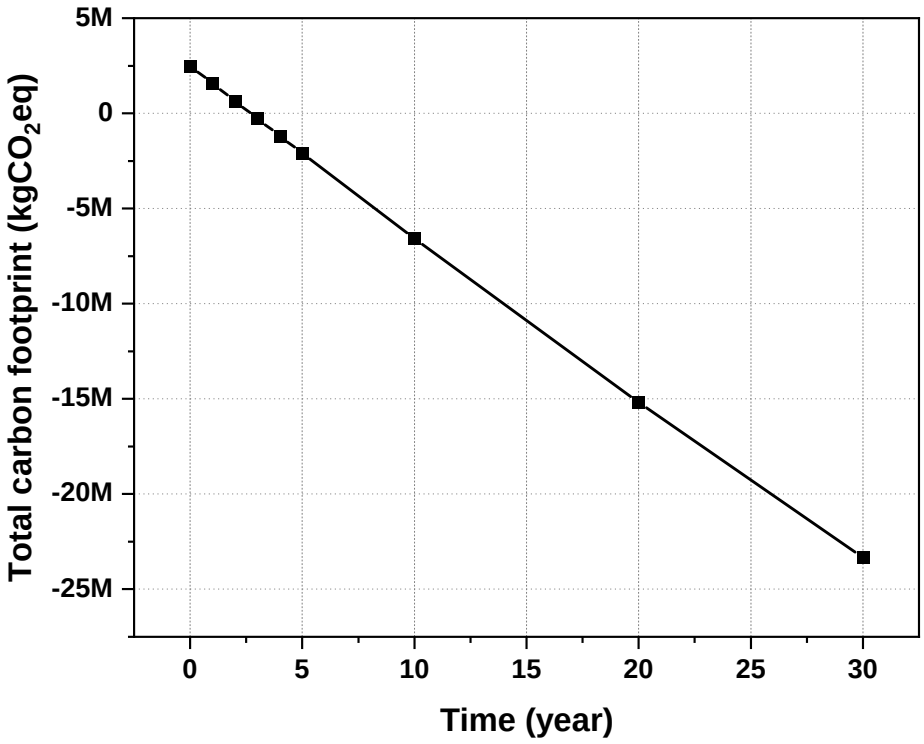

Figure B.2: The change in the total carbon footprint over time.

manufacturing process. Also, if we could develop and include ecosystems, such as green roofs, local bushes, and trees, in the study, they could contribute to the footprint in a negative way. Moreover, since vehicles in the parking lot are shaded by the solar panels, it helps keep the parked vehicles cool during the summer and helps reduce the removal of snow during the winter, which in turn could reduce the carbon footprint as well.

Bibliography

[1] Bureau of Transportation Statistics (BTS). Commodity flow survey (cfs) data and reports. Available at: https://www.bts.gov/topics/commodity-flow-survey-reports Accessed Mar 2020.

[2] Joseph Fiksel. A systems view of sustainability: The triple value model. *Environmental Development*, 2:138–141, 2012.

[3] Bhavik R Bakshi. Toward sustainable chemical engineering: The role of process systems engineering. *Annual review of chemical and biomolecular engineering*, 10:265–288, 2019.

[4] Sriram Satagopan, Yuan Sun, Jon R Parquette, and F Robert Tabita. Synthetic co_2-fixation enzyme cascades immobilized on self-assembled nanostructures that enhance co_2/o_2 selectivity of rubisco. *Biotechnology for biofuels*, 10(1):175, 2017.

[5] Detlef P Van Vuuren, Jae Edmonds, Mikiko Kainuma, Keywan Riahi, Allison Thomson, Kathy Hibbard, George C Hurtt, Tom Kram, Volker Krey, Jean-Francois Lamarque, et al. The representative concentration pathways: an overview. *Climatic change*, 109(1-2):5, 2011.

[6] Kyuha Lee, Tapajyoti Ghosh, and Bhavik R Bakshi. Toward multiscale consequential sustainable process design: Including the effects of economy and resource constraints with application to green urea production in a watershed. *Chemical Engineering Science*, 207:725–743, 2019.

[7] Ignacio E Grossmann and Christodoulos A Floudas. Active constraint strategy for flexibility analysis in chemical processes. *Computers & Chemical Engineering*, 11(6):675–693, 1987.

[8] Patrick Heffer and Michel Prud'homme. Global nitrogen fertilizer demand and supply: Trend, current level and outlook. In *International Nitrogen Initiative Conference. Melbourne, Australia*, 2016.

[9] Bhavik R Bakshi, Timothy G Gutowski, and Dusan P Sekulic. Claiming sustainability: requirements and challenges. *ACS Sustainable Chemistry & Engineering*, 6(3):3632–3639, 2018.

[10] Bhavik R Bakshi, Guy Ziv, and Michael D Lepech. Techno-ecological synergy: A framework for sustainable engineering. *Environmental science & technology*, 49(3):1752–1760, 2015.

[11] Utkarsh Shah and Bhavik R Bakshi. Accounting for nature's intermittency and growth while mitigating no_2 emissions by technoecological synergistic design—application to a chloralkali process. *Journal of Advanced Manufacturing and Processing*, 1(1-2):e10013, 2019.

[12] Sangwon Suh. Functions, commodities and environmental impacts in an ecological–economic model. *Ecological Economics*, 48(4):451–467, 2004.

[13] Rebecca J Hanes and Bhavik R Bakshi. Process to planet: A multiscale modeling framework toward sustainable engineering. *AIChE Journal*, 61(10):3332–3352, 2015.

[14] Daniel J Garcia and Fengqi You. The water-energy-food nexus and process systems engineering: A new focus. *Computers & Chemical Engineering*, 91:49–67, 2016.

[15] Rebecca J Hanes, Varsha Gopalakrishnan, and Bhavik R Bakshi. Including nature in the food-energy-water nexus can improve sustainability across multiple ecosystem services. *Resources, Conservation and Recycling*, 137:214–228, 2018.

[16] Marlies A Thomassen, Randi Dalgaard, Reinout Heijungs, and Imke De Boer. Attributional and consequential lca of milk production. *The International Journal of Life Cycle Assessment*, 13(4):339–349, 2008.

[17] Bhavik R Bakshi, Tapajyoti Ghosh, and Kyuha Lee. Engineering, markets, and human behavior: an essential integration for decisions toward sustainability. *Current Opinion in Chemical Engineering*, 26:164–169, 2019.

[18] Arne Kätelhön, André Bardow, and Sangwon Suh. Stochastic technology choice model for consequential life cycle assessment. *Environmental science & technology*, 50(23):12575–12583, 2016.

[19] J Mason Earles and Anthony Halog. Consequential life cycle assessment: a review. *The International Journal of Life Cycle Assessment*, 16(5):445–453, 2011.

[20] M Brander, R Tipper, C Hutchison, and G Davis. Technical paper: Consequential and attributional approaches to lca: a guide to policy makers with specific reference to greenhouse gas lca of biofuels, 2008.

[21] J Reinhard and Rainer Zah. Global environmental consequences of increased biodiesel consumption in switzerland: consequential life cycle assessment. *Journal of Cleaner Production*, 17:S46–S56, 2009.

[22] Henrik Lund, Brian Vad Mathiesen, Per Christensen, and Jannick Hoejrup Schmidt. Energy system analysis of marginal electricity supply in consequential lca. *The International Journal of Life Cycle Assessment*, 15(3):260–271, 2010.

[23] Eléonore Loiseau, Lynda Aissani, Samuel Le Féon, Faustine Laurent, Juliette Cerceau, Serenella Sala, and Philippe Roux. Territorial life cycle assessment (lca): What exactly is it about? a proposal towards using a common terminology and a research agenda. *Journal of Cleaner Production*, 176:474–485, 2018.

[24] Antonino Marvuglia, Enrico Benetto, Sameer Rege, and Colin Jury. Modelling approaches for consequential life-cycle assessment (c-lca) of bioenergy: critical review and proposed framework for biogas production. *Renewable and Sustainable Energy Reviews*, 25:768–781, 2013.

[25] Ian Vázquez-Rowe, Sameer Rege, Antonino Marvuglia, Julien Thénie, Alain Haurie, and Enrico Benetto. Application of three independent consequential lca approaches to the agricultural sector in luxembourg. *The International Journal of Life Cycle Assessment*, 18(8):1593–1604, 2013.

[26] Ian Vázquez-Rowe, Antonino Marvuglia, Sameer Rege, and Enrico Benetto. Applying consequential lca to support energy policy: land use change effects of bioenergy production. *Science of the Total Environment*, 472:78–89, 2014.

[27] Faye Duchin and Stephen H Levine. Sectors may use multiple technologies simultaneously: The rectangular choice-of-technology model with binding factor constraints. *Economic Systems Research*, 23(3):281–302, 2011.

[28] Faye Duchin and Stephen H Levine. The rectangular sector-by-technology model: not every economy produces every product and some products may rely on several technologies simultaneously. *Journal of Economic Structures*, 1(1):3, 2012.

[29] Hannah Förster and Johan Lilliestam. Modeling thermoelectric power generation in view of climate change. *Regional Environmental Change*, 10(4):327–338, 2010.

[30] Michelle TH Van Vliet, David Wiberg, Sylvain Leduc, and Keywan Riahi. Power-generation system vulnerability and adaptation to changes in climate and water resources. *Nature Climate Change*, 6(4):375, 2016.

[31] Jørgen E Olesen and Marco Bindi. Consequences of climate change for european agricultural productivity, land use and policy. *European journal of agronomy*, 16(4):239–262, 2002.

[32] Philip K Thornton, Peter G Jones, Gopal Alagarswamy, Jeff Andresen, and Mario Herrero. Adapting to climate change: agricultural system and household impacts in east africa. *Agricultural systems*, 103(2):73–82, 2010.

[33] Yi Yang, Wesley W Ingwersen, and David E Meyer. Exploring the relevance of spatial scale to life cycle inventory results using environmentally-extended input-output models of the united states. *Environmental modelling & software*, 99:52–57, 2018.

[34] Yi Yang and Reinout Heijungs. A generalized computational structure for regional life-cycle assessment. *The International Journal of Life Cycle Assessment*, 22(2):213–221, 2017.

[35] Xinyu Liu, Guy Ziv, and Bhavik R Bakshi. Ecosystem services in life cycle assessment-part 2: Adaptations to regional and serviceshed information. *Journal of cleaner production*, 197:772–780, 2018.

[36] Roy Haines-Young and Marion B Potschin. Common international classification of ecosystem services (cices) v5. 1 and guidance on the application of the revised structure. *European Environment Agency*, 53, 2018.

[37] International Organization for Standardization. *Environmental Management: Life Cycle Assessment; Principles and Framework*. Number 2006. ISO, 2006.

[38] Jane Bare. Traci 2.0: the tool for the reduction and assessment of chemical and other environmental impacts 2.0. *Clean Technologies and Environmental Policy*, 13(5):687–696, 2011.

[39] Yi Yang, Wesley W Ingwersen, Troy R Hawkins, Michael Srocka, and David E Meyer. Useeio: A new and transparent united states environmentally-extended input-output model. *Journal of cleaner production*, 158:308–318, 2017.

[40] National Renewable Energy Laboratory (NREL). U.s. life cycle inventory database (uslci). Available at: https://www.lcacommons.gov/ Accessed November 2018.

[41] Anne-Marie Boulay, Jane Bare, Lorenzo Benini, Markus Berger, Michael J Lathuillière, Alessandro Manzardo, Manuele Margni, Masaharu Motoshita, Montserrat Núñez, Amandine Valerie Pastor, et al. The wulca consensus characterization model for water scarcity footprints: assessing impacts of water consumption based on available water remaining (aware). *The International Journal of Life Cycle Assessment*, 23(2):368–378, 2018.

[42] Argonne National Laboratory. The greenhouse gases, regulated emissions, and energy use in transportation (greet) model, 2018 version.

[43] Rolf Frischknecht, Niels Jungbluth, Hans-Jörg Althaus, Gabor Doka, Roberto Dones, Thomas Heck, Stefanie Hellweg, Roland Hischier, Thomas Nemecek, Gerald Rebitzer, et al. The ecoinvent database: Overview and methodological framework (7 pp). *The international journal of life cycle assessment*, 10(1):3–9, 2005.

[44] U.S. Bureau of Economic Analysis (BEA). Interactive access to industry economic accounts data: Input-output. Available at: https://apps.bea.gov/iTable/itable.cfm?reqid=52&step=1 Accessed September 2019.

[45] U.S. Bureau of Economic Analysis (BEA). Regional input-output modeling system (rims ii). Available at: https://apps.bea.gov/regional/rims/ Accessed September 2019.

[46] Scott A Lindall, Douglas C Olson, and Gregory S Alward. Deriving multi-regional models using the implan national trade flows model. *Journal of Regional Analysis and Policy*, 36(1100-2016-89756), 2006.

[47] US EPA. Inventory of us greenhouse gas emissions and sinks: 1990–2017, 2019.

[48] World Resources Institute (WRI). Cait climate data explorer, 2015.

[49] U.S. Environmental Protection Agency (USEPA). 2014 national emissions inventory (nei) report. Available at: https://www.epa.gov/air-emissions-inventories Accessed November 2018.

[50] Brian R Pickard, Jessica Daniel, Megan Mehaffey, Laura E Jackson, and Anne Neale. Enviroatlas: A new geospatial tool to foster ecosystem services science and resource management. *Ecosystem Services*, 14:45–55, 2015.

[51] Andreas Ciroth. Ict for environment in life cycle applications openlca—a new open source software for life cycle assessment. *The International Journal of Life Cycle Assessment*, 12(4):209, 2007.

[52] Mark Goedkoop, Anne De Schryver, Michiel Oele, Sipke Durksz, and Douwe de Roest. Introduction to lca with simapro 7. *PRé Consultants, The Netherlands*, 2008.

[53] Sabrina Spatari, Michael Betz, Harald Florin, Martin Baitz, and Michael Faltenbacher. Using gabi 3 to perform life cycle assessment and life cycle engineering. *The International Journal of Life Cycle Assessment*, 6(2):81, 2001.

[54] Christopher Weber, Deanna Matthews, Aranya Venkatesh, Christine Costello, and H Matthews. The 2002 us benchmark version of the economic input-output life cycle assessment (eio-lca) model. *Green Design Institute, Carnegie Mellon University*, 2009.

[55] Shweta Singh and Bhavik R Bakshi. Eco-lca: A tool for quantifying the role of ecological resources in lca. In *2009 IEEE International Symposium on Sustainable Systems and Technology*, pages 1–6. IEEE, 2009.

[56] Tapajyoti Ghosh, Kyuha Lee, and Bhavik R Bakshi. Integrating market models and price effects in a multiscale sustainable process design framework. In *Computer Aided Chemical Engineering*, volume 47, pages 175–180. Elsevier, 2019.

[57] Andreas Jørgensen, Agathe Le Bocq, Liudmila Nazarkina, and Michael Hauschild. Methodologies for social life cycle assessment. *The international journal of life cycle assessment*, 13(2):96, 2008.

[58] Cheryl A Dieter, Molly A Maupin, Rodney R Caldwell, Melissa A Harris, Tamara I Ivahnenko, John K Lovelace, Nancy L Barber, and Kristin S Linsey. *Estimated use of water in the United States in 2015*. Number 1441. U.S. Geological Survey, 2018.

[59] U.S. Energy Information Administration. State energy data system (seds): 1960-2018. Available at: https://www.eia.gov/state/seds/seds-data-complete.php Accessed June 2020.

[60] Guobao Song, Mingjing Li, Henry Musoke Semakula, and Shushen Zhang. Food consumption and waste and the embedded carbon, water and ecological footprints of households in china. *Science of the Total Environment*, 529:191–197, 2015.

[61] Sonia Graham, Heinz Schandl, Liana J Williams, and Tira Foran. The effects of climate and socio-demographics on direct household carbon dioxide emissions in australia. *Geographical Research*, 51(4):424–438, 2013.

[62] Marja Salo, MK Mattinen-Yuryev, and Ari Nissinen. Opportunities and limitations of carbon footprint calculators to steer sustainable household consumption–analysis of nordic calculator features. *Journal of cleaner production*, 207:658–666, 2019.

[63] David Tilman and Michael Clark. Global diets link environmental sustainability and human health. *Nature*, 515(7528):518–522, 2014.

[64] Joseph Poore and Thomas Nemecek. Reducing food's environmental impacts through producers and consumers. *Science*, 360(6392):987–992, 2018.

[65] Christopher L Weber and H Scott Matthews. Quantifying the global and distributional aspects of american household carbon footprint. *Ecological economics*, 66(2-3):379–391, 2008.

[66] Angela Druckman and Tim Jackson. The carbon footprint of uk households 1990–2004: a socio-economically disaggregated, quasi-multi-regional input–output model. *Ecological economics*, 68(7):2066–2077, 2009.

[67] Christopher M Jones and Daniel M Kammen. Quantifying carbon footprint reduction opportunities for us households and communities. *Environmental science & technology*, 45(9):4088–4095, 2011.

[68] Yin Long, Yoshikuni Yoshida, Kai Fang, Haoran Zhang, and Maya Dhondt. City-level household carbon footprint from purchaser point of view by a modified input-output model. *Applied energy*, 236:379–387, 2019.

[69] Joe F Bozeman, Rayne Bozeman, and Thomas L Theis. Overcoming climate change adaptation barriers: A study on food–energy–water impacts of the average american diet by demographic group. *Journal of Industrial Ecology*, 24(2):383–399, 2020.

[70] Annika Carlsson-Kanyama, Marianne Pipping Ekström, and Helena Shanahan. Food and life cycle energy inputs: consequences of diet and ways to increase efficiency. *Ecological economics*, 44(2-3):293–307, 2003.

[71] Emily Huddart Kennedy, Harvey Krahn, and Naomi T Krogman. Egregious emitters: Disproportionality in household carbon footprints. *Environment and Behavior*, 46(5):535–555, 2014.

[72] Hussien Wa'el A, Fayyaz A Memon, and Dragan A Savic. An integrated model to evaluate water-energy-food nexus at a household scale. *Environmental modelling & software*, 93:366–380, 2017.

[73] Chelsea Mackie and Aaron P Wemhoff. Comparing greenhouse gas emissions associated with food away from home versus food at home in the united states. *Journal of Cleaner Production*, page 120930, 2020.

[74] U.S. Energy Information Administration. Weekly retail gasoline and diesel prices. Available at: https://www.eia.gov/dnav/pet/PET_PRI_GND_DCUS_NUS_A.htm Accessed June 2019.

[75] Hao Cai, Andrew Burnham, Michael Wang, Wen Hang, and Anant Vyas. The greet model expansion for well-to-wheels analysis of heavy-duty vehicles. Technical report, Argonne National Laboratory, IL, 2015.

[76] Leslie Eudy, Matthew Post, and M Jeffers. Fuel cell buses in u.s. transit fleets: Current status 2016. Technical report, National Renewable Energy Laboratory, 2016.

[77] U.S. Department of Energy. Clean cities alternative fuel price report. Technical report, 2018.

[78] U.S. Bureau of Transportation Statistics. Average passenger revenue per passenger-mile. Available at: https://www.bts.gov/content/average-passenger-revenue-passenger-mile Accessed June 2019.

[79] Wesley Ingwersen and Yi Yang. Useeio v1.1 - matrices. Available at: https://catalog.data.gov/dataset/useeio-v1-1-matrices Accessed October 2018.

[80] U.S. Energy Information Administration. Residential energy consumption survey (recs), 2015 recs survey data. Available at: https://www.eia.gov/consumption/residential/data/2015/ Accessed June 2020.

[81] Wen-Hsiu Huang. The determinants of household electricity consumption in taiwan: Evidence from quantile regression. *Energy*, 87:120–133, 2015.

[82] Christopher F Clark, Matthew J Kotchen, and Michael R Moore. Internal and external influences on pro-environmental behavior: Participation in a green electricity program. *Journal of environmental psychology*, 23(3):237–246, 2003.

[83] LC Zelezny, P Chua, and Christina Aldrich. Elaborating on gender differences in environmentalism-statistical data included. *Journal of Social Issues*, 56(3):443–445, 2000.

[84] Markus Vinnari, Pekka Mustonen, and Pekka Räsänen. Tracking down trends in non-meat consumption in finnish households, 1966-2006. *British Food Journal*, 2010.

[85] George A Olah, GK Surya Prakash, and Alain Goeppert. Anthropogenic chemical carbon cycle for a sustainable future. *Journal of the American Chemical Society*, 133(33):12881–12898, 2011.

[86] Jens Artz, Thomas E Müller, Katharina Thenert, Johanna Kleinekorte, Raoul Meys, André Sternberg, André Bardow, and Walter Leitner. Sustainable conversion of carbon dioxide: an integrated review of catalysis and life cycle assessment. *Chemical reviews*, 118(2):434–504, 2018.

[87] James Barber and Phong D Tran. From natural to artificial photosynthesis. *Journal of The Royal Society Interface*, 10(81):20120984, 2013.

[88] Iain McConnell, Gonghu Li, and Gary W Brudvig. Energy conversion in natural and artificial photosynthesis. *Chemistry & biology*, 17(5):434–447, 2010.

[89] Francesco Cherubini and Gerfried Jungmeier. Lca of a biorefinery concept producing bioethanol, bioenergy, and chemicals from switchgrass. *The International Journal of Life Cycle Assessment*, 15(1):53–66, 2010.

[90] Spencer M Whitney, Robert L Houtz, and Hernan Alonso. Advancing our understanding and capacity to engineer nature's co_2-sequestering enzyme, rubisco. *Plant Physiology*, 155(1):27–35, 2011.

[91] John A Raven. Rubisco: still the most abundant protein of earth? *New Phytologist*, 198(1):1–3, 2013.

[92] Wei Kang, Jiahui Liu, Jianpeng Wang, Yunyu Nie, Zhihong Guo, and Jiang Xia. Cascade biocatalysis by multienzyme–nanoparticle assemblies. *Bioconjugate chemistry*, 25(8):1387–1394, 2014.

[93] Shaowei Ding, Allison A Cargill, Igor L Medintz, and Jonathan C Claussen. Increasing the activity of immobilized enzymes with nanoparticle conjugation. *Current opinion in biotechnology*, 34:242–250, 2015.

[94] Quentin M Dudley, Ashty S Karim, and Michael C Jewett. Cell-free metabolic engineering: biomanufacturing beyond the cell. *Biotechnology journal*, 10(1):69–82, 2015.

[95] Wolf-Dieter Fessner. Systems biocatalysis: Development and engineering of cell-free "artificial metabolisms" for preparative multi-enzymatic synthesis. *New biotechnology*, 32(6):658–664, 2015.

[96] Se Hye Kim, Jonah A Kaplan, Yuan Sun, Aileen Shieh, Hui-Lung Sun, Carlo M Croce, Mark W Grinstaff, and Jon R Parquette. The self-assembly of anticancer camptothecin–dipeptide nanotubes: a minimalistic and high drug loading approach to increased efficacy. *Chemistry–A European Journal*, 21(1):101–105, 2015.

[97] Ines Mandl and Carl Neuberg. Preparation of d (+)-2-phosphoglyceric acid. *Methods in enzymology*, 3:214–216, 1957.

[98] Andrea Weckbecker, Harald Gröger, and Werner Hummel. Regeneration of nicotinamide coenzymes: principles and applications for the synthesis of chiral compounds. In *Biosystems Engineering I*, pages 195–242. Springer, 2010.

[99] Richard H Fish, John B Kerr, and Christine H Lo. Agents for replacement of nad+/nadh system in enzymatic reactions, April 6 2004. US Patent 6,716,596.

[100] Sriram Satagopan, Sum Chan, L Jeanne Perry, and F Robert Tabita. Structure-function studies with the unique hexameric form ii ribulose-1, 5-bisphosphate carboxylase/oxygenase (rubisco) from rhodopseudomonas palustris. *Journal of Biological Chemistry*, 289(31):21433–21450, 2014.

[101] Sriram Satagopan and F Robert Tabita. Rubisco selection using the vigorously aerobic and metabolically versatile bacterium ralstonia eutropha. *The FEBS journal*, 283(15):2869–2880, 2016.

[102] Daisuke Kobayashi, Masahiro Tamoi, Toshio Iwaki, Shigeru Shigeoka, and Akira Wadano. Molecular characterization and redox regulation of phosphoribulokinase from the cyanobacterium synechococcus sp. pcc 7942. *Plant and cell physiology*, 44(3):269–276, 2003.

[103] John Villadsen, Jens Nielsen, and Gunnar Lidén. Chemicals from metabolic pathways. In *Bioreaction engineering principles*, pages 7–62. Springer, 2011.

[104] Petra Peters-Wendisch, Michael Stolz, Helga Etterich, Nicole Kennerknecht, Hermann Sahm, and Lothar Eggeling. Metabolic engineering of corynebacterium glutamicum for l-serine production. *Appl. Environ. Microbiol.*, 71(11):7139–7144, 2005.

[105] Borja Cascales-Miñana, Jesús Muñoz-Bertomeu, María Flores-Tornero, Armand Djoro Anoman, José Pertusa, Manuel Alaiz, Sonia Osorio, Alisdair R Fernie, Juan Segura, and Roc Ros. The phosphorylated pathway of serine biosynthesis is essential both for male gametophyte and embryo development and for root growth in arabidopsis. *The Plant Cell*, 25(6):2084–2101, 2013.

[106] Tairo Hagishita, Toyokazu Yoshida, Yoshikazu Izumi, and Toshio Mitsunaga. Efficient l-serine production from methanol and glycine by resting cells of methylobacterium sp. strain mn43. *Bioscience, biotechnology, and biochemistry*, 60(10):1604–1607, 1996.

[107] K Drauz, I Grayson, A Kleemann, HP Krimmer, W. Leuchtenberger, and C Weckbecker. Amino acids. ullmann's encyclopedia of industrial chemistry, 2012.

[108] Marcelle C McManus, Caroline M Taylor, Alison Mohr, Carly Whittaker, Corinne D Scown, Aiduan Li Borrion, Neryssa J Glithero, and Yao Yin. Challenge clusters facing lca in environmental decision-making—what we can learn from biofuels. *The international journal of life cycle assessment*, 20(10):1399–1414, 2015.

[109] HJ Althaus, Mike Chudacoff, Roland Hischier, Niels Jungbluth, Maggie Osses, Alex Primas, et al. Life cycle inventories of chemicals. *Ecoinvent report*, 2, 2007.

[110] Jane Bare, Daniel Young, S Qam, Matthew Hopton, and S Chief. Tool for the reduction and assessment of chemical and other environmental impacts (traci). *Washington, DC: US Environmental Protection Agency*, 2012.

[111] World Health Organization et al. Indoor air quality: organic pollutants. 1989.

[112] Envrionmental Protection Agencey EPA. Technical overview of volatile organic compounds. *Indoor Air Quality, Washington DC*, 2016.

[113] Yi Zhang, Bhavik R Bakshi, and E Sahle Demessie. Life cycle assessment of an ionic liquid versus molecular solvents and their applications. *Environmental science & technology*, 42(5):1724–1730, 2008.

[114] J George Buta and Michael J Novak. Isolation of camptothecin and 10-methoxycamptothecin from camptotheca acuminata by gel permeation chromatography. *Industrial & Engineering Chemistry Product Research and Development*, 17(2):160–161, 1978.

[115] Gunnar Myhre, Drew Shindell, and Julia Pongratz. Anthropogenic and natural radiative forcing. 2014.

[116] Stephen J Walker, Ray F Weiss, and Peter K Salameh. Reconstructed histories of the annual mean atmospheric mole fractions for the halocarbons cfc-11 cfc-12, cfc-113, and carbon tetrachloride. *Journal of Geophysical Research: Oceans*, 105(C6):14285–14296, 2000.

[117] Palanivel Sathishkumar, Seralathan Kamala-Kannan, Min Cho, Jae Su Kim, Tony Hadibarata, Mohd Razman Salim, and Byung-Taek Oh. Laccase immobilization on cellulose nanofiber: the catalytic efficiency and recyclic application for simulated dye effluent treatment. *Journal of Molecular Catalysis B: Enzymatic*, 100:111–120, 2014.

[118] Wen-Can Huang, Wei Wang, Changhu Xue, and Xiangzhao Mao. Effective enzyme immobilization onto a magnetic chitin nanofiber composite. *ACS Sustainable Chemistry & Engineering*, 6(7):8118–8124, 2018.

[119] Dajun Yue, Shyama Pandya, and Fengqi You. Integrating hybrid life cycle assessment with multiobjective optimization: A modeling framework. *Environmental Science & Technology*, 50(3):1501–1509, 2016.

[120] Rebecca Frauzem, Pichayapan Kongpanna, Kosan Roh, Jay H Lee, Varong Pavarajarn, Suttichai Assabumrungrat, and Rafiqul Gani. Sustainable process design: sustainable process networks for carbon dioxide conversion. In *Computer Aided Chemical Engineering*, volume 36, pages 175–195. Elsevier, 2015.

[121] Mariano Martin and Ignacio E. Grossmann. On the Systematic Synthesis of Sustainable Biorefineries. *Industrial Engineering Chemistry and Research*, 52(9):3044–3064, MAR 6 2013.

[122] Temitope Falano, Harish K. Jeswani, and Adisa Azapagic. Assessing the environmental sustainability of ethanol from integrated biorefineries. *Biotechnology Journal*, 9(6):753–765, 2014.

[123] Rebecca J Hanes and Bhavik R Bakshi. Sustainable process design by the process to planet framework. *AIChE Journal*, 61(10):3320–3331, 2015.

[124] Tapajyoti Ghosh and Bhavik R Bakshi. Process to planet approach to sustainable process design: Multiple objectives and byproducts. *Theoretical Foundations of Chemical Engineering*, 51(6):936–948, 2017.

[125] Janire Pascual-González, Laureano Jiménez-Esteller, Gonzalo Guillén-Gosálbez, Jeffrey J Siirola, and Ignacio E Grossmann. Macro-economic multi-objective input–output model for minimizing co_2 emissions: Application to the us economy. *AIChE Journal*, 62(10):3639–3656, 2016.

[126] Anna Voll, Giovanni Sorda, Felix Optehostert, Reinhard Madlener, and Wolfgang Marquardt. Integration of market dynamics into the design of biofuel processes. In *Computer Aided Chemical Engineering*, volume 31, pages 850–854. Elsevier, 2012.

[127] Jian Gong and Fengqi You. Consequential life cycle optimization: general conceptual framework and application to algal renewable diesel production. *ACS Sustainable Chemistry & Engineering*, 5(7):5887–5911, 2017.

[128] Dajun Yue, Fengqi You, and Seth W Snyder. Biomass-to-bioenergy and biofuel supply chain optimization: overview, key issues and challenges. *Computers & Chemical Engineering*, 66:36–56, 2014.

[129] Xinyu Liu, Guy Ziv, and Bhavik R Bakshi. Ecosystem services in life cycle assessment-part 1: A computational framework. *Journal of Cleaner Production*, 197:314–322, 2018.

[130] Xinyu Liu and Bhavik R Bakshi. Ecosystem services in life cycle assessment while encouraging techno-ecological synergies. *Journal of Industrial Ecology*, 23(2):347–360, 2019.

[131] Harold James. Deglobalization: The rise of disembedded unilateralism. *Annual Review of Financial Economics*, 10:219–237, 2018.

[132] Rong Lan, John TS Irvine, and Shanwen Tao. Ammonia and related chemicals as potential indirect hydrogen storage materials. *International Journal of Hydrogen Energy*, 37(2):1482–1494, 2012.

[133] Asbjørn Klerke, Claus Hviid Christensen, Jens K Nørskov, and Tejs Vegge. Ammonia for hydrogen storage: challenges and opportunities. *Journal of Materials Chemistry*, 18(20):2304–2310, 2008.

[134] Stefan Seuring and Martin Müller. From a literature review to a conceptual framework for sustainable supply chain management. *Journal of cleaner production*, 16(15):1699–1710, 2008.

[135] Kannan Govindan, Roohollah Khodaverdi, and Ahmad Jafarian. A fuzzy multi criteria approach for measuring sustainability performance of a supplier based on triple bottom line approach. *Journal of Cleaner production*, 47:345–354, 2013.

[136] Lazaros G Papageorgiou. Supply chain optimisation for the process industries: Advances and opportunities. *Computers & Chemical Engineering*, 33(12):1931–1938, 2009.

[137] Leslie Jacquemin, Pierre-Yves Pontalier, and Caroline Sablayrolles. Life cycle assessment (lca) applied to the process industry: a review. *The International Journal of Life Cycle Assessment*, 17(8):1028–1041, 2012.

[138] Carla Pieragostini, Miguel C Mussati, and Pío Aguirre. On process optimization considering lca methodology. *Journal of environmental management*, 96(1):43–54, 2012.

[139] Stefan Seuring. A review of modeling approaches for sustainable supply chain management. *Decision support systems*, 54(4):1513–1520, 2013.

[140] Vered Blass and Charles J Corbett. Same supply chain, different models: Integrating perspectives from life cycle assessment and supply chain management. *Journal of Industrial Ecology*, 22(1):18–30, 2018.

[141] Wassily Leontief. Quantitative input and output relations in the economic systems of the united states. *The review of economic statistics*, pages 105–125, 1936.

[142] Wassily Leontief. Environmental repercussions and the economic structure: an input-output approach. *The review of economics and statistics*, pages 262–271, 1970.

[143] Chris Hendrickson, Arpad Horvath, Satish Joshi, and Lester Lave. Peer reviewed: economic input–output models for environmental life-cycle assessment. *Environmental science & technology*, 32(7):184A–191A, 1998.

[144] Naci Dilekli and Faye Duchin. Prospects for cellulosic biofuel production in the northeastern united states: A scenario analysis. *Journal of Industrial Ecology*, 20(1):120–131, 2016.

[145] Nathaniel P Springer. Physical, technical, and economic accessibility of resources and reserves need to be distinguished by grade: Application to the case of phosphorus. *Science of the Total Environment*, 577:319–328, 2017.

[146] Gustavo Larrea-Gallegos, Ian Vázquez-Rowe, Hugo Wiener, and Ramzy Kahhat. Applying the technology choice model in consequential life cycle assessment: a case study in the peruvian agricultural sector. *Journal of Industrial Ecology*, 23(3):601–614, 2018.

[147] U.S. Census Bureau. North american industry classification system. Available at: https://www.census.gov/eos/www/naics/ Accessed November 2018.

[148] Karen J Horowitz and Mark A Planting. Concepts and methods of the input-output accounts. 2006.

[149] Paul R Seaber, F Paul Kapinos, and George L Knapp. Hydrologic unit maps. 1987.

[150] USDA Forest Service. i-tree landscape. Available at: https://landscape.itreetools.org/ Accessed Feb 2018.

[151] Bonnie G Colby. Transactions costs and efficiency in western water allocation. *American Journal of Agricultural Economics*, 72(5):1184–1192, 1990.

[152] Charles C Callahan and James R Hanson. Principles of water rights law in ohio. *Division of Water, Department of Natural Resources, State of Ohio*, 1979.

[153] U.S. Energy Information Administration (USEIA). Electricity: Form eia-923. Available at: https://www.eia.gov/electricity/data/eia923/ Accessed April 2018.

[154] Pichayapan Kongpanna, Varong Pavarajarn, Rafiqul Gani, and Suttichai Assabumrungrat. Techno-economic evaluation of different co_2-based processes for dimethyl carbonate production. *Chemical Engineering Research and Design*, 93:496–510, 2015.

[155] Lucien H Cook. Urea synthesis process, February 20 1968. US Patent 3,370,090.

[156] Giorgio Pagani. Process for urea production involving a carbon dioxide stripping step, November 4 1997. US Patent 5,684,194.

[157] Gary R Kocis and Ignacio E Grossmann. Computational experience with dicopt solving minlp problems in process systems engineering. *Computers & Chemical Engineering*, 13(3):307–315, 1989.

[158] Lorenz T Biegler, Ignacio E Grossmann, and Arthur W Westerberg. Systematic methods for chemical process design. 1997.

[159] Warren D Seider, JD Seader, Daniel R Lewin, and Soemantri Widagdo. Product and process design principles: Synthesis, analysis, and design, 3rd edition, 2008.

[160] Mark Brouwer. Thermodynamics of the urea process. *Urea Know How*, 2009.

[161] Hannes Müller Schmied, Stephanie Eisner, Daniela Franz, Martin Wattenbach, Felix Theodor Portmann, Martina Flörke, and Petra Döll. Sensitivity of simulated global-scale freshwater fluxes and storages to input data, hydrological model structure, human water use and calibration. *Hydrology and Earth System Sciences*, 18(9):3511–3538, 2014.

[162] Wayne B Solley, Robert R Pierce, and Howard A Perlman. *Estimated use of water in the United States in 1995*. US Geological Survey, 1998.

[163] U.S. Energy Information Administration (USEIA). How much carbon dioxide is produced when different fuels are burned? Available at: https://www.eia.gov/tools/faqs/faq.php?id=73&t=11 Accessed October 2018.

[164] Corinne Le Quéré, Robbie M Andrew, Pierre Friedlingstein, Stephen Sitch, Julia Pongratz, Andrew C Manning, Jan Ivar Korsbakken, Glen P Peters, Josep G Canadell, Robert B Jackson, et al. Global carbon budget 2017. *Earth System Science Data Discussions*, pages 1–79, 2017.

[165] U.S. Energy Information Administration (USEIA). Energy and the environment explained: Where greenhouse gases come from. Available at: https://www.eia.gov/energyexplained/index.php?page=environment_where_ghg_come_from Accessed November 2018.

[166] British Petroleum. Bp statistical review of world energy 2018., 2018.

[167] U.S. Energy Information Administration (USEIA). Natural gas proved reserves, wet after lease separation. Available at: https://www.eia.gov/dnav/ng/ng_enr_wals_a_EPG0_R21_Bcf_a.htm Accessed October 2018.

[168] U.S. Energy Information Administration (USEIA). Shale gas. Available at: https://www.eia.gov/dnav/ng/ng_enr_shalegas_a_EPG0_R5301_Bcf_a.htm Accessed October 2018.

[169] U.S. Energy Information Administration (USEIA). Natural gas proved reserves, wet after lease separation. Available at: https://www.eia.gov/dnav/ng/ng_enr_wals_a_EPG0_r30_Bcf_a.htm Accessed October 2018.

[170] U.S. Energy Information Administration (USEIA). Shale gas. Available at: https://www.eia.gov/dnav/ng/ng_enr_shalegas_a_EPG0_R5302_Bcf_a.htm Accessed October 2018.

[171] U.S. Department of Agriculture (USDA). Land values 2017 summary, 2017.

[172] Dakota Gasification Company. Urea. Available at: https://www.dakotagas.com/products/fertilizers/urea Accessed October 2018.

[173] Engro Corporation Limited. World's largest urea plant starts production in pakistan. Available at: https://www.engro.com/news-center/worlds-largest-urea-plant-starts-production-pakistan/ Accessed October 2018.

[174] F Mueller-Langer, E Tzimas, M Kaltschmitt, and S Peteves. Techno-economic assessment of hydrogen production processes for the hydrogen economy for the short and medium term. *International Journal of Hydrogen Energy*, 32(16):3797–3810, 2007.

[175] Joel Martinez-Frias, Ai-Quoc Pham, and Salvador M Aceves. A natural gas-assisted steam electrolyzer for high-efficiency production of hydrogen. *International Journal of Hydrogen Energy*, 28(5):483–490, 2003.

[176] US EIA. Levelized cost of new generation resources in the annual energy outlook 2013. *Washington DC: US Energy Information Administration*, 2013.

[177] US EIA. Levelized cost and levelized avoided cost of new generation resources in the annual energy outlook 2018. *Washington DC: US Energy Information Administration*, 2018.

[178] John Deutch. The good news about gas: the natural gas revolution and its consequences. *Foreign Affairs*, pages 82–93, 2011.

[179] Tapajyoti Ghosh and Bhavik R Bakshi. Designing biofuel supply chains while mitigating harmful algal blooms with treatment wetlands. *Computers & Chemical Engineering*, 126:113–127, 2019.

[180] Jun-Ki Choi, Bhavik R Bakshi, and Timothy Haab. Effects of a carbon price in the us on economic sectors, resource use, and emissions: An input–output approach. *Energy Policy*, 38(7):3527–3536, 2010.

[181] Jun-Ki Choi, Bhavik R Bakshi, Klaus Hubacek, and Jordan Nader. A sequential input–output framework to analyze the economic and environmental implications of energy policies: Gas taxes and fuel subsidies. *Applied energy*, 184:830–839, 2016.

[182] Roy Haines-Young and Marion Potschin-Young. Revision of the common international classification for ecosystem services (cices v5. 1): a policy brief. *One Ecosystem*, 3:e27108, 2018.

[183] Joseph Fiksel, Randy Bruins, Annette Gatchett, Alice Gilliland, and Marilyn Ten Brink. The triple value model: a systems approach to sustainable solutions. *Clean Technologies and Environmental Policy*, 16(4):691–702, 2014.

[184] Dagmar Schröter, Wolfgang Cramer, Rik Leemans, I Colin Prentice, Miguel B Araújo, Nigel W Arnell, Alberte Bondeau, Harald Bugmann, Timothy R Carter, Carlos A Gracia, et al. Ecosystem service supply and vulnerability to global change in europe. *science*, 310(5752):1333–1337, 2005.

[185] M Rebecca Shaw, Linwood Pendleton, D Richard Cameron, Belinda Morris, Dominique Bachelet, Kirk Klausmeyer, Jason MacKenzie, David R Conklin, Gregrory N Bratman, James Lenihan, et al. The impact of climate change on california's ecosystem services. *Climatic Change*, 109(1):465–484, 2011.

[186] William D Nordhaus. A review of the stern review on the economics of climate change. *Journal of economic literature*, 45(3):686–702, 2007.

[187] Jeremy Martinich and Allison Crimmins. Climate damages and adaptation potential across diverse sectors of the united states. *Nature climate change*, 9(5):397, 2019.

[188] Nicholas H Stern, Siobhan Peters, Vicki Bakhshi, Alex Bowen, Catherine Cameron, Sebastian Catovsky, Diane Crane, Sophie Cruickshank, Simon Dietz, Nicola Edmonson, et al. *Stern Review: The economics of climate change*, volume 30. Cambridge University Press Cambridge, 2006.

[189] Niall Mac Dowell, Paul S Fennell, Nilay Shah, and Geoffrey C Maitland. The role of co_2 capture and utilization in mitigating climate change. *Nature Climate Change*, 7(4):243–249, 2017.

[190] Eric Masanet and Michael E Walker. Energy-water efficiency and us industrial steam. *AIChE Journal*, 59(7):2268–2274, 2013.

[191] Prakash Rao, Darren Sholes, and Joe Cresko. Evaluation of us manufacturing subsectors at risk of physical water shortages. *Environmental science & technology*, 53(5):2295–2303, 2019.

[192] Michael E Walker, Zhen Lv, and Eric Masanet. Industrial steam systems and the energy-water nexus. *Environmental science & technology*, 47(22):13060–13067, 2013.

[193] Paul CD Milly, Julio Betancourt, Malin Falkenmark, Robert M Hirsch, Zbigniew W Kundzewicz, Dennis P Lettenmaier, and Ronald J Stouffer. Stationarity is dead: Whither water management? *Science*, 319(5863):573–574, 2008.

[194] Ignacio E Grossmann, Bruno A Calfa, and Pablo Garcia-Herreros. Evolution of concepts and models for quantifying resiliency and flexibility of chemical processes. *Computers & Chemical Engineering*, 70:22–34, 2014.

[195] Wendy Francesconi, Raghavan Srinivasan, Elena Pérez-Miñana, Simon P Willcock, and Marcela Quintero. Using the soil and water assessment tool (swat) to model ecosystem services: A systematic review. *Journal of Hydrology*, 535:625–636, 2016.

[196] Valérie Masson-Delmotte, Panmao Zhai, Hans-Otto Pörtner, Debra Roberts, J Skea, PR Shukla, Anna Pirani, W Moufouma-Okia, C Péan, R Pidcock, et al. *Global Warming of 1.5 °C: An IPCC Special Report on the Impacts of Global Warming of 1.5 °C Above Pre-industrial Levels and Related Global Greenhouse Gas Emission Pathways, in the Context of Strengthening the Global Response to the Threat of Climate Change, Sustainable Development, and Efforts to Eradicate Poverty*. World Meteorological Organization Geneva, Switzerland, 2018.

[197] Keywan Riahi, Shilpa Rao, Volker Krey, Cheolhung Cho, Vadim Chirkov, Guenther Fischer, Georg Kindermann, Nebojsa Nakicenovic, and Peter Rafaj. Rcp 8.5—a scenario of comparatively high greenhouse gas emissions. *Climatic Change*, 109(1-2):33, 2011.

[198] Allison M Thomson, Katherine V Calvin, Steven J Smith, G Page Kyle, April Volke, Pralit Patel, Sabrina Delgado-Arias, Ben Bond-Lamberty, Marshall A Wise, Leon E Clarke, et al. Rcp4. 5: a pathway for stabilization of radiative forcing by 2100. *Climatic change*, 109(1-2):77, 2011.

[199] USGS Geo Data Portal. Projected future loca statistical downscaling (localized constructed analogs) statistically downscaled cmip5 climate projections for north america, 2019. Available at: https://cida.usgs.gov/gdp/ Accessed Nov 2019.

[200] David W Pierce, Daniel R Cayan, and Bridget L Thrasher. Statistical downscaling using localized constructed analogs (loca). *Journal of Hydrometeorology*, 15(6):2558–2585, 2014.

[201] Susan L Neitsch, Jeffrey G Arnold, Jim R Kiniry, and Jimmy R Williams. Soil and water assessment tool theoretical documentation version 2009. Technical report, Texas Water Resources Institute, 2011.

[202] S Khanal, R Lal, G Kharel, and J Fulton. Identification and classification of critical soil and water conservation areas in the muskingum river basin in ohio. *Journal of Soil and Water Conservation*, 73(2):213–226, 2018.

[203] Heinz G Stefan and Eric B Preud'homme. Stream temperature estimation from air temperature. *JAWRA Journal of the American Water Resources Association*, 29(1):27–45, 1993.

[204] Ross Edward Swaney and Ignacio E Grossmann. An index for operational flexibility in chemical process design. part i: Formulation and theory. *AIChE Journal*, 31(4):621–630, 1985.

[205] Qi Zhang, Ignacio E Grossmann, and Ricardo M Lima. On the relation between flexibility analysis and robust optimization for linear systems. *AIChE Journal*, 62(9):3109–3123, 2016.

[206] Hao Jiang, Bingzhen Chen, and Ignacio E Grossmann. New algorithm for the flexibility index problem of quadratic systems. *AIChE Journal*, 64(7):2486–2499, 2018.

[207] Joshua L Pulsipher, Daniel Rios, and Victor M Zavala. A computational framework for quantifying and analyzing system flexibility. *Computers & Chemical Engineering*, 126:342–355, 2019.

[208] Hagen Koch and Stefan Vögele. Dynamic modelling of water demand, water availability and adaptation strategies for power plants to global change. *Ecological Economics*, 68(7):2031–2039, 2009.

[209] Andreas M Culbertson, Jay F Martin, Noel Aloysius, and Stuart A Ludsin. Anticipated impacts of climate change on 21st century maumee river discharge and nutrient loads. *Journal of Great Lakes Research*, 42(6):1332–1342, 2016.

[210] Terrence F Yee and Ignacio E Grossmann. Simultaneous optimization models for heat integration—ii. heat exchanger network synthesis. *Computers & Chemical Engineering*, 14(10):1165–1184, 1990.

[211] Veniamin D Dimitriadis and Efstratios N Pistikopoulos. Flexibility analysis of dynamic systems. *Industrial & Engineering Chemistry Research*, 34(12):4451–4462, 1995.

[212] Ruth Dittrich, Anita Wreford, and Dominic Moran. A survey of decision-making approaches for climate change adaptation: Are robust methods the way forward? *Ecological Economics*, 122:79–89, 2016.

[213] Sarah Fletcher, Megan Lickley, and Kenneth Strzepek. Learning about climate change uncertainty enables flexible water infrastructure planning. *Nature communications*, 10(1):1782, 2019.

[214] William C Rooney and Lorenz T Biegler. Design for model parameter uncertainty using nonlinear confidence regions. *AIChE Journal*, 47(8):1794–1804, 2001.

[215] EN Pistikopoulos and TA Mazzuchi. A novel flexibility analysis approach for processes with stochastic parameters. *Computers & Chemical Engineering*, 14(9):991–1000, 1990.

[216] DA Straub and IE Grossmann. Integrated stochastic metric of flexibility for systems with discrete state and continuous parameter uncertainties. *Computers & Chemical Engineering*, 14(9):967–985, 1990.

[217] Andrew N Sharpley and Jimmy R Williams. Epic-erosion/productivity impact calculator. i: Model documentation. ii: User manual. *Technical Bulletin-United States Department of Agriculture*, (1768), 1990.

[218] David J Lampert, Hao Cai, Zhichao Wang, Jennifer Keisman, May Wu, Jeongwoo Han, Jennifer Dunn, John L Sullivan, Amgad Elgowainy, Michael Wang, et al. Development of a life cycle inventory of water consumption associated with the production of transportation fuels. Technical report, Argonne National Lab.(ANL), Argonne, IL (United States), 2015.

[219] Varsha Gopalakrishnan and Bhavik R Bakshi. Ecosystems as unit operations for local techno-ecological synergy: Integrated process design with treatment wetlands. *AIChE Journal*, 64(7):2390–2407, 2018.

[220] Luke T Miller and Chan S Park. A learning real options framework with application to process design and capacity planning. *Production and Operations Management*, 14(1):5–20, 2005.

[221] Berry Gersonius, Richard Ashley, Assela Pathirana, and Chris Zevenbergen. Managing the flooding system's resiliency to climate change. In *Proceedings of the Institution of Civil Engineers-Engineering Sustainability*, volume 163, pages 15–23. Thomas Telford Ltd, 2010.

[222] J Marques, M Cunha, D Savić, and O Giustolisi. Dealing with uncertainty through real options for the multi-objective design of water distribution networks. *Procedia Engineering*, 89:856–863, 2014.

[223] Marjolijn Haasnoot, Hans Middelkoop, Astrid Offermans, Eelco Van Beek, and Willem PA Van Deursen. Exploring pathways for sustainable water management in river deltas in a changing environment. *Climatic Change*, 115(3-4):795–819, 2012.

[224] Marjolijn Haasnoot, Jan H Kwakkel, Warren E Walker, and Judith ter Maat. Dynamic adaptive policy pathways: A method for crafting robust decisions for a deeply uncertain world. *Global environmental change*, 23(2):485–498, 2013.

[225] John W Finley and James N Seiber. The nexus of food, energy, and water. *Journal of agricultural and food chemistry*, 62(27):6255–6262, 2014.

[226] CCDF Van Ree and PJH Van Beukering. Geosystem services: a concept in support of sustainable development of the subsurface. *Ecosystem services*, 20:30–36, 2016.

[227] Marc Fasel, Christian Brethaut, Elham Rouholahnejad, Martin Ariel Lacayo-Emery, and Anthony Lehmann. Blue water scarcity in the black sea catchment: Identifying key actors in the water-ecosystem-energy-food nexus. *Environmental Science & Policy*, 66:140–150, 2016.

[228] Armağan Karabulut, Benis N Egoh, Denis Lanzanova, Bruna Grizzetti, Giovanni Bidoglio, Liliana Pagliero, Fayçal Bouraoui, Alberto Aloe, Arnaud Reynaud, Joachim Maes, et al. Mapping water provisioning services to support the ecosystem–water–food–energy nexus in the danube river basin. *Ecosystem services*, 17:278–292, 2016.

[229] Armağan Aloe Karabulut, Eleonora Crenna, Serenella Sala, and Angel Udias. A proposal for integration of the ecosystem-water-food-land-energy (ewfle) nexus concept into life cycle assessment: A synthesis matrix system for food security. *Journal of cleaner production*, 172:3874–3889, 2018.

[230] Stephan Hülsmann, Janez Sušnik, Karsten Rinke, Simon Langan, Dianneke van Wijk, Annette BG Janssen, and Wolf M Mooij. Integrated modelling and management of water resources: the ecosystem perspective on the nexus approach. *Current Opinion in Environmental Sustainability*, 40:14–20, 2019.

[231] Armağan Aloe Karabulut, Angel Udias, and Olga Vigiak. Assessing the policy scenarios for the ecosystem water food energy (ewfe) nexus in the mediterranean region. *Ecosystem services*, 35:231–240, 2019.

[232] Michael Charles, Guy Ziv, Gil Bohrer, and Bhavik R Bakshi. Connecting air quality regulating ecosystem services with beneficiaries through quantitative serviceshed analysis. *Ecosystem Services*, 41:101057, 2020.

[233] Guangyu Wang, Shari Mang, Haisheng Cai, Shirong Liu, Zhiqiang Zhang, Liguo Wang, and John L Innes. Integrated watershed management: evolution, development and emerging trends. *Journal of Forestry Research*, 27(5):967–994, 2016.

[234] Avner Vengosh, Nathaniel Warner, Rob Jackson, and Tom Darrah. The effects of shale gas exploration and hydraulic fracturing on the quality of water resources in the united states. *Procedia Earth and Planetary Science*, 7:863–866, 2013.

[235] Radisav D Vidic, Susan L Brantley, Julie M Vandenbossche, David Yoxtheimer, and Jorge D Abad. Impact of shale gas development on regional water quality. *science*, 340(6134):1235009, 2013.

[236] US EIA. Monthly energy review. 2019.

[237] Hao Cai, M Wang, A Elgowainy, and J Han. Updated greenhouse gas and criteria air pollutant emission factors and their probability distribution functions for electricity generating units. Technical report, Argonne National Lab.(ANL), Argonne, IL (United States), 2012.

[238] Robert B Finkelman, William Orem, Vincent Castranova, Calin A Tatu, Harvey E Belkin, Baoshan Zheng, Harry E Lerch, Susan V Maharaj, and Anne L Bates. Health impacts of coal and coal use: possible solutions. *International Journal of Coal Geology*, 50(1-4):425–443, 2002.

[239] US Energy Information Administration. Natural gas gross withdrawals and production. 2019.

[240] Corrie E Clark, Robert M Horner, and Christopher B Harto. Life cycle water consumption for shale gas and conventional natural gas. *Environmental science & technology*, 47(20):11829–11836, 2013.

[241] Aviva Loew, Paulina Jaramillo, and Haibo Zhai. Marginal costs of water savings from cooling system retrofits: a case study for texas power plants. *Environmental Research Letters*, 11(10):104004, 2016.

[242] Michael Mendelsohn, Travis Lowder, and Brendan Canavan. Utility-scale concentrating solar power and photovoltaic projects: A technology and market overview, 2012.

[243] EIA. Levelized cost and levelized avoided cost of new generation resources in the annual energy outlook 2019, 2019.

[244] Chunshan Song. Global challenges and strategies for control, conversion and utilization of co_2 for sustainable development involving energy, catalysis, adsorption and chemical processing. *Catalysis today*, 115(1-4):2–32, 2006.

[245] Mai Bui, Claire S Adjiman, André Bardow, Edward J Anthony, Andy Boston, Solomon Brown, Paul S Fennell, Sabine Fuss, Amparo Galindo, Leigh A Hackett, et al. Carbon capture and storage (ccs): the way forward. *Energy & Environmental Science*, 11(5):1062–1176, 2018.

[246] Guido Magneschi, Tony Zhang, and Ron Munson. The impact of co_2 capture on water requirements of power plants. *Energy Procedia*, 114:6337–6347, 2017.

[247] Jens Artz, Thomas E Muller, Katharina Thenert, Johanna Kleinekorte, Raoul Meys, Andre Sternberg, Andre Bardow, and Walter Leitner. Sustainable conversion of carbon dioxide: an integrated review of catalysis and life cycle assessment. *Chemical reviews*, 118(2):434–504, 2017.

[248] Mar Pérez-Fortes, Jan C Schöneberger, Aikaterini Boulamanti, Gillian Harrison, and Evangelos Tzimas. Formic acid synthesis using co_2 as raw material: Techno-economic and environmental evaluation and market potential. *international journal of hydrogen energy*, 41(37):16444–16462, 2016.

[249] Arun S Agarwal, Yumei Zhai, Davion Hill, and Narasi Sridhar. The electrochemical reduction of carbon dioxide to formate/formic acid: engineering and economic feasibility. *ChemSusChem*, 4(9):1301–1310, 2011.

[250] Jennifer B Dunn, Felix Adom, Norm Sather, Jeongwoo Han, Seth Snyder, Chang He, Jian Gong, Dajun Yue, and Fengqi You. Life-cycle analysis of bioproducts and their conventional counterparts in greet, 2015.

[251] Sivashunmugam Sankaranarayanan and Kannan Srinivasan. Carbon dioxide–a potential raw material for the production of fuel, fuel additives and bio-derived chemicals. 2012.

[252] Philip G Jessop, Yi Hsiao, Takao Ikariya, and Ryoji Noyori. Homogeneous catalysis in supercritical fluids: hydrogenation of supercritical carbon dioxide to formic acid, alkyl formates, and formamides. *Journal of the American Chemical Society*, 118(2):344–355, 1996.

[253] Chak Po Lau and Yu Zhong Chen. Hydrogenation of carbon dioxide to formic acid using a 6,6'-dichloro-2,2'-bipyridine complex of ruthenium, cis-$[ru(6,6'\text{-}cl_2bpy)_2(h_2o)_2](cf_3so_3)_2$. *Journal of Molecular Catalysis A: Chemical*, 101(1):33–36, 1995.

[254] Philip G Jessop, Ferenc Joó, and Chih-Cheng Tai. Recent advances in the homogeneous hydrogenation of carbon dioxide. *Coordination Chemistry Reviews*, 248(21-24):2425–2442, 2004.

[255] Arno Behr and Kristina Nowakowski. Catalytic hydrogenation of carbon dioxide to formic acid. In *Advances in Inorganic Chemistry*, volume 66, pages 223–258. Elsevier, 2014.

[256] Tristram O West and Wilfred M Post. Soil organic carbon sequestration rates by tillage and crop rotation. *Soil Science Society of America Journal*, 66(6):1930–1946, 2002.

[257] Alfons Weersink, Michael Walker, Clarence Swanton, and James E Shaw. Costs of conventional and conservation tillage systems. *Journal of Soil and Water Conservation*, 47(4):328–334, 1992.

[258] Petra Döll, Frank Kaspar, and Bernhard Lehner. A global hydrological model for deriving water availability indicators: model tuning and validation. *Journal of Hydrology*, 270(1-2):105–134, 2003.

[259] TP Taggart, TA Endreny, and D Nowak. Modeling the effect of urban infrastructure on hydrologic processes within i-tree hydro, a statistically and spatially distributed model. In *AGU Fall Meeting Abstracts*, 2014.

[260] RH Kadlec. The effects of wetland vegetation and morphology on nitrogen processing. *Ecological Engineering*, 33(2):126–141, 2008.

[261] Robert Kadlec. Large constructed wetlands for phosphorus control: A review. *Water*, 8(6):243, 2016.

[262] Gary J Whiting and Jeffrey P Chanton. Greenhouse carbon balance of wetlands: methane emission versus carbon sequestration. *Tellus B*, 53(5):521–528, 2001.

[263] Solange Filoso, Maíra Ometto Bezerra, Katherine CB Weiss, and Margaret A Palmer. Impacts of forest restoration on water yield: A systematic review. *PloS one*, 12(8):e0183210, 2017.

[264] Anne Sofie Elburg Nielsen, Andrew J Plantinga, and Ralph J Alig. New cost estimates for carbon sequestration through afforestation in the united states. *Gen. Tech. Rep. PNW-GTR-888. Portland, OR: US Department of Agriculture, Forest Service, Pacific Northwest Research Station. 35 p.*, 888, 2014.

[265] PV Townsend, RJ Harper, PD Brennan, C Dean, S Wu, KRJ Smettem, and SE Cook. Multiple environmental services as an opportunity for watershed restoration. *Forest Policy and Economics*, 17:45–58, 2012.

[266] Mark L Plummer. Assessing benefit transfer for the valuation of ecosystem services. *Frontiers in Ecology and the Environment*, 7(1):38–45, 2009.

[267] Leslie Richardson, John Loomis, Timm Kroeger, and Frank Casey. The role of benefit transfer in ecosystem service valuation. *Ecological Economics*, 115:51–58, 2015.

[268] Greg McComb, Van Lantz, Katrina Nash, and Robyn Rittmaster. International valuation databases: overview, methods and operational issues. *Ecological Economics*, 60(2):461–472, 2006.

[269] U.S. Environmental Protection Agency (EPA). Emissions & generation resource integrated database (egrid). Available at: https://www.epa.gov/energy/emissions-generation-resource-integrated-database-egrid Accessed Feb 2018.

[270] Ohio Environmental Protection Agency (Ohio EPA). Individual wastewater discharge permit information.

[271] Timothy J Skone. Life cycle analysis of coal exports from the powder river basin. Technical report, National Energy Technology Laboratory (NETL), 2016.

[272] Timothy J Skone, James Littlefield, Joe Marriott, Greg Cooney, Matt Jamieson, Chris Jones, Laura Demetrion, Michele Mutchek, Chungyan Shih, Aimee E Curtright, et al. Life cycle analysis of natural gas extraction and power generation, 2016.

[273] Ohio Environmental Protection Agency (Ohio EPA). Nutrient mass balance study for ohio's major rivers. Technical report, 2016.

[274] U.S. Energy Information Administration (EIA). Total energy consumption, price, and expenditure estimates, 2015. Available at: https://www.eia.gov/state/seds/data.php?incfile=/state/seds/sep_fuel/html/fuel_te.html&sid=US&sid=OH Accessed Apr 2018.

[275] Xuping Li, Paul Anderson, Huei-Ru Molly Jhong, Mark Paster, James F Stubbins, and Paul JA Kenis. Greenhouse gas emissions, energy efficiency, and cost of synthetic fuel production using electrochemical co_2 conversion and the fischer–tropsch process. *Energy & Fuels*, 30(7):5980–5989, 2016.

[276] Morgan Bazilian, Holger Rogner, Mark Howells, Sebastian Hermann, Douglas Arent, Dolf Gielen, Pasquale Steduto, Alexander Mueller, Paul Komor, Richard SJ Tol, et al. Considering the energy, water and food nexus: Towards an integrated modelling approach. *Energy Policy*, 39(12):7896–7906, 2011.

[277] Vaclav Smil. 21st century energy: Some sobering thoughts. *oecd Observer*, (258-259):22–24, 2006.

[278] Global formic acid market report, history and forecast 2019-2026, breakdown data by manufacturers, key regions, types and application, 2019. Available at: https://dataintelo.com/report/formic-acid-market/ Accessed May 2020.

[279] Ohio EPA. Ohio nutrient reduction strategy, 2013.

[280] Jim Waymer. Fpl plans $100 million solar plant at nasa's kennedy space center, 2019. Available at: https://www.floridatoday.com/story/news/local/environment/2019/08/09/fpl-fill-wetlands-solar-plant-nasa-kennedy-space-center/1934778001/ Accessed May 2020.

[281] Greg A Barron-Gafford, Mitchell A Pavao-Zuckerman, Rebecca L Minor, Leland F Sutter, Isaiah Barnett-Moreno, Daniel T Blackett, Moses Thompson, Kirk Dimond, Andrea K Gerlak, Gary P Nabhan, et al. Agrivoltaics provide mutual benefits across the food–energy–water nexus in drylands. *Nature Sustainability*, 2(9):848–855, 2019.

[282] Christian Dupraz, Hélène Marrou, Grégoire Talbot, Lydie Dufour, A Nogier, and Y Ferard. Combining solar photovoltaic panels and food crops for optimising land use: towards new agrivoltaic schemes. *Renewable energy*, 36(10):2725–2732, 2011.

[283] Harshavardhan Dinesh and Joshua M Pearce. The potential of agrivoltaic systems. *Renewable and Sustainable Energy Reviews*, 54:299–308, 2016.

[284] Mikhail Golosov, John Hassler, Per Krusell, and Aleh Tsyvinski. Optimal taxes on fossil fuel in general equilibrium. *Econometrica*, 82(1):41–88, 2014.

[285] Thomas Gibon, Richard Wood, Anders Arvesen, Joseph D Bergesen, Sangwon Suh, and Edgar G Hertwich. A methodology for integrated, multiregional life cycle assessment scenarios under large-scale technological change. *Environmental Science & Technology*, 49(18):11218–11226, 2015.

[286] Maxime Agez, Richard Wood, Manuele Margni, Anders H Strømman, Réjean Samson, and Guillaume Majeau-Bettez. Hybridization of complete plca and mrio databases for a comprehensive product system coverage. *Journal of Industrial Ecology*, 2020.

[287] Zhifu Mi, Jing Meng, Dabo Guan, Yuli Shan, Malin Song, Yi-Ming Wei, Zhu Liu, and Klaus Hubacek. Chinese co_2 emission flows have reversed since the global financial crisis. *Nature communications*, 8(1):1–10, 2017.

[288] Junmei Hu, Gengyuan Liu, Fanxin Meng, Yuanchao Hu, and Marco Casazza. Subnational carbon flow pattern analysis using multi-scale input-output model. *Ecological Modelling*, 431:109138, 2020.

[289] Richard Wood, Konstantin Stadler, Tatyana Bulavskaya, Stephan Lutter, Stefan Giljum, Arjan De Koning, Jeroen Kuenen, Helmut Schütz, José Acosta-Fernández, Arkaitz Usubiaga, et al. Global sustainability accounting—developing exiobase for multi-regional footprint analysis. *Sustainability*, 7(1):138–163, 2015.

[290] Thomas F. Howells III, Edward T. Morgan, Kevin B. Barefoot, Louis E. Feagans, Teresa L. Gilmore, and Chelsea K. Smith-Nelson. Preview of the 2018 comprehensive update of the industry economic accounts, 2018. Available at: https://apps.bea.gov/scb/2018/08-august/0818-industry-economic-accounts-preview.htm Accessed Mar 2020.

[291] National Agricultural Statistics Service (NASS). Nass quick stats. Available at: https://quickstats.nass.usda.gov/ Accessed Mar 2020.

[292] Economic Research Service (ERS). Fertilizer use and price. Available at: https://www.ers.usda.gov/data-products/fertilizer-use-and-price.aspx Accessed Mar 2020.

[293] USDA Forest Service. i-tree county benefits. Available at: https://county.itreetools.org/ Accessed Mar 2020.

[294] Kyuha Lee and Bhavik R Bakshi. Energy-water-co_2 nexus of fossil fuel based power generation. *Advances in Carbon Management Technologies: Carbon Removal, Renewable and Nuclear Energy, Volume 1*, page 184, 2020.

[295] Detlef P van Vuuren, Jason Lowe, Elke Stehfest, Laila Gohar, Andries F Hof, Chris Hope, Rachel Warren, Malte Meinshausen, and Gian-Kasper Plattner. How well do integrated assessment models simulate climate change? *Climatic change*, 104(2):255–285, 2011.

[296] CM Goodess, C Hanson, M Hulme, and TJ Osborn. Representing climate and extreme weather events in integrated assessment models: a review of existing methods and options for development. *Integrated Assessment*, 4(3):145–171, 2003.

[297] Jonathan D Linton and Steven T Walsh. Integrating innovation and learning curve theory: an enabler for moving nanotechnologies and other emerging process technologies into production. *R&D Management*, 34(5):517–526, 2004.

[298] Otávio Cavalett, Mateus F Chagas, Tassia L Junqueira, Marcos DB Watanabe, and Antonio Bonomi. Environmental impacts of technology learning curve for cellulosic ethanol in brazil. *Industrial Crops and Products*, 106:31–39, 2017.